pH-Triggered Dynamic Molecular Tweezers for Drug Delivery Applications

by

Cyndy G. M. Cruz

A thesis submitted to the Department of Chemistry

In conformity with the requirements for

the degree of Master of Science

Queen's University

Kingston, Ontario, Canada

September 2011

Abstract

My MSc project aims at developing pH-responsive molecular tweezers for drug delivery applications. The project began with the synthesis of our 2nd generation tweezer, whose main objective was to improve our previous model, 1st generation tweezer, which contained a pH-responsive triad spacer and two naphthalene walls known to interact with hydrophobic drugs such as Mitoxantrone®. The naphthalene interaction sites were successfully modified to contain oligoethylene glycol chains to improve their water-solubility, in anticipation for more accurate measurements of pKa and binding constants in aqueous media. However, all attempts to convert such naphthalene derivatives into their corresponding boronic acid or ester through standard protocols (halogen-lithium exchange, palladium catalyzed borylation) failed. Without the required boronic acid/ester, the final Suzuki-Miyaura coupling with the di-bromo triad spacer was not achieved.

Synthesis of the 3rd generation tweezer, which was modified to contain theophylline as the new interaction sites, was then attempted. The half-tweezer was successfully synthesized via copper (II) catalyzed coupling of theophylline with the 5-bromo-4-methoxyphenyl boronic acid. However, all attempts to convert it into the required boronic acid/ ester for the final Suzuki-Miyaura coupling reaction with 2,6-dibromopyridine failed. We then focused our attention on the conversion of the triad spacer into its corresponding diboronic acid. The synthesis of the triad diboronic acid was a success, however, the final copper (II) catalyzed reaction with theophylline to form the tweezer only yielded the mono-coupled product.

Lastly, our 4th generation tweezer was engineered to avoid the synthetic difficulties encountered in the boronic acid/ ester synthesis stage. Using the commercially available 5-formyl-2-methoxyphenylboronic acid and *o*-phenylenediamine, we successfully synthesized a benzimidazole-derived “half tweezer” through ring condensation reaction. Alkylation of this half-tweezer was also successfully achieved, although purification of the alkylated product was not

optimized. Using this crude product, we carried out the final tweezer reaction via Suzuki-Miyaura coupling with 2,6-dibromopyridine under microwave irradiation. ^{1}H NMR results show formation of new species that is believed to be the 4th generation tweezer (although the presence of impurities made integration of the signals unreliable). Much work is needed in the purification of the alkylated half tweezer boronic acid in order to avoid complicated mixtures in the final tweezer reaction.

Acknowledgements

This research project would not be possible without the support and guidance of many people. First, I would like to extend my heartfelt gratitude to my supervisor, Dr. Anne Petitjean. Her invaluable ideas and advice, patience, guidance, understanding, and dedication to her students throughout the course of this project have not only enriched my growth as a chemist, but also helped build my character.

Sincere thanks are also given to the members of the supervisory committee, Dr. Ralph Whitney, Dr. David Zechel, Dr. Donal Macartney and Dr. Guojun Liu.

I also thank the Petitjean group members, Dr. Olivier Fleischel, Dr. Ganga Bhagavathy, Weiwen Zhao, and Dr. Yi Yan, for all the help they have given me in the laboratory and for being great friends. Lastly, to my undergraduate student, Caitlin Miron, who has offered her invaluable time to help me with the syntheses of the 2nd and 4th generation tweezers, for being a great friend and for keeping me entertained in the lab through her great sense of humour.

I would also like to convey my gratitude to the Snieckus group for allowing me to perform reactions on their microwave machine. Special thanks are also given to Dr. Cedric Schneider and Dr. Matthew Kitching, for their invaluable ideas and suggestions about boronic acid/ester syntheses.

Dr. Cathleen Crudden is also acknowledged for her advice on palladium and copper-catalyzed syntheses, and Dr. Françoise Sauriol for her help in NMR spectroscopic analysis.

My deepest gratitude is also extended to Queen's University, Ontario Ministry of Research and Innovation, NSERC-DG, and the Canadian Foundation for Innovation for their financial assistance. Also, I thank the Queen's University Chemistry Department for providing the equipment and space needed to perform my experiments.

Lastly, I would like to express my love and gratitude to my family, for their undying support and guidance throughout the course of my studies: For my parents, who nurtured the

scientist in me, my brothers, who were my very first students, and for Robert T. Woods, who has continued to be my inspiration all these years.

Table of Contents

List of Figures

List of Symbols and Abbreviations

ADME	absorption, distribution, metabolism, and elimination
ASGP-R	asiaglycoprotein receptor
br	broad
n-BuLi	n-butyllithium
d	doublet
DCM	dichloromethane
dd	doublet of doublet
DDS	drug delivery systems
DMA	dimethylacetal
DMF	dimethylformamide
DMF/DMA	dimethylformamide dimethylacetal
DMSO	dimethylsulfoxide
EA	elemental analysis
EI	electron impact
EPR	enhanced permeability and retention
ESI	electrospray ionization
EtOAc	ethyl acetate
EtOH	ethanol
FR	folate receptor
g	gram
HCl	hydrochloric acid
HPLC	high performance liquid chromatography
hr	hour
HRMS	high resolution mass spectrometry

IS	interaction sites
J	Joule
J	vicinal coupling constant
kDa	kilodalton
KDN	potassium 1,3-dihydroxy-2-naphthoate
kJ	kilojoule
m	multiplet
MeCN	acetonitrile
MeOPh-Py-MeOPh	methoxyphenyl-pyridine-methoxyphenyl
mg	milligram
MHz	megahertz
min	minute
mL	millilitre
mmol	millimole
mol	mole
MS	mass spectrometry
MTX	Mitoxantrone™
NCE	new chemical entities
NMR	nuclear magnetic resonance
NOESY	nuclear overhauser effect spectroscopy
^{o}C	degree Celsius
ortho-Py	2,6-bis-(2'-methoxyphenyl)-pyridine
ortho-PyNaph	1st generation "naked" tweezer
PEG	polyethylene glycol
Ph	phenyl
PhPin	phenyl- pinacol

PLA	polylactic acid
pLys	poly-Lysine
ppm	parts per million
Py	pyridine
R&D	research and development
Rf	retention factor
ROESY	rotating frame overhauser spectroscopy
RT	room temperature
S	spacer
s	singlet
S_NAr	nucleophilic aromatic substitution
t	triplet
TBAB	tetrabutylammonium bromide
TFA	trifluoroacetic acid
THF	tetrahydrofuran
TLC	thin layer chromatography
TMS-Cl	chlorotrimethylsilane
TMS-F	fluorotrimethylsilane
TOCSY	total correlation spectroscopy
UNIT 1 PEG	1-bromo-2,7-bis(2-methoxyethoxy) naphthalene
UNIT 2 PEG	1-bromo-2,7-bis(2-(2-methoxyethoxy)ethoxy) naphthalene
UV	ultraviolet
δ	chemical shift
λ	wavelength

Chapter 1: Introduction

Supramolecular Architectures for Drug Delivery Applications

1.1 Drug Discovery and Development: A Brief Overview

Discovering and developing new drugs is a very lengthy and expensive process. In order to be commercially available, drug candidates must first undergo various different screening and testing protocols and pass clinical trials.[1,2] Drug discovery begins by the identification of a "target" (e.g. protein) that exhibits a strong relationship to the specific disease being investigated. The next step would be to screen tens of thousands of new chemical entities (NCE's) against this target, where only those with the desired biological activity (referred to as "hits") would be selected for further testing and optimization. These screening and optimization processes (drug development) are repeated several times until only a small number of these NCE's (now referred to as "leads") remain for testing in pharmacological models. Compounds that show the best results would then be evaluated in clinical trials, which is the last stage of drug development.

Drug discovery and development take about an average of 12-15 years to complete. Furthermore, the cost of drug R&D is currently estimated to be greater than $800 million dollars and continues to increase each year.[1] Still, only 40% of the proposed drug candidates reach Phase I clinical trials (evaluation in humans), which gives a very high attrition rate (90%).[1] In other words, only 1 in 10 drug candidates that are tested in humans will become marketable.

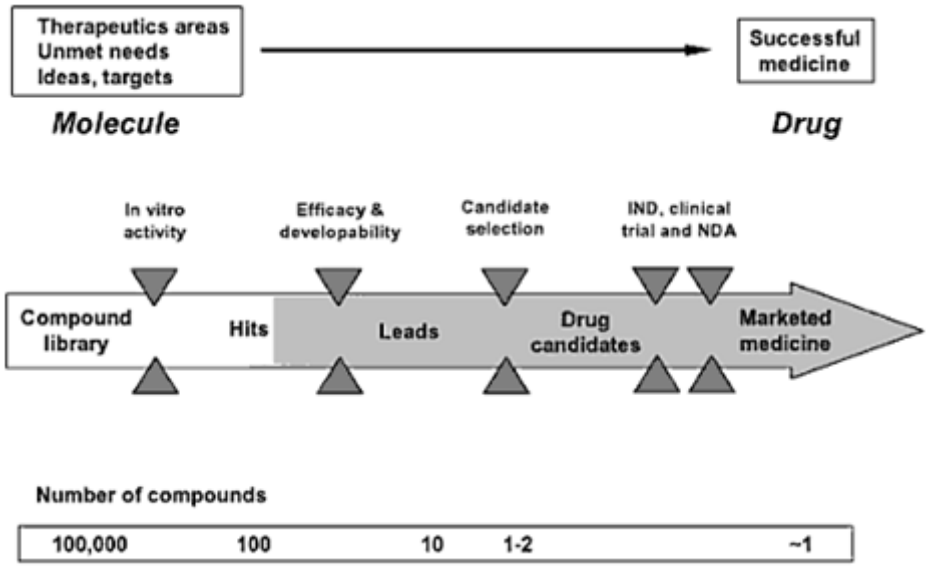

Figure 1.1: Schematic of the drug discovery and development process, highlighting the estimated number of compounds chosen for each step.[1]

1.1.1. Improving the Efficiency of Drug R&D

The economic disadvantages of drug R&D have driven the pharmaceutical industries to reduce their overall costs, as well as the time to make an NCE commercially available. The late stages of drug development (clinical trials) is known to be the most expensive part of drug R&D and account for more than 50% of its overall budget.[1] Therefore, to avoid expensive failures at the clinical trial stage, it is crucial to identify the factors that may potentiate these failures while still in the discovery stage.

A study by Prentis *et al.* in 1988 examined the causes of the high attrition rates of the NCE's.[3] Their results showed that the majority of NCE's failure can be attributed to their poor pharmacokinetic properties and not to their lack of biological activities.[3,2] Thus, improving the pharmacokinetic properties of drugs has become one of the main focuses of pharmaceutical research today.

1.1.2. Pharmacokinetics and Drug Efficacy

Pharmacokinetics is defined as the quantitative study of drug absorption, distribution, metabolism, and elimination (ADME) from the body.[4] It influences the therapeutic efficacy of drugs primarily by controlling its bioavailability, which refers to the extent and rate at which an administered drug reaches systemic circulation and subsequently its physiological target.[5] The route of entry and the mode of administration of drugs affect their bioavailability due to the physiological differences that exist between the tissues that the drug must cross before entering systemic circulation. For example, drugs that are administered intravenously would have a higher bioavailability than those taken orally because they are directly injected into the bloodstream.[5,6] Drugs that are taken orally must first pass through various obstacles, such as overcoming solubility issues in the gastrointestinal fluid, metabolism by the gut wall and intestinal flora, and absorption through the intestinal wall, to name a few.[5] It is important to note, however, that the therapeutic efficacy of drugs is not 100% even if their bioavailability is.[6] Regardless of the technique used, partial degradation of the drug always happens before it reaches their site of action.

1.1.3. The Role of Drug Delivery Systems

Many commercially available drugs have limited therapeutic effects because they are partially degraded by enzymes as they enter the body. Drug delivery systems (DDS) have great potential to conquer this problem because they are designed to deliver medications intact to their site of action. Most DDS are composed of nanoparticles, whose synthetic versatility enables fine tuning of their size, shape, and surface characteristics- all of which play a key role in influencing their biodistribution *in vivo*, which in turn, enhance the drugs' bioavailability.[7] Furthermore, nanoparticles can be designed to incorporate targeting ligands, which can be used for the selective targeting of the drug in question. Historically, liposomes were among the first types of nanoparticles used for drug delivery applications.[7] Liposomes are synthetic spherical

vesicles composed of a lipid bilayer. They can encapsulate hydrophobic and hydrophilic agents (such as drugs, proteins, or imaging agents), thus shielding their cargo from enzymatic attack as they circulate throughout the body.[8]

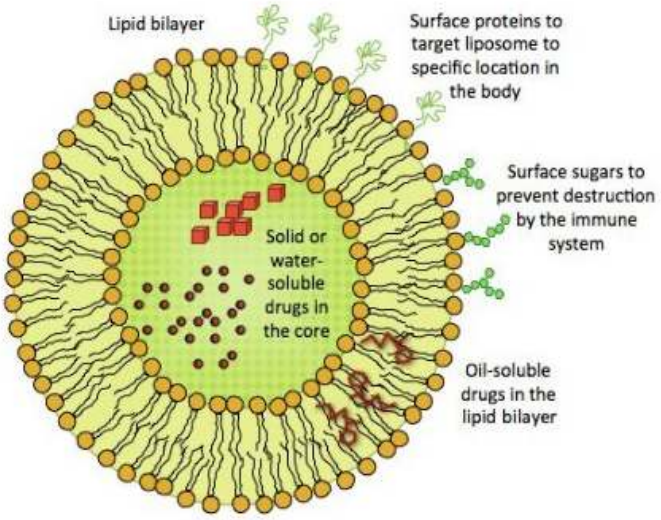

Figure 1.2: Basic structure of a liposome used as a DDS.[29]

Liposomes are examples of particulate drug carriers, or nanoparticles that carry physically entrapped drugs.[8,10] Another type of drug carriers described in literature belongs to a class called macromolecular conjugates, in which the drug is chemically linked to a macromolecule such as a synthetic polymer or an endogenous protein. [9] An example of this is the polyethylene glycol (PEG)–L-asparaginase drug conjugate for the treatment of acute lymphocytic leukemia.[7]

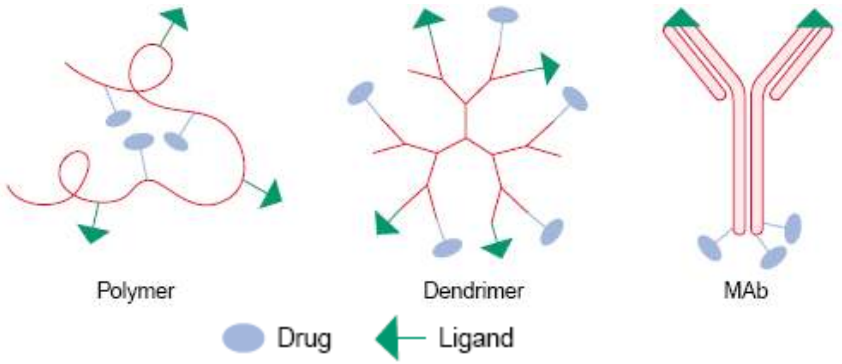

Figure 1.3: Schematic representation of macromolecular conjugates (Mab Monoclonal antibodies)[9]

1.1.4. Drug Delivery Systems as Applied to the Field of Oncology

Cancer has been the leading cause of premature death in North America for the past decade. Chemotherapy remains to be the most common mode of treatment although it is often associated with many adverse side effects. Most of the commercially available anticancer drugs have a narrow therapeutic window because of their high systemic toxicity and lack of tumour selectivity.[11,12] Thus, in order to overcome these limitations, selective targeting of these anticancer drugs is required.

The therapeutic efficacy of cancer drugs can be improved by the targeted delivery approach, which may or may not involve the use of a DDS. Targeted delivery currently falls into two categories. The first approach involves blocking novel pathways or proteins that emerge or become overexpressed in cancer cells.[13] These pathways are crucial for the survival of the tumour cells, but are either absent or not needed by normal cells. For example, the kinase inhibitor chemotherapeutic drug, Gleevec, exhibits its anticancer properties by targeting the fusion protein bcr/abl that arises solely from the chromosomal translocation during tumorigenesis.[13] The second approach, on the other hand, involves the use of homing ligands that bind specifically to a receptor that is primarily expressed on malignant cells. Attaching the

therapeutic drug to a corresponding ligand would then allow the non-selective drug to be carried only to the tumour cell.

There are currently two types of selective drug targeting processes as applied to the field of oncology, namely active and passive targeting. The former encompasses ligand-targeted therapy while the latter exploits the anomalies of malignant tissues at the vasculolymphatic level. Following these approaches, accumulation of drugs in the tumour tissue can be achieved by employing macromolecules as inert drug carriers that do not necessarily interact with the cancer cells, but strongly influence the drugs' biodistribution.[11]

1.1.5. Active Targeting

Active targeting encompasses ligand-targeted therapy, whose aim is to develop antibodies or receptor-affinity ligands that will interact specifically with their cellular target. Upon binding of the DDS to their target receptor, they are then internalized into the cell via receptor mediated endocytosis. Once inside the cell, the drug is then released either in the endosomes or lysosomes depending on the route of cellular trafficking of the receptor in question.

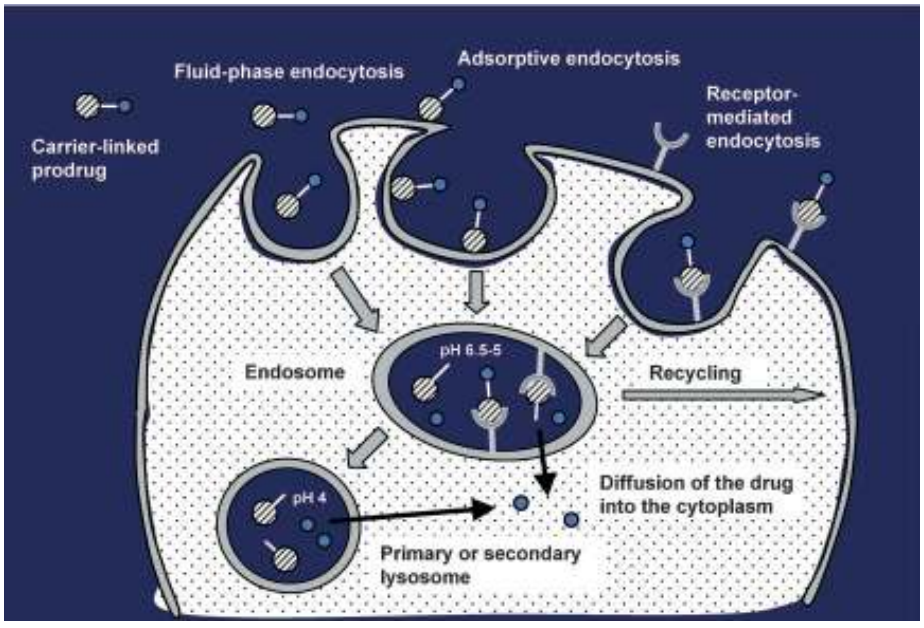

Figure 1.4: Mechanism of active targeting.[11]

As applied to the field of oncology, this approach should recognize the differences in cell surface antigen or receptor expression between normal and cancer cells. There have been many tumour-associated receptors that have been investigated in receptor targeting approaches. For example, the receptor ErbB2, a growth factor that is overexpressed in 20-30% of human breast carcinomas, has been a target of antibody-based anticancer drugs for the treatment of breast cancer.[12] On the other hand, asiaglycoprotein galactose receptor (ASGP-R) has been widely investigated for the treatment of liver cancer.[12] Another very promising target is the folate receptor (FR), which has emerged as an optimal targeting ligand for the selective delivery of attached imaging and therapeutic agents to cancer tissues and sites of inflammation.[12,13] FR is overexpressed in approximately 40% of human cancers and activated macrophages. Meanwhile, FR in normal cells is limited primarily in the proximal tubule of the kidneys.

1.1.6. Passive Targeting

Unlike active targeting, which DDS rely heavily on a target receptor, passive targeting depends on the anomalies of malignant tissues at the vasculolymphatic level. It exploits a universal property of tumour tissues, called the Enhanced Permeability and Retention (EPR) effect that arises from the rapid vascularization required to support the fast-growing cancer cells.[15] As a result of this uncontrolled growth, tumour blood vessels are often defective. As can be seen from the following figure, normal tissues have relatively uniform blood vessels that are sufficiently close together to evenly distribute nutrients (i.e. oxygen, folate) to their surrounding cells.[16] In contrast, tumour blood vessels are tortuous and contain many fenestrations that arise from the misalignment of endothelial cells and absence of a basement membrane. This makes tumour blood vessels leaky, enabling macromolecules, such as polymeric DDS, to pass through very easily.

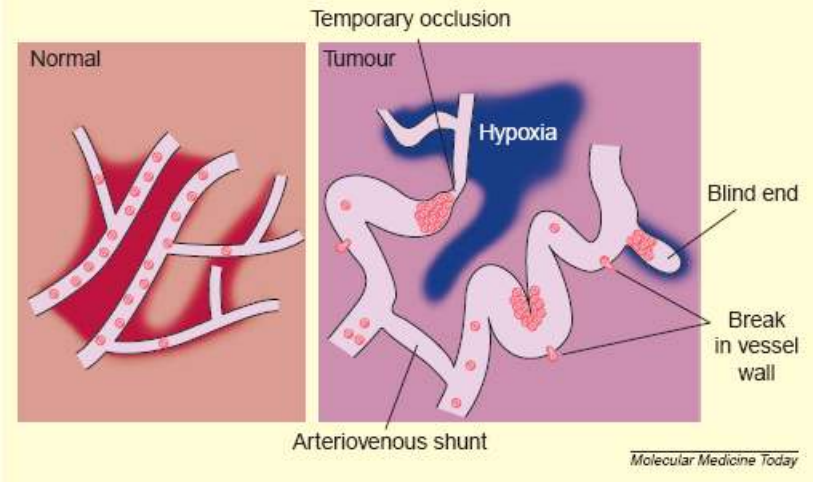

Figure 1.5: Differences in the vasculature of normal versus tumour tissues.[16]

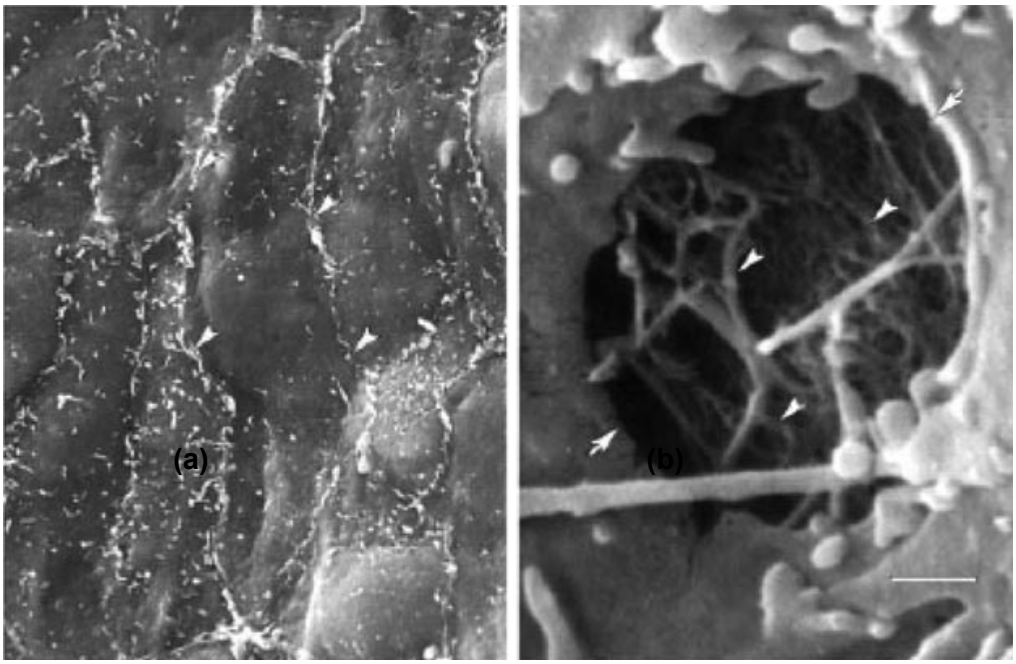

(a) **(b)**

Figure 1.6: Scanning electron micrographs of the luminal surface of a) healthy mouse mammary gland and b) tumour blood vessels.[11]

Tumour tissues also have impaired or missing lymphatic drainage. As a result, macromolecules that are able to pass through the leaky blood vessels are easily retained within

the tumour tissue. As a rule of thumb, macromolecules that are larger than 40 kDa are preferentially retained due to their ability to escape renal clearance.[11]

1.1.7. Controlled Release by pH

Drug release can be triggered by a stimulus such as light, temperature, redox potential, and pH.[17,18] These stimuli are typically recognized on cell surfaces and usually differ between normal and diseased cells.[11,19] Drug release by pH is a popular strategy employed when developing drug carriers in the field of cancer research. Indeed, pH has been observed to differ between normal and tumour tissues. For example, the extracellular pH of normal tissues is held constant at 7.4 (similar to blood pH), while the intracellular pH is 7.2. In tumour cells, however, the external pH is lowered by 0.5-1.0 unit, making them acidic.[11,20] The difference in pH between normal and tumour tissues was initially attributed from the high rate of glycolysis in cancer cells in both aerobic and non-aerobic conditions.[20] Newer evidence, however, suggests that this pH difference is due to the anomalous regulation of hydrogen ion dynamics of proton transporters within the cancerous cell.[21] It was also hypothesized that the acidic conditions benefit the cancer cells by providing an invasive environment that tears the extracellular matrix and destroys surrounding normal cells.[20,21]

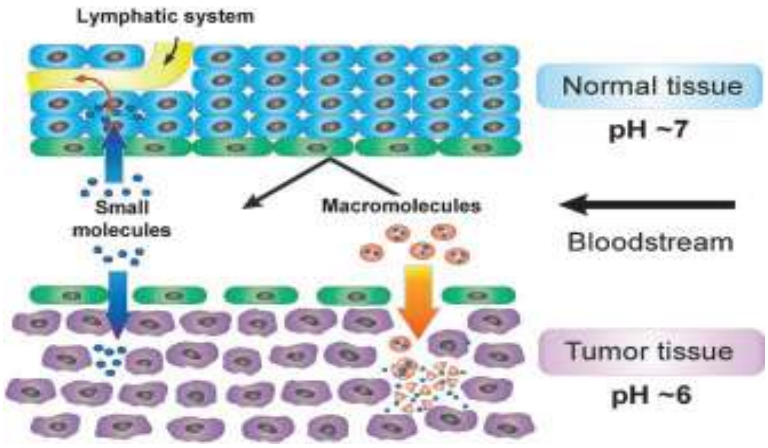

Figure 1.7: EPR effect and the differences in pH between normal and tumour tissues.[11]

The majority of reported systems in literature involves the covalent attachment of drugs and relies on pH-dependent chemical hydrolysis for its release. For example, Frechét *et al.* developed a library of acid-degradable polymers for DDS applications that uses a dimethyl ketal monomer as its acid degradable component.[22] At physiological pH (7.4), the polymers are stable but are quickly degraded at mildly acidic pH such as that in endosomes or in tumour tissues.

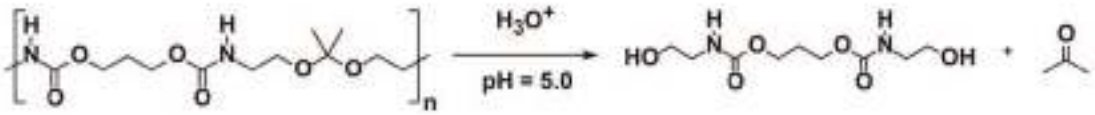

Figure 1.8: Acid-catalyzed hydrolysis of poly(ketal)-based polymers.[22]

Another example is the polymer-drug conjugate developed by Bae *et al.*[20] This macromolecular conjugate is covalently attached to the anticancer drug Doxorubicin by an acid-sensitive, acyl hydrazone bond. At pH values below 6.0, the acyl hydrazone bond is hydrolyzed, thus releasing the bound Doxorubicin into the medium. Although a very effective design, drug release rates in these systems are often very difficult to control due to the high lability or stability of the covalent bonds involved. Due to this, research in the area of non-covalent release systems has gained increasing popularity.

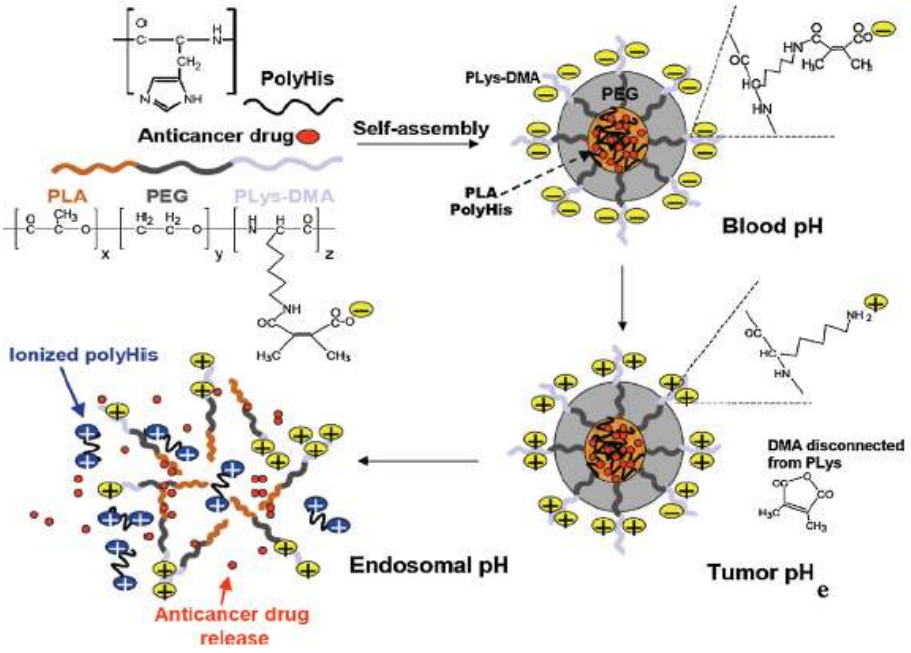

Figure 1.9: Schematic diagram of pH-controlled drug release of polycationic micelle, PLA-*b*-PEG-*b*-pLys-DMA.

Non-covalent binding is much desirable as it offers greater tunability of the binding and release properties of the drug substrate. Unlike covalent systems, whose degradation kinetics may take hours (thus increasing the probability of the DDS to be eliminated from the body prior to releasing its bound drug), non-covalent based systems release their bound drugs almost instantaneously.

1.2 Molecular Tweezers

Molecular tweezers are simple synthetic receptors. Their basic structure is composed mainly of two interaction sites (**IS**) that are held together by a spacer group (**S**).[23] Guests are bound via non-covalent interactions such as hydrogen bonding, metal coordination, hydrophobic forces, van der Waals forces, π-π interactions, and/or electrostatic effects. There are currently

three classes of molecular tweezers described in literature, all of which are defined by the nature and flexibility of the **S** group.[24] They are either 1) flexible, 2) rigid, or 3) switchable.

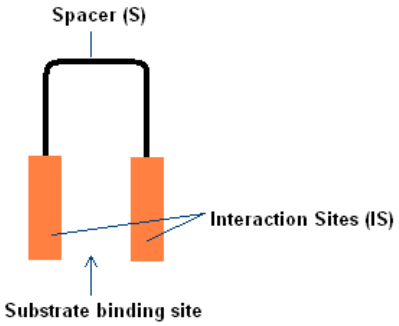

Figure 1.10: General structure of a molecular tweezer.

1.2.1 Flexible Tweezers

Flexible tweezers allow various molecular conformations through bond rotations that occur in the **S** group, typically composed of a linear chain (or aromatic groups held by aliphatic hinges for semi-flexible tweezers). The nature of the substrate dictates the conformation of the tweezer that optimizes the degree of binding between host and guest, much like the "induced fit" model described in biological systems. This type of tweezer usually involves strong intermolecular forces (e.g. coordination bonds, synergistic effects of weak intermolecular forces such as ion-dipole and donor-acceptor interactions) in order to compensate for the loss of entropy in the event of substrate binding.[24]

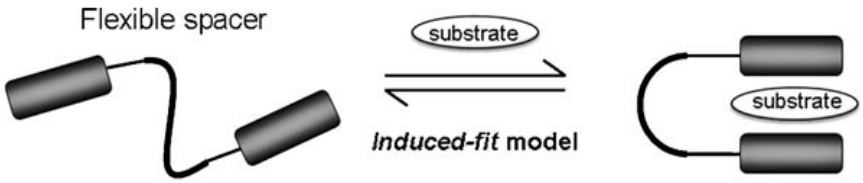

Figure 1.11: Cartoon representation of flexible tweezers illustrating the "induced fit" mechanism.[24]

An example is the water-soluble caffeine tweezer, developed by Chen and Whitlock in 1978. This molecular tweezer is composed of two theophylline moieties (IS) that are held together by a flexible, alkyl-diyne spacer (S). It selectively binds hydrophobic benzoate and naphthoate anionic guests such as the potassium salt of 1,3-dihydroxy-2-naphthoate (KDN) via combination of π-π stacking and ion-dipole interactions.[25]

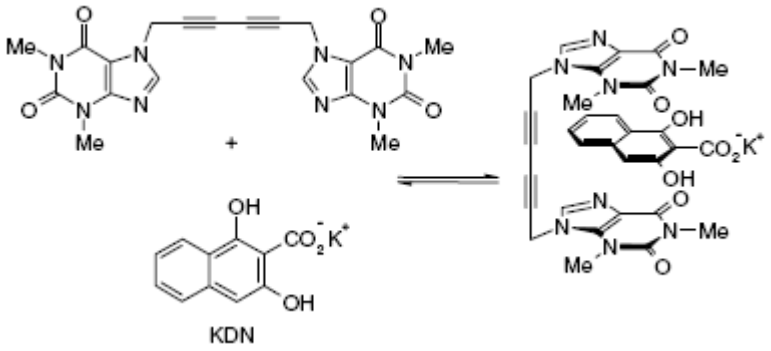

Figure 1.12: Chen and Whitlock's molecular tweezer illustrating the conformational changes upon guest binding.[23]

1.2.2 Rigid Tweezers

The rigidity of the spacer group is crucial for two main reasons. First, it provides some degree of pre-organization to the molecule which enhances its guest binding ability. Second, it keeps the two binding units at a required distance apart, thus leaving enough space in between for guest molecules to bind. Overall, both S and IS must also prevent self-association or dimerization to ensure proper guest molecule binding.[23]

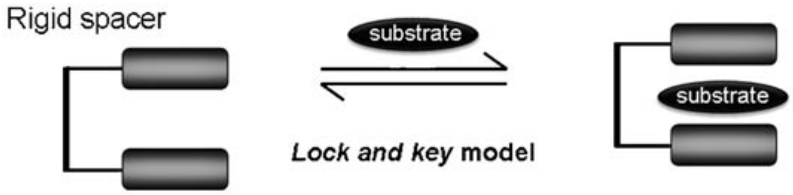

Figure 1.13: Cartoon representation of flexible tweezers illustrating the "lock and key" mechanism.[24]

An example is the “buckycatcher”, created by Sygula and co-workers in 2007. Its binding units are composed of corannulene molecules which bind C60 fullerene by a combination of structure complementarity and hydrophobic interactions.[25] Another example is the chiral molecular tweezer developed by Harmata and his co-workers in 2004. This static tweezer is made from two Kagan’s ether units that form a single diastereomer.[23,26] This chiral molecular tweezer effectively binds electron deficient guests such as trinitrobenzene and is able to separate enantiomers of trinitrobenzene analogues at high %ee.[23,26]

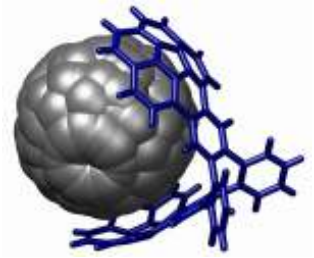

Figure 1.14: 3D model of the “buckycatcher” developed by Sygula *et al.*[25]

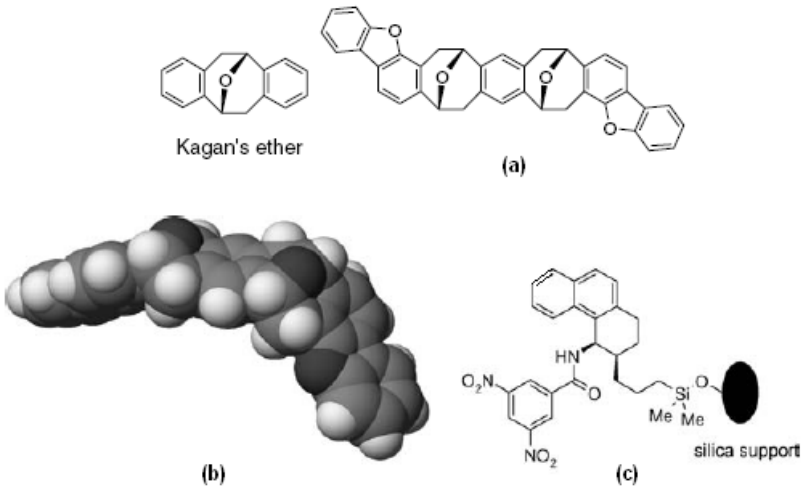

Figure 1.15: a) Harmata’s chiral molecular tweezer using Kagan’s ether as the S, and dibenzofuran as IS. b) Molecular model of the chiral tweezer and c) the chiral guest that forms part of the π-acidic stationary phase, a (3*R*,4*S*) Whelk-O 1 silica-based chromatography column.[23,26]

1.2.3 Switchable Tweezers

Switchable molecular tweezers more or less exist in one conformation in the absence of a particular stimulus and switch conformations when the required stimulus is present.

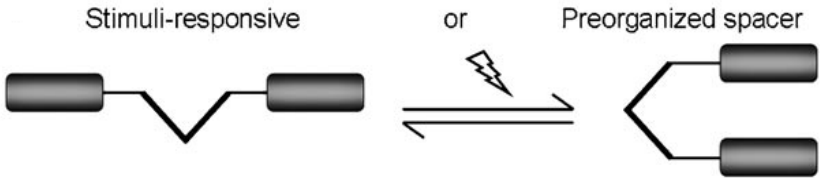

FIgure 1.16: Cartoon representation of stimuli-responsive and pre-organized spacers.[24]

For example, Petitjean *et al.* developed ion-controlled dynamic molecular tweezers, the conformational state of which is controlled by the amount of Cu(I) ions in solution.[27] At very low concentrations of Cu(I), the tweezer is in a "U" binding conformation, where it binds its aromatic guest (i.e. trinitrofluorenone) via donor/acceptor π-π interactions. Substrate release is induced by increasing concentrations of Cu(I) where the tweezer adopts a "W" (release) conformation due to the ion-dipole interactions that occur between the nitrogen lone pair electrons of the spacer group and the Cu(I) ion.

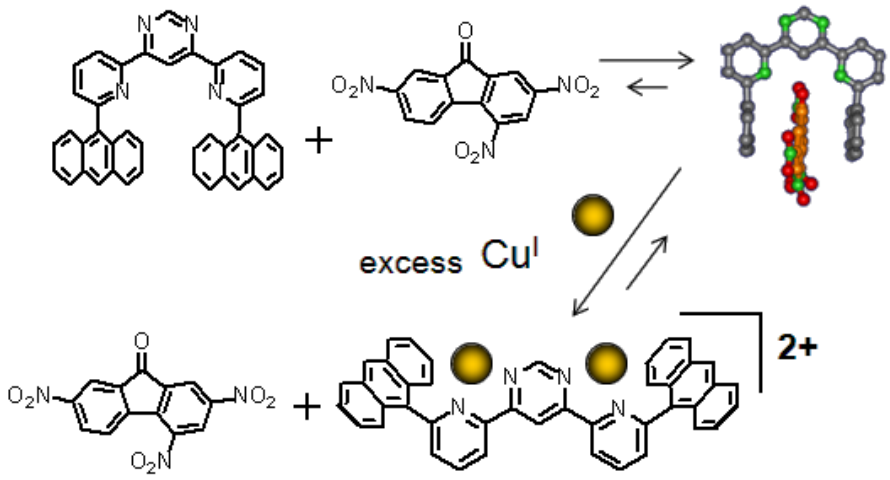

Figure 1.17: Mechanism of substrate binding and release of the ion-controlled molecular tweezer developed by Petitjean *et al.*[27]

1.2.4 pH Triggered Molecular Tweezer for Drug Delivery

Molecular tweezers are excellent receptors as they can be engineered to selectively bind guest molecules. For this reason, their current applications have been heavily focused in the field of molecular recognition and sensing[23] due to their synthetic versatility and ability to selectively bind guest molecules. Interestingly, their applications in the field of drug delivery have only been explored recently. We have successfully synthesized our first generation pH-triggered molecular tweezer that changes its conformation from a closed (binding) state into an open (release) state upon acidification.[28] It binds the anticancer drug, Mitoxantrone™ (MTX), non-covalently via π-π interactions with the naphthalene receptors.

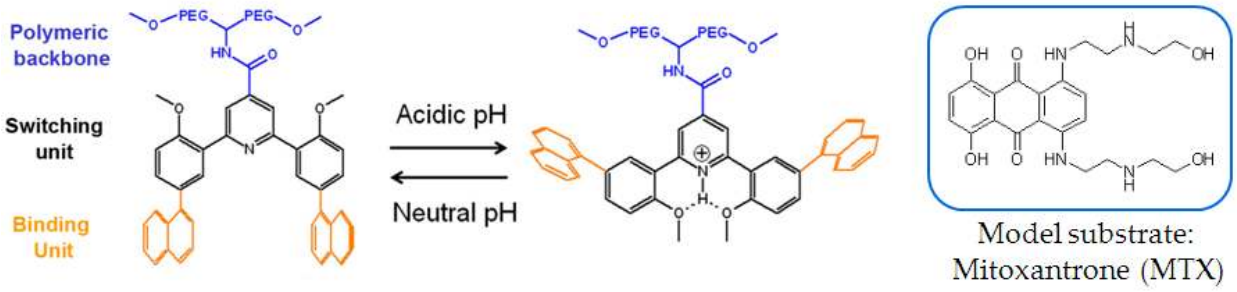

Figure 1.18: First generation molecular tweezer and its model substrate, MTX.[28]

1.3 Design of 2nd, 3rd and 4th Generation Molecular Tweezer

In this project, we aim to discover new pH-controlled, dynamic molecular tweezers for drug delivery applications. We have initially set our goal in improving our first generation tweezer, however, several difficulties encountered during the synthesis stage, led us to into investigating new designs. Just like our first generation tweezer, the new tweezers will bind aromatic guests, such as the breast cancer drug MTX. Guest binding is achieved through a combination of non-covalent interactions, mainly π-π interactions, hydrophobic effects, or possibly donor/acceptor interactions under physiological environments.

1.3.1 Target Structures

The new tweezers will follow the basic design of our first generation tweezer. It will use the same pH-responsive triad spacer (**S**) as our first generation tweezer, but will have different receptors (**IS**) for guest binding. By varying the type of **IS** used, we will then be able to assess the differences in binding affinities of MTX, and ultimately decipher the stoichiometries and strength of host to guest binding.

Overall, the new tweezers will be composed of three major components: 1) switching unit/ spacer (**S**), composed of methoxyphenyl-pyridine-methoxyphenyl triad that changes its conformation upon protonation of the lone pair nitrogen atom, 2) two binding units (**IS**), each composed of naphthalene, theophylline, and benzimidazole groups, and finally 3) solubilizing groups, made up of short oligoethylene glycol chains.

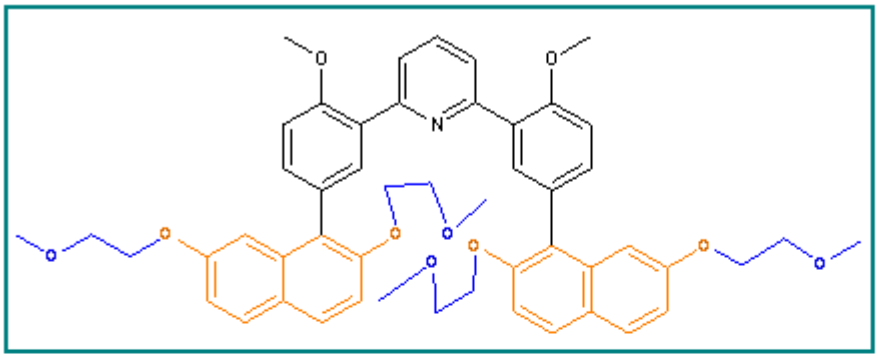

Target A

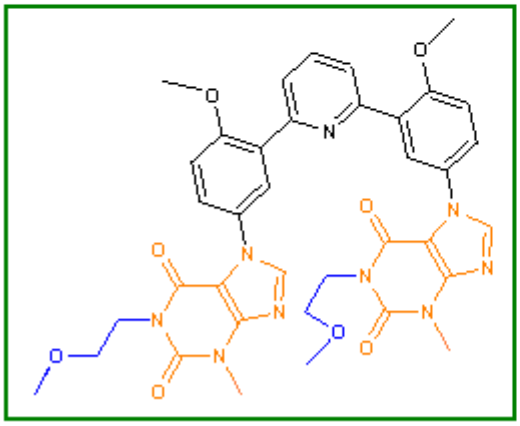

Target B

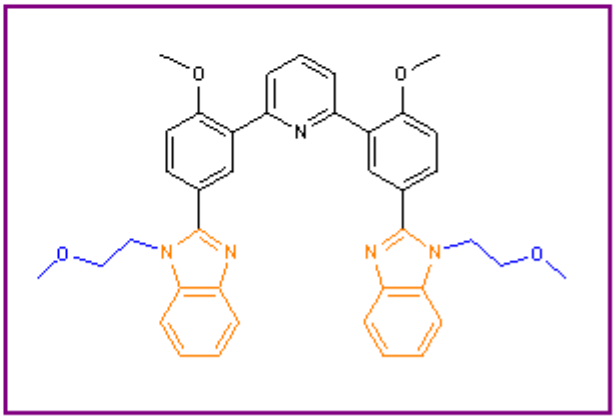

Target C

1.3.2 Retrosynthetic Analysis

The components for the new molecular tweezers can be achieved according to the following retrosynthetic analyses. All tweezers would be assembled via coupling of **S** with **IS**, either through Suzuki coupling or Cu(II) catalyzed coupling methods.

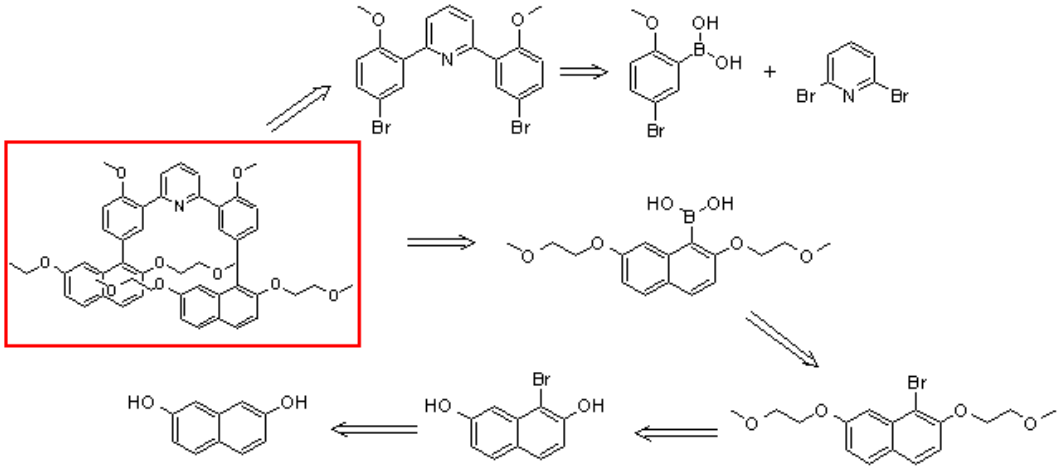

Scheme 1.1: Retrosynthesis route to Target A.

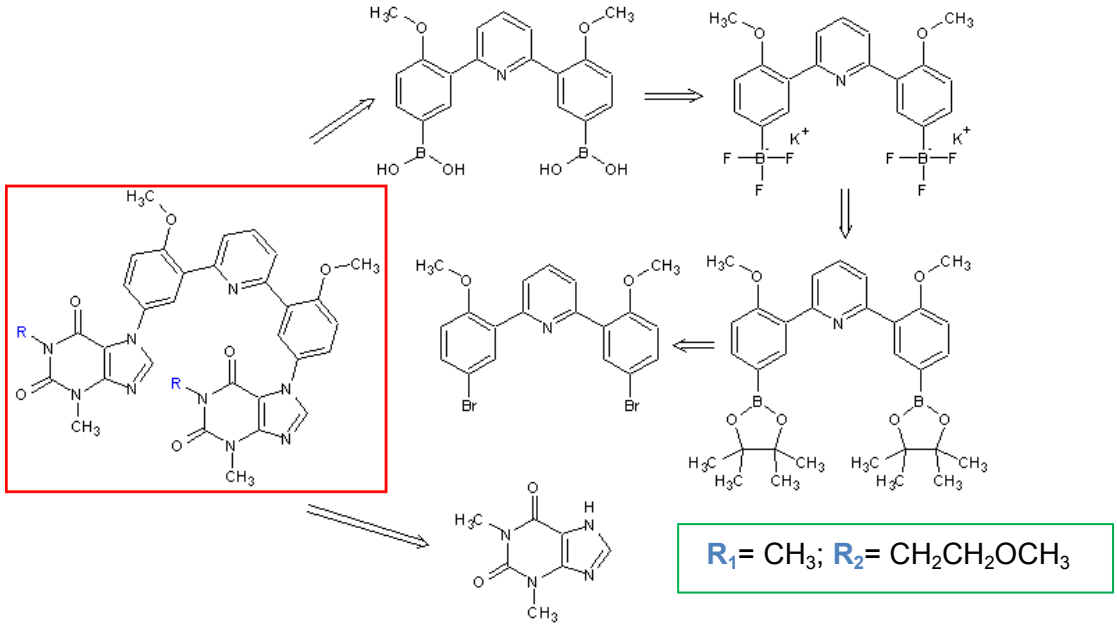

Scheme 1.2: Retrosynthesis route to Target B. (R_1 is the test reaction with theophylline as the IS, while R_2 represents the derivatized theophylline IS).

Alternatively, Target B may be synthesized via the following route. This route is designed to minimize the steric effects associated with the coupling of two theophylline IS with the triad S.

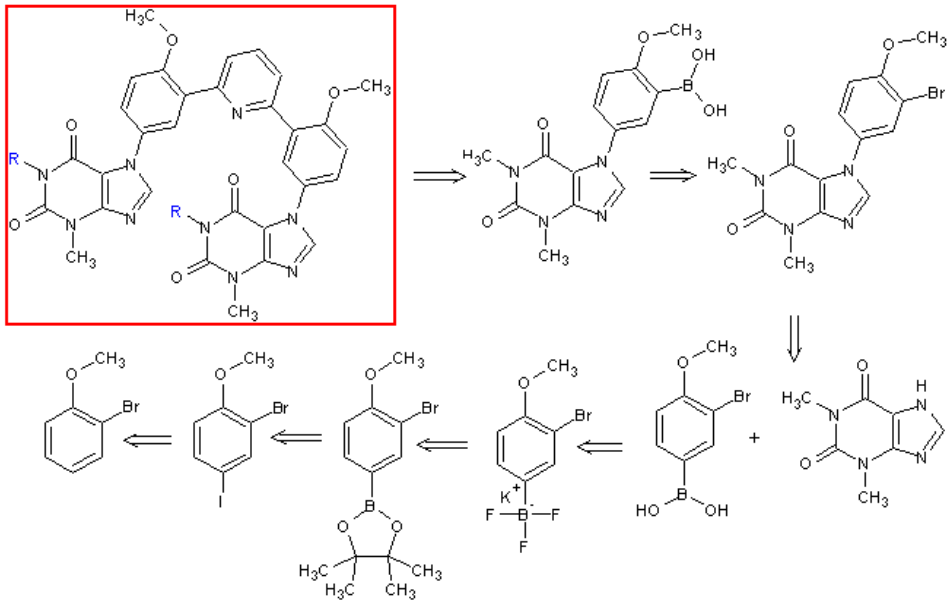

Scheme 1.3: Alternative retrosynthesis route to Target B.

And, to install the short oligoethylene chains on the theophylline IS, we may follow the following route.

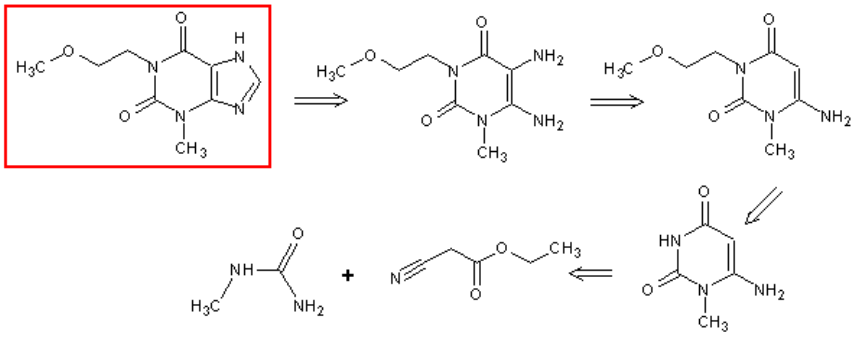

Scheme 1.4: Retrosynthesis route to alkylated theophylline IS.

One last target (Target C, Scheme 1.5) is finally considered in order to (i) remedy the difficulty to install a boronic acid on the anisol unit (see further chapters) and (ii) to investigate a

coupling to the IS units which would not involve transition metal catalysis (organic condensation).

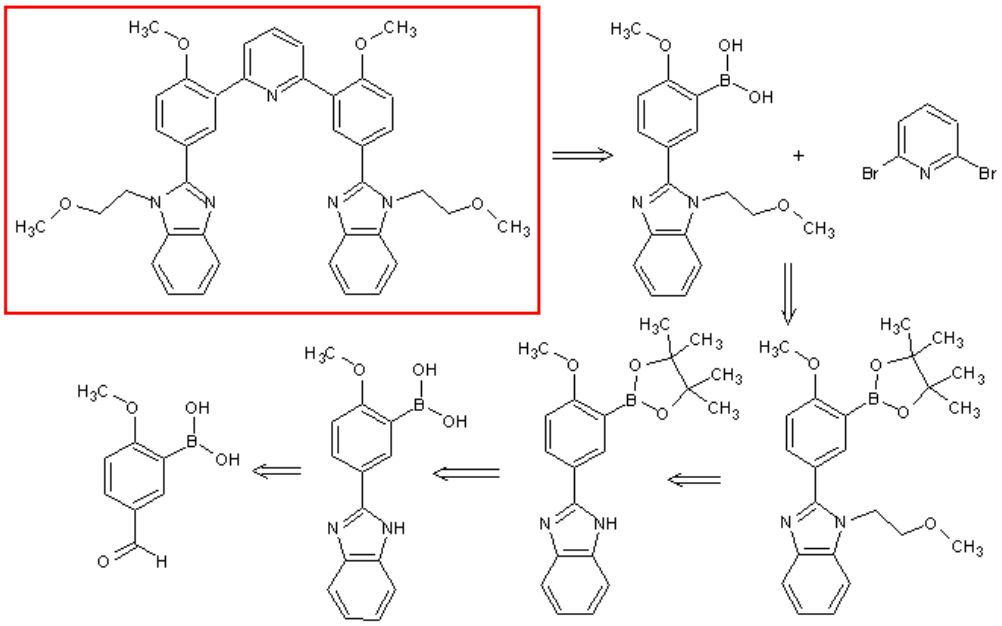

Scheme 1.5: Retrosynthesis route to Target C.

1.3.3 Goals of Thesis

Chapter 2: Synthesis of 2nd Generation Molecular Tweezer

2.1: Introduce the development of our 1st generation tweezer

2.2: Discuss how to improve the 1st generation tweezer via synthesis of the 2nd Generation Tweezer

2.3: Conclusion

Chapter 3: Synthesis of 3rd Generation Molecular Tweezer

3.1: Insights on the caffeine derived IS: Discussion of the ideas that led to the creation of our 3rd generation tweezer.

3.2: Discussion of the synthetic routes and challenges of the 3rd Generation Tweezer

3.3: Conclusion

Chapter 4: Synthesis of 4th Generation Molecular Tweezer

4.1: Insights on the Benzimidazole-derived IS: Simplifying the synthesis of the tweezer via using commercially available reagents and avoiding metal-catalyzed coupling reactions.

4.2: Discussion of the synthetic routes and challenges in the creation of the 4th generation tweezer.

4.3: Conclusion

Chapter 5: Experimental Section

Chapter 6: Conclusion

Appendix

References:

1. Wang, B.; Siahaan, T.; Soltero, R.; *Drug Delivery: principles and applications.* J. Wiley & Sons Inc.: New Jersey, 2005; pp. 1-5
2. Bonate, P.; Howard, D.; *Pharmacokinetics in Drug Development: Regulatory and Development paradigms.* AAPS Press; USA, 2004; pp. 3-23
3. Prentis, R. A.; Lis, Y.; Walker, S. R.; *Br. J. Clin. Pharmac.* **1988**, 25, 387-396
4. Burton, M. E.; Shaw, L. M.; Schentag, J. J.; Evans, W. E.; *Applied pharmacokinetics & pharmacodynamics: principles of therapeutic drug monitoring.* Lippincott Williams & Wilkins: Maryland, 2006; pp. 3-4
5. Mannhold, R.; Kubinyi, H.; Folkers, G.; *Drug Bioavailability: Estimation of Solubility, Permeability, Absorption and Bioavailability.* 2nd Ed.; Wiley- VCH: Weinheim, 2009; Vol. 40, pp. 1-5
6. Vogelson, C. T.; *Nanotechnology.* **2001**, 4, 49-50

7. Petros, R. A.; DeSimone, J. M.; *Nat. Rev. Drug Discovery.* **2010**, 9, 615-627
8. Düzgüneş, N.; *Methods in Enzymology: Liposomes.* Elsevier: California, 2005, pp. 8-12
9. Marcucci, F.; Lefoulon, F.; *Drug Discovery Today.* **2004**, 219-228
10. De Villiers, M. M.; Aramwit, P.; Kwon, G. S.; *Nanotechnology in Drug Delivery*. Springer: New York, 2009; pp. 600-603
11. Kratz, F.; Muller, I. A.; Ryppa, C.; Warnecke, A.; *Chem. Med. Chem.* **2008**, 3, 20-53
12. Brannon-Peppas, L.; Blanchette, J. O.; *Adv. Drug Delivery Rev.* **2004**, 56, 1649-1659
13. Xia, W.; Low, P. S.; *J. Med. Chem.* **2010**, 53, 6811-6824
14. Low, P. S.; Kularatne, S. A.; *Curr. Opin. Chem. Biol.* **2009**, 13, 256-262
15. Matsumura, Y.; Maeda, H.; *Cancer Res.* **1986**, 46, 6387-6392
16. Brown, J. M.; *Molecular Medicine Today.* **2000**, 6, 157-162
17. Yoon, H. J.; Jang, W. D.; *J. Mater. Chem.* **2010**, 20, 211-222
18. Kaasgaard, T.; Andresen, T. L.; *Expert Opin. Drug Deliv.* **2010**, 7, 225-243
19. Du, J. Z.; Sun, T. M.; Song, W. J.; Wu, J.; Wang, J.; *Angew. Chem. Int. Ed.* **2010**, 122, 3703 –3708
20. Lee, E. S.; Gao, Z.; Bae, Y. H.; *J. Controlled Release.* **2008**, 132, 164-170
21. Harguindey, S; Arranz, J. L.; Wahl, M. L.; Orive, G., Reshkin, S.; *Anticancer Res.* **2009**, 29, 2127-2136
22. Paramonov, S.; Bachelder, E. M.; Baudette, T. T.; Standley, S. M.; Lee, C. C.; Dashe, J.; Fréchet, J. M. J.; *Bioconjugate Chem.* **2008**, 19, 911–919
23. Steed, J. W.; Atwood, J. L.; *Supramolecular Chemistry.* John Wiley & Sons Ltd.: Wiltshire, 2009; pp. 336-340
24. Leblond, J.; Petitjean, A.; *Chem. Phys. Chem.* **2011**, 12, 1043-1051
25. Sygula, A.; Fronczek, F. R.; Sygula, R.; Rabideau, P. W.; Olmstead, M. M.; *J. Am. Chem. Soc*. **2007**, 129, 3842-3843
26. Harmata, M.; *Acc. Chem. Res.* **2004**, 37, 862–873

27. Petitjean, A.; Lehn, J. M.; Khoury, R.G.; Kyritsakas, N.; *J. Am. Chem. Soc*. **2004**, 126, 6637-6647
28. Leblond, J.; Gao, H.; Petitjean, A.; Leroux, J.-C. *J. Am. Chem. Soc*. **2010**, 132, 8544-8545
29. Image retrieved from https://sitn.hms.harvard.edu/sitnflash_wp/2011/06/materials-for-drug-delivery/ on August 2011

Chapter 2

Synthesis of 2nd Generation Molecular Tweezer

2.1 Introduction: 1st generation tweezer

The first generation tweezer mentioned herein refers to the pH-responsive molecular tweezer synthesized by Leblond *et al.* in 2010.[1] The tweezer was designed for DDS applications in cancer therapy, using two naphthalene groups as the **IS** that will specifically interact with the anticancer drug substrate, MTX. The design of the **S** (a.k.a. triad) group is unique as it is capable of switching its conformation from a closed "U" binding state to an open "W" release state at low pH.

2.1.1 Components of the 1st Generation Tweezer

The first generation tweezer is composed of three major elements: 1) the pH active **S** composed of methoxyphenyl-pyridine-methoxyphenyl triad 2) two naphthalene **IS** and finally 3) polymeric backbone composed of polyethylene glycol (PEG) chains.

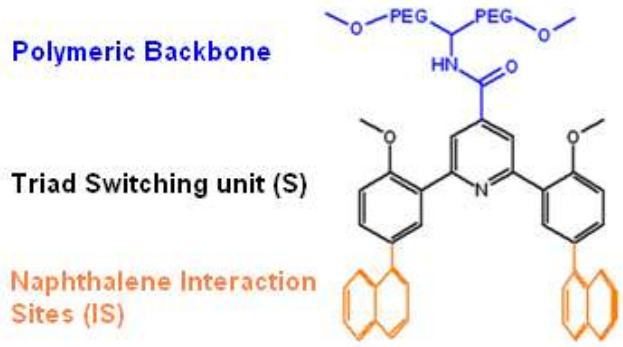

Figure 2.1: Structure of the first generation tweezer illustrating its basic components.[1]

2.1.1.1: The pH- Active Triad (S)

To assess the pH responsiveness of the triad **S**, the following model compound was first synthesized via Kumada-Corriu-Tamao coupling.

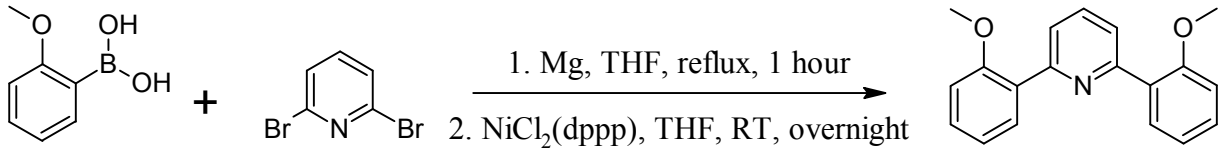

Yield: 28- 70 %

Scheme 2.1: Reaction scheme of the model triad, 2,6-bis-(2'-methoxyphenyl)-pyridine (***ortho*-Py**).[1]

***ortho*-Py** changes its conformation upon protonation of the central nitrogen atom, as confirmed by NOESY experiments in 1:1 $CDCl_3/CD_3OD$.[1]

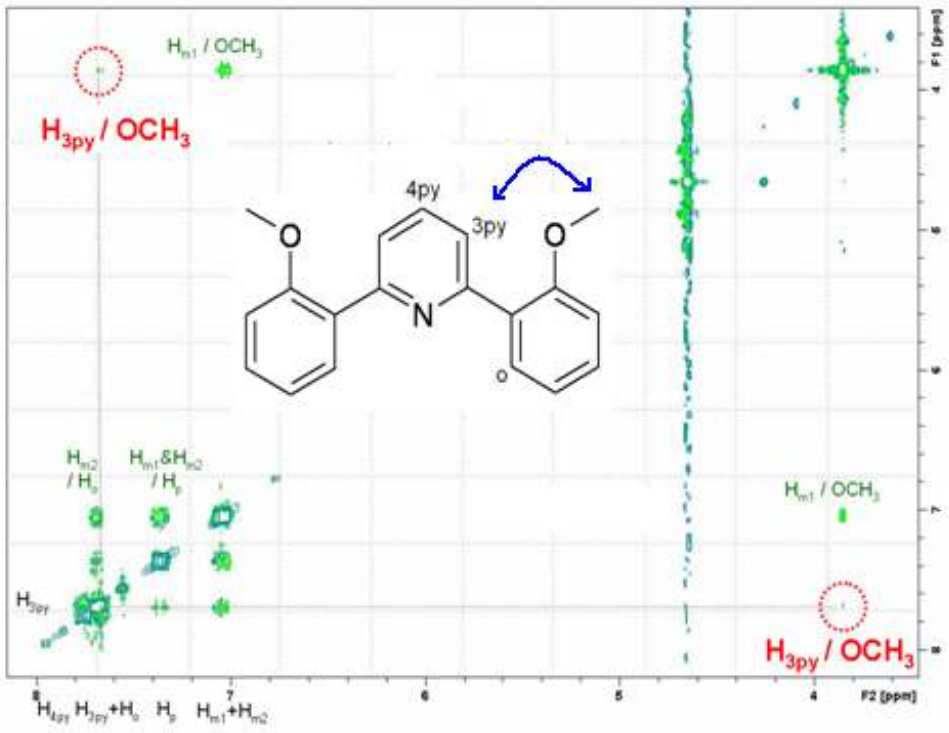

(a)

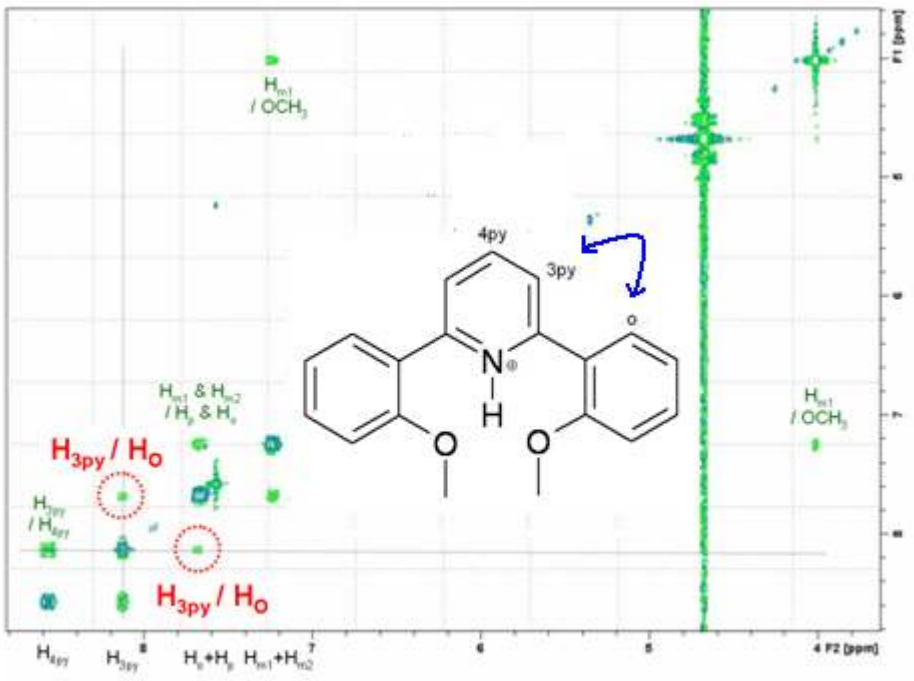

Figure 2.2: 400 MHz NOESY spectra of (a) the neutral (before H^+ addition, using trifluoroacetic acid (TFA) as titrant) and (b) the protonated (after H^+ addition) *ortho*-Py triads in 1:1 $CDCl_3/CD_3OD$.[1]

At high pH, ***ortho*-Py** exists as the conformation shown in Figure 2.2a due to the weak C-H---O hydrogen bonds that occur between the lone pair oxygen atoms of the phenyl substituent and the pyridine hydrogen atoms. Rotation is hindered between the C-C bonds that connect the phenyl rings to the central pyridine molecule, as the hydrogen bonded structure completes a stable 6-membered ring. When the pH is lowered, the central nitrogen atom is protonated, which also becomes a new source of hydrogen bonds. The N-H---O hydrogen bonds (12-16 kJ/mol) are a lot stronger than the C-H---O hydrogen bonds from the pyridine centre (<12 kJ/mol),[2] which makes it the main driving force of the conformational change of the model triad.

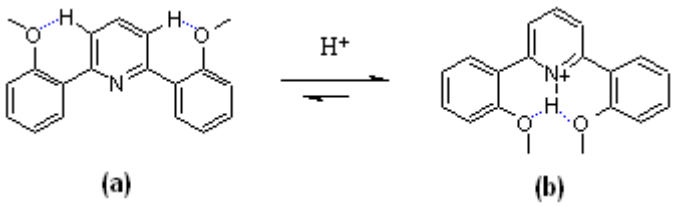

Figure 2.3: pH-triggered model **S** (H-bonds: blue dotted lines).[1]

Confirmation of the conformational changes that occurred with the ***ortho*-Py** at neutral and acidic pH prompted the synthesis of the actual triad **S**. The compound was synthesized via Suzuki-Miyaura coupling of the commercially available 5-bromo-2-methoxyphenyl boronic acid with 2,6-dibromopyridine, which gave a yield of 60 % after recrystallization in ethanol.

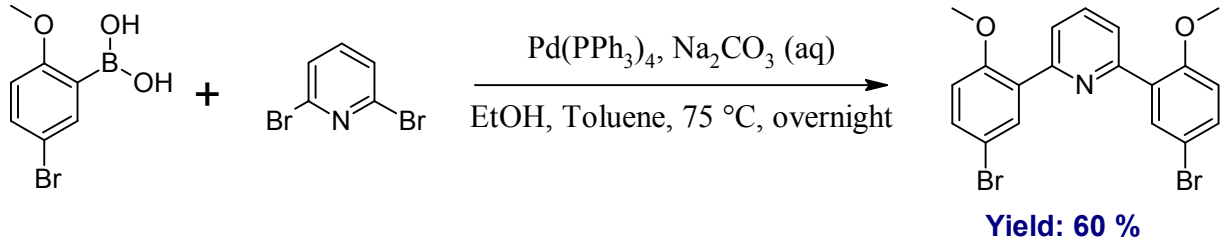

Scheme 2.2: Reaction scheme of the triad **S**.[1]

2.1.1.2: Naphthalene IS

Naphthalene was chosen as the **IS** due to its propensity to favour hydrophobic interactions and lower toxicity when compared to other polyaromatic hydrocarbons such as pyrene or anthracene.[3] The naphthalene-derived binding units may bind aromatic guests via π-π stacking, donor-acceptor interactions, and hydrophobic effects. However, X-ray studies of the first generation tweezer show that, in the solid state, the naphthalene rings are not held parallel to each other due to the edge-to-face interaction that occurs between them. The twisted orientation of the binding units makes characterization of the binding location a lot more difficult. We still do not know where the guest molecule binds in the first generation tweezer. If the

naphthalene rings are held parallel, however, the guest molecule would most likely be bound in between the two naphthalene rings.[4]

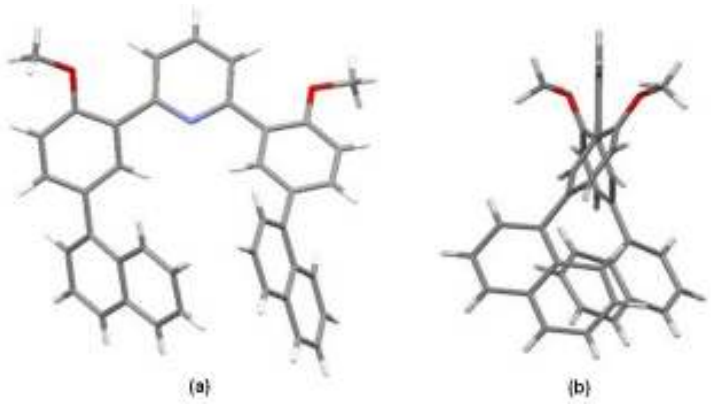

Figure 2.4: Crystal structure of Leblond *et al.*'s "naked" (without PEG) molecular tweezer**.** a) front and b) side views.[1]

To determine whether the conformational changes of the triad is maintained in the presence of naphthalene **IS,** ^{1}H NMR titration of the "naked" tweezer (without the PEG backbone, ***ortho*-PyNaph**) with varying concentrations of TFA was conducted.

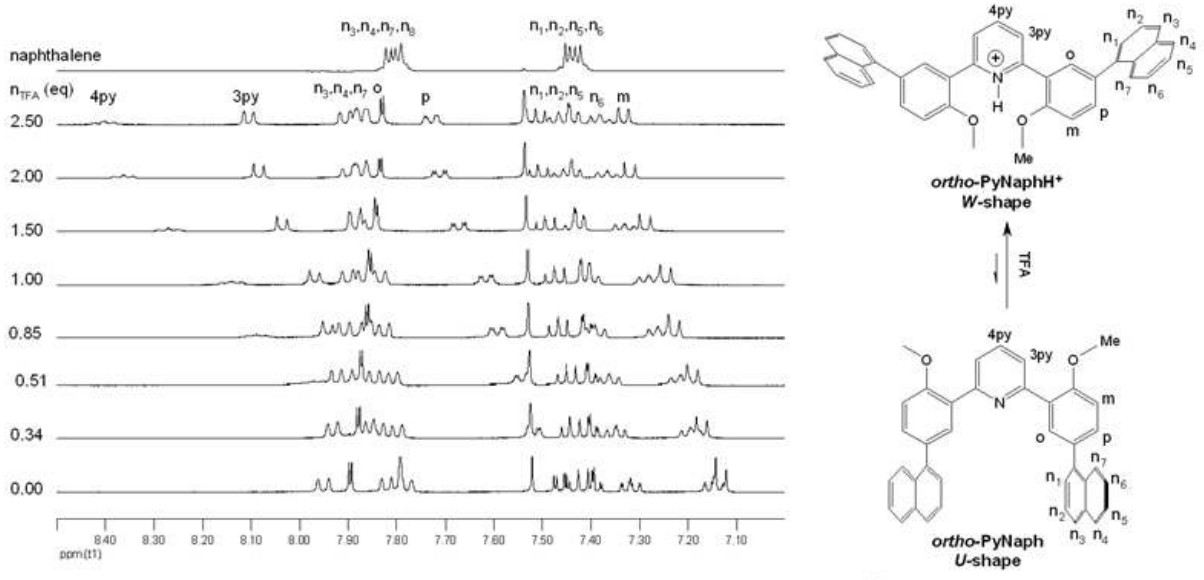

Figure 2.5: 400 MHz ^{1}H NMR spectra of ***ortho*-PyNaph** (5.9 μM) upon addition of TFA in 1:1 $CDCl_3$ / CD_3OD.[1]

The titration data in Figure 2.5 show that the switching property of the triad was maintained in the presence of the naphthalene **IS**. At 0 equiv. of TFA, the naphthalene protons were spread out in the aromatic region of the spectrum and were significantly lower than the chemical shifts of the free naphthalene. This is because at neutral state, the naphthalene groups face each other, thus causing mutual shielding of the aromatic protons.[1] In contrast, as TFA concentration is increased, the naphthalene protons become de-shielded and eventually, they merge into two clusters, resembling the spectrum of the free naphthalene. This is consistent with the observation that at low pH, the tweezer exists in an open, "W" state, where the naphthalene groups no longer feel the shielding effects of its counterpart.[1]

2.1.1.3: PEG Polymeric Backbone

To make the tweezer water soluble, and hence much more suited for drug delivery applications, it was derivatized with PEG at the fourth carbon position (4Py) of the central pyridine ring (Figure 2.1). PEG functionalization was achieved via following peptide coupling reaction.[1]

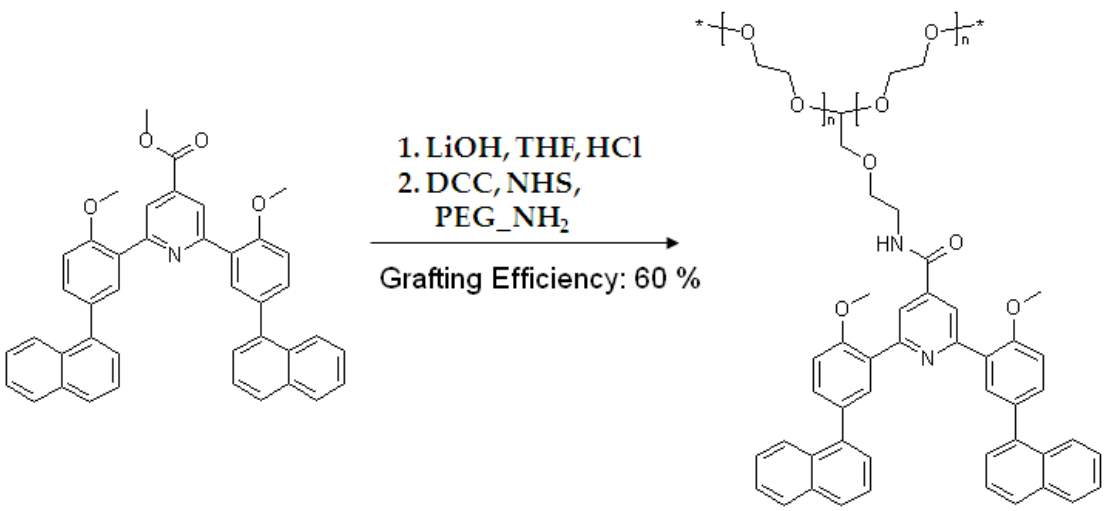

Scheme 2.3: Reaction scheme of the PEG tweezer.[1]

PEG was chosen due to its high biocompatibility and water solubility.[5] Furthermore, the high molecular weight of PEG will allow the targeting of tumour cells via EPR effect.[6] Lastly, the branched structure of PEG is hypothesized to prevent the partial degradation of the attached tweezer by shielding it from enzymatic attack as it enters the body, much like an umbrella.

2.1.2 Binding with MTX

Drug binding and release properties of both the ***ortho*-PyNaph** and the PEG tweezer were investigated using the anticancer drug, MTX, as the substrate. MTX binds to the naphthalene **IS** via aromatic stacking, donor/acceptor, and hydrophobic interactions.[1] Substrate binding was monitored via observing the fluorescence of the tweezers at pH = 4 and pH = 8, with varying concentrations of MTX.[1]

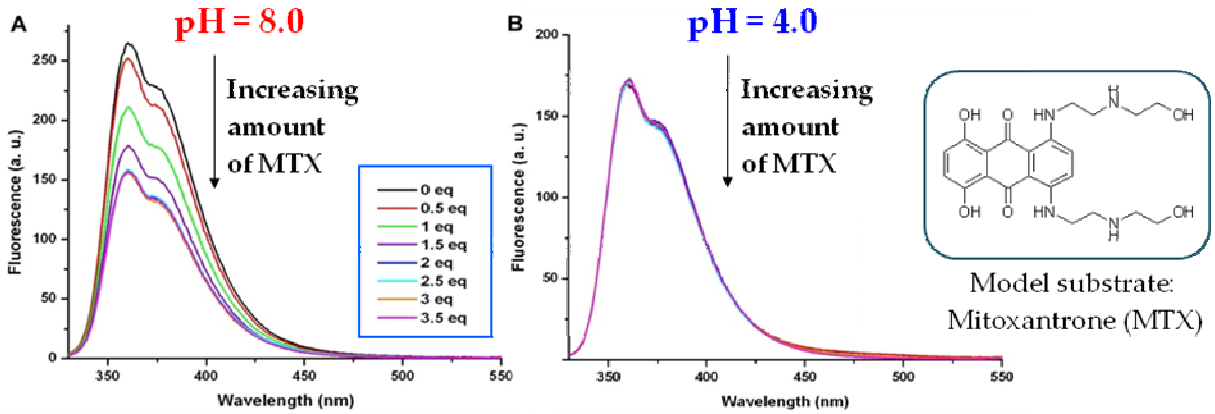

Figure 2.6: Fluorescence of the naphthalene binding units of ***ortho*-PyNaph** (1.8 μM buffer with 1% THF) with MTX (0-6.3 μM).[1]

The fluorescence data show that binding occurs at pH = 8. The decreasing fluorescence signals of the naphthalene **IS** at increasing concentrations of MTX suggests MTX-induced

quenching.[1] In contrast, no quenching was observed at pH = 4, which means that the MTX does not interact with the naphthalene at low pH.

The fluorescence experiment was also conducted with the PEG tweezer, with the results summarized by the following figure.

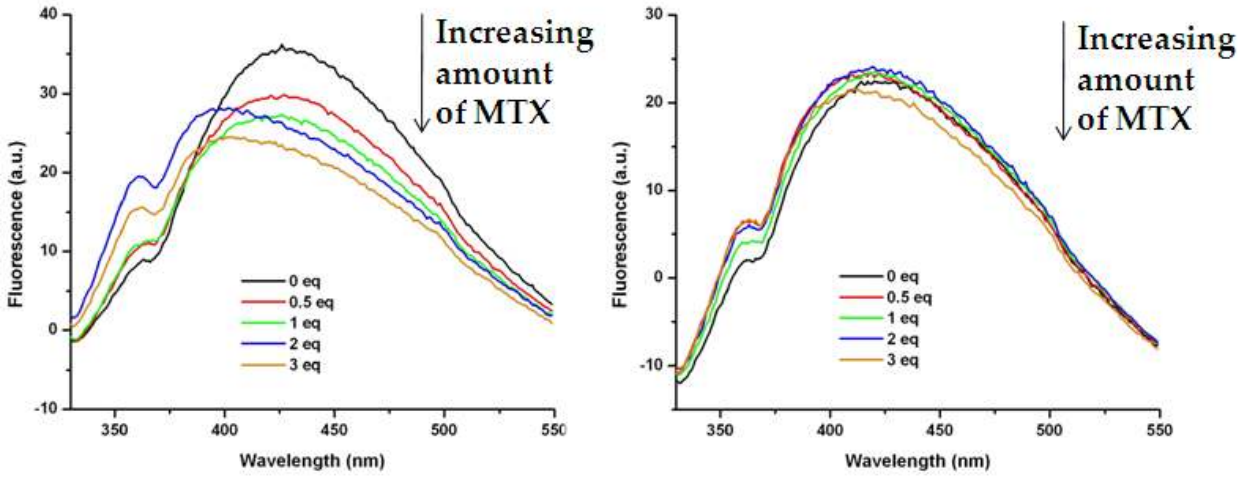

(a) **(b)**

Figure 2.7: Fluorescence of the PEG Tweezer (5 μM in buffer) at a) pH = 7.4 and b) pH = 4 upon addition of MTX (0-3 equivalents).[1]

The fluorescence data is consistent with the results of the ***ortho*-PyNaph** tweezer, but significant broadening of the spectra is now evident. This is suggestive of excimer formation, suggesting the partial aggregation of the naphthalene units in the buffer solution in the absence of THF.

2.1.3 Improving the 1st Generation Tweezer

Our 1st generation tweezer showed great potential for use as a DDS, however, several limitations have yet to be overcome. First, the twisting of the **IS**, which may have resulted in discrepancies with the stoichiometry of tweezer:MTX binding. Second, due to the poor water

solubility of the naked tweezer, we are only able to estimate its pKa in aqueous solution based on experiments in organic solvents. Lastly, the binding constants are still missing from our initial data. We have therefore designed our 2nd generation tweezer in order to address the aforementioned limitations. This new tweezer design is focused mainly in correcting the twisted orientations of the **IS.**

2.2: Synthesis of the 2nd Generation Tweezer

Synthesis of the 2nd generation tweezer proved to be a very challenging task. As can be seen from Scheme 1.1, the tweezer is assembled in three parts, namely 1) synthesis of the spacer (**S**), 2) synthesis of the binding units (**IS**) and finally, 3) coupling of **S** to **IS**.

2.2.1: Investigating New pH Active Spacer Groups

Initially, we have investigated two compounds for their potential use as a switching unit component. The first **S** was *N,N'*-bis(4-methylphenyl)pyridine-2,6-dicarboxyamide (Triad 1), which was synthesized via condensation reaction of the commercially available *p*-toluidine with dipicolinic acyl chloride.

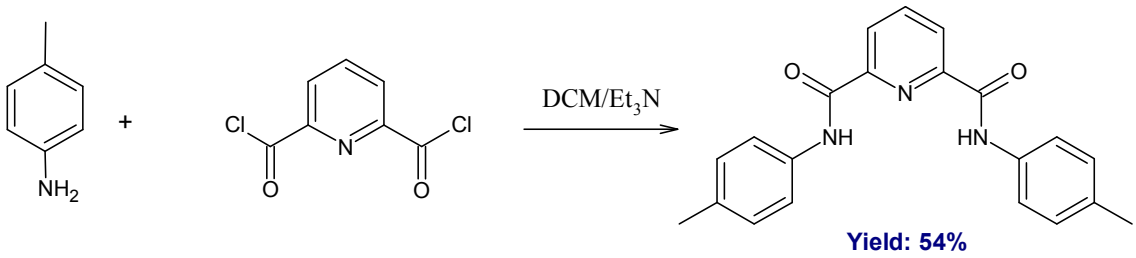

Scheme 2.4: Synthesis of *N,N'*-bis(4-methylphenyl)pyridine-2,6-dicarboxyamide.[7]

The reaction proceeded with a moderate yield of 54 %. However, when the switching behaviour was investigated via ^{1}H NMR upon titration with TFA in 1:1 $CDCl_3$/ MeOD, no signs of

conformational changes was observed. The chemical shifts of the protons at 1.5 equivalents of TFA remained almost identical to those with 0 equivalent of TFA.

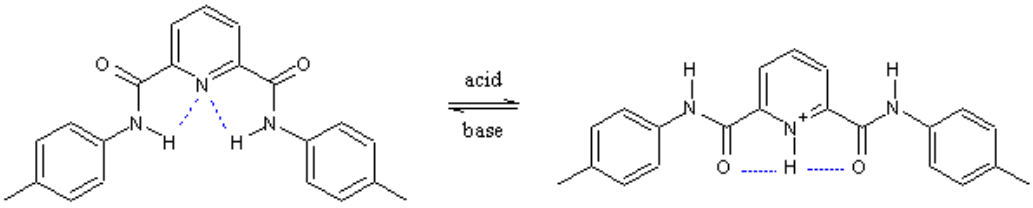

Scheme 2.5: Desired conformational changes of Triad 1 in response to acidic/ basic pH.

To understand why the conformational switching did not occur, we examined the pKa values of the central pyridine ring. Pyridine is a weak Brønsted base with a pKa of ~ 5.2.[8] The basicity of the nitrogen lone pairs is influenced by the functional groups attached to the pyridine ring. Electron donating groups generally enhance the basicity of the nitrogen atom, whereas electron withdrawing groups decreases its basicity. The central pyridine in the triad is attached to two amide groups, which are both electron-withdrawing. Therefore, the pKa of the nitrogen atom is dramatically decreased, which is estimated to be < 2 by Kurosaki and co-workers.[9] Also, the hydrogen bonds that occur between the two N-H groups and the central nitrogen forms a stable 5-membered ring structure. Conformational switching from acidification would result in the disruption of these stable structures, and thus, protonation of the central nitrogen atom is highly disfavoured.

To avoid complications from Triad 1, we have carefully designed our next model compound so that its pKa would fall within our desired range (5-6). The triad would have consisted of two uracil molecules that are attached to the central pyridine molecule in the 2,6 position, as shown below.

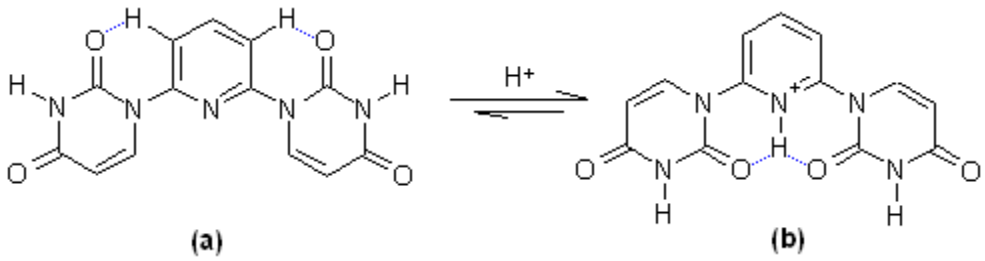

Scheme 2.6: pH-triggered uracil switching triad (Triad 2).

We have estimated the pKa of this triad to be around 5.8 via comparison with similar compounds in literature.[1,10] At high or neutral pH, the triad would exist in the conformation seen in scheme 2.5a due to the weak hydrogen bonding that occurs between the lone pair oxygen atoms of the uracil substituents and the C---H bonds of the pyridine ring. As the pH is lowered, the central nitrogen atom will be protonated and this would create a stronger O---H-N hydrogen bonds, resulting in a conformational change. The reaction should have proceeded via S_NAr mechanism. The 2-chloro-4-nitropyridine-*N*-oxide acts as an electrophile that could attack the NH groups in the uracil. However, electrophilic attack was anticipated at the NH group that is *para* to one of the carbonyl groups because the other one is more sterically hindered. In the presence of a base, such as Cs_2CO_3 used in this reaction, the nitrogen loses a proton, thus enhancing its nucleophilicity. However, the presence of the neighbouring carbonyl groups counteracts this increase in the nucleophilicity because they withdraw electrons from the nitrogen through resonance. This makes the uracil a poor nucleophile; hence, it is not surprising that the synthesis failed.

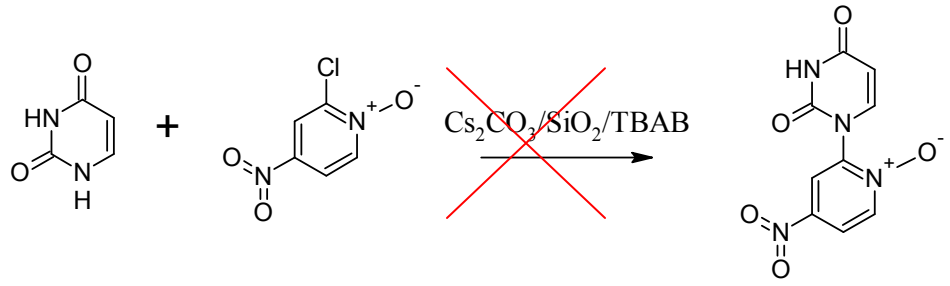

Scheme 2.7: Synthesis of 1-(4-nitro-1-oxidopyridin-2-yl)dihydropyrimidine-2,4(1*H*,3*H*)-dione.[11]

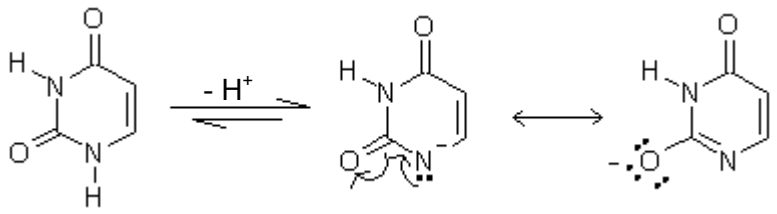

Scheme 2.8: Electron withdrawal from the nitrogen through resonance.

2.2.2: Synthesis of UNIT 1 and UNIT 2 PEG IS

To correct the twisting of the naphthalene **IS** from our 1st generation tweezer, we attempted to replace it with 2,7-dihydroxynaphthalene in order to attach short oligoethylene glycol chains on its 2,7 position. The steric bulk of the ether chains would prevent the edge-to-face interaction that arise from the naphthalene **IS**, hence, creating a more parallel orientation of the **IS**. Furthermore, the ether chains would help improve the water solubility of the naked tweezer, allowing us to determine the binding constants and pKa values in aqueous media via NMR studies. The length of the ether chains may also be varied, in order to fine-tune the water solubility of the tweezer. UNIT 1 PEG will be attached to two 2-methoxyethanol chains, while UNIT 1 PEG will instead be attached to two 2-(2-methoxyethoxy)ethanol chains. The synthetic route planned for both UNIT 1 and 2 PEG is summarized by the following two-step procedure.

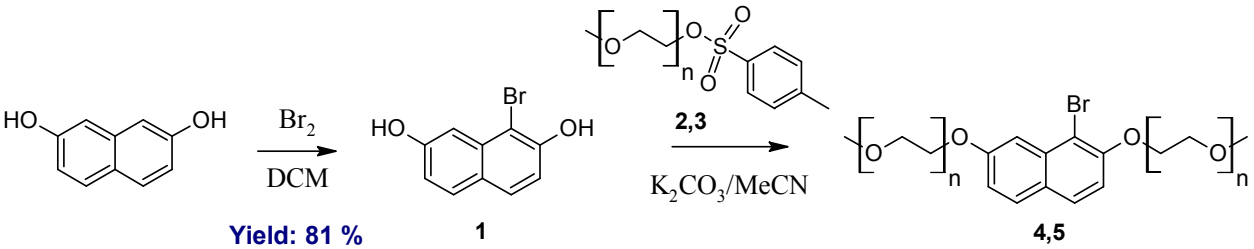

Scheme 2.9: Synthetic route to UNIT 1 (n= 1, compound 4) and UNIT 2 (n= 2, compound 5) PEG.

The commercially available 2,7-dihydroxynaphthalene was first brominated using the procedure developed by R. D. Wilson.[12] The bromination was allowed to take place in the dark, as the starting compound was observed to photo-oxidize (grey crystals become purple upon prolonged exposure to light and air) especially when left in solution for more than a day. The bromination reaction proceeded in 81 % yield. The crude product was pure, as represented by the clean ^{1}H NMR spectrum; hence no further purifications were performed.

The next step was to introduce the oligoethylene chains using the procedure developed by Badjic *et al.*[13] This step occurs via S_N2 reaction mechanism, using the deprotonated bromonaphthalene diol as the nucleophile. The reaction proceeded readily, although purification of the crude was tricky, especially for UNIT 2 PEG. The contaminants in the crude were always the unreacted starting tosylate and the TsO^- anion, although they can be removed by recrystallization in ethanol in the case of UNIT 1 PEG. In contrast, purification of UNIT 2 PEG was very challenging because the compound was an oil, hence re-crystallization was not an option. We have also tried chromatography to purify the product, but were unsuccessful because the compound streaked on either silica or alumina. The best separation was achieved on pretreated TLC plates using as an eluent 1 % methanol in dichloromethane and 2 drops of triethylamine. However, the Rf values were very close and would require preparative HPLC to successfully obtain a pure sample.

As our last resort, we have used the protocol developed by Heathcote *et al.* as a "sacrificial" method to destroy the remaining tosylate.[14] After treating the oil with 40 % methylamine in water, it became possible to remove the tosylate, which had reacted with the amine, through extraction. An attempt to monitor this reaction by TLC produced no observable changes between 2 hours to 4 days, suggesting that the reaction had gone as close to completion as possible during the first 2 hours. The NMR spectrum of the oil isolated from the organic layer only shows trace amounts of TsO^- impurities, suggesting that the purification

method was a success. The purification process gave a yield of 0.836 g (84 %) of the desired product.

2.2.3: Challenges in the UNIT 1 PEG boronic acid synthesis

Conversion of UNIT 1 PEG to its corresponding boronic acid/ ester is the most challenging part of the synthesis. In this reaction, we have chosen UNIT 1 PEG as our test compound for ease of analyzing the ^{1}H NMR spectrum. Various methods were attempted to generate the desired boronic acid, however, all of them were unsuccessful. We initially started the halogen-lithium exchange reaction with n-BuLi as our lithium source and triisopropylborate, then replaced it with a less bulky, trimethylborate, as our boron source. As for solvents, we initially chose anhydrous diethyl ether but due to solubility problems of our starting material, we have replaced it with anhydrous tetrahydrofuran. The choice of solvents and boron source had very little effect on the reaction, since none of them have produced our desired boronic acid (see below for analysis of the reaction).

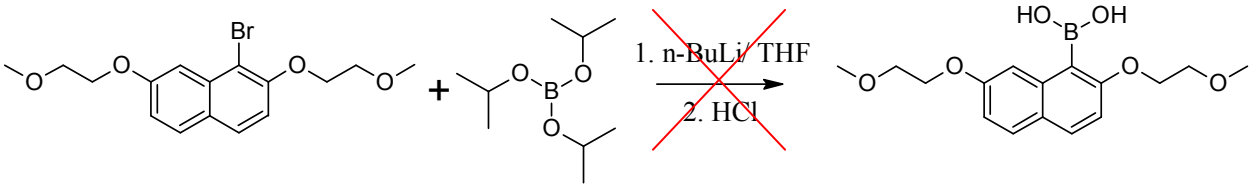

Scheme 2.10: Attempted Halogen-lithium exchange reaction.[15]

The Grignard method was also used to generate our boronic acid. Through careful analysis of the ^{1}H NMR spectrum of the crude products for both types of reactions, we saw that debrominated starting material, 2,7-bis(2-methoxyethoxy)naphthalene was the major product. This was marked by the disappearance of the H8 signal and the formation of new peaks around 6.98-7.05 ppm. Although there were minor peaks present that may correspond to our boronic

acid, we could not find any conditions for which to isolate and characterize it. Thus, we proceeded to investigate other methods.

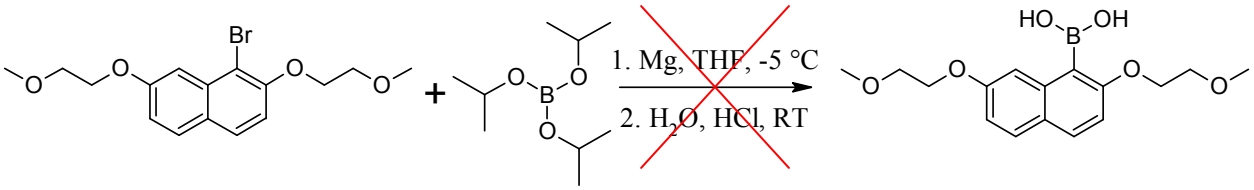

Scheme 2.11: Attempted Grignard reaction.[16]

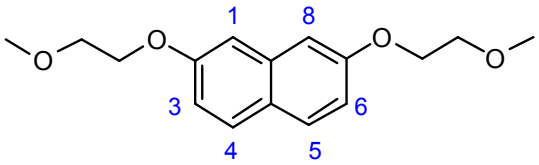

Figure 2.8: 2,7-bis(2-methoxyethoxy)naphthalene, debrominated product.

We have deduced two possible reasons for the formation of the major product; 1) failure of the lithiated species (or Grignard reagent) to interact with the boron source due to steric hindrance and 2) instability of the carbon-boron bond, which is common for this type of reaction. The small oligoethylene glycol chains introduce a lot of steric hindrance to our molecule by blocking the site of attack from incoming electrophiles. Furthermore, lithiation of the molecule introduces a new source for non-covalent interactions. It is highly possible that the lithium is interacting with the oxygen lone pair electrons through ion-dipole interactions since lithium is a hard acid and oxygen is a hard base. Because it is very difficult for the two substituents to interact, the binding units stay lithiated until it is later protonated by the addition of 1 M HCl. Indeed, the protonated product would generate the 2,7-bis(2-methoxyethoxy)naphthalene, as observed.

To test whether the C-B bond is forming, we have taken an aliquot of the sample prior to the HCl quenching step. The ^{1}H NMR should show peaks corresponding to the triisopropyl group that is still attached to the boron, but we did not see such peaks. Synthesis of the

corresponding pinacol boronic ester would also test this hypothesis. The methyl groups from the pinacol ester should be visible by ^{1}H NMR if the C-B bond has successfully formed.

2.2.4: Challenges in the UNIT 1 PEG pinacolboronic ester synthesis

Due to the lack of success in the direct synthesis of UNIT 1 PEG boronic acid, we then attempted to synthesize it indirectly via palladium-catalyzed cross-coupling reaction with pinacolborane and bis(pinacolato)diboron.[18,20] Once the desired pinacol boronic ester is made, it will then be hydrolyzed into its corresponding boronic acid via mild deprotection methods.[17]

Our first attempt on the synthesis of the pinacol boronic ester followed the protocol developed by Murata *et al.* in 2000, which uses pinacolborane as the boron source.[18] We have ideally chosen this method over the much popular palladium catalyzed cross-coupling reaction developed by Ishiyama *et al.* because pinacolborane was thought to introduce less steric problems to our molecule than the bulkier bis(pinacolato)diboron.[18] Sterics play a big role for the success of this reaction. The palladium-catalyzed coupling reaction mechanism proceeds in 3 steps: 1) oxidative addition, 2) transmetallation, and 3) reductive elimination.[19,21] Both oxidative addition and transmetallation steps require the attachment of the boron source and the alkyl halide. If both reagents are bulky, access to the palladium metal would be very difficult, so the reaction would either be very slow or not proceed at all. The size of the catalyst also influences whether the reaction would take place or not. When we carried out the reaction using the $PdCl_2$(dppf) catalyst, we saw via ^{1}H NMR analysis some formation of new peaks in the aromatic region. However, when we used the bulkier $PdCl_2(PPh_3)_2$, no such observations were made.

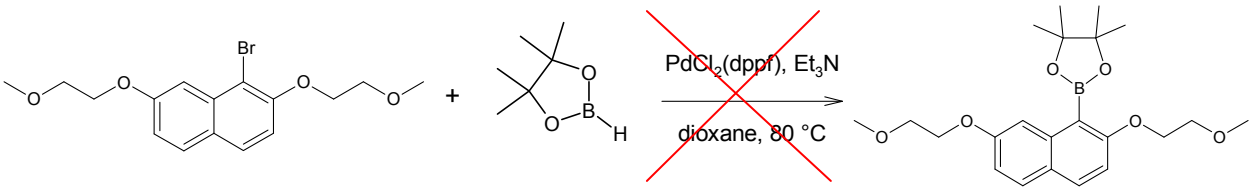

Scheme 2.12: Synthetic route for the UNIT 1 PEG pinacol ester using pinacolborane as the boron source.[18]

In the reaction depicted in Scheme 2.10, a solution of the catalyst was first prepared in anhydrous dioxane. Then, UNIT 1 PEG, triethylamine and then pinacolborane were added. The reaction was monitored via TLC and allowed to take place overnight. However, the reaction did not go to completion, which may be due to the catalyst going inactive. When the crude was analyzed by ^{1}H NMR, we saw that it was mostly composed of the starting materials. There were signs of new species that formed. However, a closer examination of its chemical shifts revealed the presence of 2,7-bis(2-methoxyethoxy)naphthalene, also observed in the lithium-halogen exchange and Grignard reactions performed earlier. This is not surprising since pinacolborane can behave as a hydride source.[18]

To eliminate this problem, we replaced the pinacolborane with the less atom economical, bis(pinacolato)diboron, and followed the protocol developed by Ishiyama *et al.*[20] The reaction was a lot easier to perform, due to the stability of the boron source in air, unlike pinacolborane. However, the reaction was also unsuccessful as the crude is composed only of unreacted starting material and a few traces of the dehalogenated 2,7-bis(2-methoxyethoxy) naphthalene.

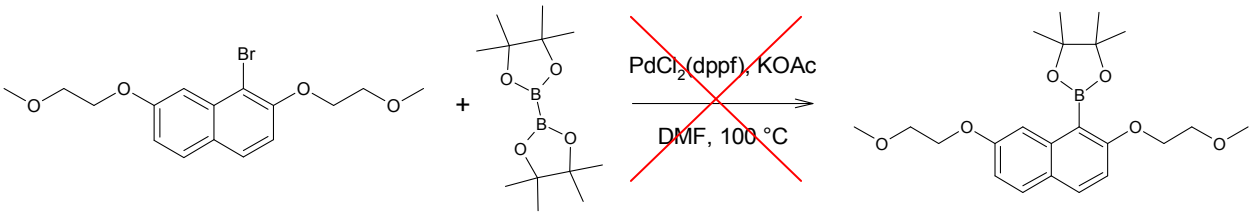

Scheme 2.13: Synthetic route for the UNIT 1 PEG pinacol ester using bis(pinacolato)diboron as the boron source.[20]

2.2.5: Triad bearing the boronic acid unit

The synthesis of 2,7-bis(2-methoxyethoxy) naphthalene boronic acid proved to be very challenging, thus we investigated alternative routes in synthesizing the tweezer. Suzuki coupling is still considered to be our best choice due to its versatility, and ease of work-up. Most importantly, the low-toxicity of Suzuki coupling partners makes this method an ideal candidate for synthesizing DDS compounds, when compared to other carbon-carbon coupling methods that uses toxic metal catalysts such as nickel or tin.[21]

In the synthesis of our 1st generation tweezer, the pH-active triad functioned as the aryl halide, while the naphthalene **IS** was used as the electrophile for the final Suzuki-coupling reaction. Due to the lack of success during the synthesis of the 2,7-bis(2-methoxyethoxy) naphthalene boronic acid, we have considered using our pH-switching triad as the new boronic acid, while keeping the 1-bromo-2,7-bis(2-methoxyethoxy) naphthalene to act as the aryl halide.

Conversion of the pH-switching triad to its corresponding di-boronic acid was successful. The conversion took place over three steps, as outlined by the following scheme.

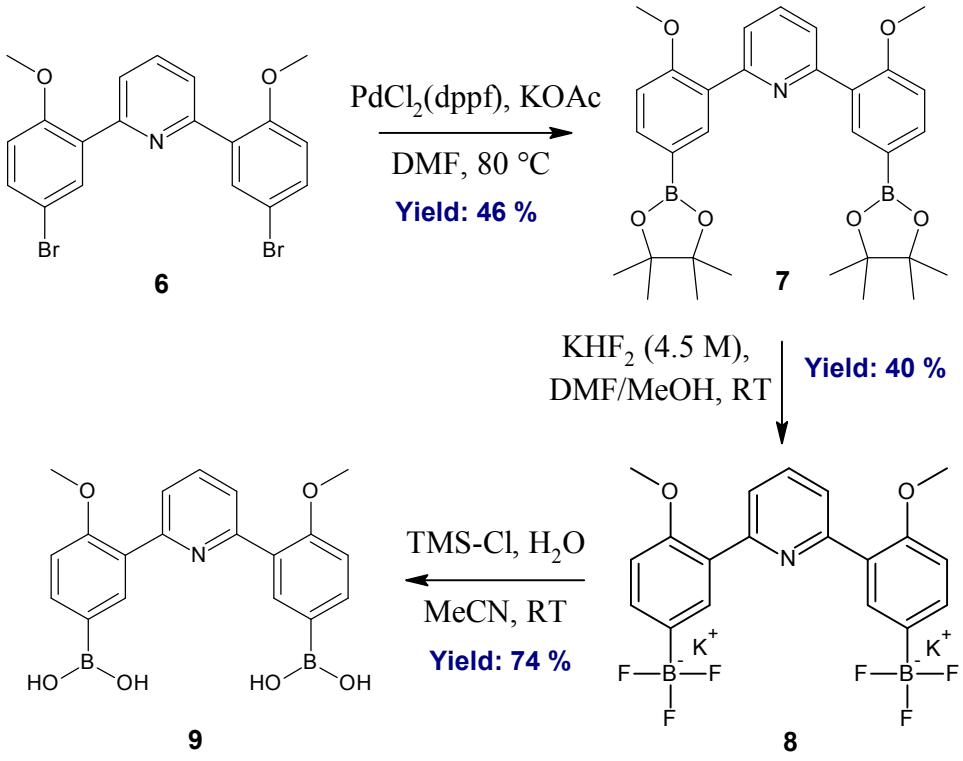

Scheme 2.14: Synthetic route of the Triad diboronic acid.[17]

The first step of the reaction involves the conversion of the triad into its corresponding pinacol ester. This was achieved by using the protocol developed by Ishiyama *et al.*.[20] The procedure was modified by doubling the required amount of the base, boron source and the catalyst in order to achieve the bis-functionalization of the triad. To make the pinacol diester, a solution of all reagents was made in dry DMF, under argon. The reaction took place overnight under argon atmosphere, and was complete after approximately 20 hours, as verified by ^{1}H NMR. The crude only contained the unreacted bis(pinacolato)diboron as the contaminant which was removed via re-crystallization from toluene:hexanes.

The purification step was the most challenging part of the synthesis, as the pinacol diester does not form crystals, but instead a dirty-looking suspension in organic solvents. Recrystallization was almost a “trial and error” event, and when it works (in the case of using

toluene:hexanes as solvent), a significant amount of the compound was lost in the filtrate. Isolation of the “recrystallized” compound via filtration was also very tricky because it forms a very fine suspension, thus it requires a high-porosity filter paper for filtration.

The next step in the synthesis is to hydrolyze the pinacol diester, using the mild deprotection method developed by Yuen and Hutton in 2005.[17] A solution of the pinacol diester was made in DMF/ methanol, and then treated with 4.5 M of potassium hydrogen fluoride. DMF was added due to the pinacol diester’s poor solubility in methanol. The reaction took place at RT, under open atmosphere, and was complete in 1 hour. Purification of crude involved re-crystallization with acetone:ether, however, no crystals were observed to form, but a brown suspension, making it again very difficult to isolate via filtration. However, this problem was once again solved via filtration using a fine-porosity filter paper.

The final step of the hydrolysis required treatment of the triad bis(trifluoroborate) salt with TMS-Cl, once again using the protocol developed by Yuen and Hutton.[17] Treatment of a strong base, such as lithium hydroxide, may also be used for hydrolysis of the salt, however, this process takes longer (24 hours) to achieve, and requires longer work-up procedures.[17] In contrast, hydrolysis via TMS-Cl is complete in one hour. The reaction is driven by the formation of TMS-F, which consequently results in the formation of the corresponding difluoroborane that reacts with water to form the desired boronic acid.

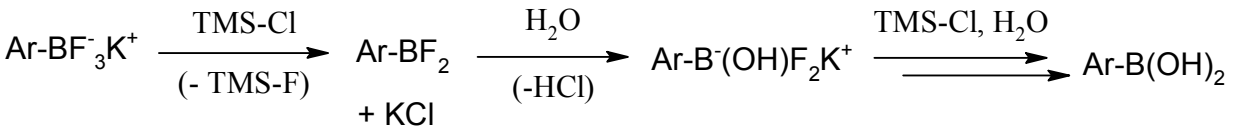

Scheme 2.15: Presumed potassium phenyltrifluoroborate hydrolysis pathway using TMS-Cl.[17]

General procedure of this reaction requires a solution of the trifluoroborate in acetonitrile. Water was added and while stirring at RT under open atmosphere, then TMS-Cl was added.

After 1 hour, the reaction was quenched with saturated sodium bicarbonate, causing a precipitate to form. Work-up was fairly simple: water was removed via Pasteur pipette and the remaining solution was dried with Na_2SO_4. Evaporation of the solvent in vacuo yielded the desired diboronic acid in high yield and purity.

2.2.6: Assembling the 2nd Generation Tweezer

To assemble the 2nd generation tweezer, we have followed the Suzuki-coupling protocol reported by Leblond *et al.* used for the synthesis of the 1st generation tweezer.[1] We have used the pinacolyl boronate ester for our first attempt, as they are also used as Suzuki-coupling substrates. However, the reaction proceeded sluggishly, as monitored by ^{1}H NMR, even when placed under microwave conditions for 24 hours. This is not very surprising because many Suzuki coupling reactions are most efficient with (or sometimes absolutely requires) using boronic acids as a coupling partner.[17] Furthermore, both the pinacolyl boronate ester and the UNIT 1 PEG are very bulky molecules. The sterics introduced by both groups make it very difficult for transmetallation to proceed.[21]

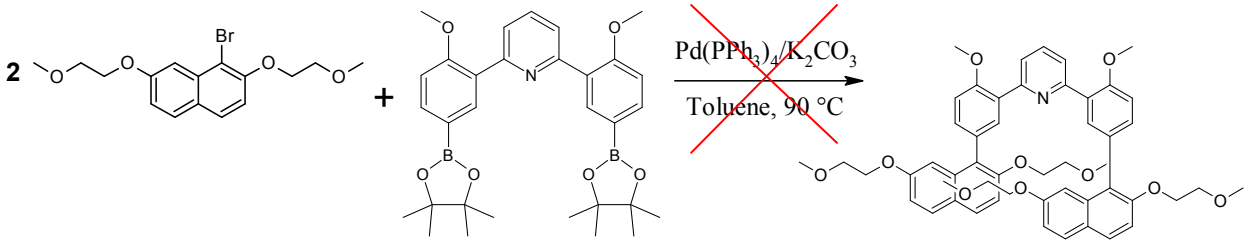

Scheme 2.16: First attempt on the 2nd generation tweezer.[1]

Analysis of the crude ^{1}H NMR spectrum was very unreliable due to the many overlapping peaks that arise. However, it can be seen that most of the starting materials were still present. TLC was also attempted in order to discern the identity of the side products formed. However, due to the presence of the oligoethylene glycol chains in the **IS**, we are unable to get

a clear separation of the components. Instead, we get a large smear on the TLC plates in all solvent-combinations we tried. Lastly, we resorted to mass spectrometry. Analysis of the crude product mixture was conducted using high resolution mass spectrometry (ESI, negative mode) showed small peaks in the range of our desired molecular weight.[23] This may suggest the formation of the tweezer. However, due to the difficulties we encountered in purifying the crude and extremely low yields, the protocol illustrated in Scheme 2.13 was disregarded.

To minimize the problems associated with sterics, we have attempted to synthesize half of the tweezer first. Once made, the two "half-tweezers" would then be coupled with the very reactive 2,6-dibromopyridine to assemble our 2nd generation tweezer.

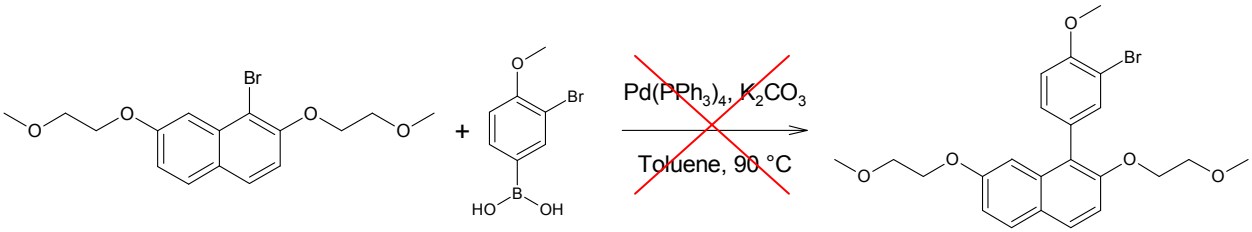

Scheme 2.17: Synthesis of the "half"- 2nd generation tweezer.

The boronic acid used for the reaction was synthesized according to Scheme 3.7. 5-Bromo-4-methoxyphenylboronic acid was used instead of the triad diboronic acid because it is less sterically hindered and its shape is not pre-organized, unlike the diboronic acid. Self-coupling of the 5-bromo-4-methoxyphenylboronic acid, although feasible, was not taken as a big concern. The bromide in the *ortho* position showed almost no reactivity towards palladium-catalyzed borylation, during the synthesis of its precursor, 2-(3-bromo-4-methoxy-phenyl)-4,4,5,5-tetramethyl-[1,3,2]dioxaborolane (Scheme 3.7).

The reaction was carried out under the conditions described in Scheme 2.14 and took place for 2 days. However, it did not work. Analysis by ^{1}H NMR shows that the starting materials did not react, but there were also signs that the debrominated product formed. Eventually, we realized that the catalyst used was probably not active enough. Thus, we are currently

investigating new methods that involve the use of a more active palladium catalyst ($Pd(dba)_2/PCy_3$ or $PdCl_2$(POPD)), used for the borylation of inactive haloarenes (e.g. *ortho*-substituted chloroarenes).[22]

2.3: Conclusion

The synthesis of the 2nd generation tweezer has proven to be very challenging. It is now known that the 2,7-bis(2-methoxyethoxy)naphthalene boronic acid can be made neither using lithium-halogen exchange, nor via Grignard method. The use of palladium-catalyzed cross coupling reaction with organoboron reagents was also without success. Nevertheless, it is worth attempting this coupling procedure with a more active palladium catalyst, such as $Pd(dba)_2/PCy_3$ or $PdCl_2$(POPD).

Although the synthesis of the triad diboronic acid was very successful, we now know that Suzuki coupling to 1-bromo-2,7-bis(2-methoxyethoxy)naphthalene is highly unlikely to proceed based on the results obtained from coupling with 5-bromo-4-methoxyphenyl boronic acid. Once again, the use of highly active palladium catalyst ($Pd(dba)_2/PCy_3$ or $PdCl_2$(POPD) for the next reaction attempts is highly recommended.

References:

1. Leblond, J.; Gao, H.; Petitjean, A.; Leroux, J.-C. *J. Am. Chem. Soc.* **2010**, 132, 8544-8545
2. Steed, J. W.; Atwood, J. L.; *Supramolecular Chemistry.* John Wiley & Sons Ltd.: Wiltshire, 2009; p. 30
3. a) Stohs, S. J.; Ohia, S.; Bagchi, D. *Toxicology*. **2002**, 180, 97-105; b) Bonnet, J. L.; Guiraud, P.; Dusser, M.; Kadri, M.; Laffosse, J.; Steiman, R.; Bohatier, J. *Ecotoxicol.*

Environ. Safety **2005**, 60, 87–100; c) Herner, H. A.; Trosko, J. E.; Masten, S. J. *Environ. Sci. Technol*. **2001**, 35, 3576-3583

4. a) Petitjean, A.; Lehn, J. M.; Khoury, R.G.; Kyritsakas, N. *J. Am. Chem. Soc*. **2004**, 126, 6637-6647; b) Petitjean, A.; Kyritsakas, N.; Lehn, J. M. *Chem. Eur. J.* **2005**, 11, 618-628
5. Joralemon, M. J.; McRae, S.; Emrick, T. *Chem. Commun.* **2010**, 46, 1377-1393
6. Matsumura, Y.; Maeda, H. *Cancer Res.* **1986**, 46, 6387-6392
7. a) Sharghi, H.; Hosseini-Sarvari, M.; Moeini, F. *Can. J. Chem.* **2008**, 86, 1044-1051; b) Shirin, Z.; Thompson, J.; Liable-Sands, L.; Yap, G. P. A.; Rheingold, A. L.; Borovik; A. S. *J. Chem. Soc., Dalton Trans.* **2002**, 1714-1720
8. Grandberg, I. I.; Faizova, G. K.; Kost, A. N. *Chem. Heterocycl. Compd.* **1967**, 2, 421-425
9. Kurosaki, H.; Sharma, R. K.; Aoki, S.; Inoue, T.; Okamoto, Y.; Sugiura, Y.; Doi, M.; Ishida, T.; Otsuka, M.; Goto, M. *J. Chem. Soc., Dalton Trans.* **2001**, 441-447
10. a) Jones, R. A.; Katritzky, A. R. *J. Chem. Soc.* **1959**, 1317-1319; b) Rauckman, B. S.; Roth, B. *J. Med. Chem.* **1980**, 23, 384-391
11. Khalafi-Nezhad, A.; Zare, A.; Parhami, A.; Rad, M. N. S.; Nejabat, G. R. *Synth. Commun.* **2006**, 36, 3549-3562
12. Wilson, R. D. *J. Chem. Soc.* **1965**, 3304-3312
13. Badjic, J. D.; Ronconi, C. M.; Stoddart, J. F.; Balzani, V.; Silvi, S.; Credi, A; *J. Am. Chem. Soc.* **2006**, 128, 1489-1499
14. Heathcote, R.; Howell, J. A. S.; Jennings, N.; Cartlidge, D.; Cobden, L.; Coles, S.; Hurtshouse, M.; *Dalton Trans.* **2007**, 13, 1309-1315
15. Genov, M.; Almorín, A.; Espinet, P. *Chem. Eur. J.* **2006**, 12, 9346-9352
16. Malkov, A. V.; Ramirez-Lopez, P.; Biedermannova, L.; Rulisek, L.; Dufkova, L.; Kotora, M.; Zhu, F.; Kocovsky, P. *J. Am. Chem. Soc.* **2008**, 130, 5341-5348
17. a) Yuen, A. K. L.; Hutton, C. A. *Tetrahedron Lett.* **2005**, 46, 7899-7903; b) Molander, G. A.; Biolatto, B. *J. Org. Chem.* **2003**, 68, 4302-4314

18. Murata, M.; Ovama, T.; Watanabe, S.; Masuda, Y. *J. Org. Chem.* **2000**, 65, 164-168

19. Snead, D. R.; Inagaki, S.; Abboud, K. A.; Hong, S. *Organometallics* **2010**, 29, 1729-1739

20. Ishiyama, T.; Murata, M.; Miyaura, N. *J. Org. Chem.* **1995**, 60, 7508-7510

21. Suzuki, A. *Chem. Commun.* **2005**, 4759-4763

22. Fang, H.; Kaur, G.; Yan, J.; Wang, B. **2005**, *Tetrahedron Lett.* 46, 1671-1674

23. Russell, D.H.; Edmondson, R. D. *J. Mass Spectrom.* **1997**, 32, 263-276

Chapter 3

Synthesis of 3rd Generation Molecular Tweezer

3.1 Insights on the Caffeine- derived IS

Our 3rd generation tweezer is inspired by the preliminary work of Chen and Whitlock, who developed a molecular tweezer that is composed of two theophylline **IS** held together by an alkyl-diyne **S**.[1] Using caffeine as our new **IS** offers many benefits to our new tweezer design. First, caffeine is water-soluble unlike the naphthalene-derived **IS** from our previous models. Therefore, it is highly likely that the tweezer derived from caffeine would also be water-soluble, especially that there would be two caffeine molecules per tweezer. Furthermore, having a water-soluble tweezer will allow us to conduct experiments in aqueous media. This will serve as a better scope for the tweezer's behavior *in vivo*.

Second, the low toxicity (192 mg/kg, rat (oral)) of caffeine makes it much more suited for DDS applications.[2] Caffeine is metabolized in the liver by the enzyme, cytochrome P450, into three primary metabolites, namely, paraxanthine, theobromine and theophylline, each of which have their own biological effects.[3]

Third, the synthetic pathways that lead to caffeine-derived molecules are well-studied. Hence, derivatization of the caffeine **IS** should be a less challenging task, unlike that of the naphthalene **IS**. From an analytical point of view, caffeine is also an attractive unit considering the simplicity of its ^{1}H NMR signals and the fact that they are located in very distinct parts of the NMR spectrum (compared to naphthalene). For instance, the intense (N-)CH_n peaks are very attractive probes for NMR titrations and NOESY experiments. Lastly, caffeine is a very cheap reagent (<$10 per 100 g), which makes large-scale synthesis of this tweezer a lot more attractive.

We have designed our 3rd generation tweezer to use the same pH-responsive triad **S** from our previous tweezers. This new tweezer will contain theophylline as its new **IS** (&

theophilline differs from caffeine by replacing the methyl group at the N-7 position with a hydrogen), and will also be used for the selective delivery of the anticancer drug, MTX™.

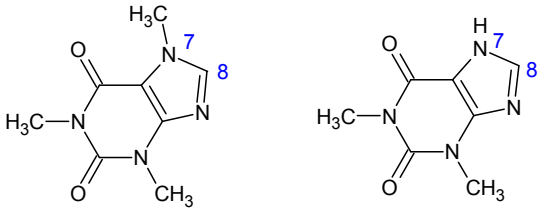

Figure 3.1: Chemical Structure of Caffeine and Theophylline.

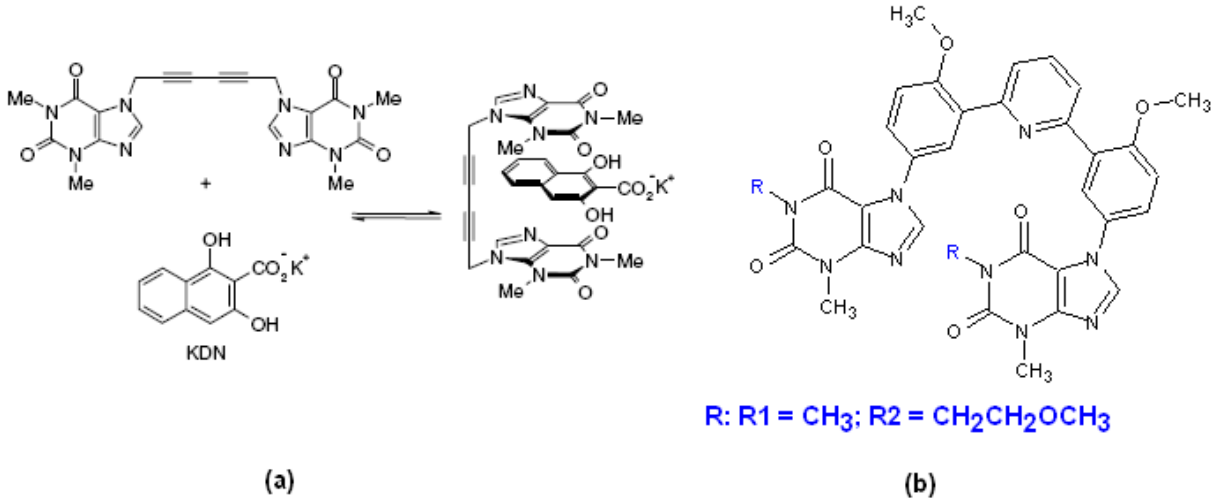

Figure 3.2: Caffeine-based molecular tweezers. a) Chen and Whitlock's Molecular Tweezer; b) 3rd Generation Molecular Tweezer.[1]

3.1.1 Caffeine and MTX Binding

Caffeine has been observed to reduce the efficacy of a number of anticancer drugs, such as MTX.[4] It has been suggested that caffeine acts as an "interceptor" of biologically active molecules, by forming hetero-association complexes with them.[4] The formation of these association complexes is presumed to lower the concentration of the free ligand *in vivo*, which decreases the pharmacological activity of drugs.[4]

A study conducted by Davies *et al.* in 2001 examines the hetero-association of caffeine with MTX in an attempt to understand the basis of the reduction of the efficacy of the drug.[4] Through NMR studies in aqueous media (^{1}H NMR, 2D TOCSY and 2D ROESY), the hetero-association between caffeine and MTX was investigated as a function of concentration and temperature. No intermolecular cross-peaks were detected in the 2D ROESY experiments between the MTX and caffeine protons in their mixed solutions, even at higher concentrations. Furthermore, the proton chemical shifts of MTX were shifted to high frequencies, suggesting a shielding effect by the caffeine molecules. This implies that various hetero-association complexes between MTX and caffeine are most likely forming, with the association constant (K_{Het}) calculated to be 256 (± 30) M^{-1}.[4]

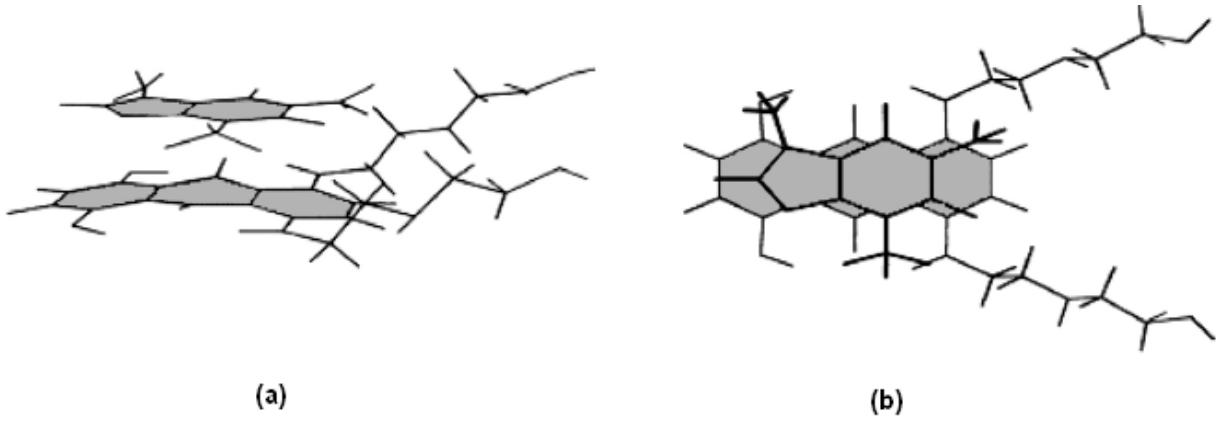

Figure 3.3: Davies *et al.'s m*odel structure of the 1:1 MTX:Caffeine hetero-association complex determined by the analysis of the calculated values of the induced proton chemical shifts in the dimer. The spatial representation of the structures were obtained using "Mathematica 2.2" software (Wolfram Res. Inc.) **a)** side-view; **b)** top view.[4]

3.2: Synthesis of the 3rd Generation Tweezer

Just like the 2nd generation tweezer, synthesis of the 3rd generation tweezer was a very challenging task. The tweezer can be assembled in two ways, as outline in Scheme 1.2 and Scheme 1.3. It may be assembled by coupling the theophylline **IS** with the triad diboronic acid,

mentioned in Scheme 2.11, or via synthesis of the “half-tweezers” that will subsequently be coupled to 2,6-dibromopyridine to form the 3rd generation tweezer.

3.2.1: Alkylation of Theophylline

In order to improve the water solubility of the tweezer, and thus avoid the same issues encountered our 1st generation tweezer, we are installing short oligoethylene glycol chains in the theophylline rings. To do this, the following synthetic route was proposed.

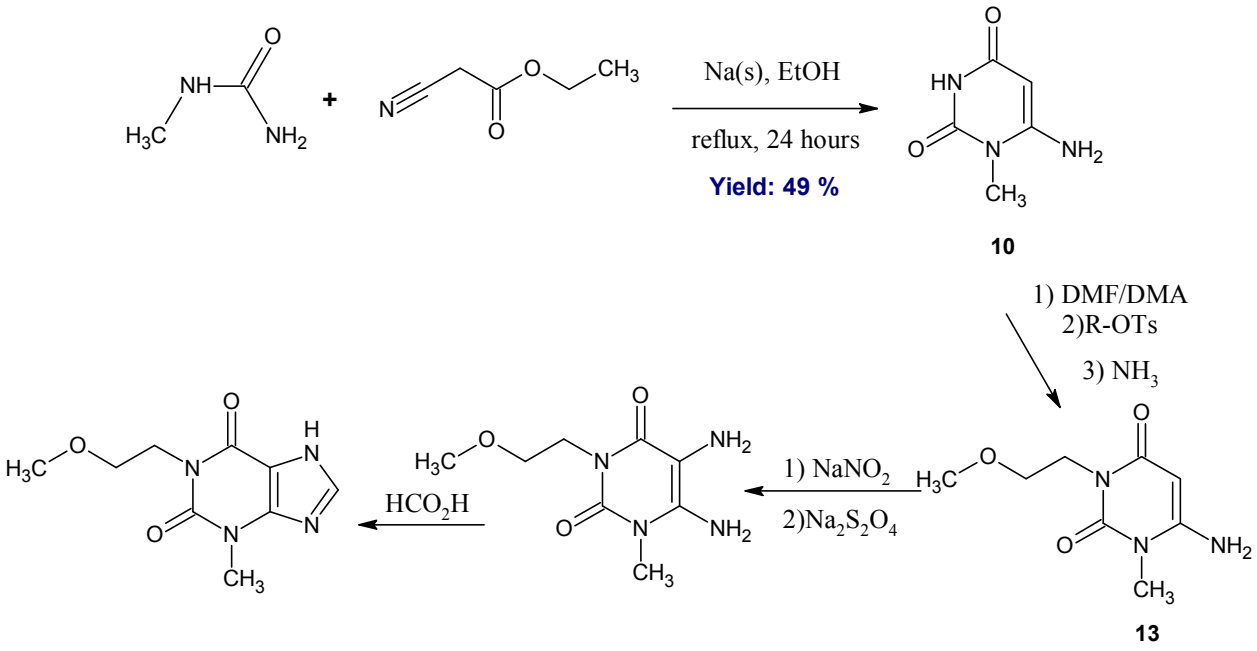

Scheme 3.1: Synthetic route for the alkylated theophylline **IS**.[5]

The first step involves condensation of the commercially available 1-methylurea with ethyl-2-cyanoacetate in the presence of sodium ethoxide as base to give compound **10**. The reaction is very simple as it gives excellent yields (literature: 95 %) and the resulting product does not require further purification.[5] This reaction is identical to that in the literature. The next step, which is new, is to synthesize the intermediate compound (Scheme 3.2) by treatment of dimethyl formamide dimethyl acetal (DMF/DMA) in DMF at 40 ˚C, and immediately alkylate it

with 2-methoxyethyl-4-methoxybenzene sulfonate, using potassium carbonate as base at 90 ˚C. Deprotection of the *N,N*-dimethyl-aminomethylene group is then achieved by treatment of the crude solid with aqueous ammonia in methanol.

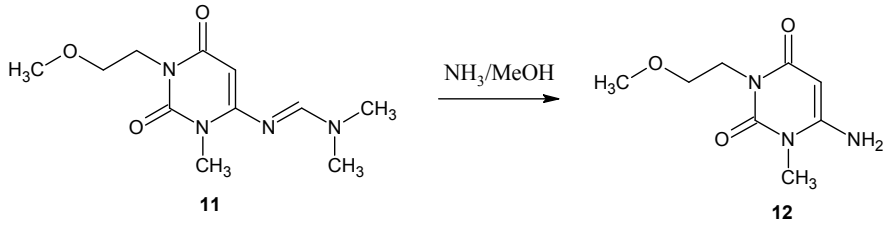

11 **12**

Scheme 3.2: Deprotection of the intermediate formamidine with aqueous ammonia in methanol.[5]

The alkylation step was carried out according to the protocol developed by Elzein *et al.* in 2008.[5] The procedure was modified by using a tosylate (2-methoxyethyl-4-methoxybenzene sulfonate) as an alkyl source, instead of an alkyl halide. The synthesis worked well, as it is able to generate the desired product (compound 3.2b), however, the purification step failed. Using column chromatography (SiO_2; 1.8:0.2 DCM:MeOH) to separate the components of the crude, we were able to remove the majority of the contaminants (i.e. unreacted starting materials). However, we were unsuccessful in removing the unwanted suspected side product, 6-amino-4-(2-methoxyethoxy)-1-methyl-3,4-dihydropyrimidin-2-(1*H*)-one (Figure 3.4) that would arise from the alkylation of the tautomeric form of the starting dione. Both compounds have the same Rf values (0.26), hence, cannot be purified via chromatography. Re-crystallization was also attempted using various solvent-combinations but was also unsuccessful. To avoid complicated mixtures in the next step of the reaction, the synthesis was stopped at this stage.

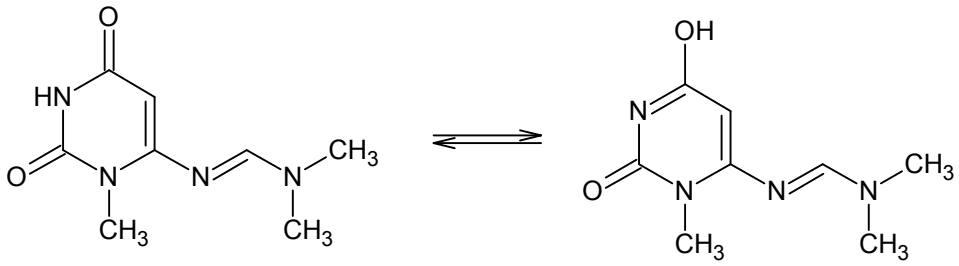

(a) **(b)**

Scheme 3.3: Tautomeric forms of the intermediate dione (before the alkylation step).

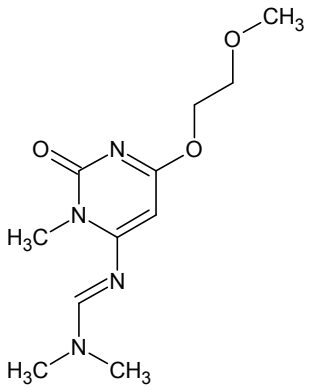

Figure 3.4: Chemical structure of the alkylated "enol" tautomer of the intermediate.

3.2.2: Synthesis of the "Half" Theophylline Tweezer

The synthesis of the "half-tweezer" was attempted in order to minimize the steric hindrance that we think we identified from our preliminary work of coupling the **IS** directly with the triad **S**. Once made, the two "half-tweezers" would then be coupled with the very reactive 2,6-dibromopyridine to assemble our 3rd generation tweezer.

The half-theophylline tweezer was synthesized via 5-step reaction, described in Scheme 3.7. Starting from the commercially available 2-bromoanisole, the 5-bromo-4-methoxy-phenyl boronic acid was synthesized which was then coupled to theophylline via copper (II) catalysis.

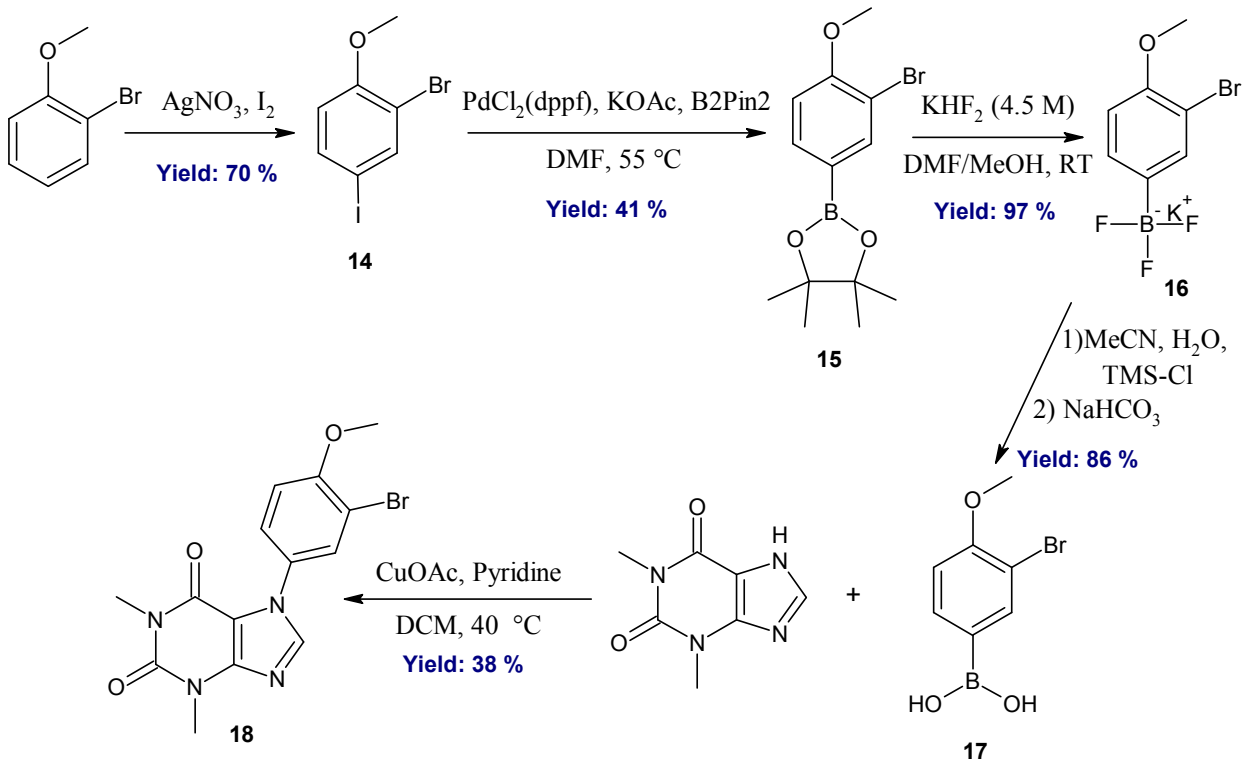

Scheme 3.7: Reaction Scheme of the "half-theophylline" tweezer.[6,7,8,10]

3.2.2.1: Synthesis of 2-(3-bromo-4-methoxy-phenyl)-4,4,5,5-tetramethyl-[1,3,2]dioxaborolane (PhPin Boronic Ester)

Synthesis of the ester was conducted in two steps: first, iodination of the commercially available 2-bromoanisole to produce 2-bromo-4-iodoanisole, followed by its palladium-catalyzed borylation using bis(pinacolato)diboron as the boron source.

The iodination step was carried out according to the solvent-free protocol developed by Yusubov *et al.* with no complications.[7] The 2-bromo-4-iodoanisole was obtained in good yield (70 %) and can either be purified using recrystallization (ethanol) or via column chromatography (SiO_2, hexanes/DCM; 2.5:0.5). The next step, however, was more complicated.

Conversion of 2-bromo-4-iodoanisole to PhPin Boronic ester was achieved using the protocol developed by Ishiyama *et al.*[8] The protocol was modified in order to carefully control

the borylation, since borylation can occur in two places due to the presence of both iodine and bromine in the starting molecule. This problem is solved by lowering the temperature of the reaction to 55 ˚C and by limiting the ratio of 2-bromo-4-iodoanisole and bis(pinacolato)diboron to 1:1. Since it is known that organic iodides are much more reactive than organic bromides towards palladium-catalyzed borylation, they should not require high temperatures to proceed.[9] Furthermore, since there is only 1.1 equivalent of bis(pinacolato)diboron, it should favour the functionalization of the aryl iodide over the aryl bromide.

The course of the reaction was monitored by ^{1}H NMR (300 MHz, $CDCl_3$). Analysis of the spectra showed that the desired PhPin Boronic ester was forming. No coupling was observed at the bromide position, however, there was a significant amount of the self-coupled product that formed (~15 %) (Figure 3.6), while the rest of the peaks correspond to the starting materials. After 24 hours, the reaction was stopped. The crude was a mixture of the starting materials, the self-coupled product, and PhPin Boronic ester. All attempts at this reaction do not reach completion, even with the addition of more catalyst (after 24 hrs), longer reaction times (extending to 4 days), or slightly higher temperatures (60 ˚C). However, this was not a big concern as the crude is easily purified using column chromatography. Purification via column chromatography using using silica gel column and hexanes/DCM (1:1) as eluent afforded a yellow oil, with a moderate yield of 41 %.

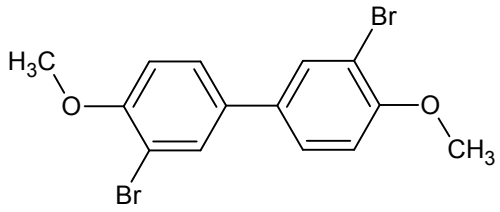

Figure 3.5: Self-coupled product of PhPin Boronic Ester.

3.2.2.2: Synthesis of 5-bromo-4-methoxy-phenyl boronic acid (Ph Boronic Acid)

The Ph boronic acid was obtained by hydrolysis of the PhPin boronic ester, once again by using the methods developed by Yuen and Hutton in 2005.[10] First, a solution of PhPin

boronic ester was prepared in methanol, then potassium hydrogen fluoride (4.5 M) was added dropwise. Unlike the pinacol diester described in Section 2.2.5, DMF was not added into the initial mixture due to PhPin boronic ester's high solubility in methanol. The reaction was carried out at RT, under open atmosphere and was complete in 30 minutes. Removal of the solvent in vacuo produced the crude, which was re-crystallized in acetone:ether. Recrystallization yielded flaky, shiny, white crystals. ^{1}H NMR revealed a very clean spectrum, and the structure was further verified by ^{13}C NMR and Mass Spectrometry analyses.

To obtain the Ph boronic acid, the recrystallized Ph salt was dissolved in acetonitrile. Water and chlorotrimethylsilane were added and the reaction was allowed to take place in 1.5 hours. Upon quenching of the reaction with saturated sodium bicarbonate, the crude was obtained via evaporation of the organic portion in vacuo. The purity of the crude Ph boronic acid varied per reaction, as it sometimes contained the boronic acid dimer (and in other cases, they are not present at all). However, the dimer was only present in trace amounts (<5 %) based on the ^{1}H NMR results, and we have found this to be insignificant for the next reaction step. When highly pure Ph Boronic ester was required, as needed for elemental analysis or ^{13}C NMR, the crude was re-crystallized using in DCM or ethyl acetate. Neither of these solvents gave good yields for re-crystallization (<30 % recovery), however, they are very successful at removing the boronic acid dimer.

^{13}C NMR and elemental analysis of the pure boronic acid gave unexpected results. The ^{13}C NMR spectrum was always missing one expected carbon signal, for unknown reasons while the elemental analysis result revealed that the major product is the boroxine derivative (as per corrected EA result, using the JASPER v2.0 software).[16] The boroxine formation is not very surprising given that boronic acids have been reported to spontaneously condense to boroxines, therefore making their analysis very difficult.[15] The fact that we were able to produce the coupling product (half-theophylline tweezer) in the next step of the reaction, suggests that we were successful in synthesizing the Ph Boronic acid intermediate.

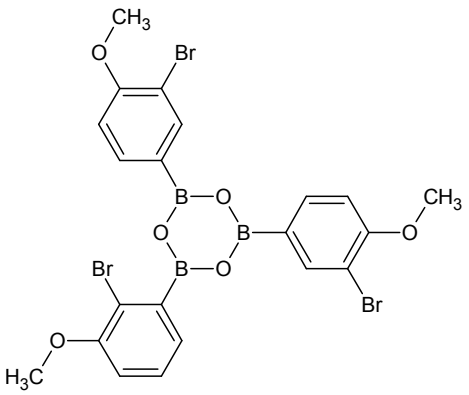

Figure 3.6: Boroxine product observed in Elemental analysis of Ph Boronic Acid

3.2.2.3: Coupling of Ph Boronic Acid with Theophylline

Due to problems associated with the alkylation of the theophylline, we have replaced the alkylated version with the just theophylline as the **IS** for our final tweezer structure. In order to synthesize the half tweezer, we followed the Cu (II) catalyzed coupling protocol that was developed by Kim *et al.* in 2010.[6] In this protocol, a suspension of the theophylline, copper(II) acetate and Ph boronic acid was made in dry DCM. While stirring under argon at RT, pyridine was added, which darkened the colour of the suspension. After 24 hours of reflux, the formation of white precipitate arising from unreacted theophylline and inorganic salt by-products was observed. The unwanted precipitate was easily removed via filtration through Celite^{TM}, while the crude was obtained from evaporating the solvent in vacuo. Purification was achieved via column chromatography (SiO_2, acetone:ether, 1.5:0.5), but since the compounds streaked a little in silica, the recovered fractions contained some trace amounts of impurities. Because the amount of these impurities were only <2 % as per ^{1}H NMR analysis, they were seen to be insignificant for the next step of the reaction. To remove them completely, however, would require re-crystallization in acetone.

3.2.3: Challenges in the Synthesis of Half-tweezer Boronic Acid

To attach the half-theophylline tweezers into 2,6-dibromopyridine, we have chosen to employ the Suzuki-Miyaura coupling method for reasons that were already mentioned in Chapter 2. For Suzuki coupling to take place, it requires a boronic acid/ ester and an organic halide. We have chosen to convert our half-theophylline tweezer to bear the boronic acid unit as conversion of 2,6-dibromopyridine into its corresponding boronic acid/ ester was well documented to be a very difficult task, which sometimes require toxic reagents.[11] Nevertheless, the conversion of the half-theophylline tweezer to its corresponding boronic acid was equally challenging.

Our first attempt to synthesize the half-theophylline tweezer boronic acid was the halogen-lithium exchange protocol, described in section 2.2.3.[12]

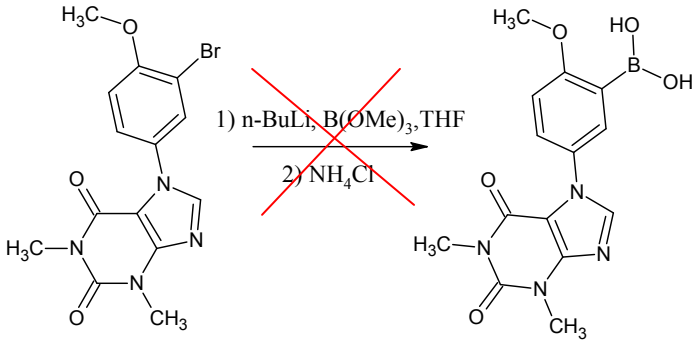

Scheme 3.8: Halogen-lithium exchange reaction of the half-theophylline tweezer.[12]

The halogen-lithium exchange reaction was first carried out using a suspension of the half-theophylline tweezer in dry THF at -70 ˚C, under argon atmosphere. When n-BuLi was added, we saw a slight colour change (turned deeper yellow) in the suspension. However, analysis of the crude showed that no reaction had occurred as the ^{1}H NMR peaks were identical to the starting materials used. We originally thought that the poor reactivity was due to the solubility problems we had with THF, as it is preferable for the starting materials to be solubilized for lithiation to occur. Since this type of reaction is very limited in its solvent choice,

we have therefore decided to control the temperature of the reaction in an attempt to solve our solubility problems.

In our next attempt at this reaction, we successfully solubilized the half-theophylline tweezer by heating the suspension of starting material to boiling. Cooling of the solution to RT did not re-crystallize the sample, however as it is further cooled to 0 ˚C, crystallization began taking place. Thus, the reaction was carried out at that temperature. However, analysis of the crude, once again, showed a failed reaction. The starting materials were untouched, despite the fact that we observed some colour change when n-BuLi was added. We later deduced that the colour change must have been from the presence of some contaminants in the starting material.

In our last attempt, we purified the half-tweezer via recrystallization with ethyl acetate. Again, we have heated it to boiling to solubilize it, and decided to carry out the reaction at RT, to prevent re-crystallization. We also reversed the order of addition of the reagents (instead of adding n-BuLi to the half-tweezer solution prior to trimethylborate, trimethylborate was added first) in order to "trap" the lithiated species, if they form at all. By adding n-BuLi last, the formed lithiated species immediately reacts with the trimethylborate in solution to produce the boronic ester. After 24 hours at RT, the reaction was quenched with saturated ammonium chloride to hydrolyze the boronic ester into a boronic acid. Analysis of the crude via ^{1}H NMR showed that the reaction failed again, however, evidence of new peaks were seen. These new peaks were later found out to be the de-brominated product, 7-(4-methoxyphenyl)-1,3-dimethyl-3,7-dihydro-purine-2,6-dione, shown below.

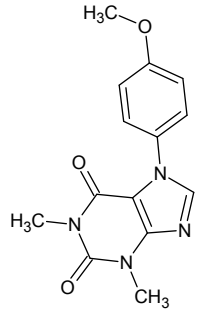

Figure 3.7: Debrominated half-theophylline tweezer.

We have also attempted the directed-*ortho*- metalation procedure developed by Snieckus *et al.* on the 7-(4-methoxyphenyl)-1,3-dimethyl-3,7-dihydro-purine-2,6-dione, synthesized previously.[13] Once again, no reaction was seen to take place.

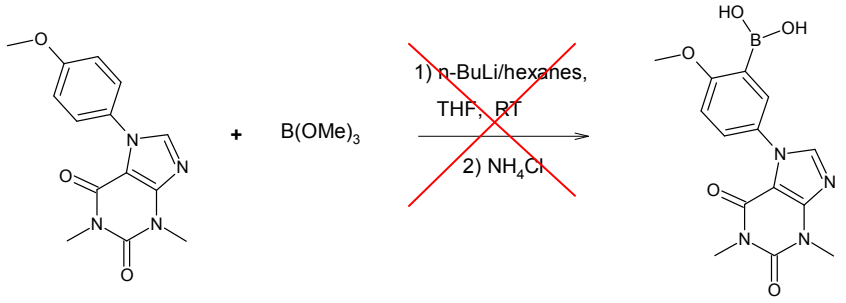

Scheme 3.9: Directed *ortho*-metalation of 7-(4-methoxyphenyl)-1,3-dimethyl-3,7-dihydro-purine-2,6-dione (a.k.a. debrominated half-theophylline tweezer).[13]

Palladium-catalyzed borylation was also attempted in order to indirectly synthesize our half-theophylline tweezer boronic acid. Our first attempt used the protocol developed by Ishiyama *et al.*, as outlined by the following reaction scheme.[8] This reaction was also very disappointing as the crude contained a large amount of the starting materials. There was also evidence of the de-brominated product forming via ^{1}H NMR analysis, but no boronic ester was seen to form.

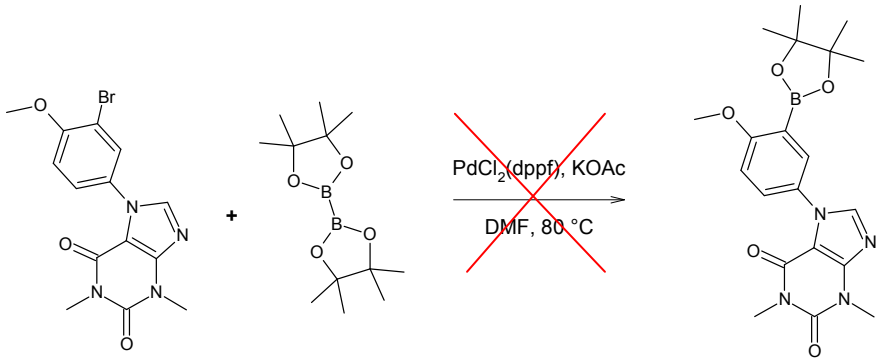

Scheme 3.10: Palladium-catalyzed borylation of half-theophylline tweezer using bis(pinacolato) diboron as the boron source.[8]

We also tried the palladium-catalyzed borylation using a less-sterically hindered boron source, bis(neopentylglycolato)diboron using the protocol developed by Fang *et al.*[14] However, we also did not observe any reactions to be taking place with the half-theophylline tweezer.

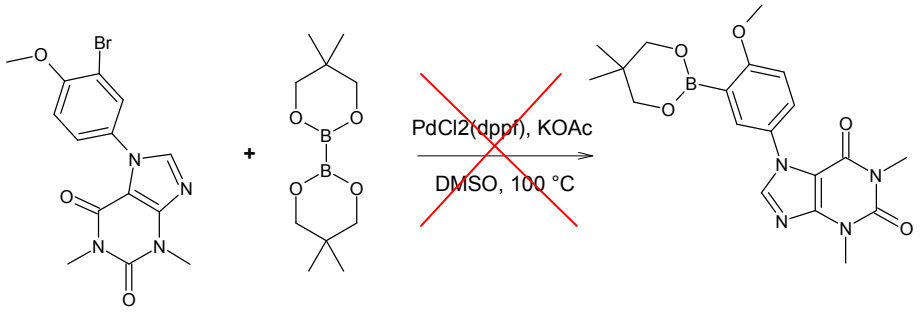

Scheme 3.11: Palladium-catalyzed borylation of half-theophylline tweezer using bis(neopently-glycolato) diboron as the boron source.[14]

We still do not know the exact causes of the half-tweezer's poor reactivity towards borylation. The presence of electron-donating groups in the structure might be responsible for the poor reactivity because it slows down the rate of oxidative addition to the palladium(0) species.[15] Hence, as a solution, we propose once again, the use highly reactive palladium catalyst ($Pd(dba)_2/PCy_3$ or $PdCl_2(POPD)$), used for the borylation of inactive haloarenes (e.g. *ortho*-substituted chloroarenes).[14,15]

3.2.4: Assembling the 3rd Generation Tweezer

Due to the problems associated with the synthesis of the half-theophylline tweezer boronic acid, we have resorted to synthesizing our 3rd generation tweezer using the triad diboronic acid, outlined in Chapter 2. Coupling of theophylline with the triad diboronic acid was performed based on the procedure developed by Kim *et al.,* as outlined by the following reaction scheme.[6]

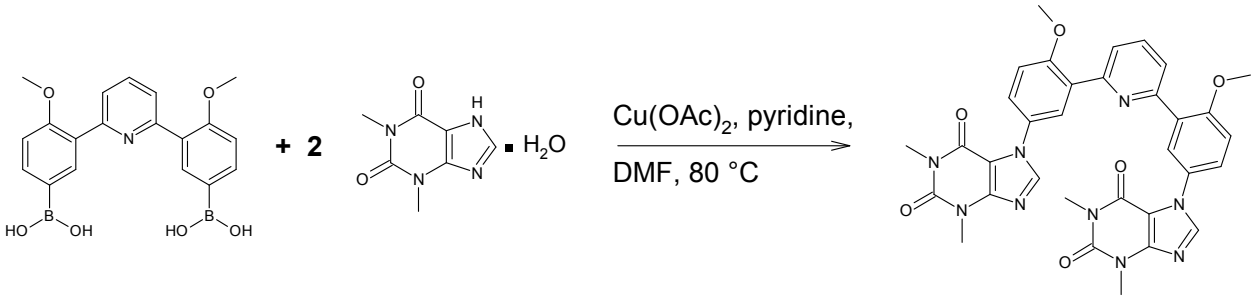

Scheme 3.12: Synthesis of the 3rd generation tweezer via Cu(II) catalyzed coupling.[6]

The first attempt in this reaction used dichloromethane as a solvent although the starting materials were not soluble. Analysis of the crude via ^{1}H NMR showed formation of new species. Purification of the crude using column chromatography allowed us to identify the new species via ^{1}H NMR, which was actually the mono-substituted tweezer. Because of this incomplete reaction, we hypothesized that our solvent choice was responsible. Hence, in our next attempt, we have chosen dimethylformamide as the new solvent.

Switching to DMF as our solvent has two main benefits. First, our starting materials were soluble in DMF, thus, the chemical reaction would occur faster since everything is dissolved. Second, DMF has a boiling point of 153 ˚C, unlike DCM that boils at 40 ˚C. We would therefore be able to carry out the reaction at higher temperatures in order to push it to completion.

Using the same protocol by Kim *et al.*, we carried out the reaction again in DMF at 100 ˚C.[6] However, the results were the same: only the mono-substituted product formed. In an attempt to push the reaction to completion, the mono-substituted tweezer was isolated and re-subjected to the same coupling reaction under microwave conditions. The sample was left to react at 100 ˚C in the microwave for 24 hours, yet there was no reaction that took place as evidenced by ^{1}H NMR analysis. We have proposed that the reaction was probably not taking place due to the steric hindrance that arose from the pre-organized structure of the triad diboronic acid. Hence, we must continue to develop ways to synthesize the 3rd generation

tweezer using the half-theophylline tweezers in order to reduce the problems associated with sterics.

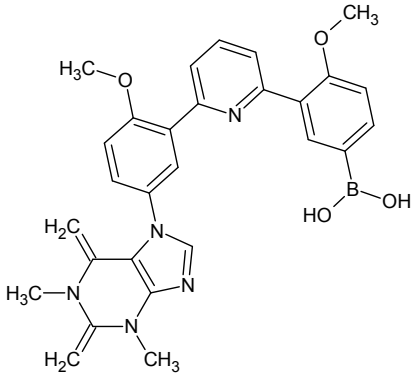

Figure 3.8: Chemical structure of the mono-substituted theophylline tweezer.

3.3: Conclusion

The synthesis of the 3rd generation tweezer was attempted via direct coupling of the triad diboronic acid with theophylline, but without any success due to problems with steric hindrance. We now know that if the synthesis of this tweezer is to be successful, we have to take the "half-tweezer" approach: that is, to synthesize the final tweezer structure via coupling of the half-theophylline tweezers with 2,6-dibromopyridine. However, we must first solve the problems that were encountered with the boronic acid synthesis. Once again, the use of highly reactive palladium catalysts ($Pd(dba)_2/PCy_3$ or $PdCl_2(POPD)$) for the next reaction attempts are highly recommended.

References:

1. Steed, J. W.; Atwood, J. L.; *Supramolecular Chemistry.* John Wiley & Sons Ltd.: Wiltshire, 2009; pp. 336-340
2. Regina, E. G.; Smith, G. M.; Keiper, C. G.; McKelvey, R. K.; *J. Appl. Psychol.* **1974**, 59, 483-489

3. Noh, K.; Seo, Y. M.; Lee, S. K.; Bista, S. R.; Kang, M. J.; Jahng, Y,; Kim, E.; Kang, W.; Jeong, T. C.; *Arch. Pharm. Res.* **2011**, 34, 119-125
4. Davies, D. B.; Veselkov, D. A.; Evstigneev, M. P.; Veselkov, A.; *J. Chem. Soc., Perkin Trans.* **2001**, 2, 61-67
5. Elzein, E.; Kalla, R. V.; Li, X.; Perry, T.; Gimbel, A.; Zeng, D.; Lustig, D.; Leung, K.; Zablocki, J.; *J. Med. Chem.* **2008**, 51, 2267-2278
6. Kim, D.; Jun, H.; Lee, H.; Hong, S.; Hong, S. *Org. Lett.* **2010**, 12, 1212-1215
7. Yusubov, M. S.; Tveryakova, E. N.; Krasnokutskaya, E. A.; Perederyna, I. A.; Zhdankin, V. V. *Synth. Comm.* **2007**, 37, 1259-1265
8. Ishiyama, T.; Murata, M.; Miyaura, N. *J. Org. Chem.* **1995**, 60, 7508-7510
9. Suzuki, A.; *Chem. Commun.* **2005**, 4759-4763
10. a) Yuen, A. K. L.; Hutton, C. A. *Tetrahedron Lett.* **2005**, 46, 7899-7903; b) Molander, G. A.; Biolatto, B. *J. Org. Chem.* **2003**, 68, 4302-4314
11. Mandolesi, S.; Vaillard, S.; Podesta, J.; Rossi, R.; *Organometallics*, **2002**, 21, 4886-4888
12. Genov, M.; Almorín, A.; Espinet, P. *Chem. Eur. J.* **2006**, 12, 9346-9352
13. Fu, J.; Snieckus, V. *Can. J. Chem.* **2000**, 78, 905-919
14. Fang, H.; Kaur, G.; Yan, J.; Wang, B.; *Tetrahedron Lett.* **2005**, 46, 1671-1674
15. Todd, M. H.; Balasubramanian, S.; Abell, C.; *Tetrahedron Lett.* **1997**, 38, 6781
16. JASPER v2.0 - JavaScript Percentage Elemental Results Calculator. Retrieved from http://www.chem.yorku.ca/profs/potvin/Jasper/jasper2.htm in August 2011

Chapter 4

Synthesis of 4th Generation Molecular Tweezer

4.1 Insights on the Benzimidazole-derived IS

Due to the difficulties that arose from the syntheses of the boronic acids required for the final coupling reactions in our 2nd and 3rd generation tweezers, we have investigated simpler synthetic schemes for our 4th generation tweezer which would not require metal-catalyzed cross-coupling reactions. The receptor platform (Figure 4.1) developed by Krebs and Jørgensen in 2001 thus became the inspiration for our latest tweezer design.[1]

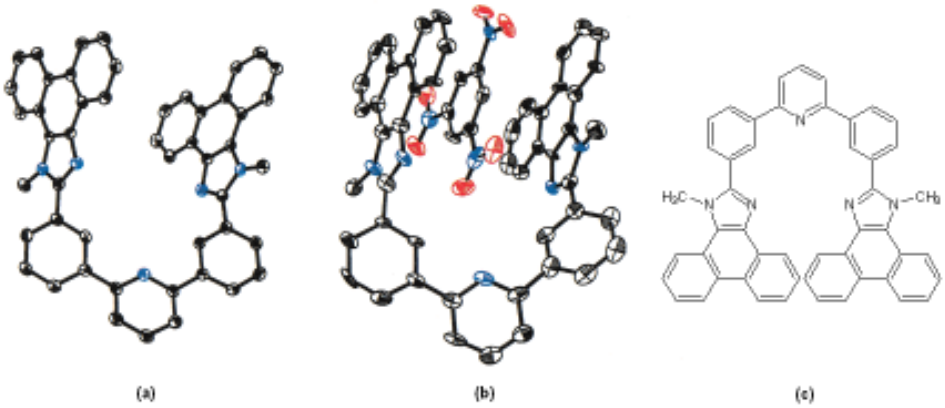

Figure 4.1: Krebs and Jørgensen's molecular tweezer. X-ray crystallography structure of the a) neutral host and b) host with 1,3,5-trinitrobenzene guest molecule, and c) chemical structure of the tweezer.

Krebs and Jørgensen's molecular tweezer has a very similar spacer (**S**) structure with our pH-responsive tweezers. Its **S** group is composed of a phenyl-pyridine-phenyl (Ph-Py-Ph) triad, whereas the latter is composed of a methoxyphenyl-pyridine-methoxyphenyl (MeOPh-Py-MeOPh) triad. Carbon-carbon bond rotation is possible for the former spacer, allowing the

tweezer structure to adopt few conformational states for guest binding. However, as depicted also by the X-ray structures in Figure 4.1, Krebs and Jørgensen's molecular tweezer prefers the benzimidazole-derived, aromatic **IS** to be in close proximity to each other.[1] Guest binding is achieved mainly via π- π interactions with the aromatic **IS**, although other types of interactions such as π-donor or π-acceptor are feasible with appropriate synthetic elaboration.[1]

Synthesis of Krebs and Jørgensen's molecular tweezer follows the "half-tweezer" synthetic route mentioned in the previous chapters, and is illustrated by the following reaction scheme.

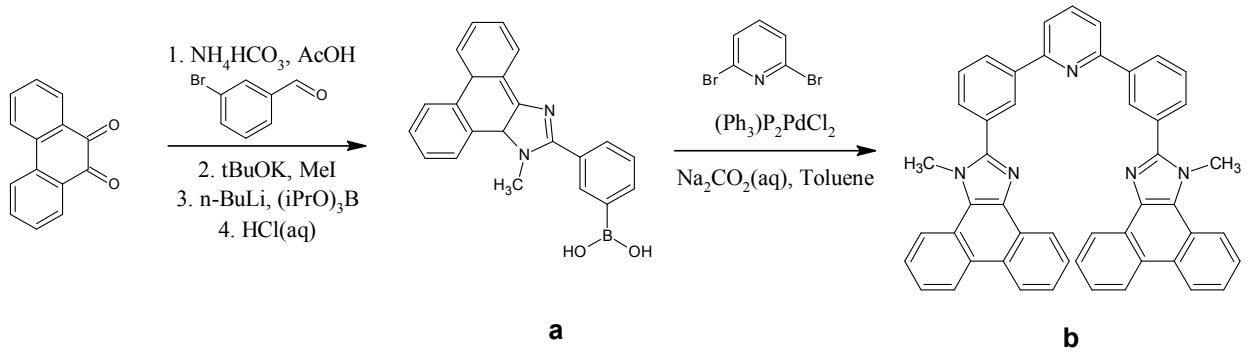

Scheme 4.1: Synthetic route of Krebs and Jørgensen's molecular tweezer.[1]

The half-tweezer, compound 4.1a, is first synthesized in three successive steps: ring condensation of the di-ketone to form the imidazole ring, then methylation, and finally, borylation via halogen-lithium exchange mechanism. The two half-tweezers are then used to assemble the tweezer (compound 4.1b) via Suzuki-Miyaura coupling with 2,6-dibromopyridine.

4.2 Synthesis of the 4th Generation Tweezer

The 4th generation tweezer will also be synthesized using the half-tweezer approach, as outlined in Scheme 4.2. Using the commercially available 5-formyl-2-methoxyphenylboronic acid and *o*-phenylenediamine as starting materials, the benzimidazole **IS** was constructed via ring condensation. The next step is then to protect the boronic acid group via condensation with

pinacol, hence forming its corresponding pinacol boronic ester. Alkylation would then be carried out next, using a tosylate as the alkyl source. Finally, the half-tweezers are assembled into the 4th generation tweezer via Suzuki-Miyaura coupling of 2,6-dibromopyridine with either the alkylated pinacol boronic ester or the alkylated boronic acid. This work was done in collaboration with our summer student, Caitlin Miron.

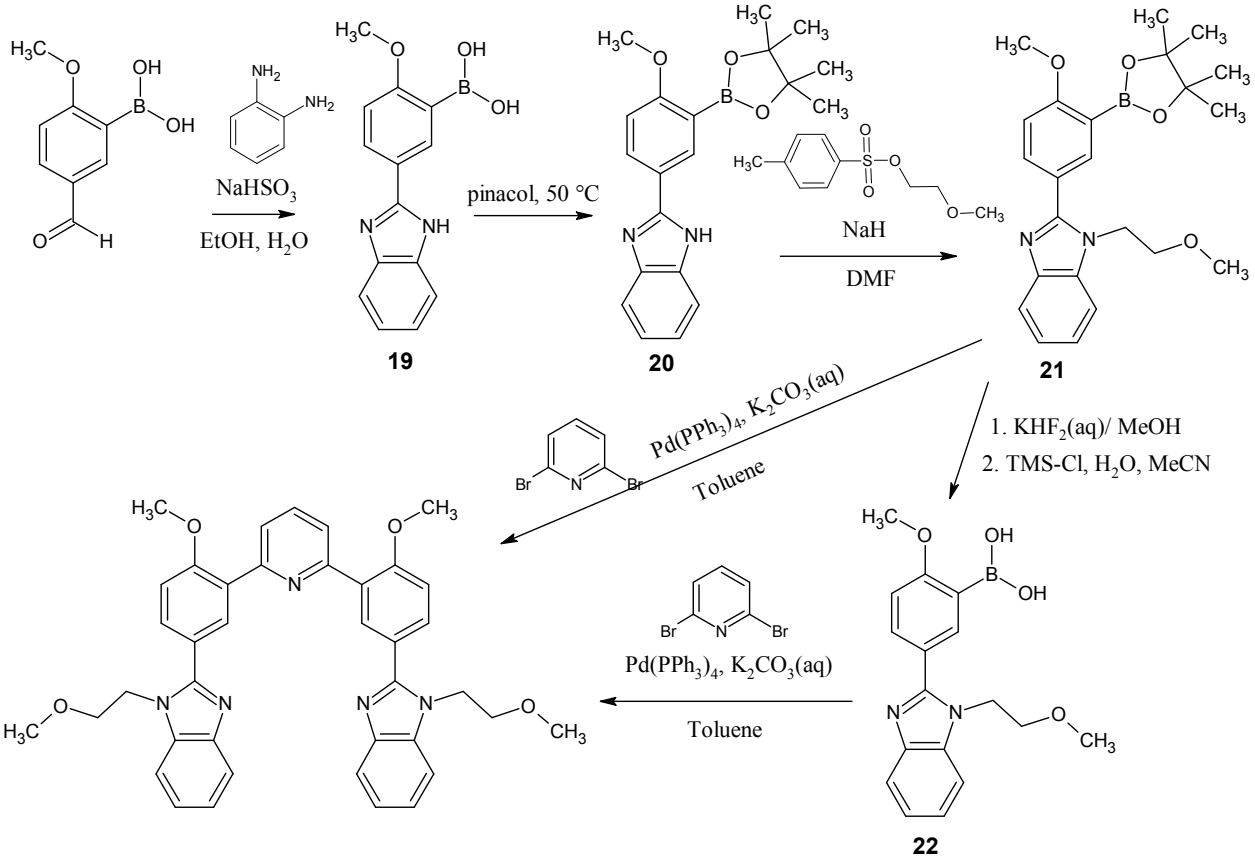

Scheme 4.2: Reaction scheme of the 4th generation tweezer.

4.2.1: Test Reactions: Ring Condensation and Alkylation

Before we proceeded with the synthesis of the 4th generation tweezer, we first carried out two test reactions outlined in Schemes 4.3 and 4.4 to see if the commercially available 5-formyl-2-methoxyphenylboronic acid can be used as a starting material.

To test the ring condensation, we have used the protocol developed by Duffy *et al.* using *p*-anisaldehyde instead of the more expensive boronic acid.[2] In this reaction, the *p*-anisaldehyde and *o*-phenylenediamine in ethanol were combined into an aqueous solution of sodium bisulfite and stirred under reflux for 1 hour. After removing any insoluble material via vacuum filtration, the mother liquor was then evaporated in vacuo to afford the crude product. Purification was achieved via recrystallization in ethyl acetate to afford pure, white crystals, although the yield was only 25 %. Despite the low yield, we have later used this protocol to synthesize our actual benzimidazole-derived **IS**, due to its simplicity and very short reaction times.

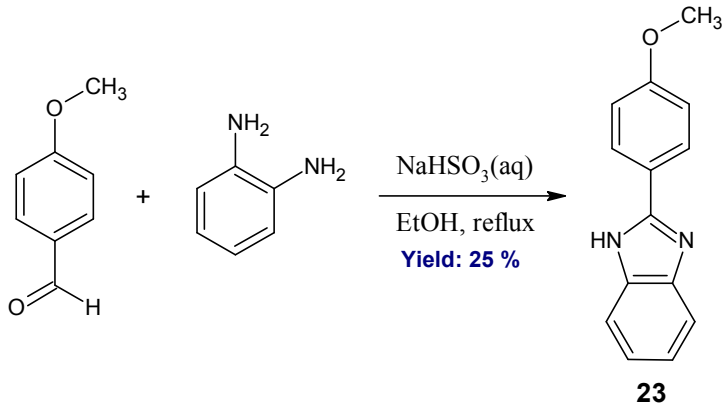

Scheme 4.3: Synthesis of 2-(4'-methoxyphenyl)benzimidazole.[2]

We have then used the product in Scheme 4.3 for the alkylation test. Using the protocol developed by Iemura *et al.*, we have successfully alkylated the 2-(4'-methoxyphenyl) benzimidazole, which required the use of the strong base, sodium hydride (NaH), to deprotonate the N-H group in the benzimidazole ring.[3] In this reaction, a suspension of NaH in DMF was prepared under argon and to this, the 2-(4'-methoxyphenyl)benzimidazole was added, followed by the tosylate. The reaction was performed at 70 ˚C and was complete in 5 hours, upon which, cold MilliQ water was added. The crude product was then isolated via extraction

with ethyl acetate, with good yields (84 %). ^{1}H NMR analysis showed that the crude did not contain any impurities, hence further purifications were avoided.

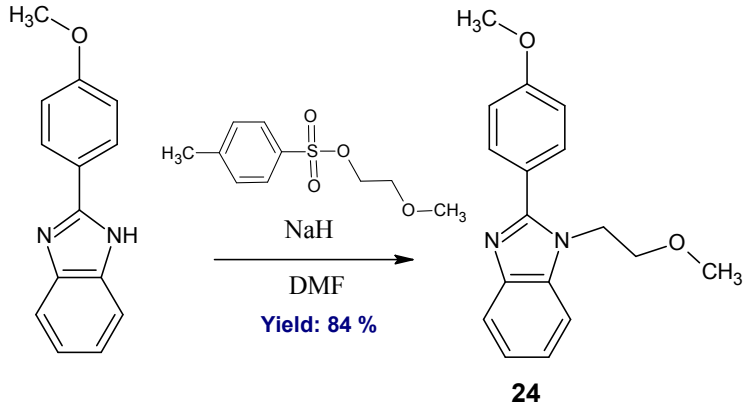

24

Scheme 4.4: Synthesis of 1-(2-methoxyethyl)-2-(4-methoxyphenyl)benzimidazole.[3]

4.2.2: Synthesis of 5[-(1H-1,3-benzodiazol-2-yl)-2-methoxyphenyl]boronic acid (Bim Boronic Acid)

The boronic acid was synthesized according to the protocol used in the test reaction, without any modifications.[2] Once again, the crude isolated via filtration did not contain any other organic impurities as per ^{1}H NMR analysis. Hence, it was not subjected into further purifications.

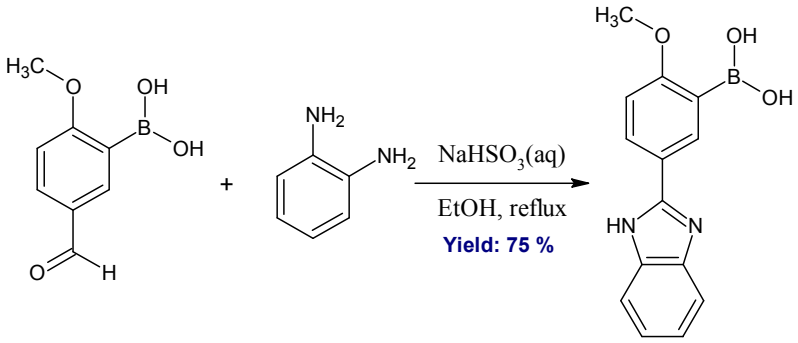

19

Scheme 4.4: Synthesis of 5[-(1H-1,3-benzodiazol-2-yl)-2-methoxyphenyl]boronic acid.[2]

4.2.3: Synthesis of 2-[4-methoxy-3-(tetramethyl-1,3,2-dioxaborolan-2-yl)phenyl]-1H-1,3-benzodiazole (Bim Pinacol Boronic ester)

Before the alkylation step was carried out, we have protected the boronic acid group by converting it to its corresponding pinacol ester. This is necessary in order to ensure that the alkylation proceeds only in the NH group of the benzimidazole ring, as the boronic acid group may be deprotonated and become a nucleophile itself. To generate our pinacol boronic ester, we have first tested the protocol developed by Morandi *et al.*, which involved a reaction of the corresponding boronic acid with pinacol using THF as a solvent at room temperature.[4] However, our Bim boronic acid is poorly soluble in THF, and to aid the reaction, we have carried out the reaction at 50 ˚C, instead of RT, as suggested by the literature protocol. We have also extended the reaction time to 24 hours instead of 1 hour. However, as per ^{1}H NMR analysis, the reaction still did not reach completion. Approximately 1 equivalent of boronic ester and 0.2 equivalents of boronic acid were present in the crude.

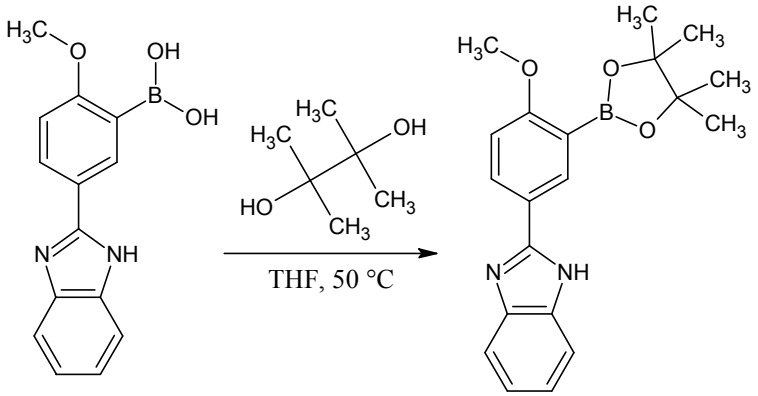

20

Scheme 4.5: First attempt at the synthesis of Bim pinacol boronic ester.[4]

We have initially hypothesized that the reaction was incomplete because of the poor solubility of the Bim boronic acid in THF. To confirm this hypothesis, we have therefore replaced the solvent with deuterated methanol, and carried the reaction at a micro scale in order to also

monitor its progress via ^{1}H NMR analysis. Even with excellent solubility in methanol, the reaction was still unable to reach completion. We therefore hypothesized that the water produced as a side product of the reaction may be responsible, similar to the reversible reaction of the formation of carbon-based esters.

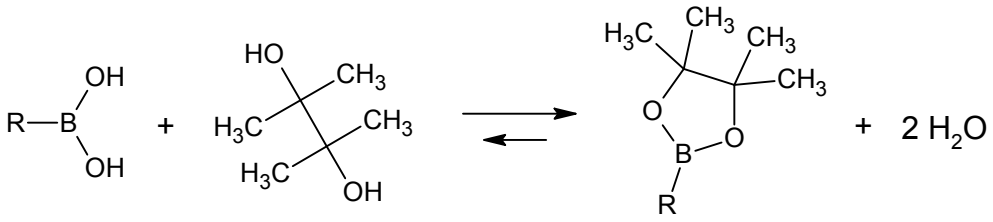

Scheme 4.6: Esterification of boronic acids.

To remedy this problem, we have increased the concentration of the pinacol in the solution in order to push the equilibrium towards the formation of the boronic ester. As predicted, esterification proceeded in greater yields. Eventually, we have decided to use pinacol as our solvent in order to optimize the pinacol concentration in solution. Since pinacol melts at 40 ˚C, we have to first heat the reaction mixture in order to melt the pinacol and obtain a solution.

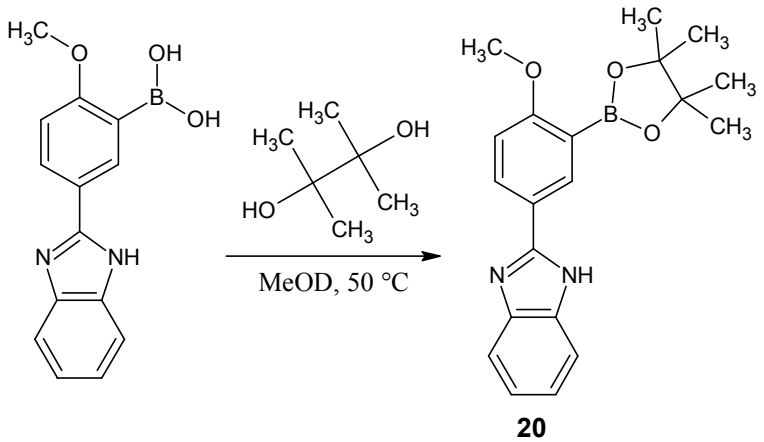

20

Scheme 4.7: Second attempt at the synthesis of Bim pinacol boronic ester.[4]

Our first attempt at using pinacol as our solvent required an overnight heating of the reaction mixture at 50 ˚C. However, the reaction did not proceed into completion and about 20 % of the boronic acid still remained in the crude. In our next attempt, we have increased the temperature of the reaction to 80 ˚C, while still carrying it out for ~24 hours. Surprisingly, the Bim boronic acid was only present in trace amounts in the crude as per ^{1}H NMR analysis. We were also successful in removing the trace Bim boronic acid via precipitating it in acetone (since the Bim pinacol boronic ester was highly soluble in acetone). The Bim boronic acid was removed via vacuum filtration, while evaporation of the filtrate in vacuo gave the pure Bim pinacol boronic ester product in good yields.

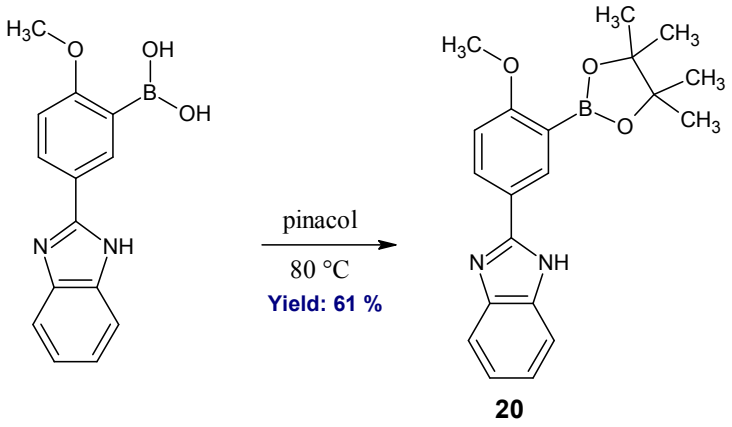

20

Scheme 4.8: Third and final attempt at the synthesis of Bim pinacol boronic ester.

4.2.4: Synthesis of 1-(2-Methoxyethyl)-2-[4-methoxy-3-(4,4,5,5-tetramethyl-[1,3,2]dioxa-borolan-2-yl)-phenyl]-1*H*-benzoimidazole (Alkyl Bim pinacol boronic ester)

Alkylation of the Bim pinacol boronic ester was carried out according to the protocol used in the test reaction, but with slight modifications.[3] The reaction time was increased to 4 days, and heating was performed for 20 hours instead of only 5 hours. The ^{1}H NMR spectrum of the crude solid contained many overlapping peaks thus, is impossible to ascertain whether the reaction has gone to completion. TLC also did not give conclusive results as the Rf values of the

starting materials and the products were nearly identical, and the spots tend to smear under the conditions used. Thus, we pursued further purification of the sample in order to properly identify the product of interest.

After work-up procedures (see Chapter 5), we have obtained a yellow oil as our crude sample. Hexanes were added to this oil in an attempt to remove the unreacted tosylate, however, we were surprised to see the formation of a white precipitate, which was later isolated via vacuum filtration. After a ^{1}H NMR analysis of this precipitate, we found out that it actually contained the Bim boronic ester starting material, while the oil recovered from the filtrate contained our desired product. However, this oil still contained impurities, namely the tosylate starting material, plus an unknown impurity that we believe to be the alkylated Bim Boronic acid. It is possible that the alkylated Bim pinacol boronic ester has been hydrolyzed to its corresponsing boronic acid due to water during work-up. In an attempt to further purify the oil, we have resorted to column chromatography in silica medium and using 1:1 acetone/hexanes as the eluent. However, the procedure failed, which is most likely due to the high polarity of the eluent used. Further purification attempts were put on hold because there was not enough material left (only 100 mg of recovered crude) and also due to time constraints. It is therefore recommended that the polarity of the eluent be decreased in the next column chromatography purification attempts, in order to avoid getting mixed fractions.

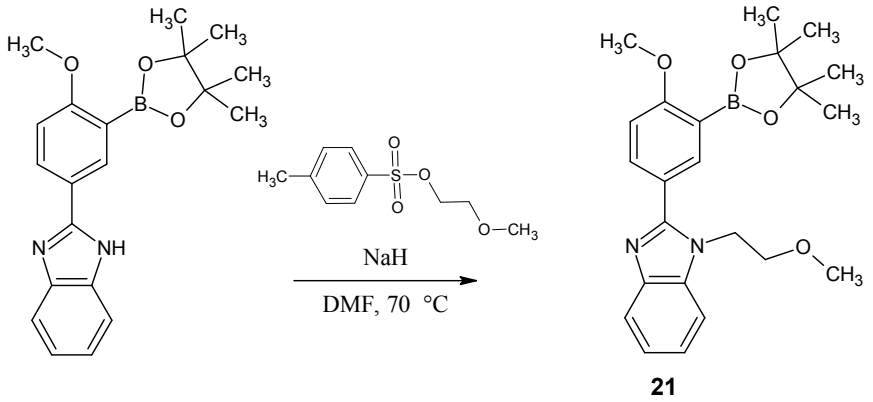

21

Scheme 4.9: Alkylation of Bim pinacol boronic ester.[3]

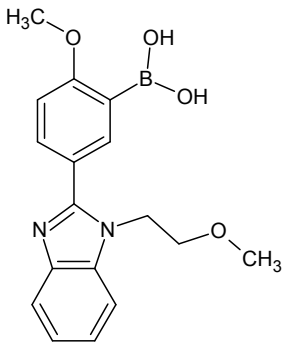

22

Figure 4.2: Alkylated Bim boronic acid (proposed side-product).

4.2.5: Assembling the 4th Generation Tweezer

Using the crude Alkyl Bim boronic ester, we have attempted to synthesize our 4th generation tweezer using the Suzuki-coupling protocol used by Leblond *et al.* in the synthesis of the 1st generation tweezer.[5] The reaction was carried out under microwave conditions in order to minimize the formation of the mono-substituted product.

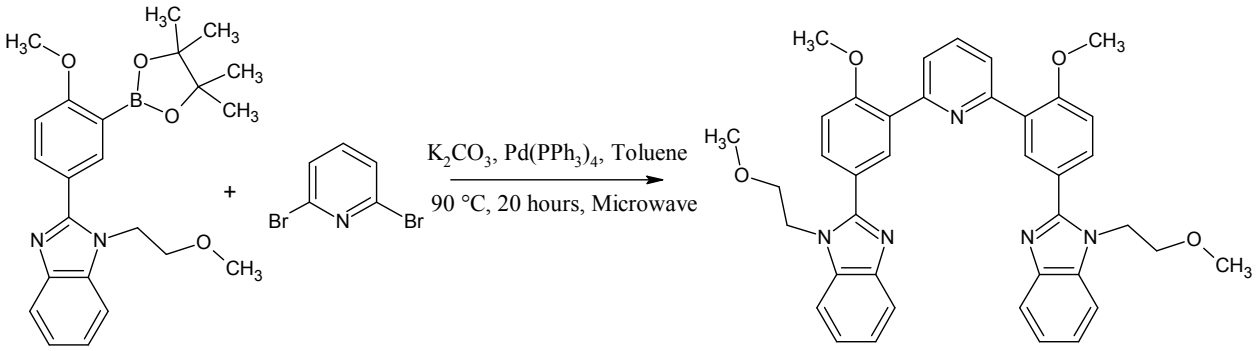

21 **25**

Scheme 4.10: Microwave- assisted synthesis of the 4th generation tweezer.[5]

Prior to work-up, a small aliquot of the sample (with the solvent removed via evaporation in vacuo) was analyzed with ^{1}H NMR. The spectrum was impossible to analyze as it is filled with

many overlapping peaks, especially in the aromatic region, that belonged to the starting materials, catalyst, and new products.

To properly analyze the mixture, we have tried to separate its components using preparative TLC (SiO_2 plate). Using 1.3: 0.7 hexanes/ acetone as eluent, we were able to partially separate the components of the mixture, but not very successfully. Streaking of the sample in the TLC plate was observed, which resulted in the contamination of some fractions. However, the purity of the fractions was enough to provide a much resolved ^{1}H NMR spectrum.

We have found by ^{1}H NMR that the fraction at Rf = 0.36 contained new species (since their chemical shifts are different from the starting materials) that might belong to our 4th generation tweezer. As proof, the ^{1}H NMR spectrum was fairly symmetric in the aromatic region, and the characteristic triplet from the central pyridine ring was present, suggesting that the di-bromopyridine has been successfully coupled to the alkyl Bim boronic ester. Although there is a possiblility that this triplet belongs to the mono-substituted product, it is less likely because we only observe one set of signals that correspond to the methoxyphenyl ring of the **S** group. If it was the mono-substituted tweezer, however, we should see two sets of these signals in the aromatic region.

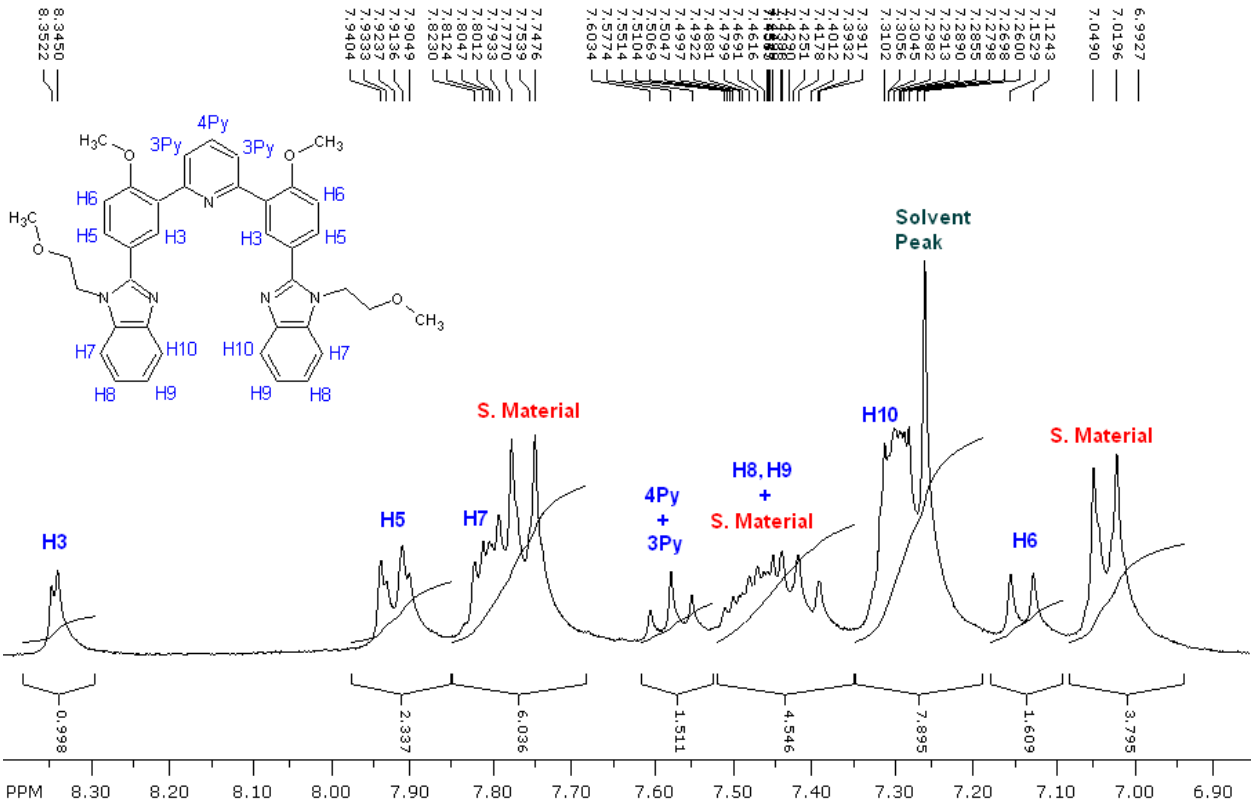

Figure 4.3: ^{1}H NMR spectrum of the aromatic region of the 4th generation tweezer test reaction. (300 MHz, $CDCl_3$, 25 ˚C).

In the aliphatic region, we can clearly observe the disappearance of the singlet that corresponds to the CH_3 groups from the pinacol protecting group of the Alkylated Bim boronic ester. We can also see the presence of the triplets at δ = 3.77 and δ = 4.40 that represents the CH_2 groups of the alkyl chain (Note that their δ is different from what is observed in the starting materials. However, just like in the starting material, we observe two sets of singlets that should correspond to the $–OCH_3$ groups of the alkyl chain and the methoxyphenyl group. The singlets have slightly different chemical shifts than the starting materials, which makes it very difficult to identify which peaks belong to the 4th generation tweezer. Correlation between the peaks were verified with 2D NMR (COSY) analysis.

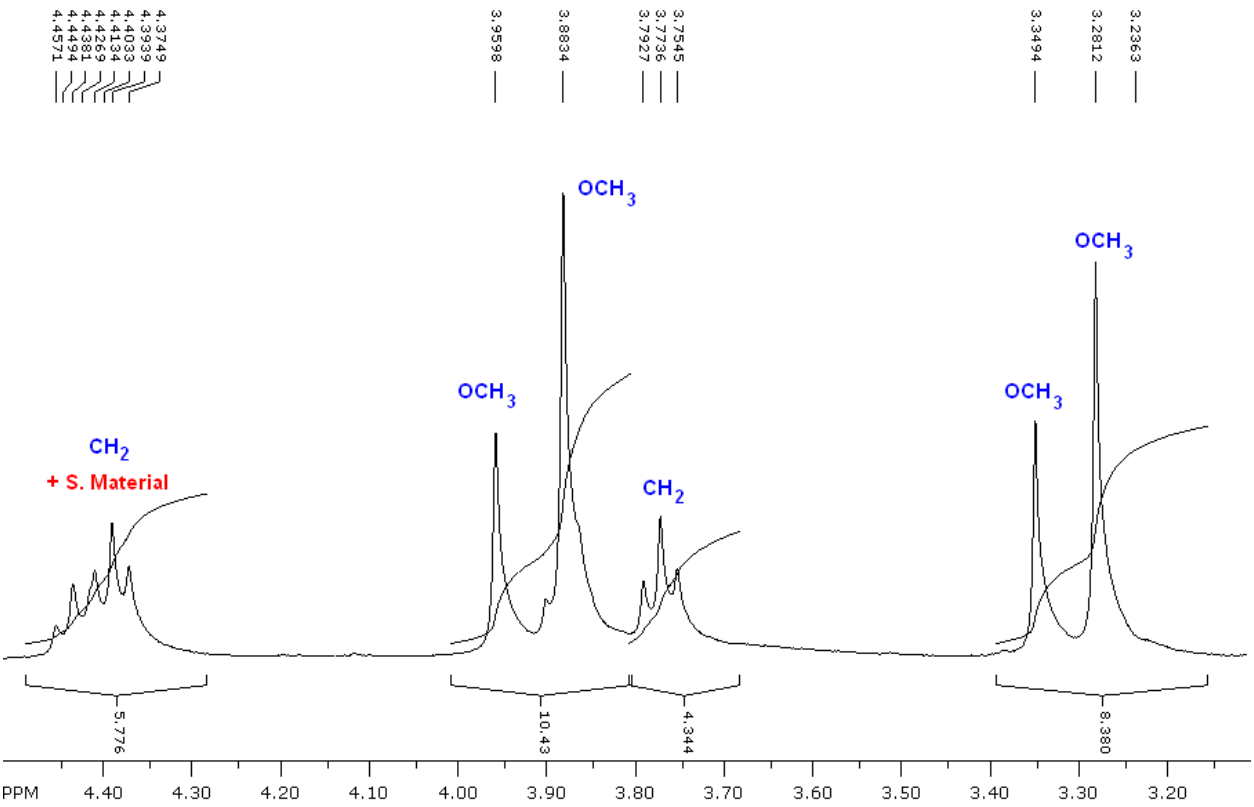

Figure 4.4: ^{1}H NMR spectrum of the aliphatic region of the 4th generation tweezer test reaction. (300 MHz, $CDCl_3$, 25 ˚C). Note: There are four OCH_3 groups present in the spectrum, but we still do not know which one actually belongs to the 4th generation tweezer.

4.3 Conclusion

The 4th generation tweezer was likely synthesized based on the ^{1}H NMR studies conducted. However, the reaction still needs more work and further optimization is highly required especially in the purification process. It is highly recommended therefore, that impurities be removed from the starting materials before carrying out the tweezer reaction to avoid complicated mixtures that are difficult to separate, and to achieve an accurate determination of the yield of the reaction.

References:

1. Krebs, F. C.; Jørgensen, M. *J. Org. Chem.* **2001**, 66, 6169-6173
2. Duffy, K.J.; Price, A.T.; Delorme, E.; Dillon, S.B.; Duquenne, C.; Erickson-Miller, C.; Giampa, L.; Huang, Y.; Keenan, R.M.; Lamb, P.; Liu, N.; Miller, S. G.; Rosen, J.; Shaw, A.N.; Smith, H.; Wiggall, K.J.; Zhang, L.; Luengo, J.I. *J. Med. Chem.* **2002**, 45, 3576-3578
3. Iemura, R.; Kawashima, T.; Fukuda, T.; Ito, K.; Tsukamoto, G. *J. Med. Chem.* **1986**, 29, 1178-1181
4. Morandi, S.; Caselli, E.; Forni, A.; Bucciarelli, M.; Torre, G.; Prati, F. *Tet. Asymm.* **2005**, 16, 2918-2926
5. Leblond, J.; Gao, H.; Petitjean, A.; Leroux, J.-C. *J. Am. Chem. Soc.* **2010**, 132, 8544-8545

Chapter 5
Experimental Section

5.1 General Methods

Commercially available compounds were purchased from Aldrich, Alfa Aesar, and Acros Organics and were used as received, with an exception to the 2,7-dihydroxynaphthalene which was re-crystallized in toluene prior to use. Anhydrous dichloromethane, tetrahydrofuran, and acetonitrile were dried by passing through an activated alumina column according to the manufacturer's instructions (Innovative Technology). Anhydrous dimethylformamide was purchased from EMD (DriSolv) and degassed by bubbling argon into it. All reactions were performed under Argon (Ar) unless stated otherwise. Deuterated solvents (Cambridge Isotopes) were used as received. ^{1}H NMR and ^{13}C NMR were performed using 300 MHz, 400 MHz, and 500 MHz Bruker instruments. Peak listings for all NMR spectra are given in ppm and referenced against the solvent residual signal. Thin layer chromatography (TLC) analysis was performed on *EMD Inc. silica gel* with a pore diameter of 60 Angstroms or activated basic Aluminum oxide with a pore diameter of 58 Angstroms. Column chromatography was performed with *Silia-P flash silica gel* with a particle size of 40-63 μm and a pore diameter of 60 Angstroms. Melting points were recorded on a MEL-TEMP (laboratory Device.USA) apparatus. Mass spectrometry was performed on a Waters/Micromass GC-TOF EI-MS or ESI –MS spectrometer. Elemental analyses were conducted at the Elemental Analysis service at the Université de Montréal.

5.2 Experimental Details

N,N'-bis(4-methylphenyl)pyridine-2,6-dicarboxyamide[1]

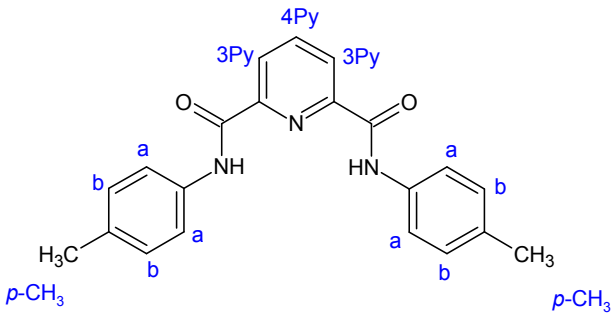

Picolinic acyl chloride (0.217 g, 1.06 mmol) was dissolved in 5 mL DCM. Any insoluble material was removed via vacuum filtration. Then, the solvent was evaporated from the filtrate in vacuo, giving a cream-coloured solid (0.210 g, 97 %).

The recovered acyl chloride (0.210 g, 1.03 mmol, 1 equiv) was dissolved in dry DCM under argon. The resulting peach coloured solution was cooled to 0 °C. While stirring, *p*-toluidine (0.566 g, 5.28 mmol, 5 equiv) was added to it as a solid, resulting in precipitate formation. The reaction mixture was stirred at 0 °C for another 2 hours, and then warmed to RT. Dry triethylamine (0.36 mL, 2.57 mmol, 2.5 equiv) was added, turning the cloudy peach solution into a clear brown mixture. The reaction mixture was further stirred at RT for 2 hours then heated to 40 °C for 2 more hours. Finally, the solution was stirred at RT for 1 hour.

The resulting solution was washed with saturated $NaHCO_3$ (5 mL) then with 2 x 5 mL of MilliQ water. The aqueous extracts were combined and washed with 3 x 5 mL DCM. All organic portions were combined then dried with Na_2SO_4. Finally, the solvent was removed in vacuo, giving a peach-coloured precipitate. Re-crystallization of the crude solid in absolute ethanol afforded white, needle-shaped crystals (0.192 g, 54 %). **TLC** (SiO_2, EtOAc/$CHCl_3$ 4:1); Rf= 0.53. **^{1}H NMR** (300 MHz; $CDCl_3$): 2.34 (s, 6 H, *p*-CH_3), 7.17 (d, 4 H; ^3J = 9 Hz, Hb), 7.62 (d, 4 H; ^3J = 9 Hz, Ha), 8.09 (t, 1 H; ^3J = 9 Hz, H4py), 8.45 (d, 2 H, ^3J = 9 Hz, H3py), 9.49 (s, 2 H, NH). **^{13}C NMR** (100 MHz; $CDCl_3$) δ 21.08, 120.5, 125.5, 129.8, 134.7, 134.8, 139.5, 149.2, 161.3. **Elemental Analysis:** Anal. Calc'd for $C_{21}H_{19}N_3O_2$: C, 73.03; H, 5.54; N, 12.17; Found: C, 72.75; H, 5.28; N, 12.00. **EI$^+$-MS:** calculated for $C_{21}H_{19}N_3O_2$: 345.15; found: 345.15 $[M]^+$, 212.10 [M-

$C_8H_8NO]^+$, 185.08 [M- $C_{10}H_{10}NO]^+$, 106.06 [M-$C_{14}H_{11}N_2O_2]^+$, 77.04 [M- $C_{15}H_{15}N_3O_3]^+$. **Melting Point:** 221.5-222.5 ˚C.

1-Bromonaphthalene-2,7-diol (Compound 1)[3]

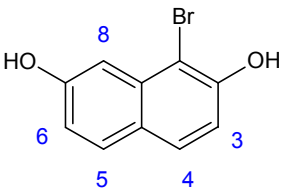

A suspension of 2,7-dihydroxynaphthalene (2.02 g, 12.6 mmol, 1 equiv) was prepared in 355 mL DCM. While stirring, the bromine solution (0.65 mL, 13.0 mmol in 185 mL of DCM, 1.03 equiv) was added dropwise using a dropping funnel. The addition took place for 4.5 hours, producing a clear yellow-orange solution. Then, the solution was concentrated in vacuo to ~ 5 % of its original volume. The white precipitate was isolated via suction filtration, washed with hexanes, and then dried under high vacuum (2.46 g, 81 %). Further purifications were not performed because the ^{1}H NMR analysis showed a clean spectrum. **TLC** (SiO_2, DCM/MeOH 2:0.1); Rf = 0.25. **^{1}H NMR** (300 MHz; $CDCl_3$): 5.18 (s, 1 H, OH), 5.88 (s, 1 H, OH), 6.99 (dd, 1 H; ^4J = 2.4, ^3J = 8.8 Hz, H6), 7.11 (d, 1 H; ^3J = 8.8 Hz, H3), 7.36 (d, 1 H, ^4J = 2.3 Hz, H8), 7.67 (t, 2 H; ^3J = 9.4 Hz, H4, H5).

2-Methoxyethyl-4-methoxybenzene sulfonate (Compound 2)[4]

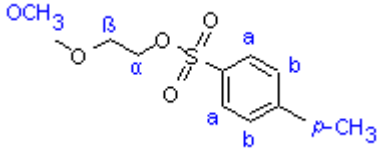

A solution of 2-methoxyethanol (5.0 mL, 63.0 mmol, 1 equiv) in 50 mL THF was prepared. To this a separate solution of NaOH (3.87 g, 96.7 mmol, 1.5 equiv) in 50 mL MilliQ water was added while stirring. The alcohol/base solution was then cooled to 0 °C using an ice/salt bath. Another solution, composed of *p*-toluenesulfonyl chloride (12.1 g, 63.6 mmol, 1.01 equiv) in 50 mL THF was prepared. Using a dropping funnel, this solution was added dropwise to the cooled alcohol/base solution. The temperature was carefully monitored so that it would not exceed 5 °C during the addition process, which took ~1 hour to complete. The entire mixture was further stirred for 3 hours under the same temperature conditions. THF

from the mixture was then removed in vacuo. Then, 150 mL of ice- water mixture was added to it, producing a cloudy-white solution that was extracted with 3 x 80 mL DCM. All of the organic extracts were combined, washed with distilled water and then with brine. After drying with Na_2SO_4, the solvent was removed in vacuo, yielding clear, pale yellow oil (11.1 g, 76 %). No further purifications were made as the ^{1}H NMR analysis showed a clean spectrum. ^{1}**H NMR** (300 MHz; $CDCl_3$): 2.43 (s, 3 H, *p*-CH_3), 3.29 (s, 3 H, OCH_3), 3.56 (t, 2 H; ^3J = 4.5 Hz, ß), 4.15 (t, 2 H; ^3J = 4.8 Hz, α), 7.34 (d, 2 H, ^3J = 8.1 Hz, Hb), 7.79 (d, 2 H; ^3J = 8.1 Hz, Ha).

2-(2-Methoxyethoxy)ethyl-4-methylbenzene sulfonate (Compound 3)[5]

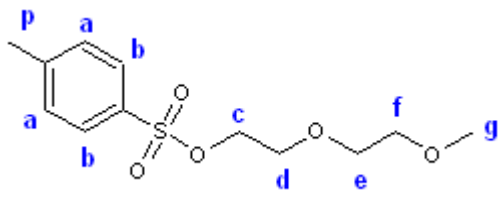

In an Erlenmeyer flask, a solution of NaOH (6.05 g, 0.150 mol, 1.5 equiv) in 20 mL MilliQ water was combined with a solution of 2-(2-methoxyethoxy) ethanol (12.0 g, 0.10 mol, 1 equiv) in 120 mL THF. To this, a solution of *p*-toluenesulfonyl chloride (22.0 g, 0.10 mol) in 30 mL THF was added dropwise, while maintaining the temperature between 0-5 ˚C throughout the addition process. Once the addition was complete, the reaction mixture was then stirred at 0 ˚C for 3 hours.

The solvent was removed in vacuo, while 50 mL of MilliQ water was added to the remaining liquid. Extraction was performed, using 3 x 20 mL DCM. All organic layers were combined, washed with 100 mL of 10 % HCl, 100 mL brine, then finally dried with Na_2SO_4. After Na_2SO_4 was removed via vacuum filtration, the filtrate was evaporated in vacuo to afford a clear, colourless oil (26.7 g, 97 %). No further purifications were made as the ^{1}H NMR analysis showed a clean spectrum. ^{1}**H NMR** (300 MHz; $CDCl_3$): 2.45 (s, 3 H, Hp), 3.35 (s, 2 H, Hg), 3.49 (m, 2 H, Hf), 3.58 (m, 2 H, He), 3.69 (t, 2 H, ^3J = 4.8 Hz, Hd), 3.93 (t, 2 H, ^3J = 4.8 Hz, Hc), 7.34 (d, 2 H, ^3J = 8.1 Hz, Ha), 7.80 (d, 2 H, ^3J = 8.1 Hz, Hb).

1-Bromo-2,7-bis(2-methoxyethoxy) naphthalene (UNIT 1 PEG, Compound 4)[6]

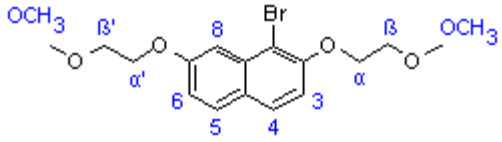

A solution of 1-bromonaphthalene-2,7-diol (2.01 g, 8.39 mmol, 1 equiv), 2-methoxyethyl-4-methoxy-benzene sulfonate (4.84 g, 21.0 mmol, 2.5 equiv) and K_2CO_3 (3.81 g, 27.6 mmol, 3.3 equiv) in 19 mL acetonitrile was prepared. The cloudy grey solution was refluxed at 82 °C overnight, then the K_2CO_3 precipitate was isolated via suction filtration, then washed with 50-60 mL of acetonitrile. The filtrate was collected and the solvent was removed under reduced pressure, yielding a mouldy green oily residue. The oily residue was re-dissolved in 30 mL DCM, washed until the aqueous layer is no longer blue (used 3 x 20 mL MilliQ water). All aqueous extracts were combined, then washed with 2 x 10 mL DCM. All organic extracts were combined and dried with Na_2SO_4. Finally, the solvent was removed in vacuo, giving a mouldy green oily residue. The crude product was re-crystallized with 95 % EtOH and activated charcoal, yielding yellow fibrous crystals (2.45 g, 82 %). **^{1}H NMR** (300 MHz; $CDCl_3$): 3.49 (s, 3 H, -OCH_3), 3.51 (s, 3 H, -OCH_3), 3.83-3.86 (m, 4 H, ß, ß' CH_2), 4.29-4.32 (m, 4 H, α, α' CH_2), 7.09-7.14 (m, 2 H, H3, H6), 7.52 (d, 1 H; ^4J = 2.3 Hz, H8), 7.67 (d, 1 H; ^3J = 8.6 Hz, H4), 7.70 (d, 1 H; ^3J = 8.6 Hz, H5). **^{13}C NMR** (100 MHz; $CDCl_3$) δ 59.38, 59.61, 67.43, 70.00, 71.07, 71.28, 105.8, 109.0, 113.2, 117.8, 125.7, 128.7, 129.9, 134.7, 154.0, 158.6. **Elemental Analysis:** Anal. Calc'd for $C_{16}H_{19}O_4Br$: C, 54.10; H, 5.39; Found: C, 54.29; H, 5.23. **EI$^+$-MS:** calculated for $C_{16}H_{19}$ O_4Br: 354.05; found: 354.05 $[M]^+$, 296.02 $[M\text{-}C_3H_7O]^+$, 237.97 $[M\text{-}\ C_6H_{14}O_2]^+$, 59.05 $[M\text{-}C_{13}H_{12}O_3Br]^+$. **Melting Point:** 56-57°C.

1-Bromo-2,7-bis(2-(2-methoxyethoxy)ethoxy) naphthalene (UNIT 2 PEG, Compound 5)[6]

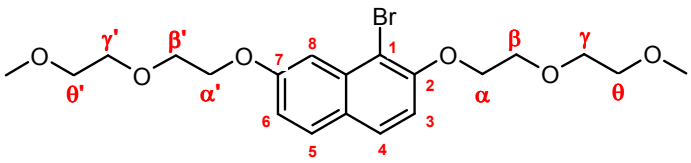

In a round-bottom flask, a solution of 1-bromo-2,7-dihydroxy-naphthalene (1.02 g, 4.28 mmol, 1 equiv.), 2-(2-methoxyethoxy)ethyl-4-methylbenzene sulfonate (3.54 g, 12.9 mmol, 3.0 equiv), and potassium

carbonate (1.93 g, 13.9 mmol, 3.3 equiv) in 17 mL was prepared. The solution was refluxed at 82 ^{o}C overnight, and then the K_2CO_3 precipitate was removed via vacuum filtration and washed with MeCN (~ 30 mL) until no colour was observed in the residue. The filtrate was then evaporated in vacuo to yield a brown oil. The crude product was dissolved in DCM (30 mL); the solution was transferred into a separatory funnel and washed with MilliQ water (15 mL increments) until no colour was observed in the aqueous phase. The combined aqueous extracts were washed with DCM (2 x 15 mL). The organic layers were combined and dried using Na_2SO_4. After removal of Na_2SO_4 via vacuum filtration, the filtrate was evaporated in vacuo to produce a brown oil (1.54 g, 81 %). By ^{1}H NMR, this oil contained approximately 0.75 equiv. of tosylate reagent, 0.75 equiv. of tosylate anion, and 1.0 equiv. of the expected product.

Purification of 1-bromo-2,7-bis(2-(2-methoxyethoxy)ethoxy) naphthalene (UNIT 2 PEG)[7]

A mixture of 1-bromo-2,7-bis(2-(2-methoxyethoxy)ethoxy) naphthalene (~1.00 g, 2.25 mmol, 1 equiv) and 2-(2-methoxyethoxy)ethyl-4-methylbenzene sulfonate (~1.30 g, 3.93 mmol, 1.7 equiv) was treated with 40 % methylamine in 1.6 mL water. The mixture was refluxed while vigorously stirring at 50 ^{o}C for 3-4 hours and then at room temperature for another 4 days. The solution was acidified with 0.1 M HCl (~ 0.5 mL), and then rinsed with 2 mL MilliQ water along with ~ 2 mL of DCM. The organic layer was further washed with 1-2 mL increments of 0.1 M NaOH, MilliQ water, 0.1 M HCl, and finally MilliQ water again. The extracted organic layer was dried with excess sodium sulphate, filtered to remove the drying agent, and concentrated to give a golden brown oil (0.836 g, 84 %). By NMR, this product still contains a small fraction of the tosylate anion but the trace amounts were not judged significant enough to attempt further purification of the oil. **TLC** (SiO_2 with DCM + 3 drops Et_3N, 1% MeOH in DCM + 2 drops Et_3N); Rf = 0.40 ^{1}**H NMR** (300 MHz; $CDCl_3$): 3.39, 3.40 (two overlapping s, 6H, O-CH_3), 3.59 (m, 4 H,

Hθ), 3.79 (dm, 4 H, Hγ), 3.95 (m, 4 H, Hβ), 4.32 (m, 4 H, Hα), 7.09 (m, 2 H, H3, H6), 7.50 (d, 1 H ; ^4J = 2.3 Hz, H8), 7.67 (m, 2 H, H4, H5).

2,6-Bis(5-bromo-2-methoxyphenyl) pyridine (MeOPh-Py-MeOPh, Compound 6)[2]

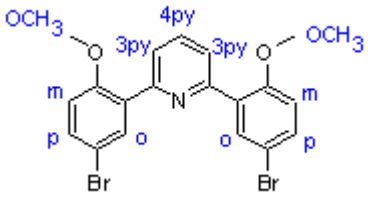

A solution consisting of 2.12 M Na_2CO_3 (4 mL, 8.48 mmol, 2.4 equiv), 3.5 mL of 95% EtOH, 5-bromo-2-methoxyphenyl boronic acid (1.71 g, 7.42 mmol, 2.1 equiv), 2,6-dibromopyridine (0.845 g, 3.57 mmol, 1 equiv) and 8.5 mL of toluene was degassed under high vacuum, and then purged with argon gas. While stirring, tetrakis(triphenylphosphine)palladium ($Pd(PPh_3)_4$, 12 mg, 1.04 x 10^{-5} mol, 3 x 10^{-3} equiv) was added to the degassed solution and the resulting mixture was purged again with argon gas. After that, the reaction mixture was refluxed under argon at 75 °C overnight. Then, it was stirred at room temperature for 1 more day, while still under argon. MilliQ water (85 mL) and EtOAc (110 mL) were then added, the organic layer was isolated, while the aqueous layer was further extracted with 3 x 30 mL EtOAc. All organic extracts were combined, washed with brine, and then dried with Na_2SO_4. Finally, the solvent was removed in vacuo yielding a yellow-orange residue. Recrystallization of the crude in 95 % EtOH afforded peach-coloured crystals (0.952 g, 60 %). ^{1}**H NMR** (300 MHz; $CDCl_3$): 3.87 (s, 6 H, OCH_3), 6.89 (d, 2 H; ^3J = 8.8 Hz, Hm), 7.46 (dd, 2 H; ^4J = 2.6, ^3J = 8.8 Hz, Hp), 7.73-7.76 (m, 3 H, H3py, H4py), 8.00 (d, 2 H; ^4J = 2.6 Hz, Ho).

Triad di-boronic ester (Compound 7)[9]

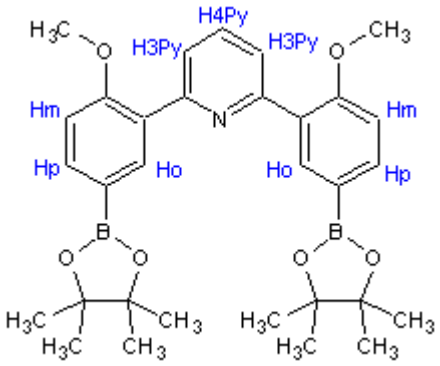

In a flame-dried round bottomed flask, 2,6-bis(5-bromo-2-methoxyphenyl) pyridine (0.672 g, 1.50 mmol, 1 equiv), bis(pinacolato) diboron (1.21 g, 4.78 mmol, 3.2 equiv), potassium acetate (0.907 g, 9.24 mmol, 6.2 equiv) and bis-[(diphenylphosphino)ferrocene]dichloropalladium(II) ($PdCl_2$(dppf), 0.164 g, 0.225 mmol, 0.15 equiv) were all combined. The solid mixture was then degassed via cycle of argon purge in high vacuum for 30 min. Then, 10 mL of previously degassed dry DMF was added, producing a yellow orange solution, which was degassed again for 15 min by bubbling argon into it. Finally, reaction mixture was heated to 80˚C for 24 hours. The reaction mixture was filtered through Celite™, obtaining a black precipitate which was rinsed with 100 mL EtOAc and 50 mL MilliQ water . The bi-phasic filtrate was then poured into a separatory funnel and the organic portion was isolated. The remaining aqueous layer was further extracted with 3 x 30 mL EtOAc. All organic extracts were then combined, washed with 3 x 50 mL MilliQ water , 50 mL brine, and dried with Na_2SO_4. After removal of Na_2SO_4 via filtration, the filtrate was evaporated in vacuo to give a brown, oily residue. Purification of the crude was achieved via recrystallization with toluene/hexanes (5:10 mL). No crystals formed, but instead a brown suspension, which was later isolated via vacuum filtration using a fine-porosity filter paper (0.365 g, 46 %). ^{1}**H NMR** (300 MHz; $CDCl_3$): 1.32 (s, 24 H, CH_3), 3.90 (s, 6 H, OCH_3), 6.99 (d, 2 H, ^3J = 8.1 Hz, H_m), 7.59 (d, 2 H; ^3J = 6.6 Hz, H_3Py), 7.67 (m, 1 H, H_4Py), 7.81 (dd, 2 H, ^3J = 8.1, ^4J = 1.5 Hz, Hp), 8.20 (d, 2 H, ^4J = 1.5 Hz, Ho).

Triad Trifluoroborate Salt (Compound 8)[10]

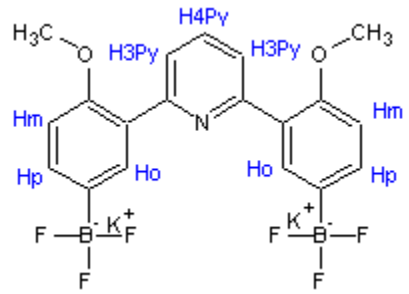

In a plastic round bottomed flask, the triad diboronic ester (0.365 g, 0.672 mmol, 1 equiv) was dissolved in 10 mL methanol and 5 mL DMF. While stirring under open atmosphere, 5 mL of 4.5 M of potassium hydrogen fluoride (KHF_2, 1.76 g, 22.5 mmol, 33 equiv) was added dropwise, immediately forming a white precipitate. The resulting slurry was then stirred at RT for 1.5 hour. The precipitate was removed via vacuum filtration and rinsed with hot acetone. The filtrate was evaporated in vacuo to give a brown solid, which was immediately recrystallized in acetone/ether (5:15 mL). The resulting brown precipitate was then isolated via vacuum filtration and rinsed with ether (0.132 g, 40 %). **^{1}H NMR** (300 MHz; Acetone-d_6): 3.85 (s, 6 H, OCH_3), 6.88 (d, 2 H, ^3J = 8.1 Hz, H_m), 7.48 (d, 2 H, ^3J = 8.1 Hz, H_3Py), 7.65 (t, 1 H, ^3J= 8.4 Hz , H_4Py), 7.85 (d, 2 H, ^3J = 7.8 Hz, Hp), 8.42 (s, 2 H, Ho).

Triad di-boronic acid (Compound 9)[10]

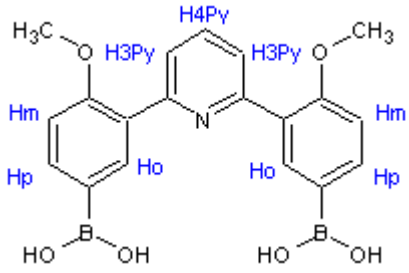

The triad trifluoroborate salt (0.132 g, 0.261 mmol, 1 equiv) was suspended in 15 mL acetonitrile and then sonicated for 5 min. To this, 0.20 mL (1.57 mmol, 6 equiv) of TMS-Cl and 30 µL (1.57 mmol, 6 equiv) of MilliQ water was added using a micropipette, changing its colour from brown to orange. The resulting suspension was then stirred at RT for 2 hours under open atmosphere. Finally, the reaction was quenched with saturated $NaHCO_3$. The resulting white precipitate was removed via vacuum filtration, while the filtrate was evaporated in vacuo to give a pale brown solid. The solid was re-dissolved in 10 mL DCM and washed with 50 mL MilliQ water. The aqueous portion was then washed with 3 x 20 mL DCM. All organic extracts were combined and dried in Na_2SO_4.

After Na_2SO_4 was removed via filtration, the solvent was removed in vacuo to afford a pale-brown solid (0.0730 g, 74 %). No further purifications were necessary as the ^{1}H NMR analysis showed a clean spectrum. ^{1}**H NMR** (300 MHz; Acetone-d_6): 3.92 (s, 6 H, OCH_3), 7.07 (s, 4 H, OH), 7.13 (d, 2 H, ^3J = 8.4 Hz, H_m), 7.73 (m, 3 H, H3Py, H4Py), 7.93 (dd, 2 H, ^3J = 8.1, ^4J = 1.5 Hz, Hp), 8.29 (d, 2 H, ^4J = 1.5 Hz, Ho).

6-Amino-1-methylpyrimidine-2,4(1*H*,3*H*)-dione (Compound 10)[18]

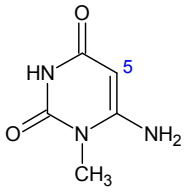

Into a flame-dried round-bottomed flask containing 55 mL of anhydrous ethanol, sodium metal (1.87 g, 81.3 mmol, 2 equiv) was added while stirring under argon atmosphere to produce the base (sodium ethoxide) in situ. Then, 4.16 mL of ethyl cyanoacetate (4.41 g, 39.0 mmol, 1 equiv) was added via syringe, causing the solution to become cloudy until white precipitate formed. After that, methylurea (2.92 g, 39.5 mmol, 1 equiv) was added and the resulting suspension was heated to 78 ˚C overnight. The brown suspension was cooled to RT, then the solvent was removed in vacuo. The recovered pale-yellow residue was then re-dissolved in 25 mL MilliQ water and the resulting clear brown solution was acidified to pH 4 using 1M HCl. The resulting pale brown precipitate was then isolated via vacuum filtration and then washed with MilliQ water (2.69 g, 49 %). No further purifications were conducted as it yielded a clean ^{1}H NMR spectrum. ^{1}**H NMR** (300 MHz; DMSO-d_6): 3.17 (s, 3 H, CH_3), 4.54 (s, 1 H, H_5), 6.76 (s, 2 H, NH_2), 10.31 (s, 1 H, NH).

6-Amino-3-(2-methoxyethyl)-1-methylpyrimidine-2,4(1*H*,3*H*)-dione (Compound 13)[18]

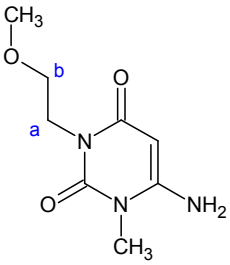

To a suspension of 6-amino-3-(2-methoxyethyl)-1-methylpyrimidine-2,4(1*H*,3*H*)-dione (0.500 g, 3.55 mmol, 1 equiv) in 17.3 mL DMF was added 1.90 mL (14.2 mmol, 4 equiv) of DMF/DMA. The mixture was heated to 40 ˚C for 1 hour, changing its colour from pale brown to yellow. After the

disappearance of the starting material (TLC, 10:1 DCM:MeOH), potassium carbonate (0.737 g, 5.33 mmol, 1.5 equiv) was added, followed by the 2-methoxyethyl-4-methoxybenzene sulfonate (1.24 g, 5.38 mmol, 1.5 equiv). The reaction was continued at 40 ˚C for another 20 hours.

The reaction mixture was cooled to RT, then DMF was removed via distillation in vacuo. The resulting yellow precipitate was then boiled in 200 mL of 95 % EtOH and any insoluble material was removed via vacuum filtration. The filtrate was then evaporated in vacuo to afford a yellow residue (~ 3 g), which was redissolved in 50 mL MeOH. To this solution, 90 mL of 28 % ammonium hydroxide was added and the entire mixture was stirred at RT overnight. Finally, the solvent was removed in vacuo to afford a crude, yellow solid. Purification of the crude solid was attempted using column chromatography (SiO_2, size: 17 x 3.5 cm) using 1.7:0.3, DCM/MeOH as eluent. This yielded a white solid (0.410 g, 63 %), but was still impure as per ^{1}H NMR analysis. The impurity possibly resulted from the alkylation of the enol tautomer of the starting material, as described in Chapter 3. **TLC** (SiO_2, DCM/MeOH 1.7:0.3); Rf = 0.26. **^{1}H NMR** (400 MHz; DMSO-d_6): 3.21 (s, 3 H, CH_3), 3.23 (s, 3 H, OCH_3), 3.40 (t, 2 H, ^3J = 6.4 Hz, H_b), 3.89 (t, 2 H, ^3J = 6.4 Hz, H_a), 4.67 (s, 1 H, CH), 6.79 (s, 2 H, NH_2).

2-Bromo-4-iodoanisole (Compound 14)[8]

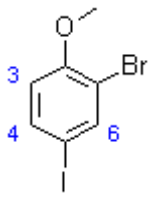

In a small mortar, silver nitrate (0.85 g, 5.03 mmol, 1.1 equiv) and iodine (1.22 g, 4.80 mmol, 1 equiv) were combined and ground into a homogeneous mixture using a pestle. Then, 2-bromoanisole (0.52 mL, 4.78 mmol, 1 equiv) was added, producing a dark brown paste. The reaction mixture was blended until the colour changed into pale yellow orange. MilliQ water (40 mL) and EtOAc (20 mL) were added into the mixture and the insoluble silver iodide was removed via suction filtration. The mother liquor was extracted with 3 x 10 mL MilliQ water and the combined aqueous extracts were washed with 3 x 10 mL EtOAc. All organic layers were combined, dried with Na_2SO_4, and the solvent was removed in vacuo producing pink residues. The crude solid was purified via column

chromatography, using silica gel column (size 20 x 3 cm) and hexanes/DCM (2.5:0.5) as eluent, giving a white solid (1.03 g, 70 %). **TLC** (SiO_2, Hexanes/DCM 2.5:0.5); Rf = 0.27. **^{1}H NMR** (300 MHz; $CDCl_3$): 3.87 (s, 3 H, H9), 6.66 (d, 1 H; ^3J = 8.6 Hz, H3), 7.55 (dd, 1 H; ^4J = 2.1, ^3J = 8.6 Hz, H4), 7.82 (d, 1 H; ^4J = 2.2 Hz, H6). **Melting Point:** 86.5-88.5 ˚C.

2-(3-Bromo-4-methoxy-phenyl)-4,4,5,5-tetramethyl-[1,3,2]dioxaborolane (Compound 15)[9]

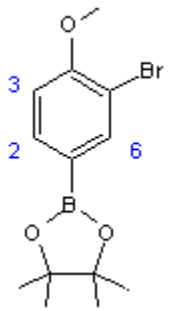

In a flame-dried round bottomed flask, the 2-bromo-4-iodoanisole (1.00 g, 3.20 mmol, 1 equiv), bis(pinacolato) diboron (0.853 g, 3.37 mmol, 1.1 equiv), potassium acetate (0.955 g, 9.73 mmol, 3 equiv) and bis[(diphenyl-phosphino)ferrocene]dichloro-palladium(II) ($PdCl_2$(dppf), 0.115 g, 0.158 mmol, 0.049 equiv) were all combined. The solid mixture was then degassed via cycle of argon purge in high vacuum for 30 min. Then, 15 mL of previously degassed dry DMF was added, producing a yellow orange solution, which was degassed again for 15 min by bubbling argon into it. The reaction mixture was heated to 55 ˚C while its progress was being monitored by ^{1}H NMR. After 24 hours, the ratio of products and starting materials no longer changes, hence, the reaction was stopped. The reaction mixture was cooled to RT and filtered through Celite™ to remove any insoluble material. The recovered black precipitate was then rinsed with ethyl acetate (~50 mL) and distilled water (~60 mL). The biphasic filtrate was then transferred into a separatory funnel and the organic portion was collected. The remaining aqueous portion was then extracted with 3 x 25 mL ethyl acetate. All organic extracts were combined, washed with 2 x 25 mL distilled water, 25 mL brine, and dried with Na_2SO_4. After removal of Na_2SO_4 by filtration, the filtrate was evaporated in vacuo to give a brown, oily residue. The crude was purified via column chromatography, using silica gel column (size 18 x 3.5 cm) and hexanes/DCM (1:1) as eluent, giving a yellow oil (0.414 g, 41 %). **TLC** (SiO_2, Hexanes/DCM 1:1); Rf = 0.26. **^{1}H NMR** (300 MHz; $CDCl_3$): 1.33 (s, 12 H, CH_3), 3.91 (s, 3 H, OCH_3), 6.88 (d, 1 H; ^3J = 8.1 Hz, H3), 7.71 (dd, 1 H; ^3J = 8.1, ^4J = 1.5 Hz, H2), 7.98 (d, 1 H, ^4J = 1.2 Hz, H6). **^{13}C**

NMR (75 MHz; $CDCl_3$) δ 24.93, 55.94, 83.31, 83.73, 111.16, 111.34, 135.42, 139.54, 158.07. **Elemental Analysis:** Anal. Calc'd for $C_{13}H_{18}BBrO_3$: C, 49.89; H, 5.80; Found: C, 51.43; H, 6.66; Corrected Calc'd (best result for $C_{13}H_{18}BBrO_3 \cdot 0.35\ C_{12}H_{24}B_2O_4$ (B2Pin2)): C, 51.41; H, 6.62; Found: C, 51.43; H, 6.66. **EI$^+$-MS:** calculated for $C_{13}H_{18}O_3BBr$: 312.05; found: 312.05 $[M]^+$, 83.95 $[M\text{-}C_7H_6BBrO_3]^+$

Potassium 5-bromo-4-methoxy-phenyl trifluoroborate (Compound 16)[10]

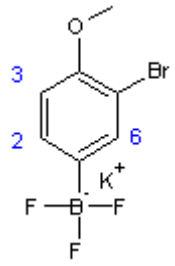

In a plastic round bottomed flask, a solution of 2-(3-bromo-4-methoxy-phenyl)-4,4,5,5-tetramethyl-[1,3,2]dioxaborolane (0.860 g, 2.76 mmol, 1 equiv) in 10 mL methanol was prepared. While stirring under open atmosphere, 3.0 mL of 4.5 M aqueous potassium hydrogen fluoride (KHF_2, 1.08 g, 13.8 mmol, 5 equiv) was added dropwise, immediately forming a white precipitate. The resulting white slurry was then stirred at RT for 30 min. The white precipitate was removed via vacuum filtration and the filtrate was evaporated in vacuo to afford a white, crystalline solid. The crude solid was recrystallized in acetone:ether (5:10 mL). To optimize the crystallization process, the solution was placed in the freezer overnight. Finally, the resulting white crystals were isolated via vacuum filtration (0.787 g, 97 %). **^{1}H NMR** (300 MHz; Acetone-d_6): 3.79 (s, 3 H, OCH_3), 6.82 (d, 1 H; ^3J = 7.9 Hz, H3), 7.89 (dd, 1 H; ^3J = 7.9 Hz, poor res., H2), 7.60 (d, 1 H, poor res, H6). **^{13}C NMR** (100 MHz; Acetone-d_6) δ 56.20, 74.81, 110.87, 112.12, 132.63, 137.12, 154.69. **Elemental Analysis:** Anal. Calc'd for $C_7H_6BBrF_3KO$: C, 28.70; H, 2.06; Found: C, 28.04; H, 2.35. Corrected Calc'd (best result for $C_7H_6BBrF_3KO \cdot 0.4\ H_2O$): C, 28.01; H, 2.28; Found: C, 28.04; H, 2.35. **ESI$^-$-HRMS:** calculated for $C_7H_6BOF_3Br^-$: 252.96; found: 252.96 $[M\text{-}K]^-$. **Melting Point:** 215-217 ˚C.

5-Bromo-4-methoxy-phenyl boronic acid (Compound 17)[10]

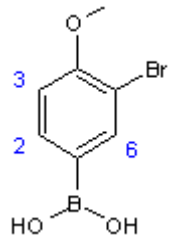

A solution of potassium 5-bromo-4-methoxy-phenyl trifluoroborate (0.348 g, 1.19 mmol, 1 equiv) was prepared in 9 mL acetonitrile. Then, 64 µL of MilliQ water was added via micropipette. While stirring under open atmosphere, 0.45 mL of TMS-Cl (0.387g, 3.57 mmol, 3 equiv) was added via syringe, immediately forming a white precipitate. The resulting suspension was then stirred at RT for 1 hour, then quenched with 2 mL of saturated $NaHCO_3$. Using a Pasteur pipette, the aqueous portion of the solution was removed, while the remaining organic portion was dried with Na_2SO_4. Upon removal of the Na_2SO_4 via vacuum filtration, the filtrate was evaporated in vacuo to afford a cream-coloured solid (0.237 g, 86 %). Further purifications were not conducted because the ^{1}H NMR analysis showed a clean spectrum. **^{1}H NMR** (300 MHz; Acetone-d_6): 3.91 (s, 3 H, OCH_3), 7.07 (d, 1 H; ^3J = 8.4 Hz, H3), 7.83 (dd, 1 H; ^3J = 8.1, ^4J = 1.5 Hz, H2), 8.02 (d, 1 H, ^4J = 1.5 Hz, H6). **^{13}C NMR** (100 MHz; Acetone-d_6) 56.42, 111.64, 112.47, 136.02, 139.80, 158.51. **Elemental Analysis:** Anal. Calc'd for $C_7H_8O_3BBr$: C, 36.42; H, 3.49; Found: C, 39.31; H, 2.46; Corrected Calc'd (best result for $C_7H_8BBrO_3 \cdot 2\ C_{21}H_{18}B_3Br_3O_6$): C, 39.03; H, 2.94; Found: C, 39.31; H, 2.46. **ESI$^-$-HRMS:** calculated for $C_7H_7BO_3Br^-$: 228.97; found: 229.00 $[M-H]^-$. **Melting Point:** 247-248 ˚C.

1-(3-bromo-4-methoxyphenyl)-1*H*-pyrazolo[4,3-*d*]pyrimidine-5,7(4*H*,6*H*)-dione (Compound 18)[11]

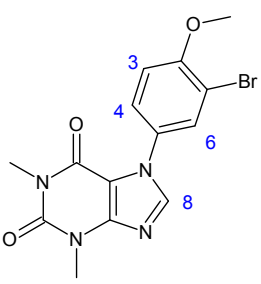

In a flame-dried flask, a suspension of theophylline (0.676 g, 3.75 mmol, 2 equiv), copper (II) acetate (0.937 g, 4.70 mmol, 2.6 equiv) and 2-bromo-4-methoxyphenyl boronic acid (0.425 g, 1.84 mmol, 1 equiv) was prepared in 10 mL of dry DCM. While stirring under argon, pyridine (0.74 mL, 9.21 mmol, 5 equiv) was added, changing the colour of the suspension from light to dark blue. The reaction mixture was then heated to 40 ˚C for 2 days.

The resulting white precipitate was isolated via filtration through a pad of Celite™ and washed with DCM. The filtrate was then evaporated in vacuo to afford a blue solid. The crude solid was purified via column chromatography, using silica gel column (size 18 x 3 cm) and acetone/ether (1.5:0.5) as eluent, giving a cream-coloured residue (0.256 g, 38 %). **TLC** (SiO_2, acetone/ether 1.5:0.5); Rf = 0.70. ^{1}**H NMR** (400 MHz; $CDCl_3$): 3.40 (s, 3 H, CH_3), 3.65 (s, 3 H, CH_3), 3.96 (s, 3 H, OCH_3), 7.00 (d, 1 H; ^{3}J = 8.8 Hz, $H3_{Ph}$), 7.43 (dd, 1 H, ^{4}J = 2.4, ^{3}J = 8.8 Hz, $H4_{Ph}$), 7.66 (d, 1 H, ^{4}J= 2.8 Hz, $H6_{Ph}$), 7.69 (s, 1 H, $H8_{theo}$). ^{13}**C NMR** (125 MHz; $CDCl_3$) 28.31, 30.09, 56.73, 107.48, 111.76, 111.87, 125.79, 128.30, 130.02, 141.25, 149.54, 151.67, 154.53, 156.71. **Elemental Analysis:** Anal. Calc'd for $C_{14}H_{13}O_3N_4Br$: C, 46.05; H, 3.59; N, 15.34; Found: C, 45.62; H, 3.33; N, 14.65. **EI^{+}-MS:** calculated for $C_{14}H_{13}BrN_4O_3$: 364.02; found: 364.02 $[M]^{+}$, 366.02 $[M+2H]^{+}$ **Melting Point:** 222-223 ˚C.

7-(4-Methoxyphenyl)-1,3-dimethyl-3,7-dihydro-purine-2,6-dione[11]

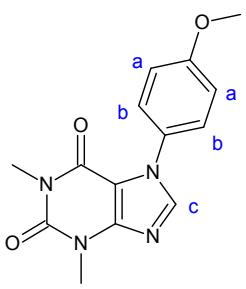

A suspension of 4-methoxyphenyl boronic acid (0.745 g, 4.90 mmol, 1 equiv) and theophylline monohydrate (1.94 g, 9.81 mmol, 2 equiv) and copper (II) acetate (2.22 g, 11.2 mmol, 2.3 equiv) was prepared in 20 mL dry DCM. While stirring under argon, 1.97 mL (24.5 mmol, 5 equiv) of pyridine was added via syringe. The reaction mixture was then heated to 40 ˚C for 22 hours. The resulting white precipitate was removed via vacuum filtration through Celite™, and rinsed with DCM. The filtrate was evaporated in vacuo to give a blue solid, which was purified via column chromatography, using silica gel column (size 18 x 3 cm) and acetone/ether (1.5:0.5) as eluent, giving a cream-coloured residue (0.346 g, 25 %). ^{1}**H NMR** (500 MHz; $CDCl_3$): 3.39 (s, 3 H, CH_3), 3.65 (s, 3 H, CH_3), 3.86 (s, 3 H, OCH_3), 7.00 (d, 2 H; ^{3}J = 8.9 Hz, Ha), 7.37 (d, 2 H, ^{3}J = 8.9 Hz, Hb), 7.69 (s, 1H, Hc).

5[-(1H-1,3-benzodiazol-2-yl)-2-methoxyphenyl]boronic acid (Compound 19)[19]

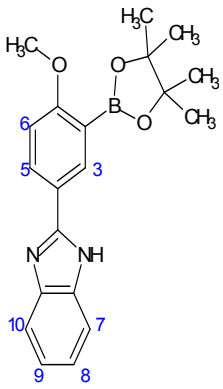

In a round-bottomed flask, 5-formyl-2-methoxyphenylboronic acid (0.367 g, 2.04 mmol, 1.1 equiv) and o-phenylenediamine (0.202 g, 1.87 mmol, 1 equiv) were combined with 31 mL ethanol. To this, a solution of sodium bisulfite (0.344 g, 1.98 mmol, 1.1 equiv) in 3.1 mL MilliQ water was added. The reaction mixture was stirred and heated under reflux for 1 hour. The mixture was cooled to slightly above room temperature and the insoluble precipitate was removed via vacuum filtration. The mother liquor was concentrated under reduced pressure and cooled further in the fridge. The crude was isolated via vacuum filtration and rinsed with MilliQ water to afford a shiny yellow-beige solid (0.374 g, 75%). ^{1}**H NMR** (300 MHz; DMSO-d_6): 3.87 (s, 3 H, OCH_3), 7.18 (m, 3 H, H6, H8, H9); 7.56 (m, 2 H, H7,10), 7.92 (s, 2 H, OH), 8.19 (dd, 1 H; ^{4}J = 2.2 Hz, ^{3}J = 8.7 Hz, H5), 8.36 (d, 1 H; ^{4}J = 2.1 Hz, H3).

2-[4-methoxy-3-(tetramethyl-1,3,2-dioxaborolan-2-yl)phenyl]-1H-1,3-benzodiazole (Compound 20) [21]

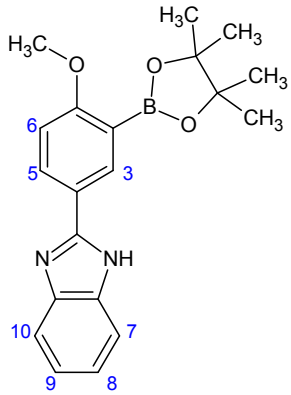

Into a round-bottomed flask, the 5[-(1H-1,3-benzodiazol-2-yl)-2-methoxyphenyl]-boronic acid (0.251 g, 0.933 mmol, 1 equiv) was mixed with pinacol (2.17 g, 19 equiv). The solid mixture was heated using a heat gun until a cloudy white solution was obtained. The resulting solution was then heated to 80 ˚C overnight, while stirring vigorously under open atmosphere. Hexanes (~50 mL) were added into the white slurry, and any insoluble material was removed via vacuum filtration. The recovered white precipitate was re-suspended in ~30 mL hexanes and sonicated for 5 min to remove any remaining pinacol. The precipitate was once again isolated via vacuum filtration, and then re-dissolved in acetone. Any insoluble material was isolated via vacuum filtration, while the filtrate was evaporated in vacuo to give a white solid. Purification of

the crude was achieved via recrystallization in acetone:hexanes (40 mL: 5 mL), yielding a cream-coloured solid (0.200 g, 61 %). **^{1}H NMR** (300 MHz; DMSO-d_6): 1.32 (s, 12 H, CH_3), 3.83 (s, 3 H, OCH_3), 7.17 (m, 3 H, H6, H8, H9); 7.48 (m, 1 H, H10), 7.61 (m, 1 H, H7), 8.22 (dd, 1 H, ^{4}J = 2.3 Hz , ^{3}J = 7.8 Hz, H5), 8.40 (d, 1 H, ^{4}J = 2.3 Hz, H3), 12.79 (s, 1 H, NH).

1-(2-Methoxyethyl)-2-[4-methoxy-3-(4,4,5,5-tetramethyl-[1,3,2]dioxaborolan-2-yl)-phenyl]-1*H*-benzoimidazole (Compound 21)[20]

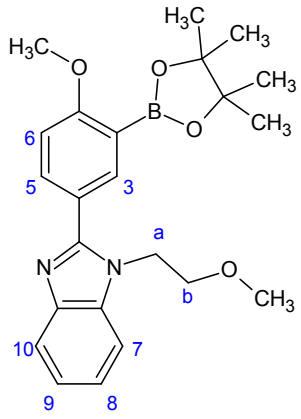

Into a flame-dried, 2-necked round-bottomed flask containing pre-washed sodium hydride (60% in mineral oil: mineral oil removed by hexanes wash; 0.0226 g, 0.942 mmol, 2.2 equiv) the previously dried 2-[4-methoxy-3-(tetramethyl-1,3,2-dioxaborolan-2-yl)phenyl]-1H-1,3-benzodiazole (0.150 g, 0.428 mmol, 1 equiv) and 2 mL anhydrous DMF were added. The reaction mixture was then stirred for 30 minutes at RT, then, 2-methoxyethyl-4-methoxybenzene sulfonate (0.148 g, 0.642 mmol, 1.5 equiv) in 1 mL anhydrous DMF was added to the reaction mixture via syringe, changing its colour from beige to red-brown. The reaction was stirred at RT for 3 days and then heated to 70^{o}C overnight. The reaction was cooled to RT, poured into ~30 mL MilliQ water, and then extracted with 4 x 25 mL ethyl acetate, with the aid of the centrifuge to break up the emulsions. All organic extracts were combined, washed with 10 mL MilliQ water and then dried with Na_2SO_4. The solvent was then removed in vacuo, yielding crude, yellow oil. To the oil, was added 5 mL of acetone and 20 mL hexanes, forming a cloudy suspension. After boiling of the suspension, white precipitate settled at the bottom of the flask. After cooling to RT, the mixture was then placed in the freezer to optimize the crystallization process. The formed cream precipitate was isolated via vacuum filtration and rinsed with hexanes, while the filtrate was evaporated in vacuo to afford yellow oil. ^{1}H NMR analysis showed that the precipitate is comprised of the starting material, while the oil recoved from the filtrate is contained the

alkylated boronic ester (0.140 g, 80 %). Furthermore, the oil seemed to contain some alkylated boronic acid, as per integration results. Accurate assignment of the ^{1}H NMR peaks is thus very difficult, hence was put on hold until we are able to obtain a pure sample. Purification was attempted with column chromatography (SiO_2, size: 14 x 2 cm) using 1:1 acetone/hexanes as eluent, but the procedure failed. The recovered product (0.103 g, 59 %) was not subjected into further purifications due to its small amount and time constraints. **TLC** (SiO_2, acetone/hexanes 1:1); Rf = 0.40.

2-(4'-methoxyphenyl)benzimidazole (Compound 23)[19]

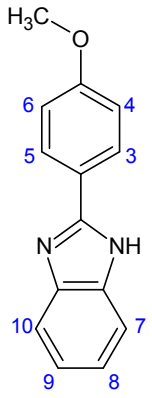

In a round-bottomed flask, p-anisaldehyde (0.903 mL, 7.42 mmol, 1.1 equiv) and o-phenylenediamine (0.730 g, 6.75 mmol, 1 equiv) were combined with 110 mL ethanol. To this, a solution of sodium bisulfite (1.18 g, 6.76 mmol, 1 equiv) in 11 mL MilliQ water was added, and the resulting mixture was heated under reflux for 1 hour. The mixture was cooled to slightly above room temperature and the insoluble precipitate that had formed was removed via vacuum filtration. The solvent was evaporated in vacuo to afford a beige precipitate. The crude was purified by recrystallization in ethyl acetate (100 mL) and hexanes (100 mL) to yield white crystals (0.379 g, 25 %). ^{1}**H NMR** (300 MHz; $CDCl_3$): 3.87 (s, 3 H, OCH_3), 7.00 (d, 2 H; ^{3}J = 8.9 Hz, H4 & H6); 7.20 (m, 2 H, H8 & H9), 7.63 (m, 2 H, H7 & H10), 8.00 (d, 2 H; ^{3}J = 8.9 Hz, H3 & H5).

1-(2-Methoxyethyl)-2-(4-methoxyphenyl)benzimidazole (Compound 24)[20]

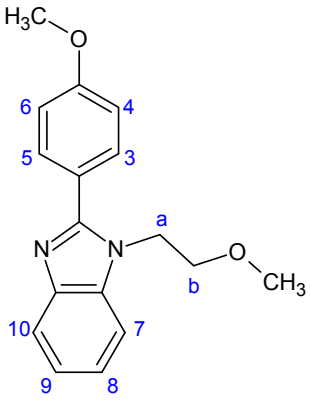

Into a flame-dried, 2-necked round-bottomed flask containing pre-washed sodium hydride (60% in mineral oil: mineral oil removed by hexanes wash; 0.0790 g, 1.98 mmol, 2.2 equiv) the previously dried 2-(4'-methoxyphenyl)benzimidazole (0.199 g, 0.889 mmol, 1.0 equiv) and 2 mL anhydrous DMF were added. The reaction mixture was then stirred for 30 minutes at RT; during this time, the evolution of gas from the mixture was observed. Next, 2-methoxyethyl-4-methoxybenzene sulfonate (0.311 g, 1.35 mmol, 1.5 equiv) in 1 mL anhydrous DMF was added to the reaction mixture via syringe, changing its colour from beige to red-brown. The reaction was stirred at RT overnight and then heated to 70°C for 5 hours. The reaction was cooled to RT, then poured into ~35 mL MilliQ water, and extracted with 2 x 15 mL ethyl acetate. All organic extracts were combined, washed with 10 mL MilliQ water and then dried with Na_2SO_4. The solvent was then removed in vacuo, yielding a crude, yellow-brown solid (0.209 g, 84%). ^{1}H NMR analysis showed a clean spectrum, thus, further purifications were not performed. **^{1}H NMR** (300 MHz; $CDCl_3$): 3.29 (s, 3 H, CH_3), 3.78 (t, 2 H; ^3J = 5.8 Hz, H_b), 3.89 (s, 3 H, OCH_3), 4.40 (t, 2 H; ^3J = 5.7 Hz, H_a), 7.04 (d, 2 H; ^3J = 8.8 Hz, H2 & H6); 7.31 (m, 2 H, H8 & H9), 7.46 (m, 1 H, H10), 7.78 (d, 2 H; ^3J = 8.7 Hz, H3 & H5); 7.81 (m, 1 H, H7).

Fourth Generation Tweezer (Compound 25)[2]

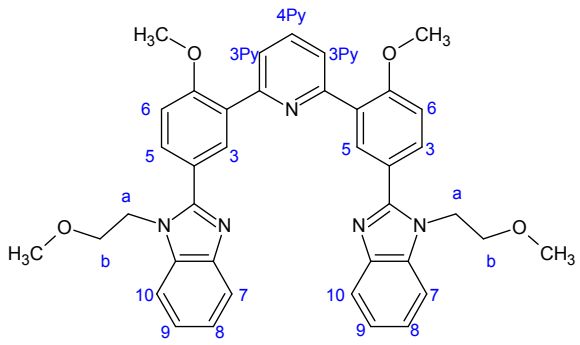

Into a 0.5-2 mL microwave vial, the 2,6-dibromopyridine (25.5 mg, 0.108 mmol, 1 equiv) was directly weighed. To this, a solution of the crude 1-(2-methoxyethyl)-2-(4-methoxyphenyl)-benzimidazole (90.0 mg,

0.220 mmol, 2.5 equiv) in toluene plus 0.30 mL (0.600 mmol, 3 equiv) of 2M potassium carbonate solution were added. The biphasic solution was then degassed by bubbling argon gas for 15 min. Then, in a nitrogen glovebox, the $Pd(PPh_3)_4$ catalyst (46.5 mg, 0.0395 mmol, 0.18 equiv) was added. The reaction was then carried out using a microwave device, set at 90 ˚C for 20 hours.

After cooling to RT, 15 mL of ethyl acetate plus 10 mL of MilliQ water were added. Using a separatory funnel, the organic layer was collected. The remaining water layer was then extracted with 3 x 5 mL ethyl acetate. All organic extracts were combined, and then washed with 10 mL MilliQ water. Using a centrifuge, the formed emulsion was removed, and the organic layer was collected, and then dried with Na_2SO_4. After filtering out the drying agent, the solvent was removed in vacuo to afford a yellow oil (0.114 g). Purification was not attempted on the crude sample due to time constraints. ^1H NMR analysis (300 MHz, $CDCl_3$) shows the presence of new peaks that most likely belong to the 4th generation tweezer, however, proper assignments of the peaks require a pure sample to resolve the ambiguity observed in the aliphatic region (please refer to section 4.2.5 for a more thorough discussion).

Failed Reactions

1-(4-Nitro-1-oxidopyridin-2-yl)dihydropyrimidine-2,4(1*H*,3*H*)-dione[12]

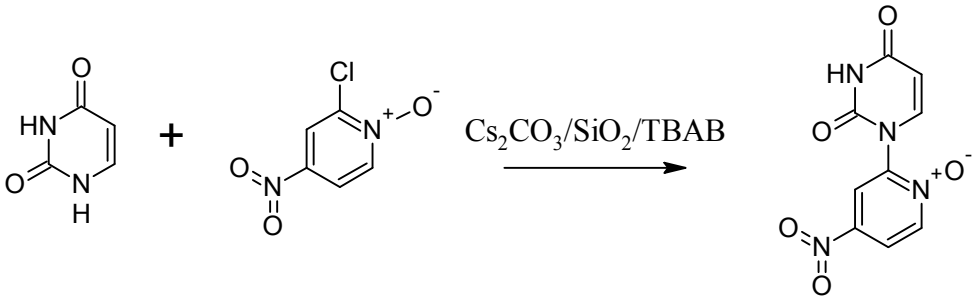

All reagents were ground separately into a fine powder using a mortar and pestle prior to use. Uracil (0.419 g, 3.73 mmol, 1.3 equiv), 2-chloro-4-nitropyridine-*N*-oxide (0.510 g, 2.87

mmol, 1 equiv), Cs_2CO_3 (0.935 g, 2.87 mmol, 1 equiv), SiO_2 (0.172 g, 2.86 mmol, 1 equiv) and tetrabutylammonium bromide (TBAB, 0.923 g, 2.86 mmol, 1 equiv) were all combined into a small test tube and stirred until a homogeneous mixture was obtained. The reaction mixture was heated to 150 °C using an oil bath, for 4 hours while stirring using a glass rod every 15 minutes. Then, it was cooled to RT, solidifying the thick brown paste. To remove the solid support, the paste was washed with 100 mL ice-cold MilliQ water, and the insolubles were removed via vacuum filtration. The mother liquor was extracted with 12 x 10 mL EtOAc. All organic extracts were combined, washed with 5 x 10 mL MilliQ water and dried with Na_2SO_4. The solvent was evaporated in vacuo, giving a dark orange solid. ^{1}H NMR analysis showed mainly the peaks corresponding to the starting material, suggesting that the reaction did not work.

2,7-Bis(2-methoxyethoxy) naphthalene boronic acid[13]

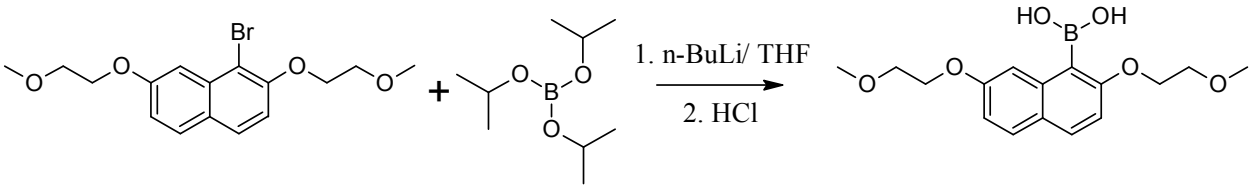

Into a flame-dried flask, a solution of the 1-bromo-2,7-bis(2-methoxyethoxy) naphthalene (1.00 g, 2.82 mmol, 1 equiv) in 10 mL dry THF was prepared under argon. The solution was cooled to -78 °C. While stirring, *n*-butyllithium (1.60 mL, 4.00 mmol, 1.4 equiv) was slowly added to the cooled solution, changing its colour from light pink to clear yellow. Then, the reaction mixture was warmed to -10 °C and stirred at that temperature for 1.5 hours. The reaction mixture was cooled again to -78 °C, then the triisopropylborate (0.90 mL, 3.90 mmol, 1.4 equiv) was slowly added while stirring under argon. The resulting mixture was warmed to RT and stirred at that temperature overnight. Then, 7 mL of 1 M HCl was added and the reaction was further stirred at RT for another hour. Extraction was performed with 3 x 20 mL DCM. All organic extracts were combined, dried with Na_2SO_4 and the solvent was removed under reduced pressure to give a

yellow solid. ^{1}H NMR analysis showed mainly the peaks corresponding to the starting material and the debrominated starting material, suggesting that the reaction did not work.

2,7-Bis(2-methoxyethoxy) naphthalene boronic acid via Grignard Method[14]

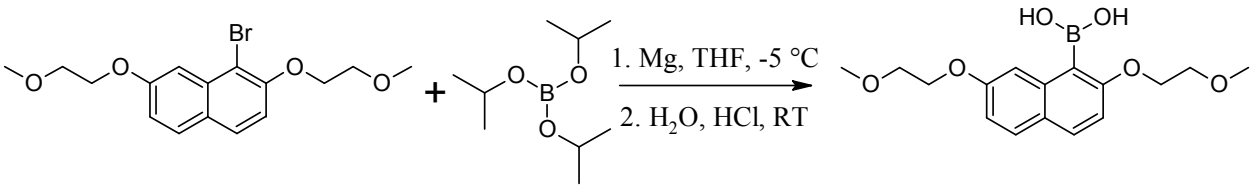

To a suspension of magnesium turnings (0.100 g, 4.11 mmol, 2.4 equiv) in dry tetrahydrofuran (1 mL), a solution of the 1-bromo-2,7-bis(2-methoxyethoxy) naphthalene (0.600 g, 1.69 mmol, 1 equiv) in dry tetrahydrofuran (5 mL) was added dropwise, forming a clear peach solution. The entire mixture was sonicated for 15 min to activate the magnesium, then a few crystals of iodine were also added. The resulting grey Grignard solution was boiled under reflux overnight, then cooled to RT. A solution of triisopropylborate (0.58 mL, 2.54 mmol, 1.5 equiv) in dry THF (3 mL) was prepared and cooled to -5 °C. To this, the Grignard solution was slowly added and then the reaction mixture was stirred at -5 °C for 1 hour and at RT overnight. MilliQ water (5 mL) was added and the solvent was evaporated in vacuo, forming a light brown residue. 1 M HCl (6 mL) was added and the solution was stirred for another 15 min. Then, the light brown precipitate was collected via vacuum filtration, washed with MilliQ water and then dried using the high vacuum apparatus under phosphorous pentoxide. ^{1}H NMR analysis showed no traces of the boronic acid, but instead shows peaks corresponding to 2,7-bis(2-methoxyethoxy)naphthalene.

2-[2,7-Bis-(2-methoxyethoxy)-naphthalen-1-yl]-4,4,5,5-tetramethyl-[1,3,2] dioxaborolane (1)[15]

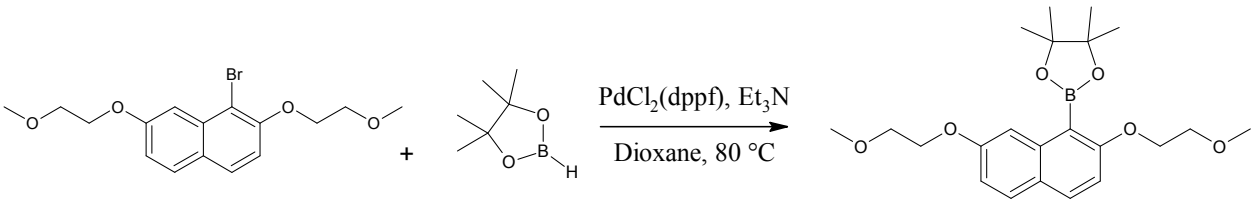

Into a flame-dried 25 mL round-bottom flask, a solution of bis-[(diphenylphosphino)-ferrocene]dichloropalladium(II) ($PdCl_2$(dppf), 31 mg, 0.42 mmol, 0.04 equiv) was prepared in anhydrous dioxane (4.61 mL, 54.0 mmol, 48 equiv). The 1-bromo-2,7-bis(2-methoxyethoxy) naphthalene (0.401 g, 1.13 mmol, 1 equiv), triethylamine (0.47 mL, 3.38 mmol, 3 equiv), and pinacolborane (0.25 mL, 1.69 mmol, 1.5 equiv) were added to the solution while stirring under argon to produce a change in colour from orange to red. The reaction mixture was refluxed at 80 ^{o}C and the reaction was monitored by TLC. The solution was dark brown after 4 hours, suggesting that the catalyst was no longer active, but TLC analysis indicated that the reaction was not complete. The reaction mixture was refluxed overnight, then cooled to room temperature and diluted in 10 mL of toluene. The addition of 5 mL MilliQ water produced an emulsion with some black precipitate that did not dissolve. The precipitate was removed partially via vacuum filtration; further filtration with Celite™ and toluene was conducted to completely remove the precipitate. The mother liquor was transferred into a separatory funnel and the aqueous layer was drained and extracted with 2 x 10 mL toluene until no UV activity could be seen by TLC. The combined organic extracts were dried with Na_2SO_4 and concentrated to yield a dark brown oil that solidified after 1 day at room temperature.

2-[2,7-Bis-(2-methoxyethoxy)-naphthalen-1-yl]-4,4,5,5-tetramethyl-[1,3,2] dioxaborolane (2)[15]

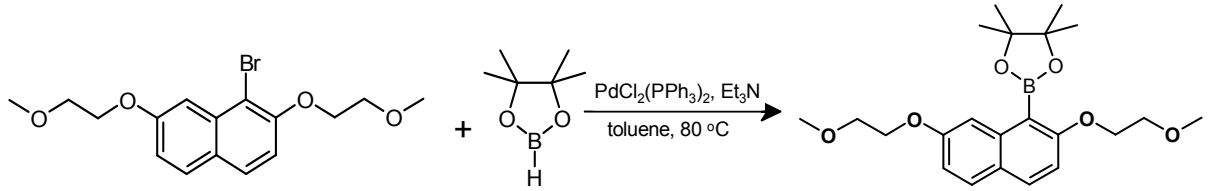

A solution of the bis(triphenylphosphine)palladium(II) dichloride ($PdCl_2(PPh_3)_2$, 51 mg, 0.072 mmol, 0.066 equiv) was prepared in 5 mL of dry, previously degassed toluene. The catalyst did not dissolve until the solution was heated. The 1-bromo-2,7-bis(2-methoxyethoxy) naphthalene mixture (0.39 g, 1.10 mmol, 1 equiv), dry triethylamine (0.47 mL, 3.38 mmol, 3 equiv, dried on potassium hydroxide), and pinacolborane (0.25 mL, 1.69 mmol, 1.5 equiv) was added to the catalyst solution while stirring under argon. The reaction mixture was refluxed at 80 ^oC overnight, then cooled to room temperature and diluted with 15 mL toluene and 10 mL MilliQ water. Because some emulsion formed, the entire biphasic solution was filtered through cotton wool. The mother liquor was transferred to a separatory funnel and the aqueous layer was collected and extracted with 3 x 10 mL toluene. The combined organic layers were dried with Na_2SO_4 and concentrated to produce a dark brown oil. ^1H NMR analysis showed only the presence of the 1-bromo-2,7-bis(2-methoxyethoxy) naphthalene, indicating that the reaction failed.

2-[2,7-Bis-(2-methoxyethoxy)-naphthalen-1-yl]-4,4,5,5-tetramethyl-[1,3,2] dioxaborolane (3)[9]

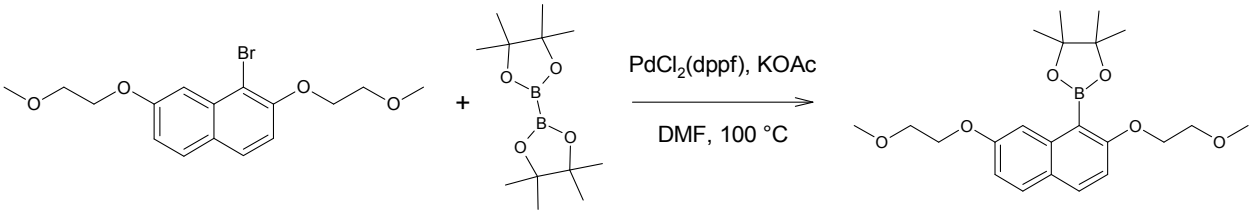

In a flame-dried round bottomed flask, 1-bromo-2,7-bis(2-methoxyethoxy) naphthalene (0.100 g, 0.282 mmol, 1 equiv), bis(pinacolato) diboron (0.081 g, 0.321 mmol, 1.1 equiv), potassium acetate (0.085 g, 0.868 mmol, 3.1 equiv) and bis(diphenylphosphino)ferrocene]-dichloropalladium(II) ($PdCl_2$(dppf), 0.019 g, 0.0264 mmol, 0.094 equiv) were all combined. The solid mixture was then degassed via cycle of argon purge in high vacuum for 30 min. Then, 5 mL of previously degassed dry dimethylformamide was added, producing a yellow orange solution, which was degassed again for 15 min by bubbling argon into it. Finally, reaction mixture was heated to 100 ˚C for 2 days. The reaction mixture was filtered through Celite™, obtaining a black precipitate which was rinsed with 30 mL EtOAc and 30 mL MilliQ water. The bi-phasic filtrate was then poured into a separatory funnel and the organic portion was isolated. The remaining aqueous layer was further extracted with 4 x 15 mL EtOAc. All organic extracts were combined, washed with 2 x 20 mL MilliQ water, 20 mL brine, and dried with Na_2SO_4. After removal of Na_2SO_4 via filtration, the filtrate was evaporated in vacuo to give a brown, oily residue. ^{1}H NMR analysis showed many overlapping peaks, but it can be seen that the major species is the unreacted 1-bromo-2,7-bis(2-methoxyethoxy) naphthalene. There were no signs of the desired boronic ester being formed, but instead, the new species was the debrominated (2,7-bis(2-methoxyethoxy) naphthalene) product.

1-(3-Bromo-4-methoxyphenyl)-2,7-bis-(2-methoxyethoxy) naphthalene[2]

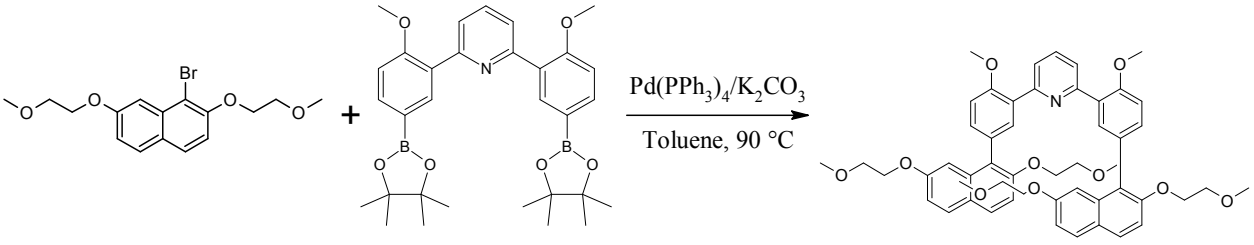

A solution of 5-bromo-4-methoxy-phenyl boronic acid (0.060 g, 0.260 mmol, 1 equiv) and 1-bromo-2,7-bis(2-methoxyethoxy) naphthalene (0.185 g, 0.520 mmol, 2 equiv) was prepared in dry tetrahydrofuran under argon. The resulting brown solution was then degassed for 5 min, by

bubbling argon into it. Then, tetrakis(triphenylphosphine)palladium ($Pd(PPh_3)_4$, 0.060 g, 0.052 mmol, 0.2 equiv) was added, and the resulting solution was degassed again for another 5 min. After stirring at RT for 15 minutes, 0.39 mL (0.780 mmol, 3 equiv) of previously degassed 2 M K_2CO_3 was added via syringe. The reaction mixture was then heated to 90 ˚C for 24 hours. An aliquot of the mixture was analyzed by ^1H NMR (300 MHz, $CDCl_3$). Results show that the reaction is not taking place, no new species were observed and all of the chemical shifts observed were that of the starting materials. Hence, the reaction was stopped.

7-[4-Methoxy-3-(4,4,5,5-tetramethyl-[1,3,2] dioxaborolan-2-yl)-phenyl]-1,3-dimethyl-3,7-dihydro-purine-2,6-dione[9]

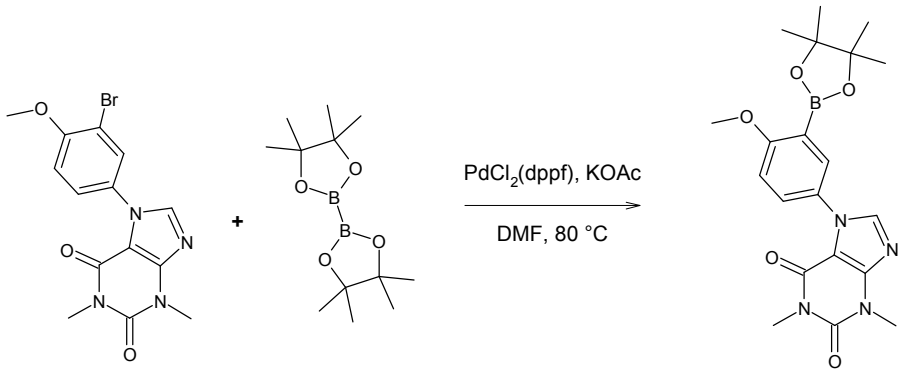

In a flame-dried round bottomed flask, 1-(3-bromo-4-methoxyphenyl)-1*H*-pyrazolo[4,3-*d*]pyrimidine-5,7(4*H*,6*H*)-dione (0.286 g, 0.783 mmol, 1 equiv), bis(pinacolato) diboron (0.239 g, 0.940 mmol, 1.2 equiv), potassium acetate (0.231 g, 2.35 mmol, 3 equiv) and bis[(diphenyl-phosphino)ferrocene]dichloropalladium(II) ($PdCl_2$(dppf), 0.057 g, 7.83×10^{-5} mol, 0.1 equiv) were all combined. The solid mixture was then degassed via cycle of argon purge in high vacuum for 30 min. Then, 5 mL of previously degassed dry DMF was added, producing a yellow orange solution, which was degassed again for 15 min by bubbling argon into it. Finally, reaction mixture was heated to 80 ˚C for 2 days. The reaction mixture was filtered through Celite™, obtaining a black precipitate which was rinsed with 30 mL EtOAc and 30 mL MilliQ water. The bi-phasic filtrate was then poured into a separatory funnel and the organic portion was isolated.

The remaining aqueous layer was further extracted with 4 x 15 mL EtOAc. All organic extracts were then combined, washed with 2 x 20 mL MilliQ water, 20 mL brine, and dried with Na_2SO_4. After removal of Na_2SO_4 via filtration, the filtrate was evaporated in vacuo to give a brown, oily residue. ^{1}H NMR analysis of the crude showed many overlapping peaks, but it can be seen that the major species is the unreacted 1-(3-bromo-4-methoxyphenyl)-1*H*-pyrazolo[4,3-*d*]pyrimidine-5,7(4*H*,6*H*)-dione. There were no signs of the desired boronic ester being formed, but instead, the new species was the debrominated (7-(4-methoxyphenyl)-1,3-dimethyl-3,7-dihydro-purine-2,6-dione) product.

1-(4-Methoxyphenyl)-1*H*-pyrazolo[4,3-*d*]pyrimidine-5,7(4*H*,6*H*)-dione boronic acid (1)[13]

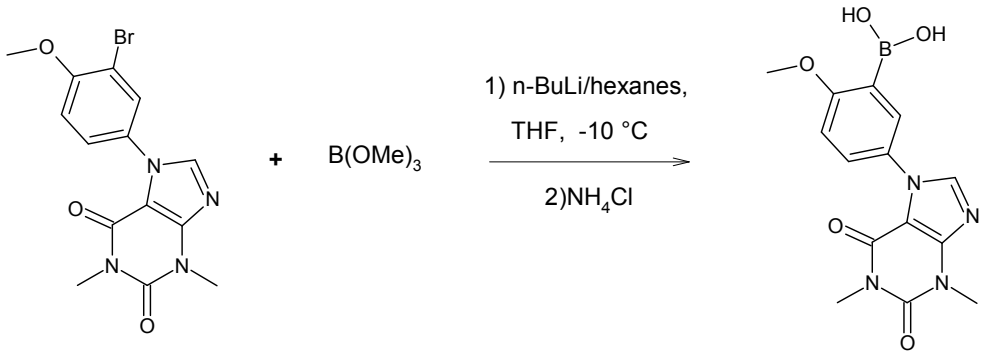

Into a flame-dried flask, the 1-(3-bromo-4-methoxyphenyl)-1*H*-pyrazolo[4,3-*d*]pyrimidine-5,7(4*H*,6*H*)-dione (0.150 g, 0.411 mmol, 1 equiv) was boiled in 3 mL dry tetrahydrofuran under argon atmosphere, in order to dissolve it. Then, 0.23 mL (2.05 mmol, 5 equiv) of trimethylborate was added. The solution was cooled to -10 ˚C, then 0.90 mL (1.44 mmol, 3.5 equiv) of 1.6 M n-butyllithium in hexanes was added dropwise. After 5 minutes, the solution became cloudy, as the starting dione began to re-crystallize. The reaction mixture was heated again until no cloudiness was observed. The reaction mixture was then stirred overnight at RT under argon. The reaction was quenched with 5 mL of saturated ammonium chloride then extracted with 3 x 15 mL EtOAc. All organic extracts were combined and dried with Na_2SO_4. After removing the Na_2SO_4 via vacuum filtration, the filtrate was evaporated in vacuo to afford a cream-coloured

solid. ^{1}H NMR analysis showed that the majority or the starting materials did not react. There were signs of new species forming, but it does not correspond to the desired boronic acid, but instead, the debrominated (7-(4-methoxyphenyl)-1,3-dimethyl-3,7-dihydro-purine-2,6-dione) product.

1-(4-Methoxyphenyl)-1*H*-pyrazolo[4,3-*d*]pyrimidine-5,7(4*H*,6*H*)-dione boronic acid (2)[16]

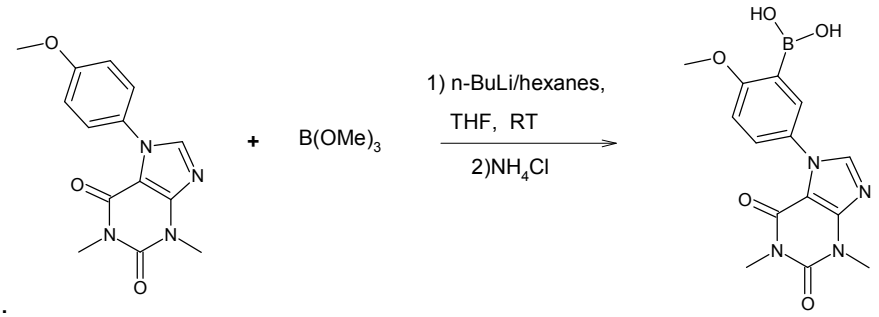

Into a flame-dried flask, a solution of 7-(4-methoxyphenyl)-1,3-dimethyl-3,7-dihydro-purine-2,6-dione (0.098 g, 0.344 mmol, 1 equiv) was prepared in 5 mL dry tetrahydrofuran under argon atmosphere. Then, 0.15 mL (1.37 mmol, 4 equiv) of trimethylborate was added. The solution was cooled to 4 ˚C (it was observed that at temperatures below 4 ˚C, the dione starts to crystallize), then 0.28 mL (0.450 mmol, 1.3 equiv) of 1.6 M n-butyllithium in hexanes was added dropwise. After 5 minutes, the solution became cloudy, as the starting dione began to re-crystallize. The reaction mixture was heated again until no cloudiness was observed. The reaction mixture was then stirred overnight at RT under argon. The reaction was quenched with 5 mL of saturated NH_4Cl, and then extracted with 3 x 15 mL EtOAc. All organic extracts were combined and dried with Na_2SO_4. After removing the Na_2SO_4 via vacuum filtration, the filtrate was evaporated in vacuo to afford a cream-coloured solid. ^{1}H NMR analysis showed that the starting materials did not react. No new species were also seen to form.

7-[3-(5,5-Dimethyl-[1,3,2]dioxaborinan-2-yl)-4-methoxyphenyl]-1,3-dimethyl-3,7-dihydro-purine-2,6-dione[17]

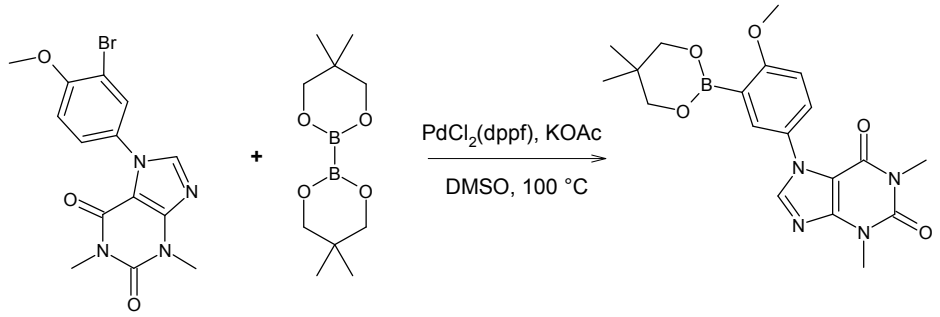

Into a flame-dried flask, the bis[(diphenylphosphino)ferrocene]dichloropalladium(II) ($PdCl_2$(dppf), 14 mg, 1.9 x 10^{-5} mol,) was directly weighed. Then, potassium acetate (19 mg, 0.188 mmol, 3 equiv) and bis(neopentylglycolato) diboron (17 mg, 0.075 mmol, 1.2 equiv) was added. The solid mixture was dried under high vacuum for 30 min, then purged with argon gas. To this, a previously degassed solution of 1-(3-bromo-4-methoxyphenyl)-1*H*-pyrazolo[4,3-*d*]pyrimidine-5,7(4*H*,6*H*)-dione (23 mg, 0.063 mmol), prepared in 1.2 mL anhydrous DMSO was added. Then, the reaction mixture was then heated to 100 ˚C for 2 days. After cooling to RT, the reaction mixture was poured into 20 mL ice-water. 10 mL of EtOAc was added, and the resulting bi-phasic mixture was poured into a separatory funnel. Extraction was performed using 3 x 10 mL EtOAc. All organic extracts were combined and dried with Na_2SO_4. After removing the Na_2SO_4 via vacuum filtration, the filtrate was evaporated in vacuo to afford an oily, brown solid. ^{1}H NMR analysis showed that the starting materials did not react. No new species were also seen to form.

Second generation tweezer[2]

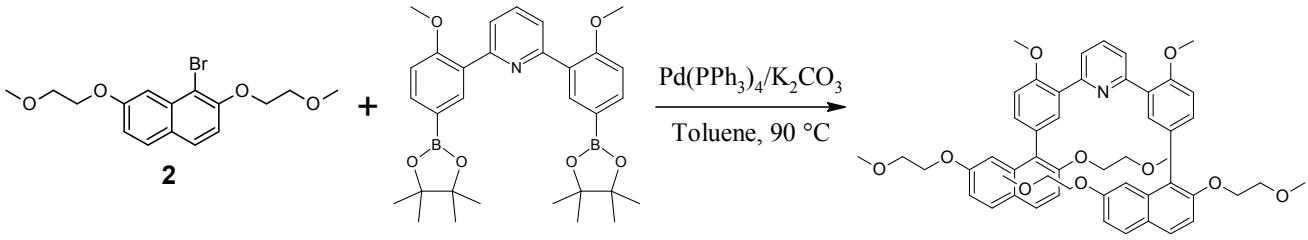

A solution of the diboronic ester (36 mg, 0.065 mmol, 1 equiv) and 1-bromo-2,7-bis(2-methoxyethoxy) naphthalene (54 mg, 0.15 mmol, 2.3 equiv) was prepared in 2 mL of previously degassed toluene, then argon gas was bubbled into the solution for 5 min. Then, tetrakis(triphenylphosphine)palladium ($Pd(PPh_3)_4$, 11 mg, 9.8 x 10^{-6} mol, 0.15 equiv) was added, and once again, the entire solution was purged with argon. The resulting deep orange solution was then stirred at RT for 15 min, then 0.18 mL (0.36 mmol, 5.5 equiv) of previously degassed 2 M K_2CO_3 was added via syringe. The reaction was allowed to take place overnight at 90 ˚C, under argon atmosphere. The reaction mixture was cooled to RT, then 3 mL of MilliQ water and 3 mL EtOAc was added. Any insoluble material was removed via vacuum filtration, while the filtrate was subjected to extraction with 4 x 3 mL EtOAc. All organic extracts were combined, washed with 2 x 5 mL MilliQ water and then dried with Na_2SO_4. After Na_2SO_4 was removed via filtration, the solvent was removed in vacuo to afford a brown, oily residue. The ^1H NMR spectrum produced many overlapping peaks in both aromatic and aliphatic regions. All purification attempts, either by recrystallization or column chromatography were unable to separate the components of the crude mixture. Finally, using ESI$^-$MS, we were able to see traces of the tweezer. However, because purification is impossible, the reaction was considered a failure.

Third generation Tweezer[11]

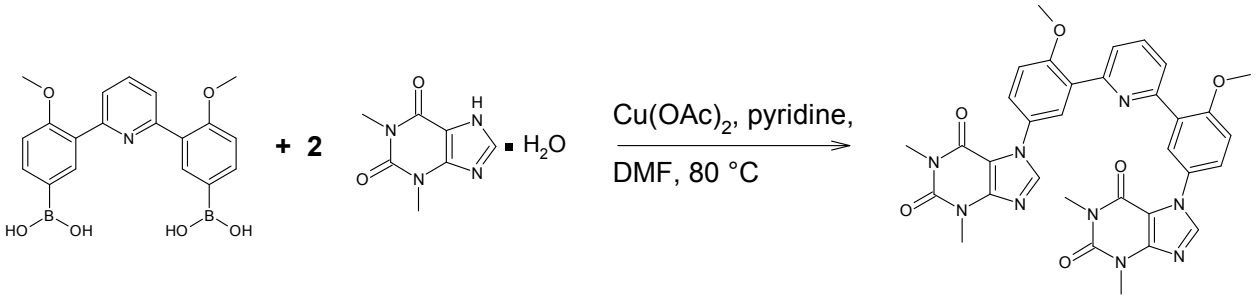

In a flame-dried flask, a suspension of theophylline (0.284 g, 1.44 mmol, 4 equiv), copper (II) acetate ($Cu(OAc)_2$, 0.430 g, 2.15 mmol, 6 equiv) and triad di- boronic acid (0.136 g, 0.359 mmol, 1 equiv) was prepared in 10 mL of dry DMF. While stirring under argon, pyridine (0.29 mL, 3.6 mmol, 10 equiv) was added, changing the colour of the suspension from light to dark blue. The reaction mixture was then heated to 80 ˚C for 4 days. The solvent was removed via distillation in vacuo, and the remaining solid was re-dissolved in DCM. The insoluble material was removed via filtration through a pad of Celite™ and washed with DCM. The filtrate was then evaporated in vacuo to afford a blue solid. The crude solid was purified via column chromatography, using silica gel column (size 18 x 3.5 cm) and acetone/ether (0.8:1.2) as eluent, but analysis of the fractions by ^1H NMR did not show any tweezer forming. Instead, the mono-substituted product was the major product.

References:

1. a) Sharghi, H.; Hosseini-Sarvari, M.; Moeini, F. *Can. J. Chem.* **2008**, 86, 1044-1051; b) Shirin, Z.; Thompson, J.; Liable-Sands, L.; Yap, G. P. A.; Rheingold, A. L.; Borovik; A. S. *J. Chem. Soc., Dalton Trans.* **2002**, 1714-1720
2. Leblond, J.; Gao, H.; Petitjean, A.; Leroux, J. *J. Am. Chem. Soc.* **2010**, 132, 8544-8545
3. Wilson, R. D. *J. Chem. Soc.* **1965**, 3304-3312
4. Ouchi, M.; Inoue, Y.; Liu, Y.; Nagamune, S.; Nakamura, S; Wada, K.; Hakushi, T. *Bull. Chem. Soc. Jpn.* **1990**, 63, 1260-1262

5. Peterca, M.; Percec, V.; Imam, M. R.; Leowanawat, P.; Morimitsu, K.; Heiney, P. A. *J. Am. Chem. Soc.* **2008**, 130, 14840-14852
6. Badjic, J. D.; Ronconi, C. M.; Stoddart, J. F.; Balzani, V.; Silvi, S.; Credi, A; *J. Am. Chem. Soc.* **2006**, 128, 1489-1499
7. Heathcote, R.; Howell, J. A. S.; Jennings, N.; Cartlidge, D.; Cobden, L.; Coles, S.; Hurtshouse, M.; *Dalton Trans.* **2007**, 13, 1309-1315
8. Yusubov, M. S.; Tveryakova, E. N.; Krasnokutskaya, E. A.; Perederyna, I. A.; Zhdankin, V. V. *Synth. Comm.* **2007**, 37, 1259-1265
9. Ishiyama, T.; Murata, M.; Miyaura, N. *J. Org. Chem.* **1995**, 60, 7508-7510
10. a) Yuen, A. K. L.; Hutton, C. A. *Tetrahedron Lett.* **2005**, 46, 7899-7903; b) Molander, G. A.; Biolatto, B. *J. Org. Chem.* **2003**, 68, 4302-4314
11. Kim, D.; Jun, H.; Lee, H.; Hong, S.; Hong, S. *Org. Lett.* **2010**, 12, 1212-1215
12. Khalafi-Nezhad, A.; Zare, A.; Parhami, A.; Rad, M. N. S.; Nejabat, G. R. *Synth. Commun.* **2006**, 36, 3549-3562
13. Genov, M.; Almorín, A.; Espinet, P. *Chem. Eur. J.* **2006**, 12, 9346-9352
14. Malkov, A. V.; Ramirez-Lopez, P.; Biedermannova, L.; Rulisek, L.; Dufkova, L.; Kotora, M.; Zhu, F.; Kocovsky, P. *J. Am. Chem. Soc.* **2008**, 130, 5341-5348
15. Murata, M.; Ovama, T.; Watanabe, S.; Masuda, Y. *J. Org. Chem.* **2000**, 65, 164-168
16. Fu, J.; Snieckus, V. *Can. J. Chem.* **2000**, 78, 905-919
17. Fang, H.; Kaur, G.; Yan, J.; Wang, B. **2005**, *Tetrahedron Lett.* 46, 1671-1674
18. Elzein, E.; Kalla, R. V.; Li, X.; Perry, T.; Gimbel, A.; Zeng, D.; Lustig, D.; Leung, K.; Zablocki, J. *J. Med. Chem.* **2008**, 51, 2267-2278
19. Duffy, K.J.; Price, A.T.; Delorme, E.; Dillon, S.B.; Duquenne, C.; Erickson-Miller, C.; Giampa, L.; Huang, Y.; Keenan, R.M.; Lamb, P.; Liu, N.; Miller, S. G.; Rosen, J.; Shaw, A.N.; Smith, H.; Wiggall, K.J.; Zhang, L.; Luengo, J.I. *J. Med. Chem.* **2002**, 45, 3576-3578

20. Iemura, R.; Kawashima, T.; Fukuda, T.; Ito, K.; Tsukamoto, G. *J. Med. Chem.* **1986**, 29, 1178-1181

21. Morandi, S.; Caselli, E.; Forni, A.; Bucciarelli, M.; Torre, G.; Prati, F. *Tet. Asymm.* **2005**, 16, 2918-2926

Chapter 6

Conclusion and Perspectives

6.1: Summary and Conclusion

The project started with the synthesis of the 2nd generation tweezer, in an attempt to improve our previously synthesized 1st generation tweezer. As described in Chapter 2, oligoethylene glycol chains were successfully incorporated in the naphthalene **IS**, however, challenges encountered in the synthesis of its corresponding boronic acid/ ester through halogen-lithium exchange mechanism and palladium catalyzed borylation were not resolved. Direct synthesis of the tweezer from Suzuki- MIyaura coupling of the triad diboronic ester (compound 7) and UNIT 1 PEG also failed. Due to this, we were unable to synthesize the 2nd generation tweezer.

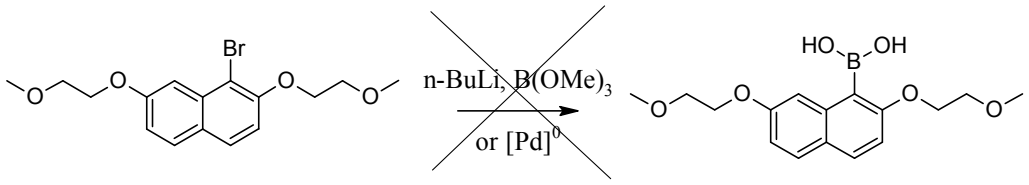

Figure 6.1: Attempted syntheses of 2,7-Bis(2-methoxyethoxy) naphthalene boronic acid.

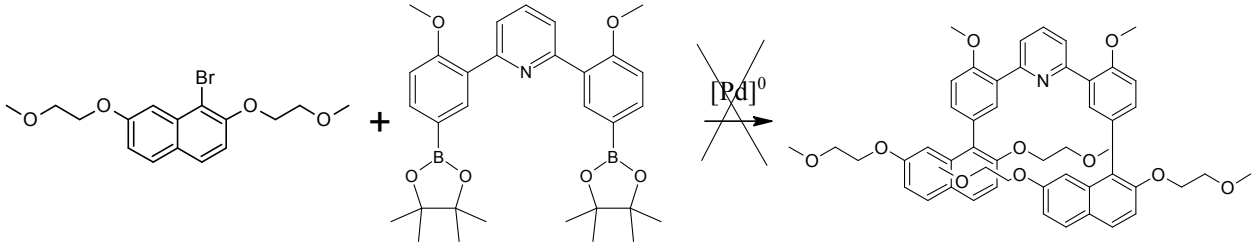

Figure 6.2: Attempted synthesis of 2nd generation tweezer through Suzuki coupling of triad diboronic ester (compound 7) and UNIT 1 PEG.

In Chapter 3, we then described our attempts in synthesizing our 3rd generation, caffeine-based tweezer. To minimize the steric hindrance that occur during coupling of the triad

S with the **IS**, we have synthesized the half-theophylline tweezers to be used later for direct coupling with 2,6-dibromopyridine. However, we were unable to produce the desired boronic acid/ester required in the final step via halogen lithium-exchange mechanism and palladium-catalyzed borylation reactions. Nevertheless, the copper (II) catalyzed coupling of the triad diboronic acid (compound 8) with theophylline, produced the mono-substituted caffeine tweezer.

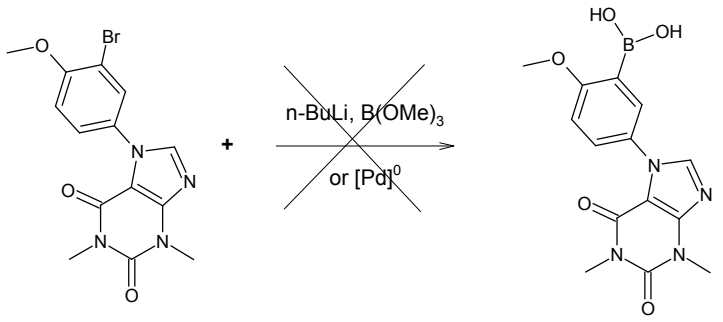

Figure 6.3: Attempted syntheses of half-theophylline tweezer boronic acid.

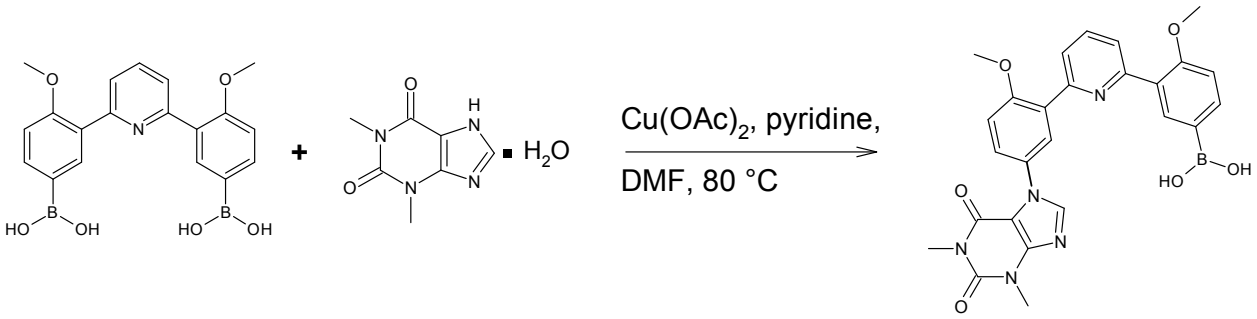

Figure 6.4: Cu (II) catalyzed reaction of triad diboronic acid with theophylline gives the mono-substituted tweezer.

Lastly, the synthesis of our 4th generation tweezer was described in Chapter 4. We have designed our 4th generation tweezer to avoid the complications that were encountered in the boronic acid/ ester syntheses. The benzimidazole-based **IS** were directly synthesized via ring condensation of the commercially available 5-formyl-2-methoxyphenylboronic acid and o-phenylenediamine. Alkylation of the **IS** with was also successfully performed via S_N2 reaction

using NaH as base. Finally, synthesis of the tweezer was carried out via Suzuki-Miyaura coupling of the Alkyl Bim boronic ester (compound 22) with 2,6-dibromopyridine. ^{1}H NMR analysis strongly suggests the formation of the 4th generation tweezer, but until we obtain a pure sample, we cannot be very certain. Much work is therefore needed to avoid complicated mixtures in the final step of the reaction, by avoiding the use of crude samples as starting materials.

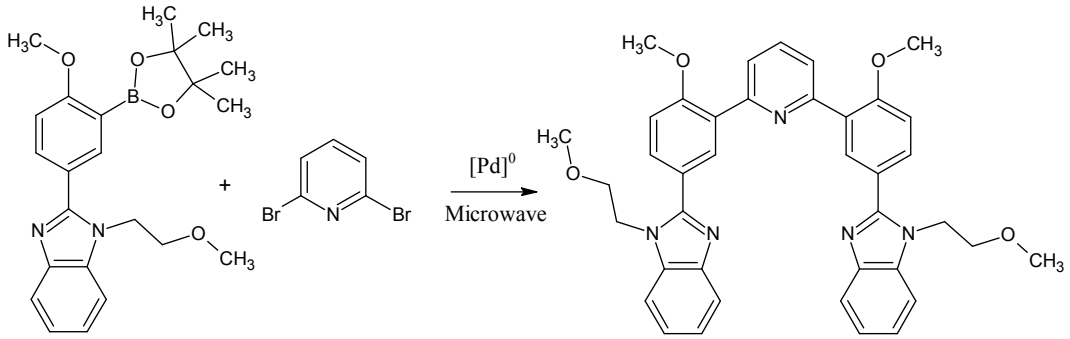

Figure 6.5: Pd (0) catalyzed reaction of Alkyl Bim boronic ester with 2,6-dibromopyridine gives the 4th generation tweezer.

6.2 Future Directions

The boronic acid and esters needed for the syntheses of both 2nd and 3rd generation tweezers may be obtained by using a highly reactive palladium catalysts, such as $Pd(dba)_2/PCy_3$ or $PdCl_2$(POPD). Thus, it is highly recommended that these catalysts be used for the next syntheses attempts.

As for the 4th generation tweezer, much work is needed to purify the Alkyl Bim boronic ester in order to prevent complicated mixtures in the next reaction step. Complete removal of the tosylate starting material and its by-product must therefore be achieved, and this could be done by optimizing the solvent conditions used for column chromatography.

Once syntheses of the tweezers are completed, the following experiments would be carried out:

1) ^{1}H NMR titration of all tweezers with varying concentrations of acid, which will help determine the binding constant of model substrates in aqueous-like media (MTX)
2) Fluorescence spectroscopy studies to characterize substrate binding at high or low pH and to determine the stoichiometry of binding between the substrate and the tweezer.
3) X-ray crystallography of the tweezers with and without the bound substrate to help visualize if the twisting of the naphthalene receptors are finally resolved (2^{nd} generation tweezer), and to determine the actual location of substrate binding.

Appendix A

NMR and MS Spectra

***N,N'*-Bis(4-methylphenyl)pyridine-2,6-dicarboxyamide**

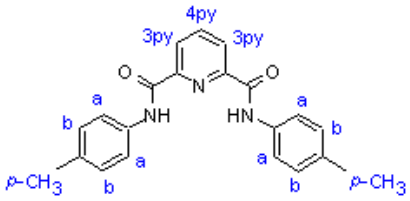

^{1}H NMR (300 MHz, $CDCl_3$)

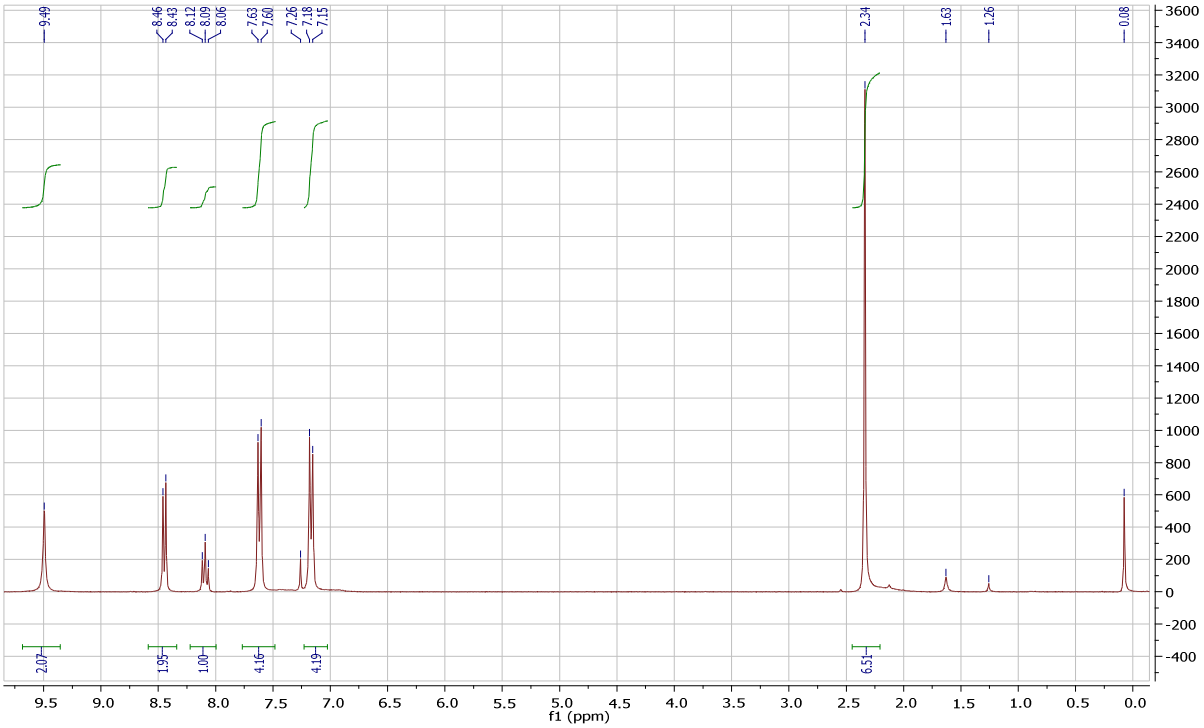

^{13}C NMR (100 MHz, $CDCl_3$)

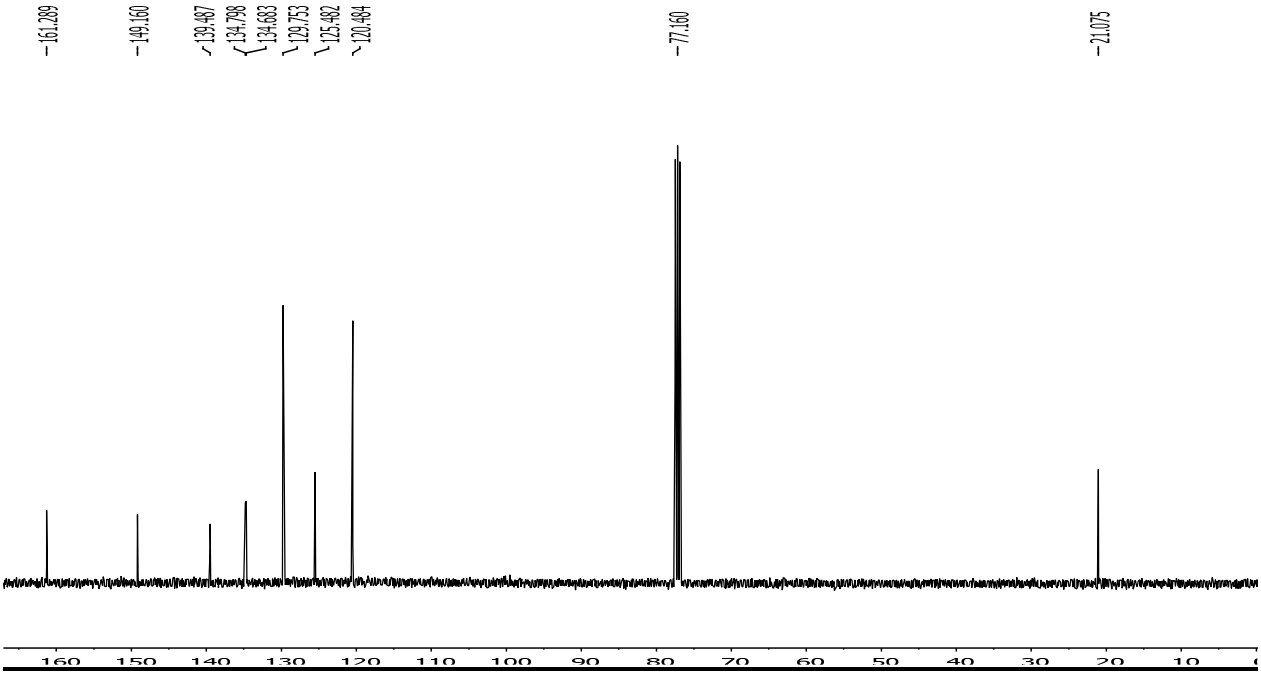

Titration with TFA to assess the switching property, (400 MHz, 1:1 $CDCl_3/CD_3OD$)

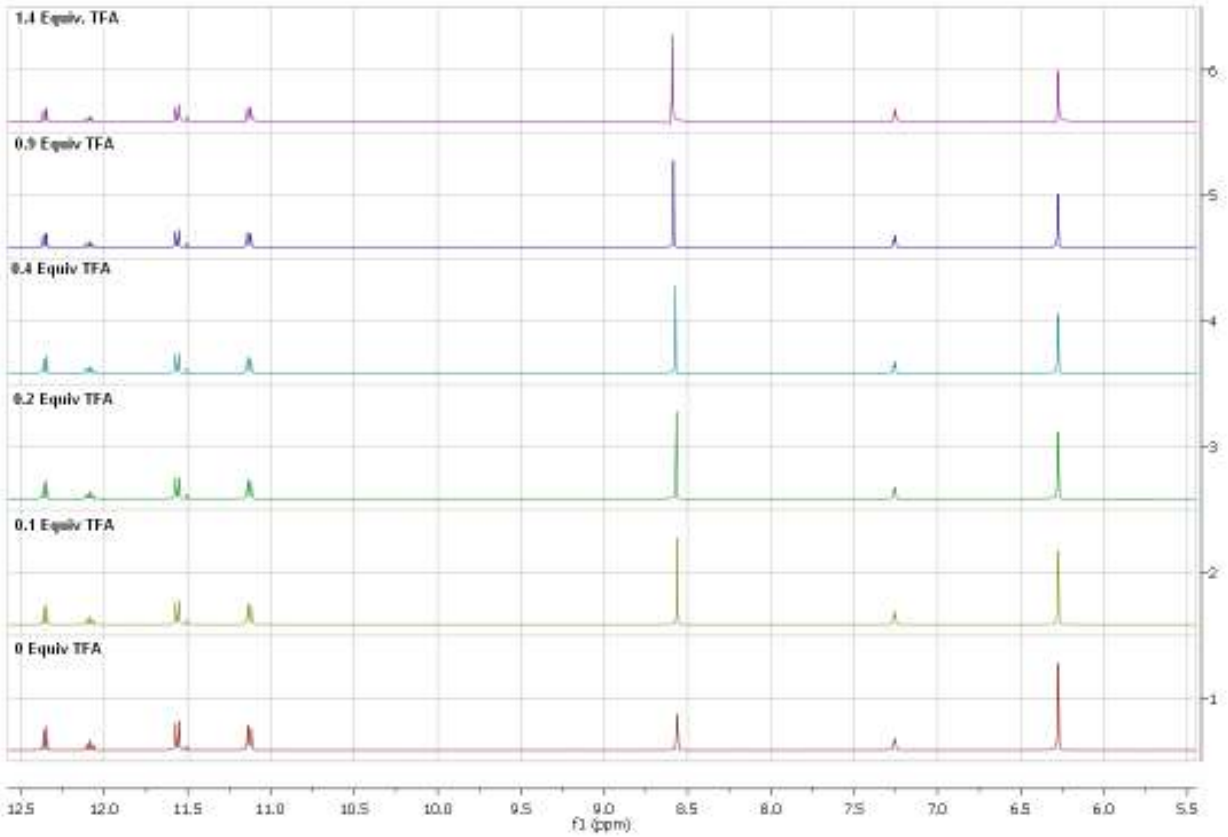

1-Bromonaphthalene-2,7-diol (Compound 1)

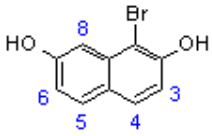

^{1}H NMR (300 MHz, $CDCl_3$)

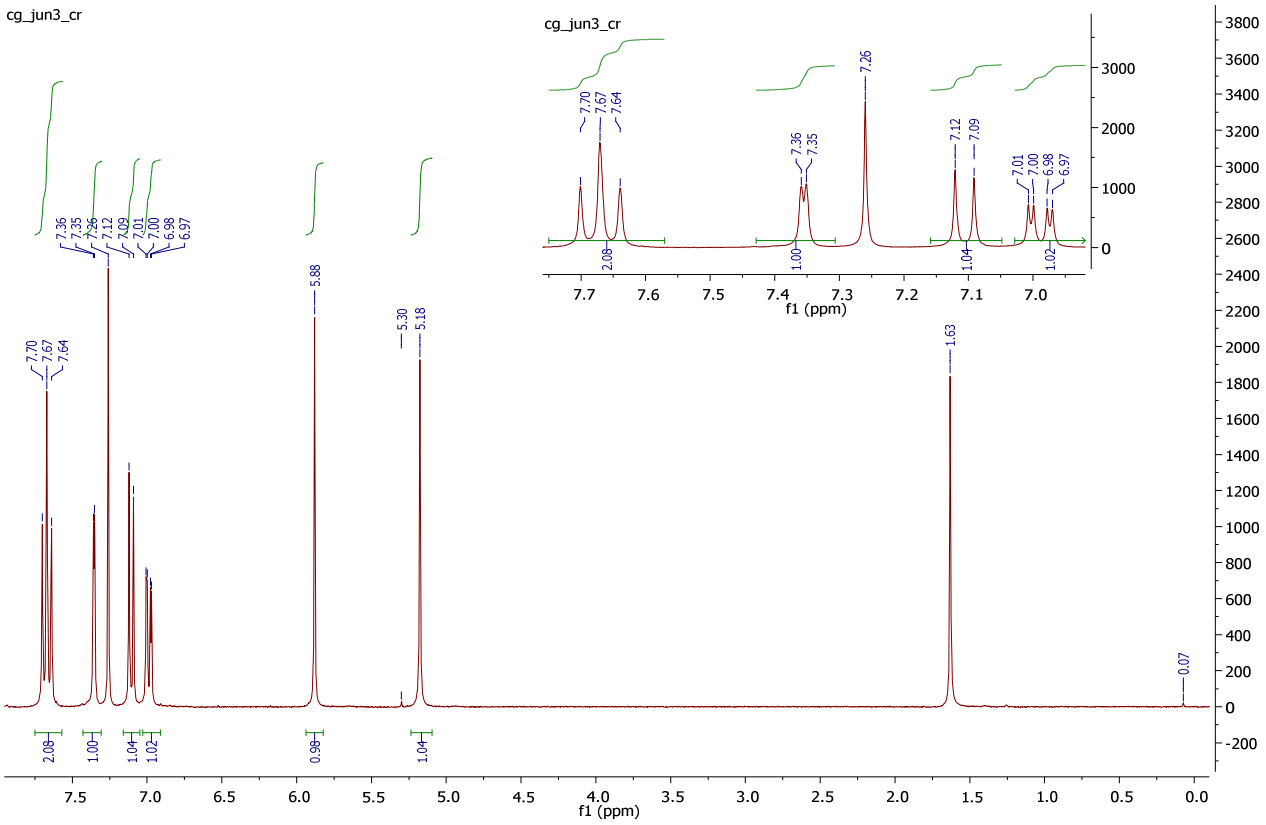

2-Methoxyethyl-4-methoxytolyl sulfonate (Compound 2)

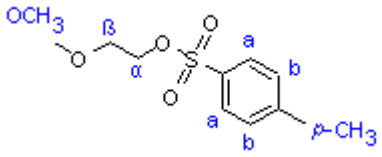

^{1}H NMR (300 MHz, $CDCl_3$)

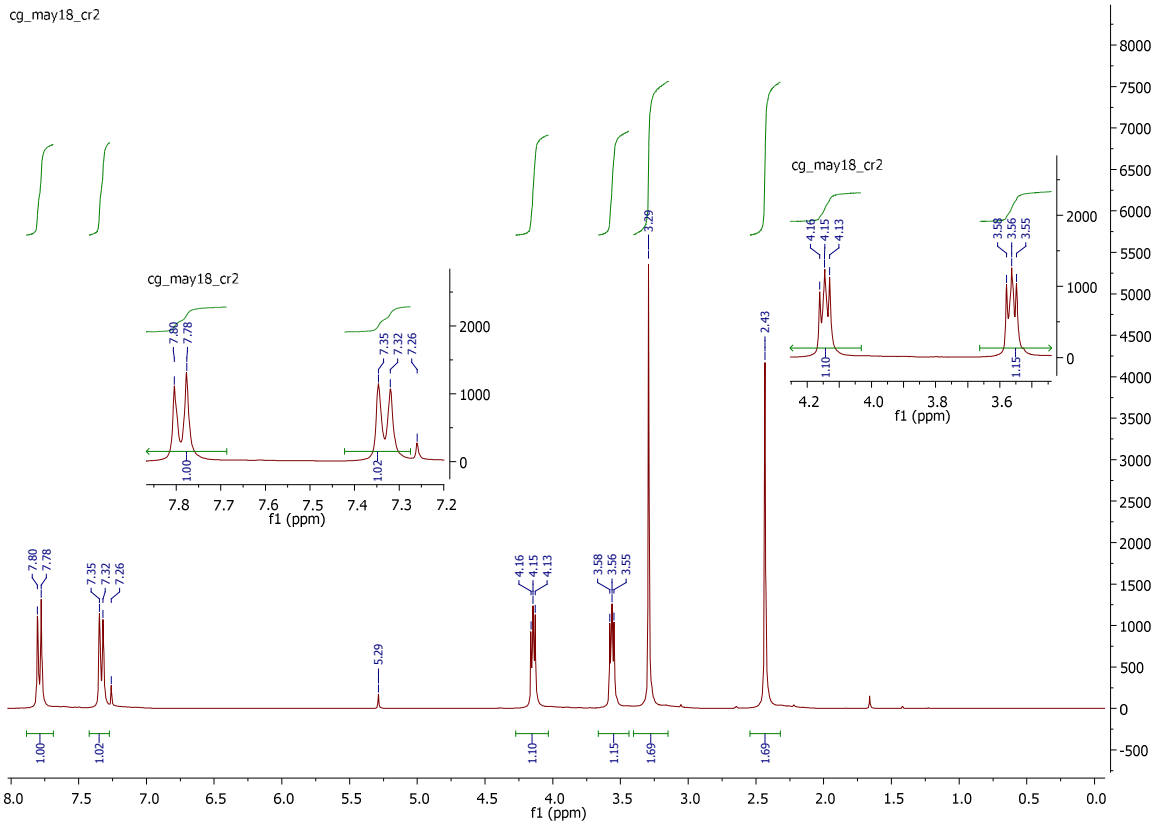

2-(2-Methoxyethoxy)ethyl-4-methylbenzene sulfonate (Compound 3)

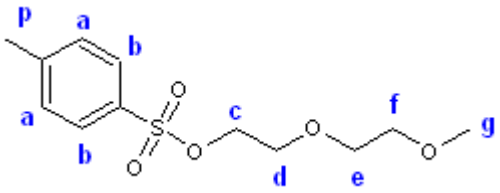

^{1}H NMR (300 MHz, $CDCl_3$)

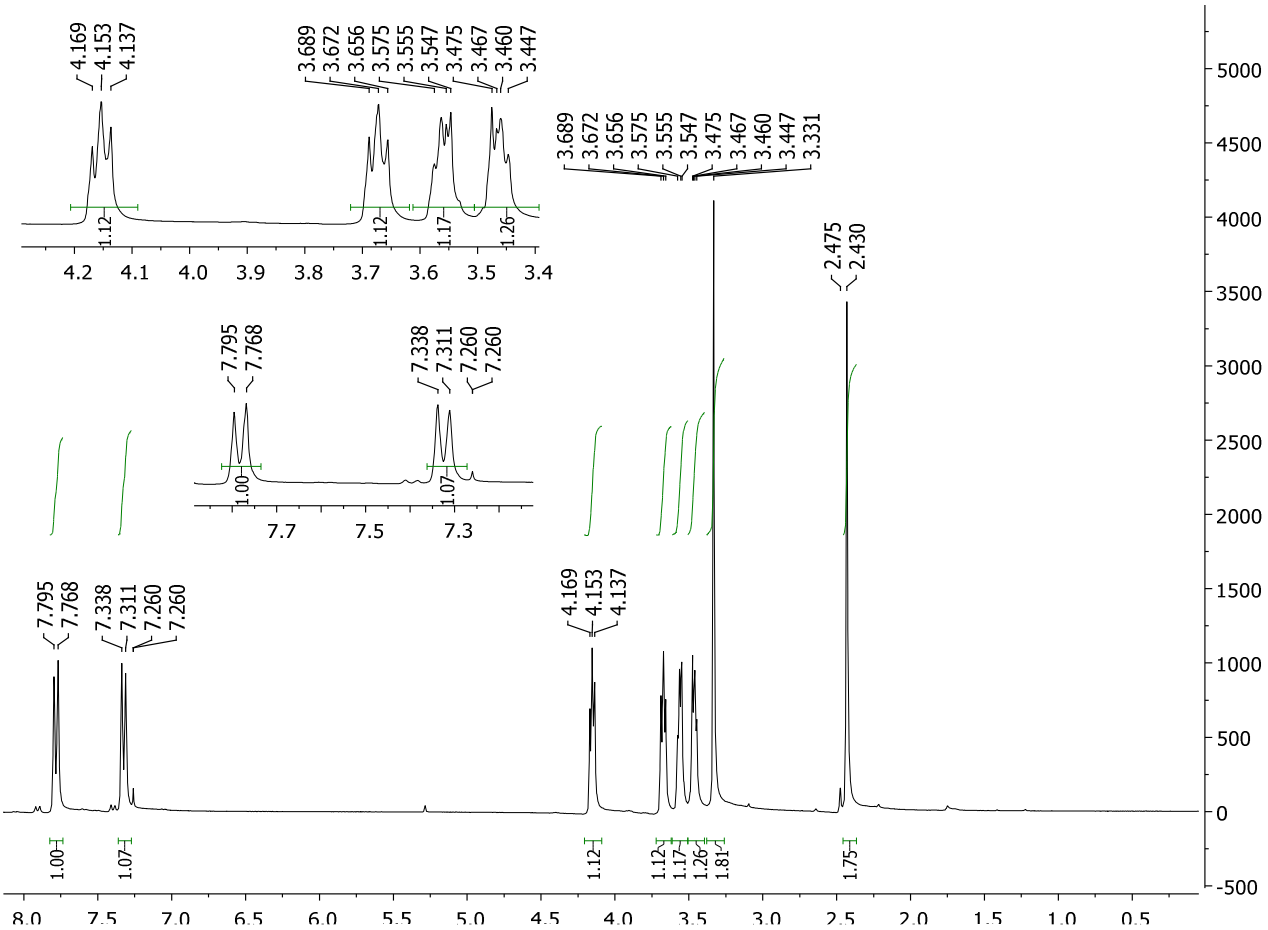

1-Bromo-2,7-bis(2-methoxyethoxy) naphthalene (UNIT 1 PEG, Compound 4)

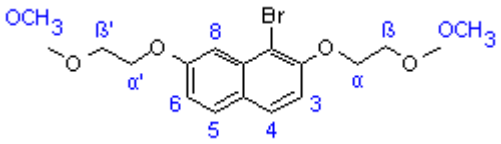

^{1}H NMR (300 MHz, $CDCl_3$)

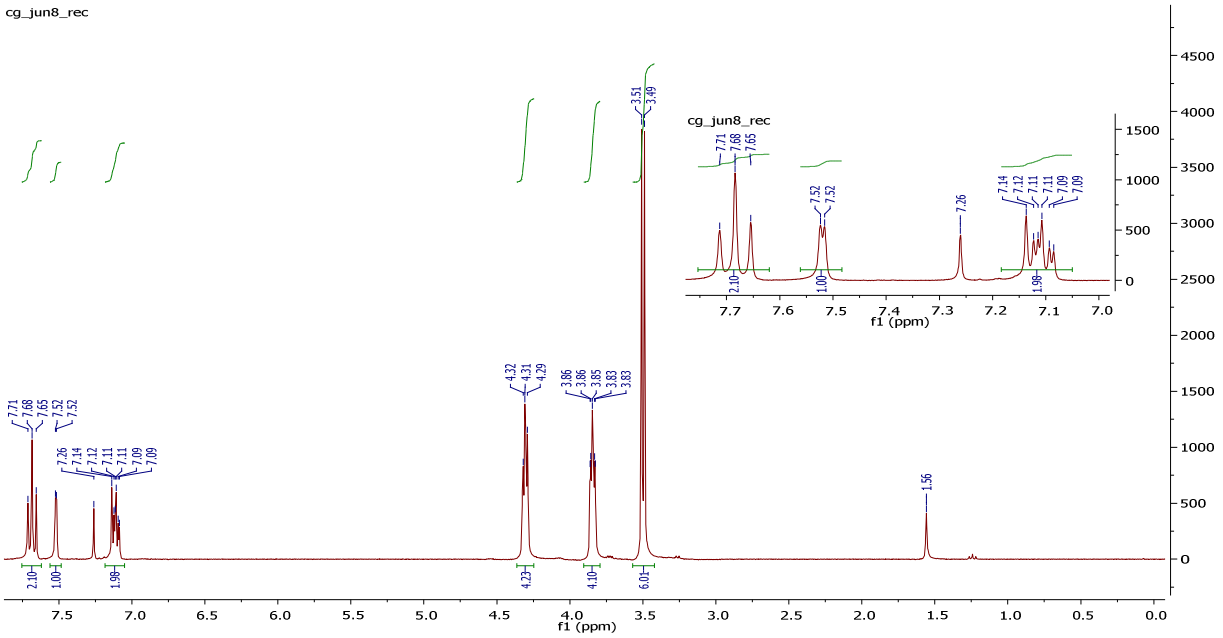

^{13}C NMR (100 MHz, $CDCl_3$)

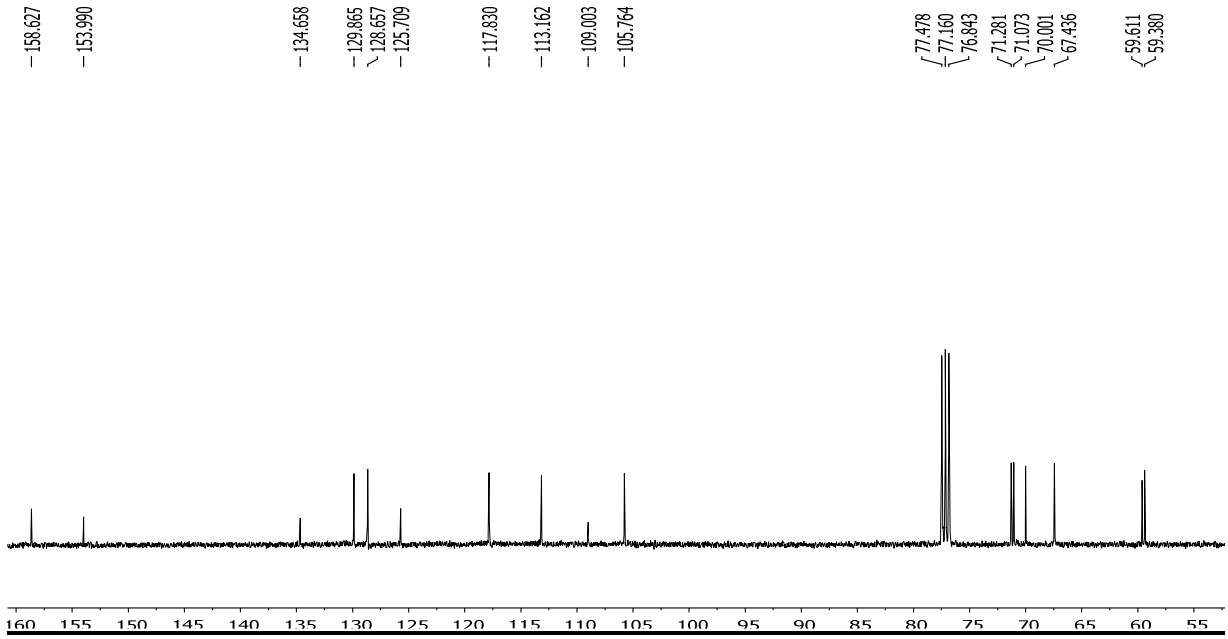

EI$^+$-MS: calculated for $C_{16}H_{19}O_4Br$: 354.05; found: 354.05 $[M]^+$, 296.02 $[M\text{-}C_3H_7O]^+$, 237.97 $[M\text{-}C_6H_{14}O_2]^+$, 59.05 $[M\text{-}C_{13}H_{12}O_3Br]^+$.

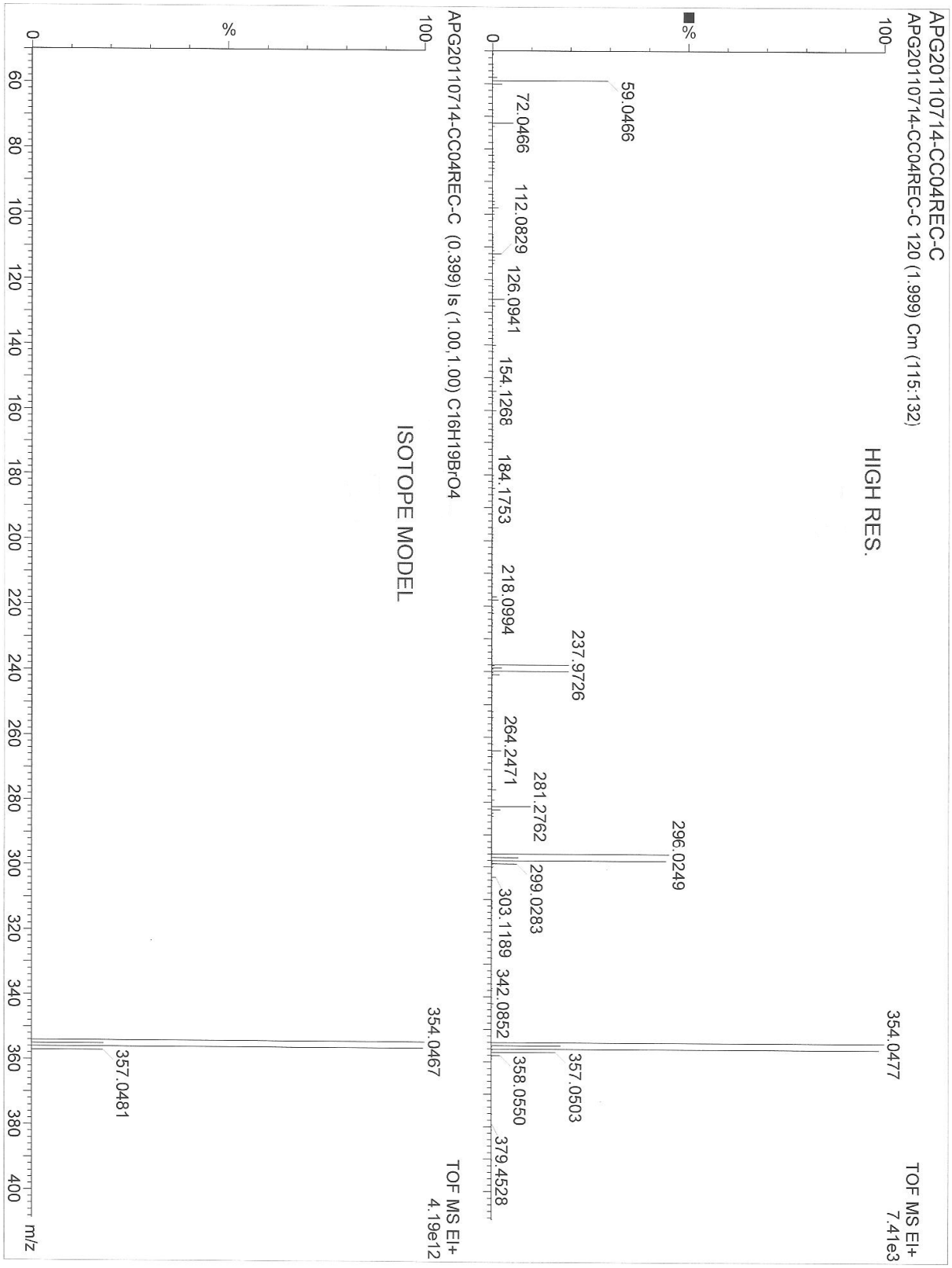

1-Bromo-2,7-bis(2-(2-methoxyethoxy)ethoxy) naphthalene (UNIT 2 PEG, Compound 5)

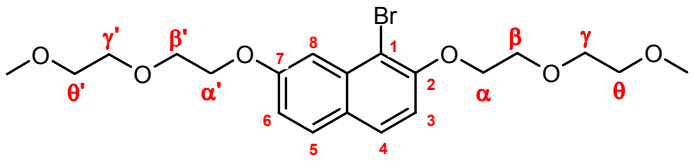

^{1}H NMR (300 MHz, $CDCl_3$)

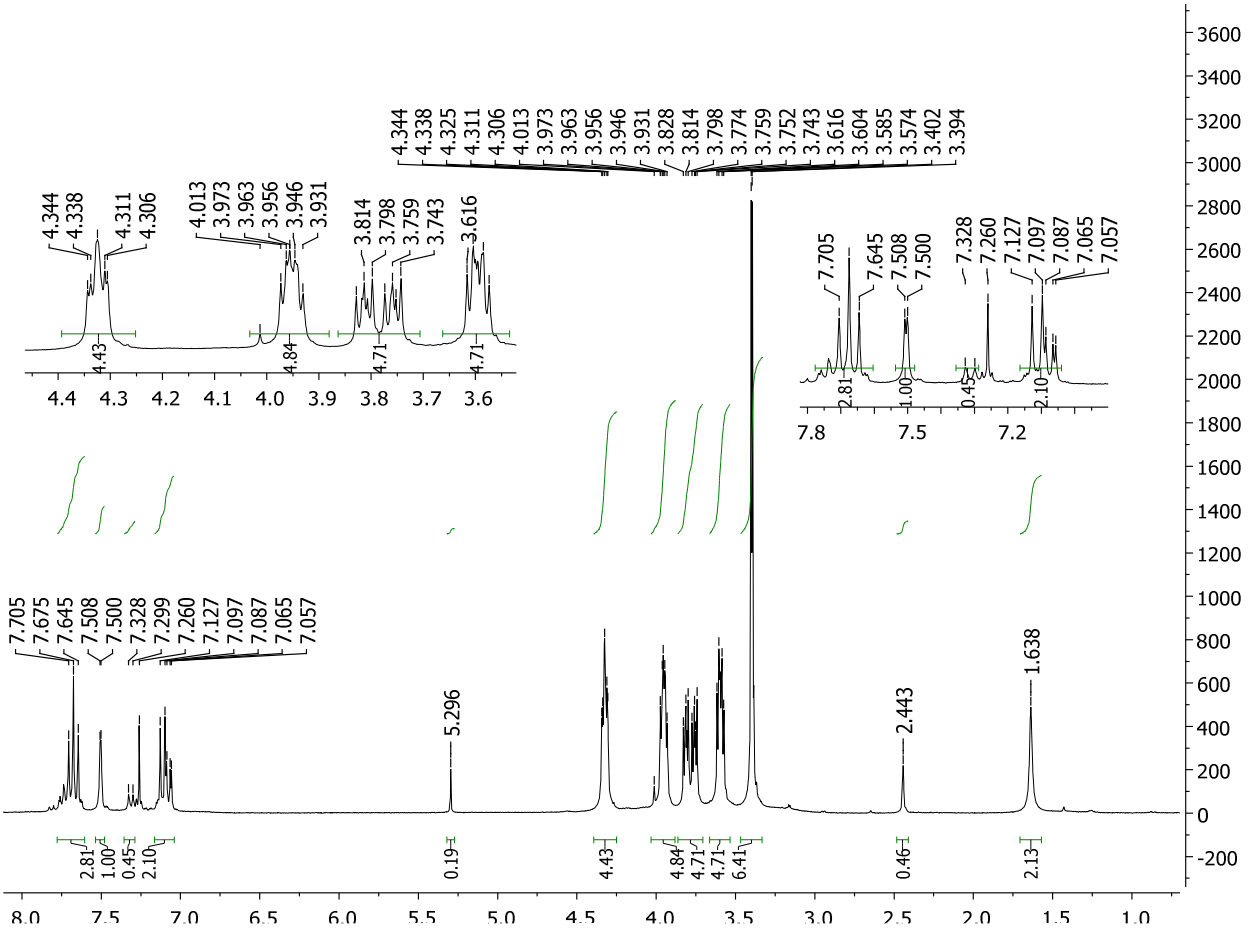

2,6-Bis(5-bromo-2-methoxyphenyl) pyridine (MeOPh-Py-MeOPh, Compound 6)

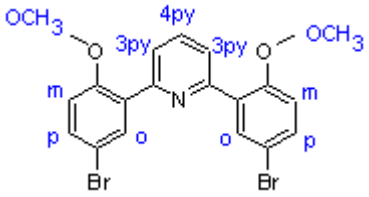

^{1}H NMR (300 MHz, $CDCl_3$)

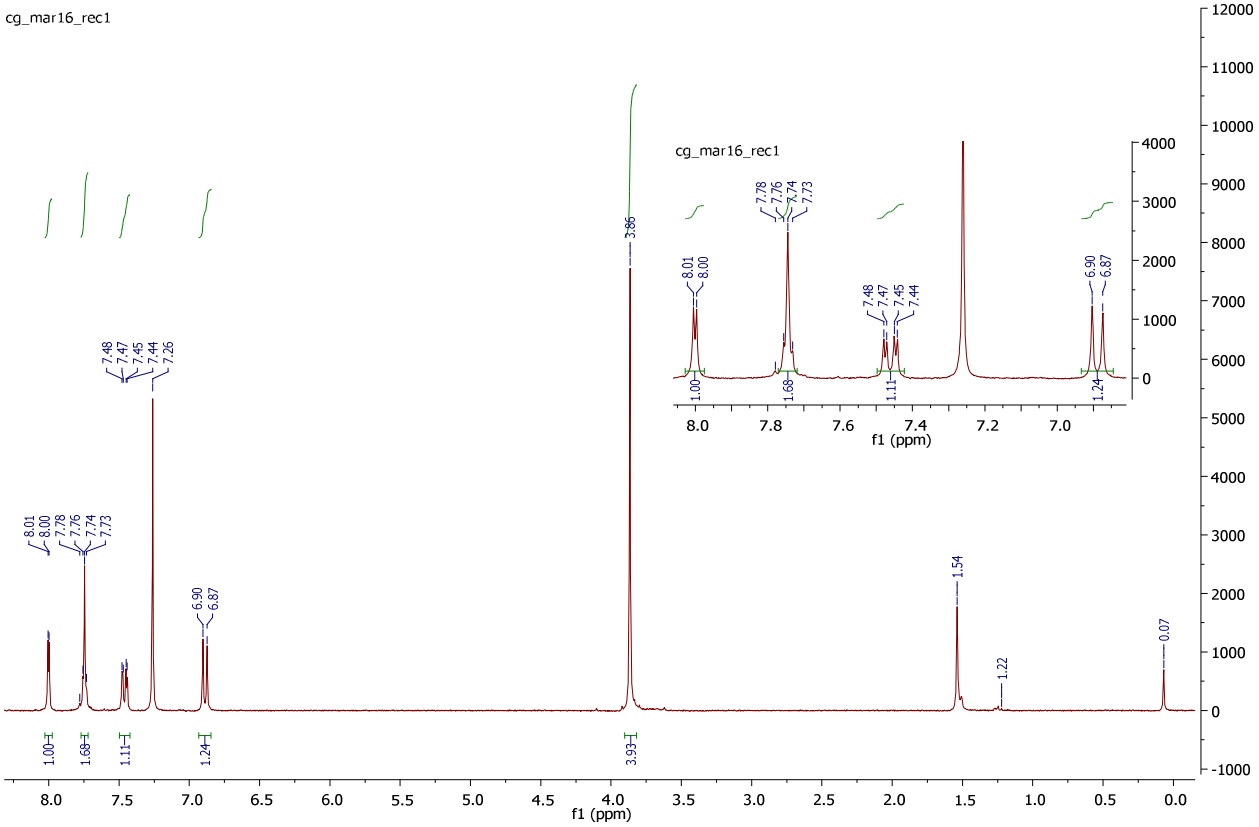

Triad di-boronic ester (Compound 7)

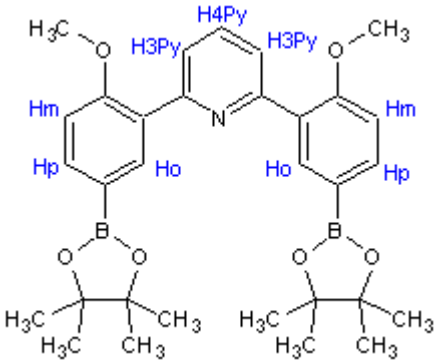

^{1}H NMR (300 MHz, $CDCl_3$)

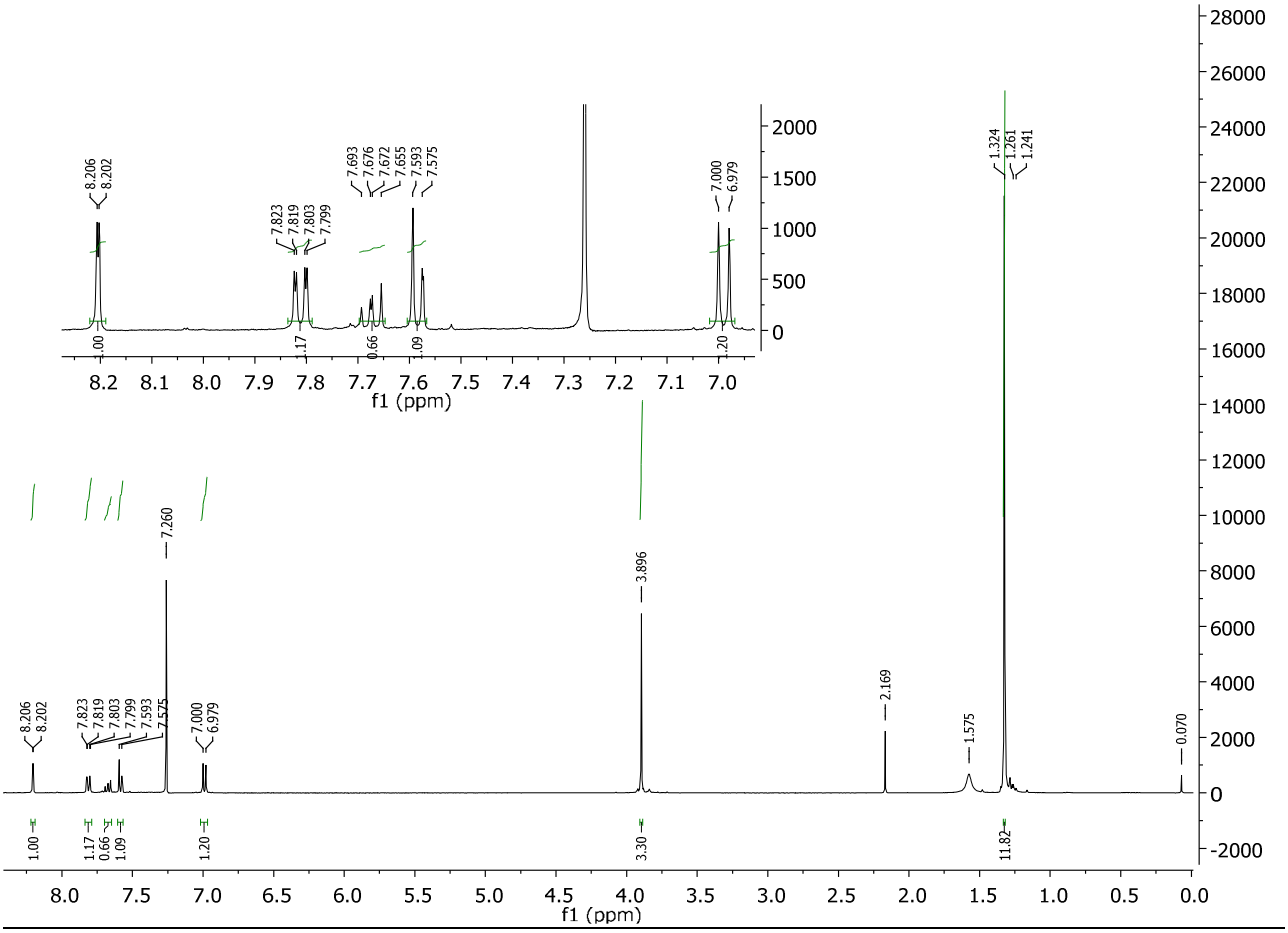

Triad Trifluoroborate Salt (Compound 8)

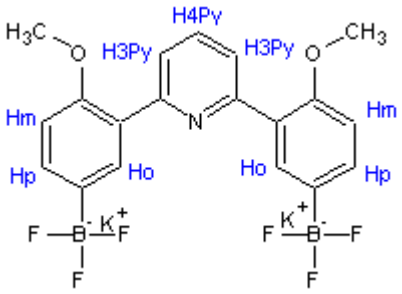

^{1}H NMR (300 MHz, Acetone-d_6)

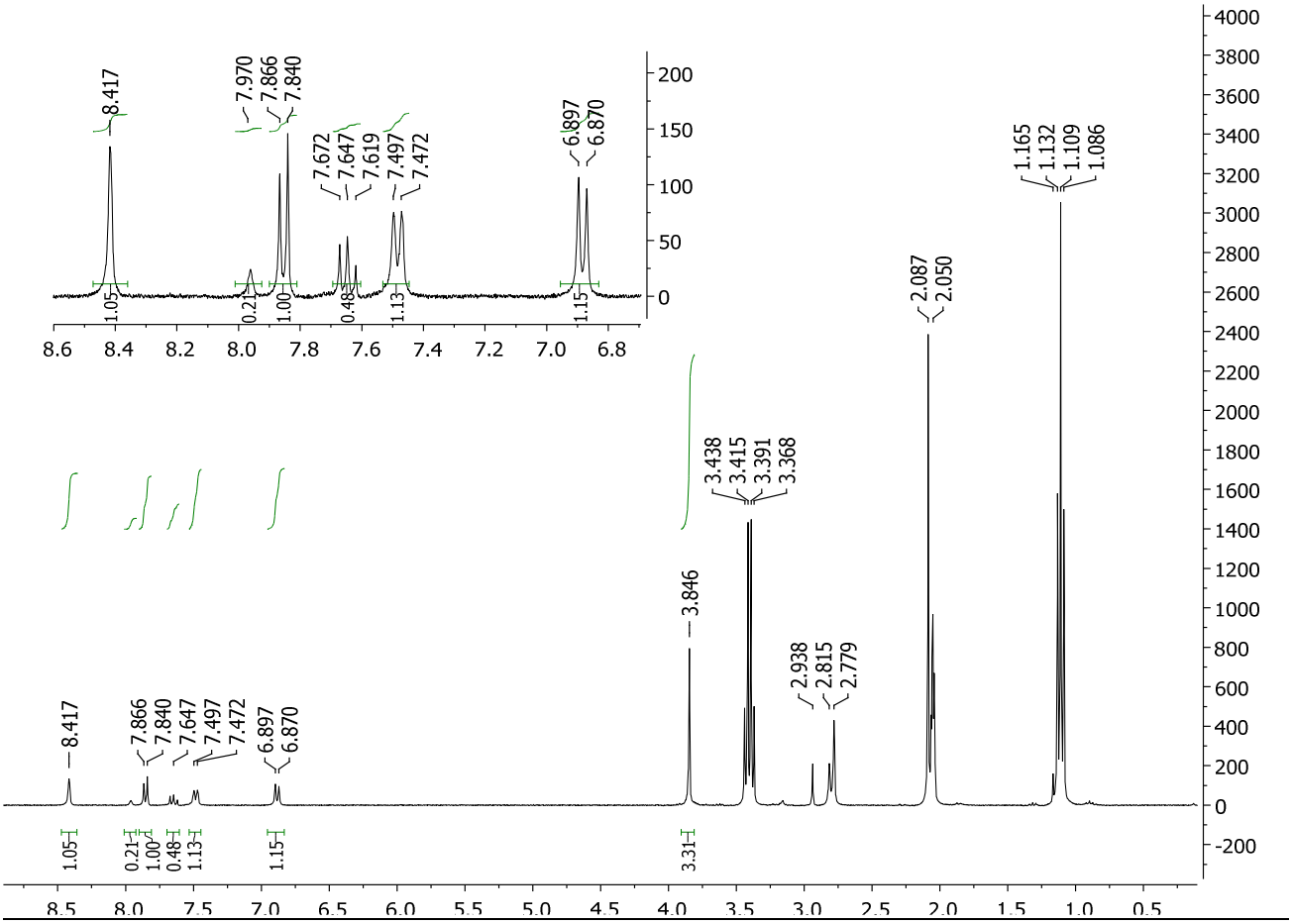

Triad di-boronic acid (Compound 9)

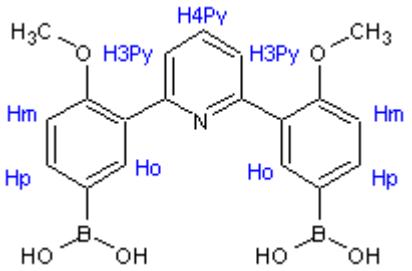

^{1}H NMR (300 MHz, Acetone-d_6)

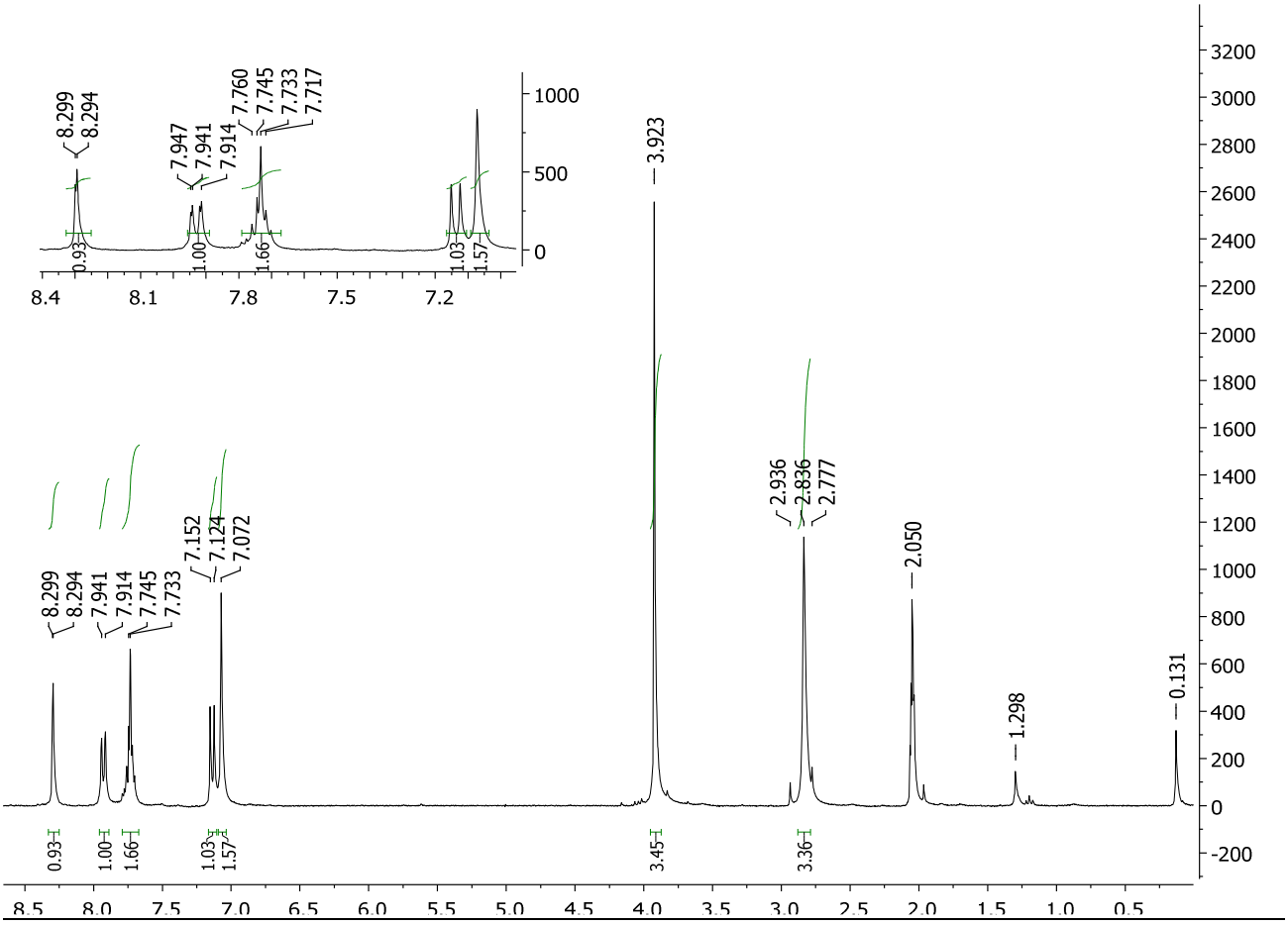

6-Amino-1-methylpyrimidine-2,4(1*H*,3*H*)-dione (Compound 10)

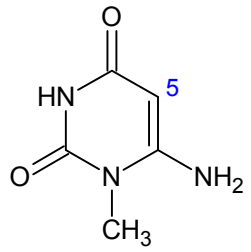

^{1}H NMR (300 MHz, DMSO-d_6)

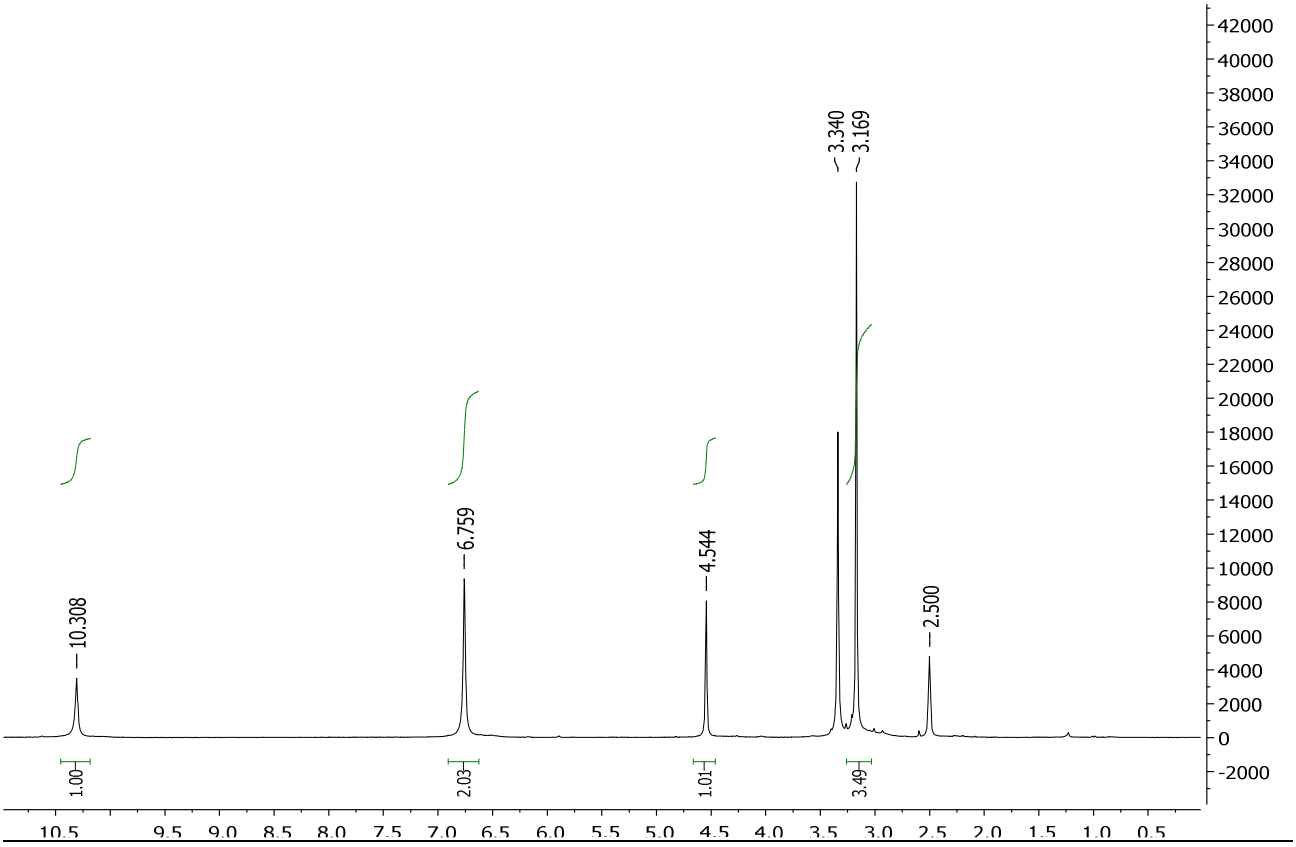

6-Amino-3-(2-methoxyethyl)-1-methylpyrimidine-2,4(1*H*,3*H*)-dione (Compound 13)

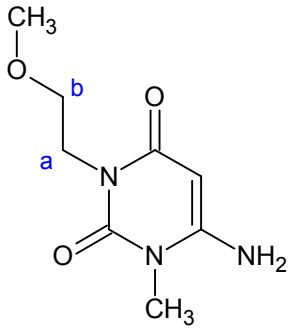

^{1}H NMR (400 MHz, DMSO-d$_6$)

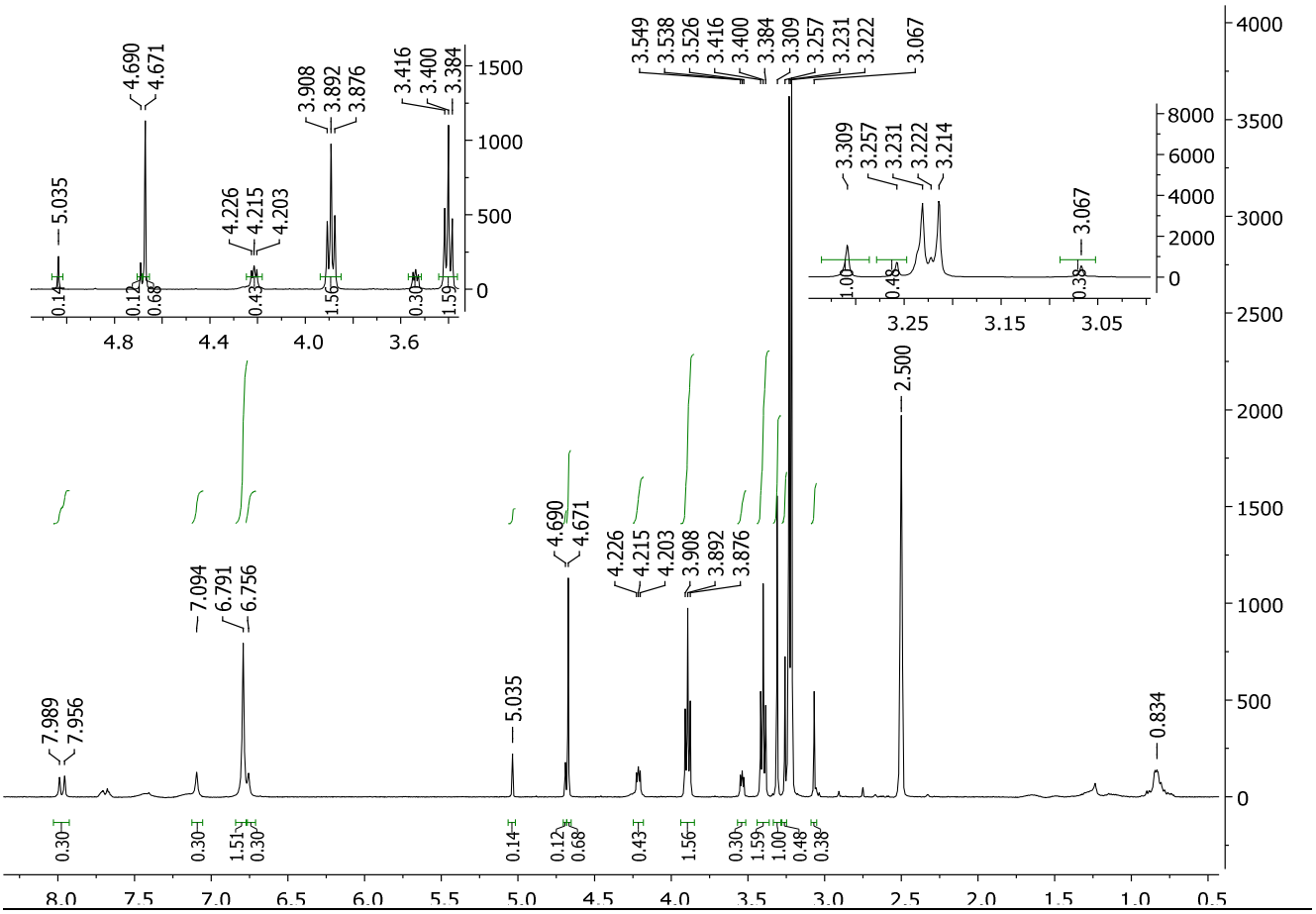

2-Bromo-4-iodoanisole (Compound 14)

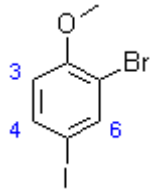

^{1}H NMR (300 MHz, $CDCl_3$)

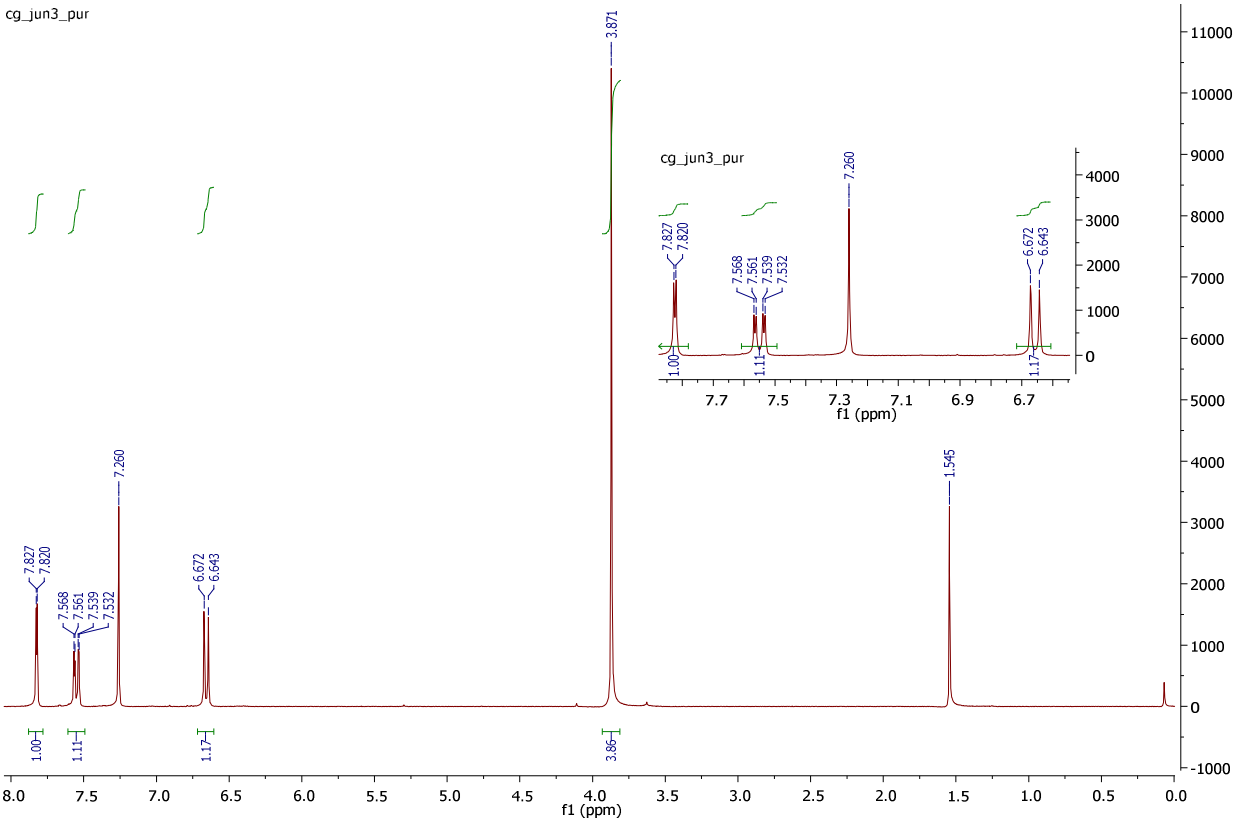

2-(3-Bromo-4-methoxy-phenyl)-4,4,5,5-tetramethyl-[1,3,2]dioxaborolane (Compound 15)

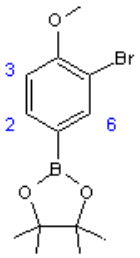

^{1}H NMR (300 MHz, $CDCl_3$)

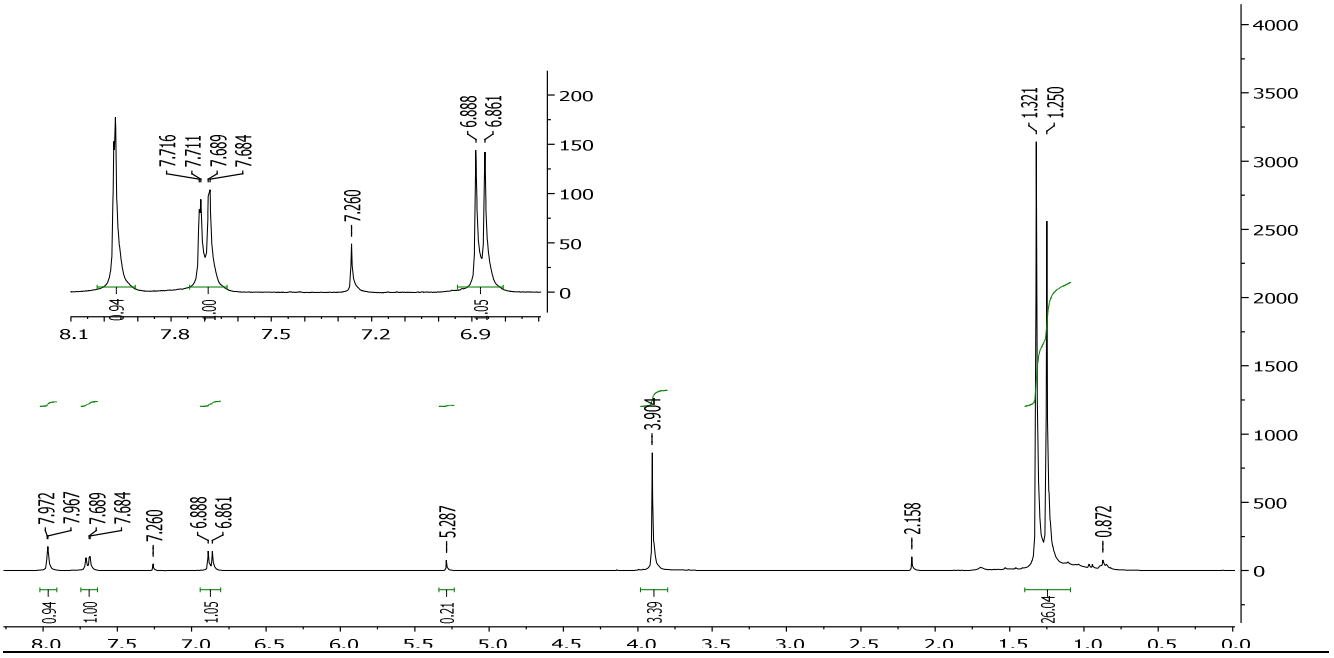

^{13}C NMR (75 MHz, $CDCl_3$)

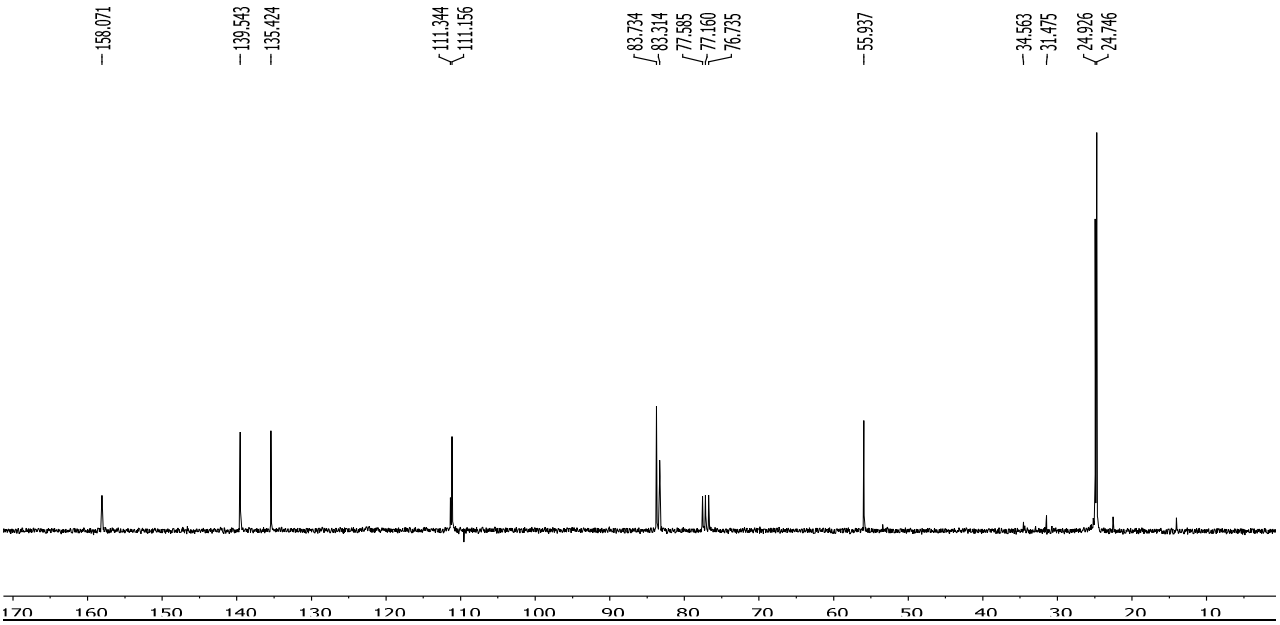

EI$^+$-MS: calculated for $C_{13}H_{18}O_3BBr$: 312.05; found: 312.05 $[M]^+$, 83.95 $[M\text{-}C_7H_6BBrO_3]^+$

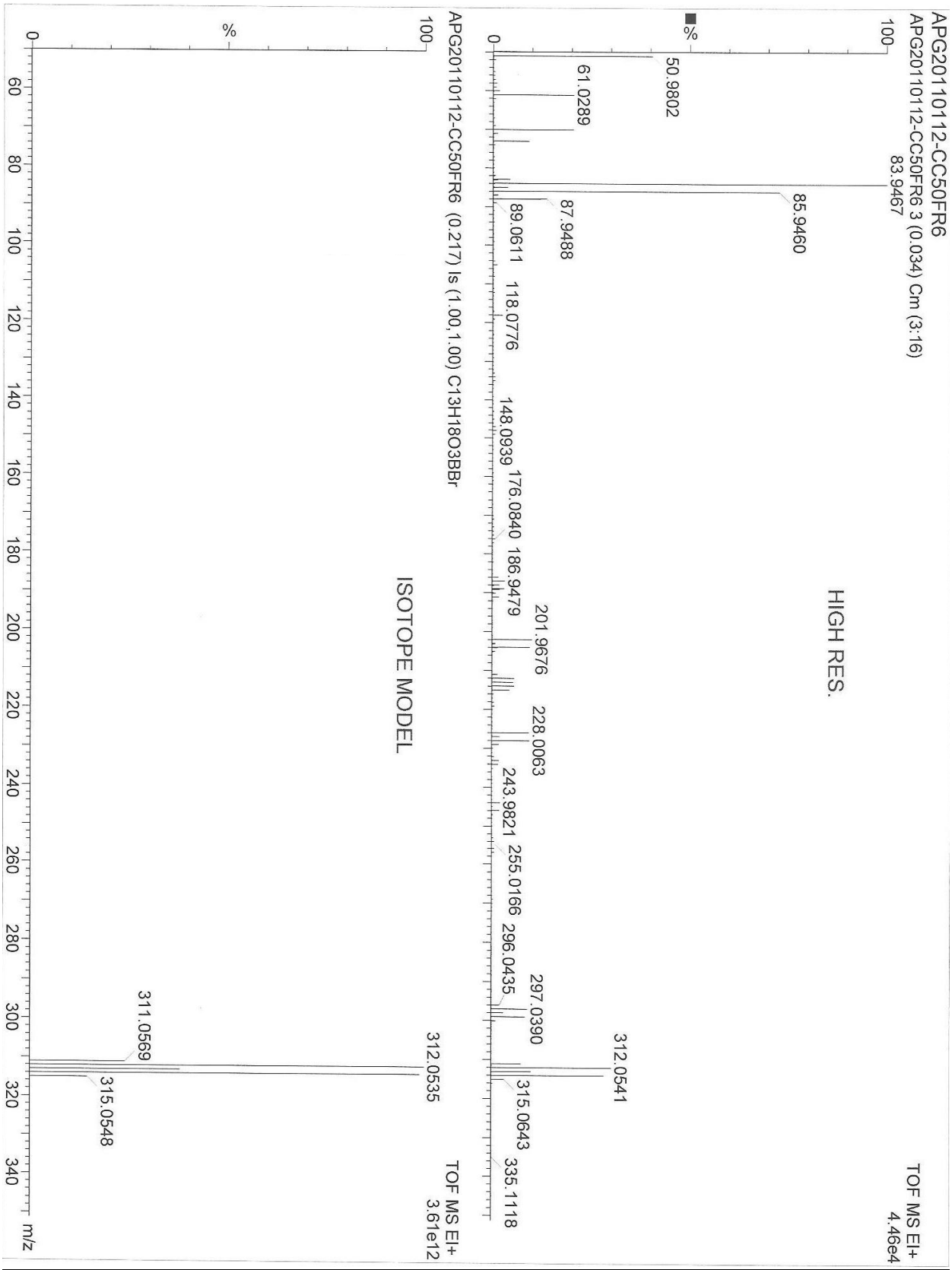

Potassium 5-bromo-4-methoxy-phenyl trifluoroborate (Compound 16)

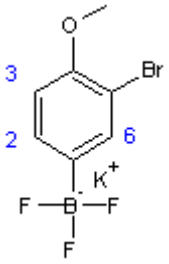

^{1}H NMR (300 MHz, Acetone- d_6)

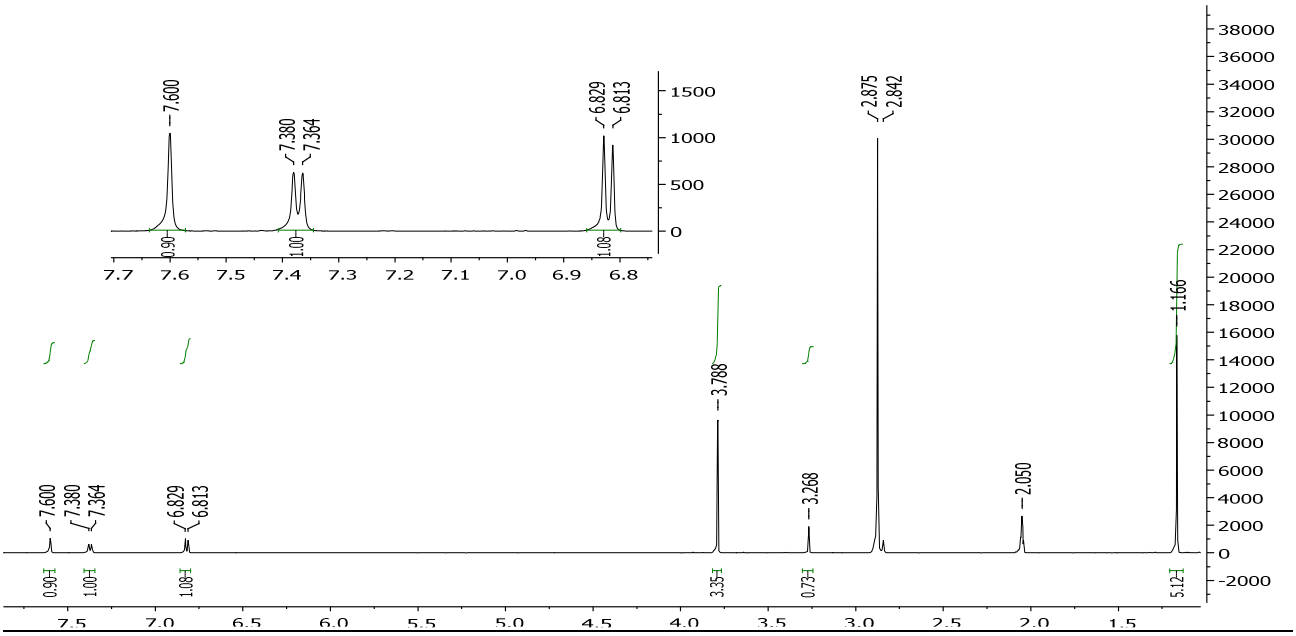

^{13}C NMR (100 MHz, Acetone- d_6)

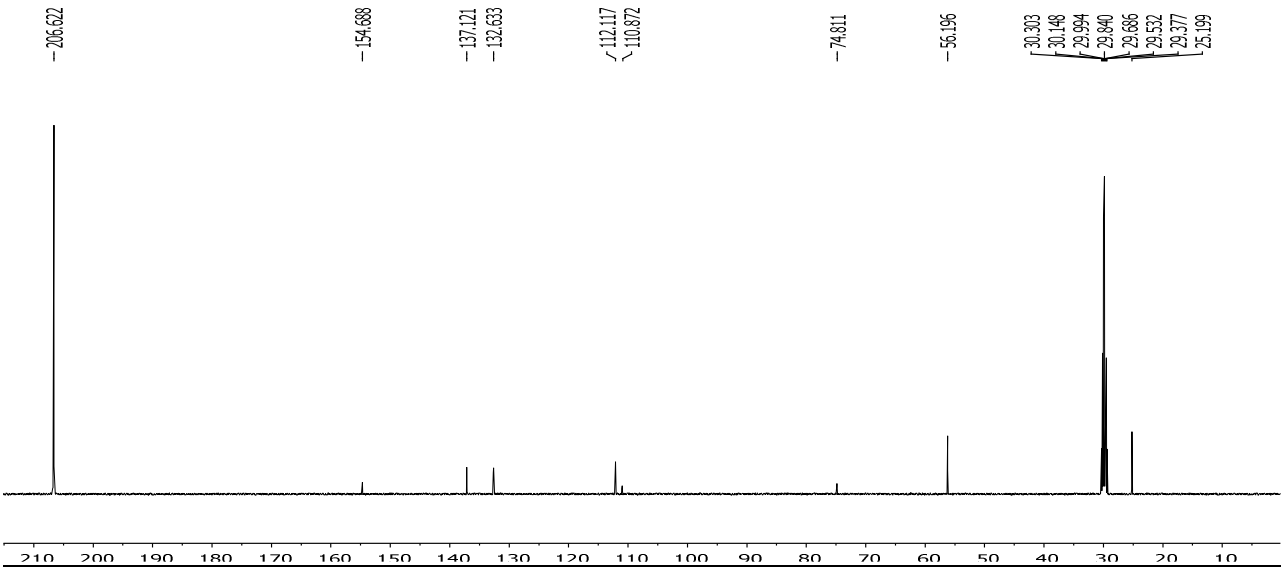

ESI$^-$-HRMS: calculated for $C_7H_6BOF_3Br^-$: 252.96; found: 252.96 $[M-K]^-$.

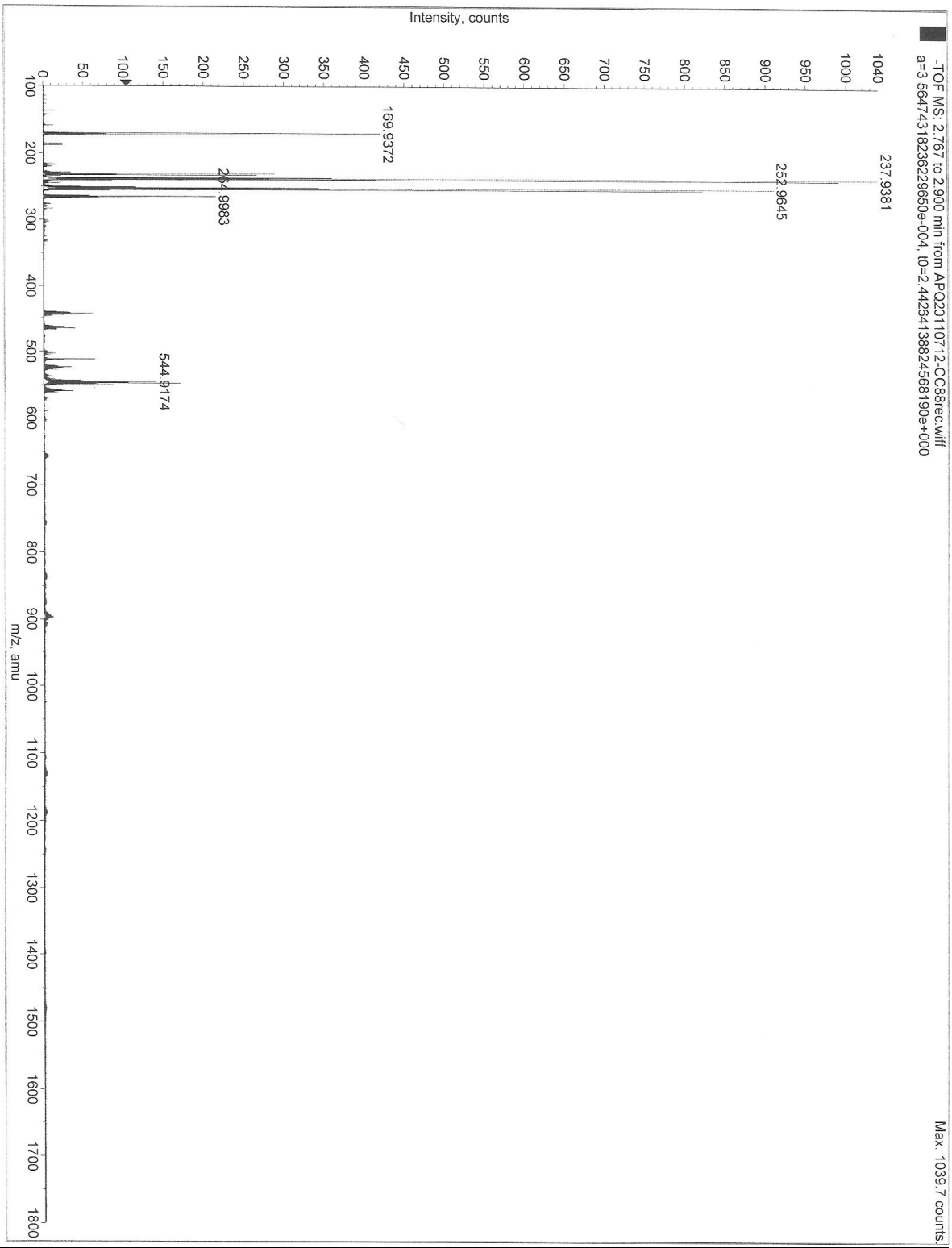

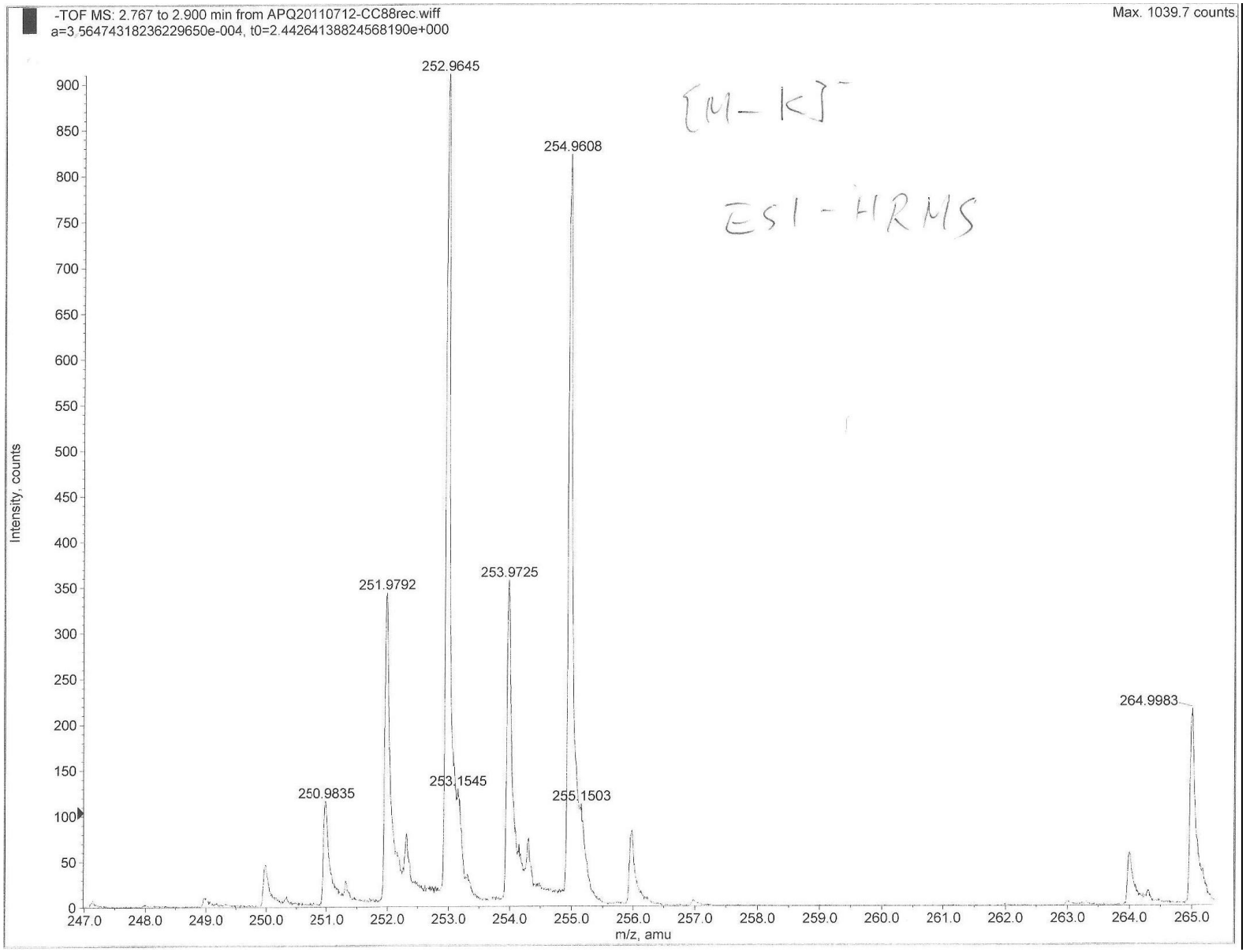
-TOF MS: 2.767 to 2.900 min from APQ20110712-CC88rec.wiff
a=3.5647431823622965e-004, t0=2.4426413882456819e+000
Max. 1039.7 counts.
[M-K]⁻
ESI-HRMS
252.9645
254.9608
251.9792
253.9725
264.9983
250.9835
253.1545
255.1503
Intensity, counts
m/z, amu

5-Bromo-4-methoxy-phenyl boronic acid (Compound 17)

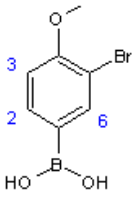

^{1}H NMR (300 MHz, Acetone- d_6)

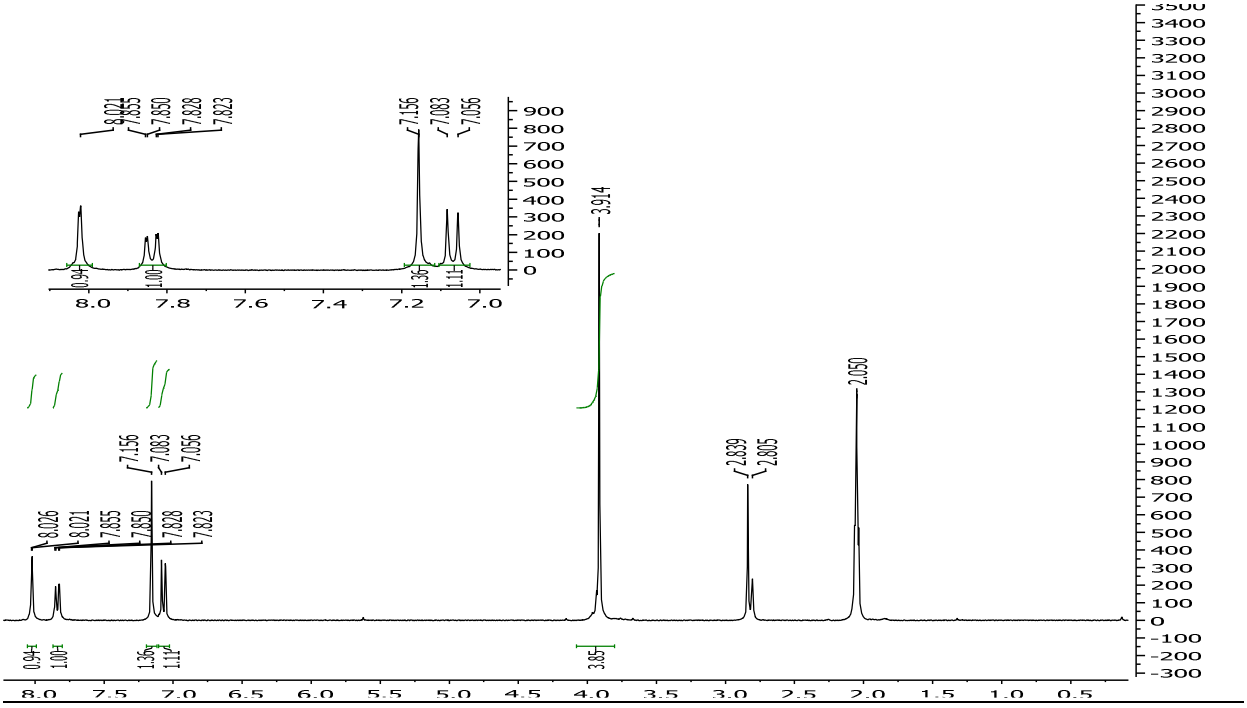

^{13}C NMR (100 MHz, Acetone- d_6)

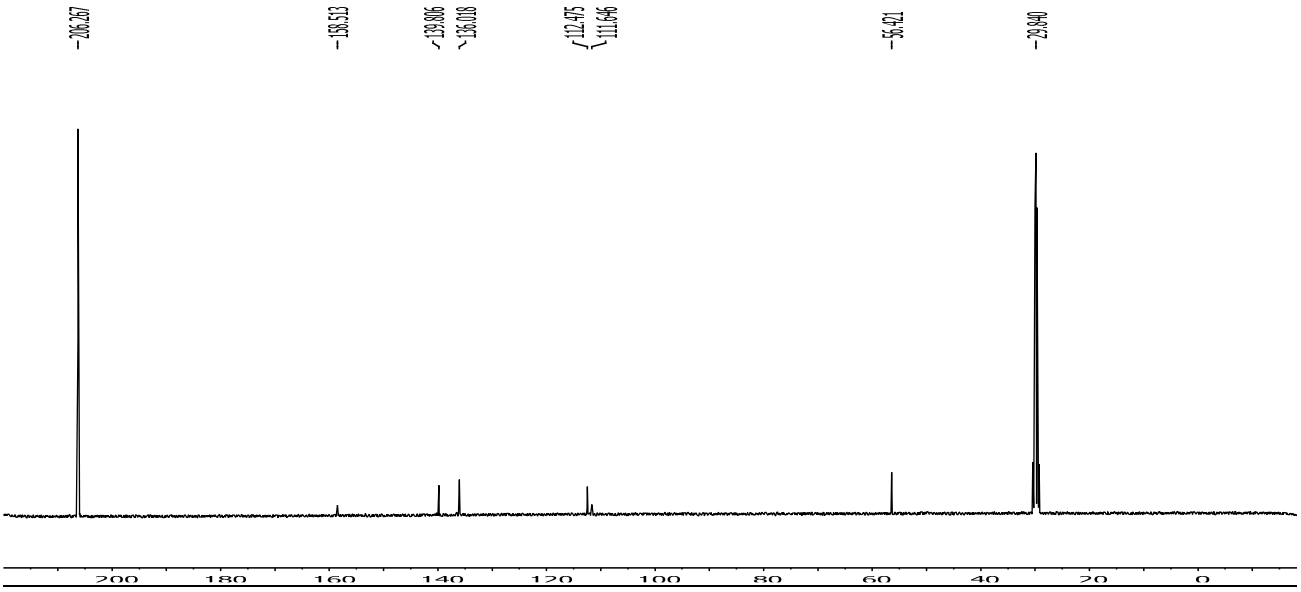

ESI$^-$-LRMS: calculated for $C_7H_7BO_3Br^-$: 228.97; found: 229.00 $[M-H]^-$.

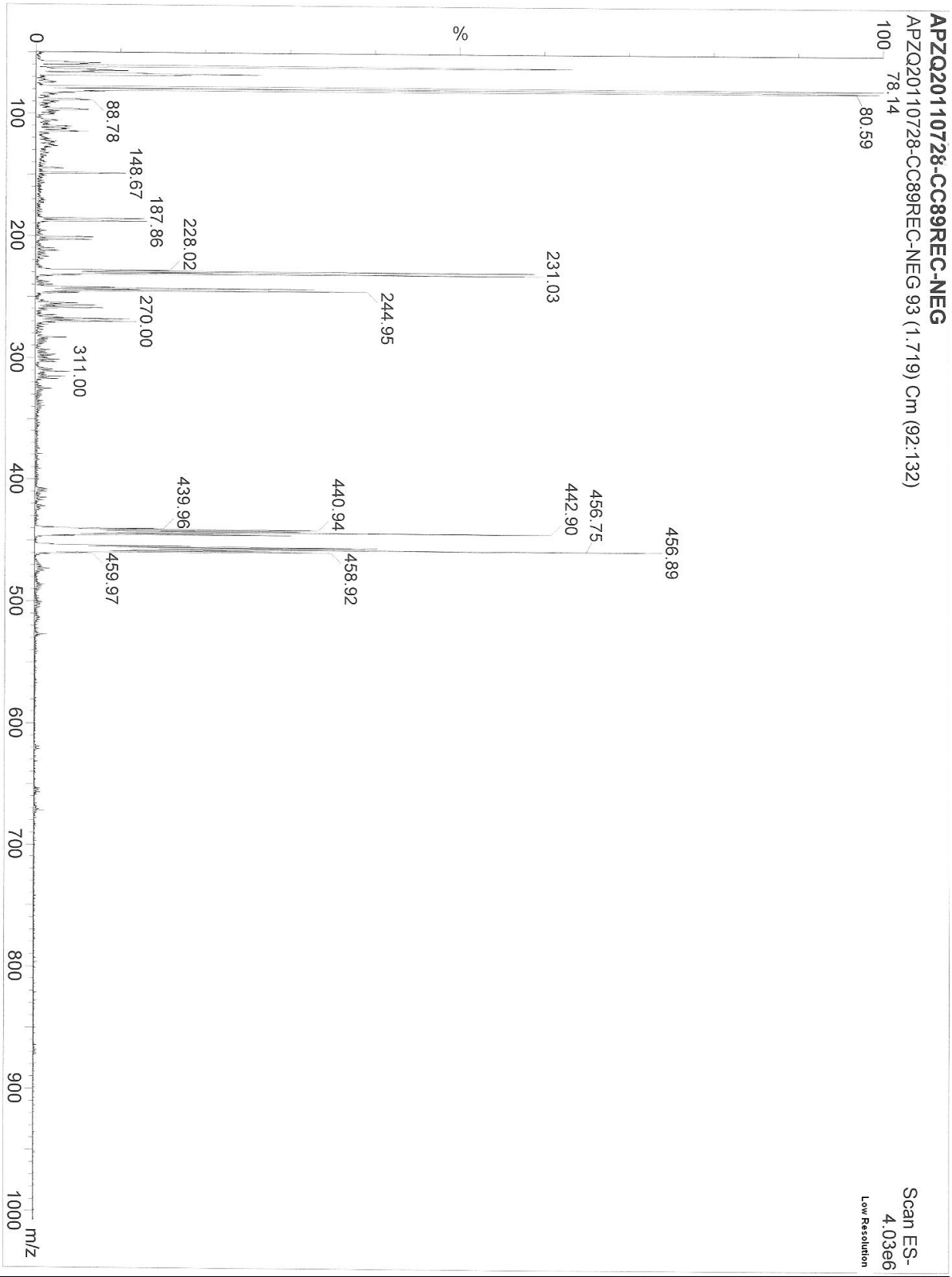

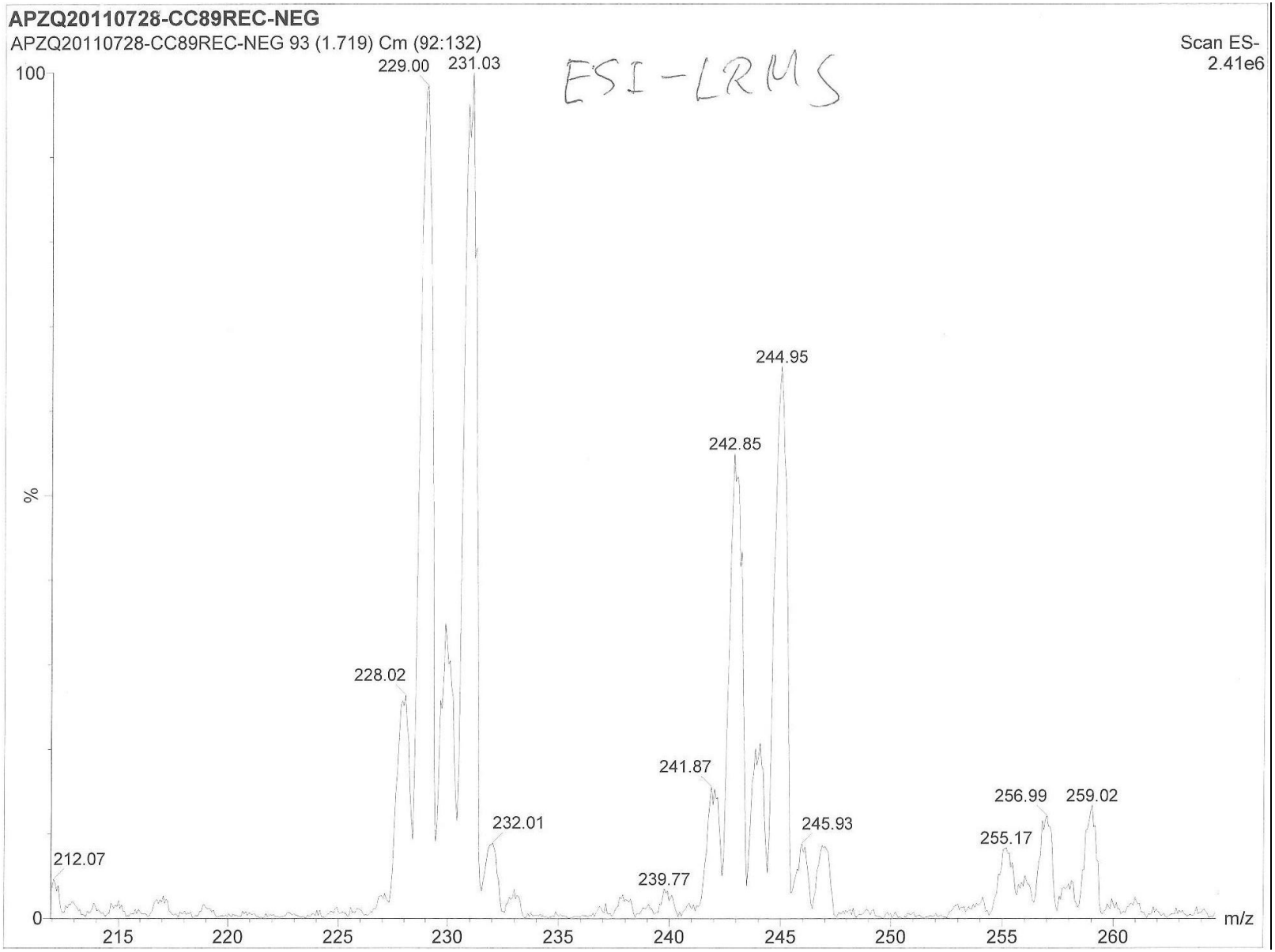
APZQ20110728-CC89REC-NEG
APZQ20110728-CC89REC-NEG 93 (1.719) Cm (92:132)
Scan ES-
2.41e6
ESI-LRMS
100
%
0
229.00
231.03
244.95
242.85
228.02
241.87
256.99
259.02
232.01
245.93
255.17
212.07
239.77
215
220
225
230
235
240
245
250
255
260
m/z

1-(3-bromo-4-methoxyphenyl)-1*H*-pyrazolo[4,3-*d*]pyrimidine-5,7(4*H*,6*H*)-dione (Compound 18)

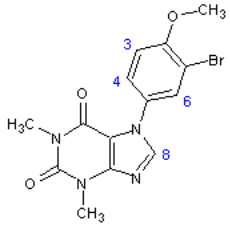

^{1}H NMR (400 MHz, $CDCl_3$)

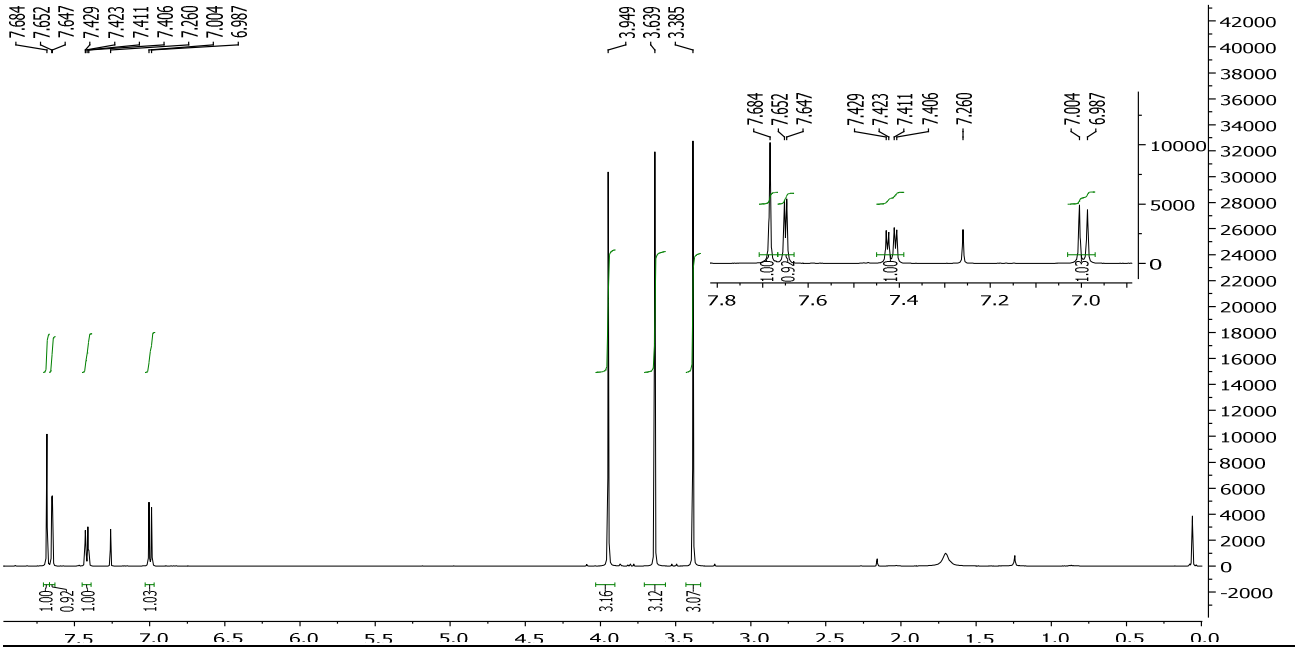

^{13}C NMR (125 MHz, $CDCl_3$)

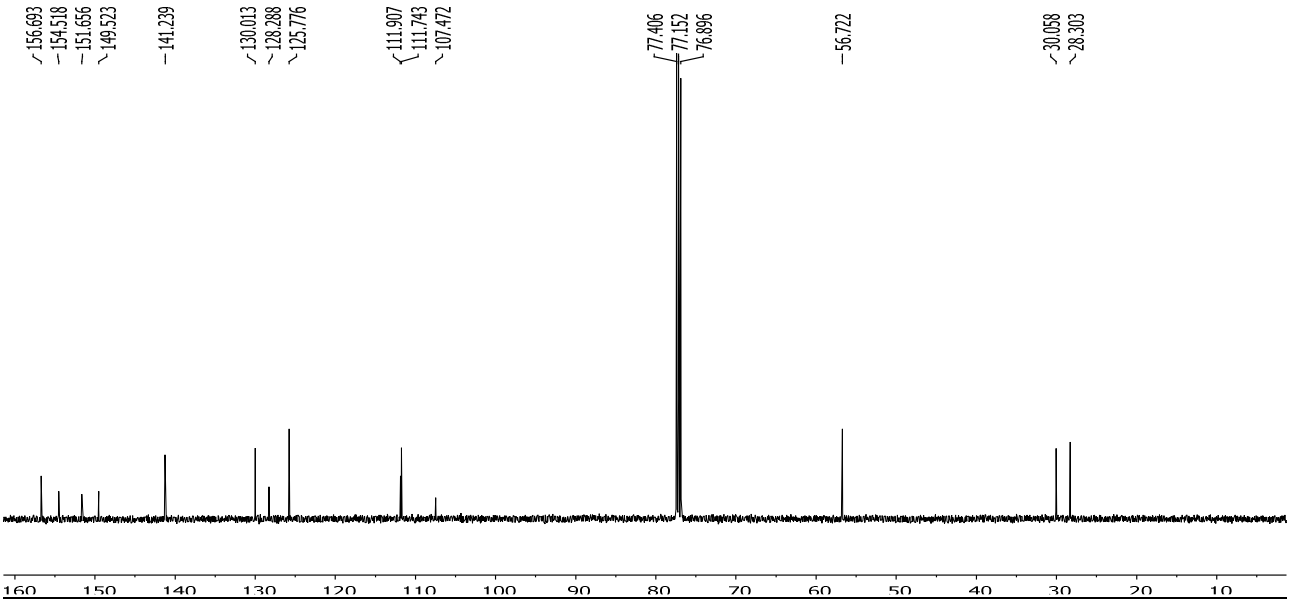

EI$^+$-MS: calculated for $C_{14}H_{13}BrN_4O_3$: 364.02; found: 364.02 $[M]^+$, 366.02 $[M+2H]^+$.

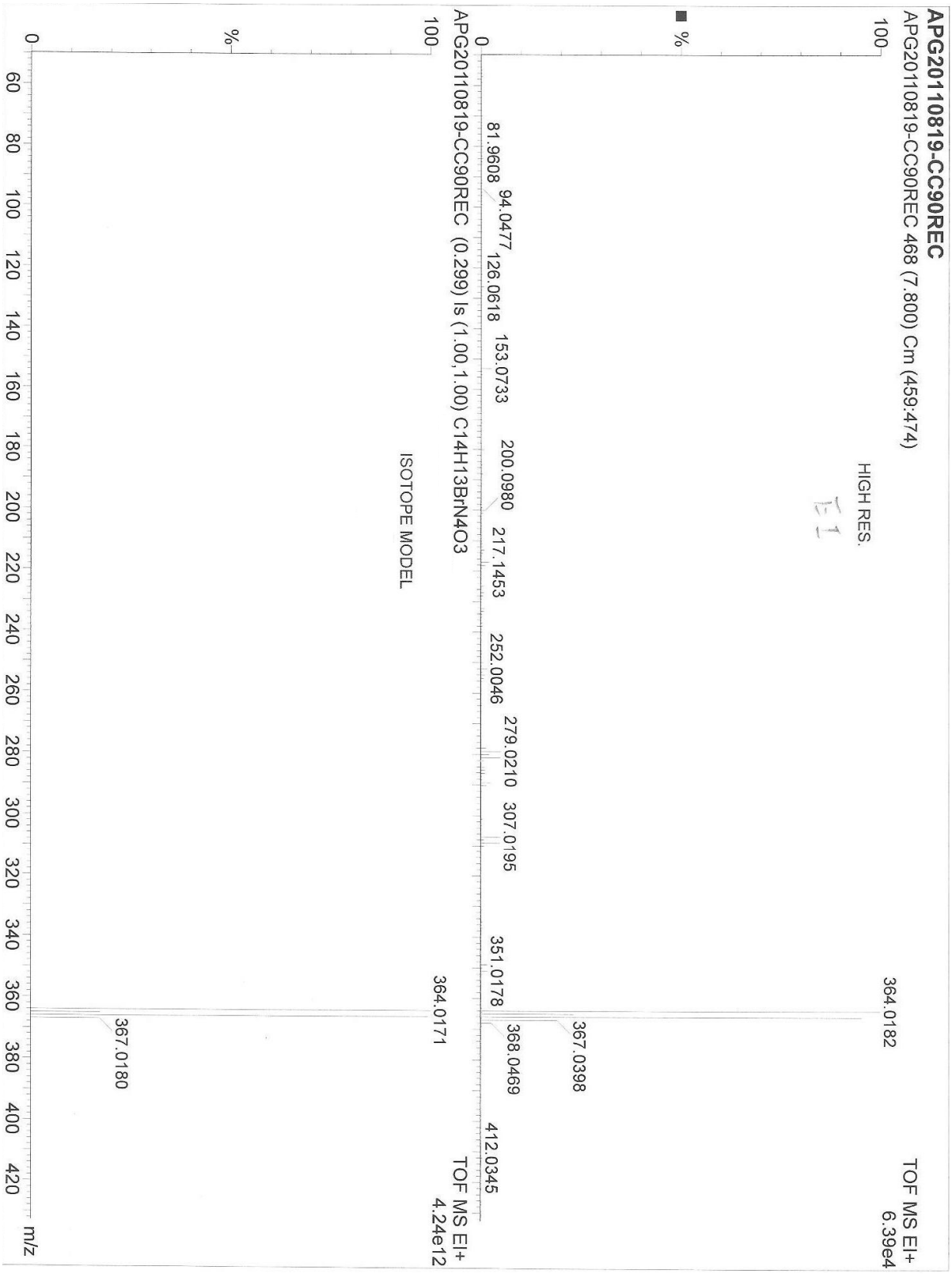

7-(4-Methoxyphenyl)-1,3-dimethyl-3,7-dihydro-purine-2,6-dione

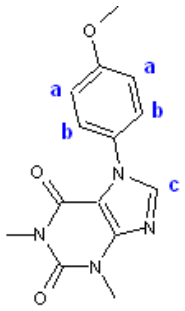

^{1}H NMR (500 MHz, $CDCl_3$)

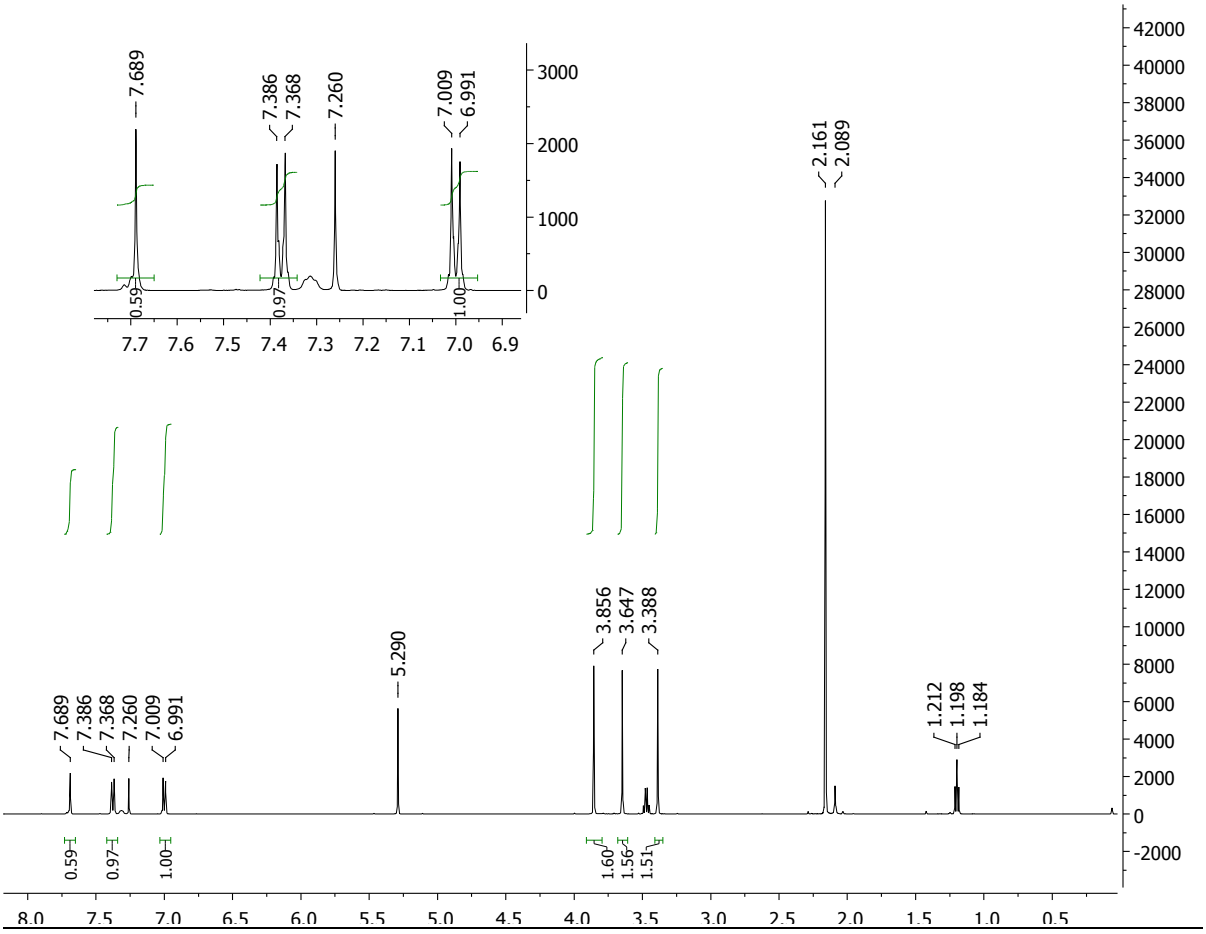

5[-(1H-1,3-benzodiazol-2-yl)-2-methoxyphenyl]boronic acid (Compound 19)

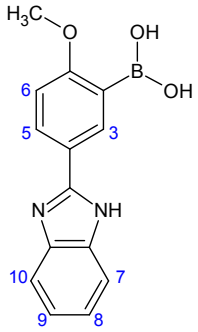

^{1}H NMR (300 MHz, DMSO-d_6)

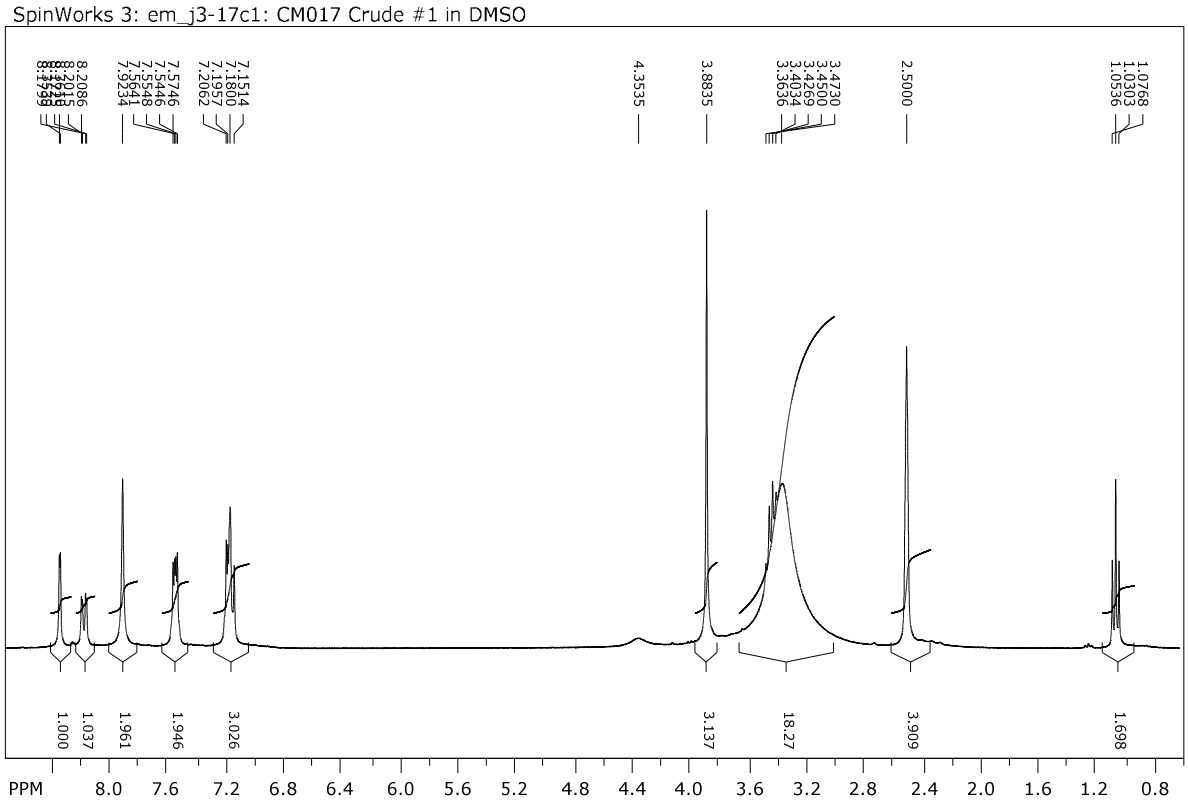

file: ...MR files\Raw Data\em_j3-17c1\2\fid expt: <zg45.fs>
transmitter freq.: 300.131501 MHz
time domain size: 32768 points
width: 7485.03 Hz = 24.9392 ppm = 0.228425 Hz/pt
number of scans: 24

freq. of 0 ppm: 300.130000 MHz
processed size: 65536 complex points
LB: 0.100 GF: 0.0000
Hz/cm: 97.502 ppm/cm: 0.32487

2-[4-methoxy-3-(tetramethyl-1,3,2-dioxaborolan-2-yl)phenyl]-1H-1,3-benzodiazole (Compound 20)

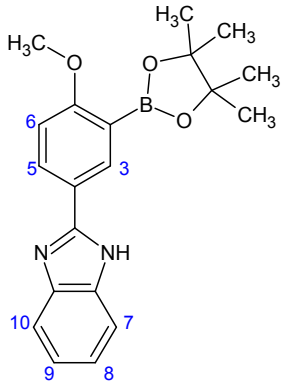

^{1}H NMR (300 MHz, DMSO-d_6)

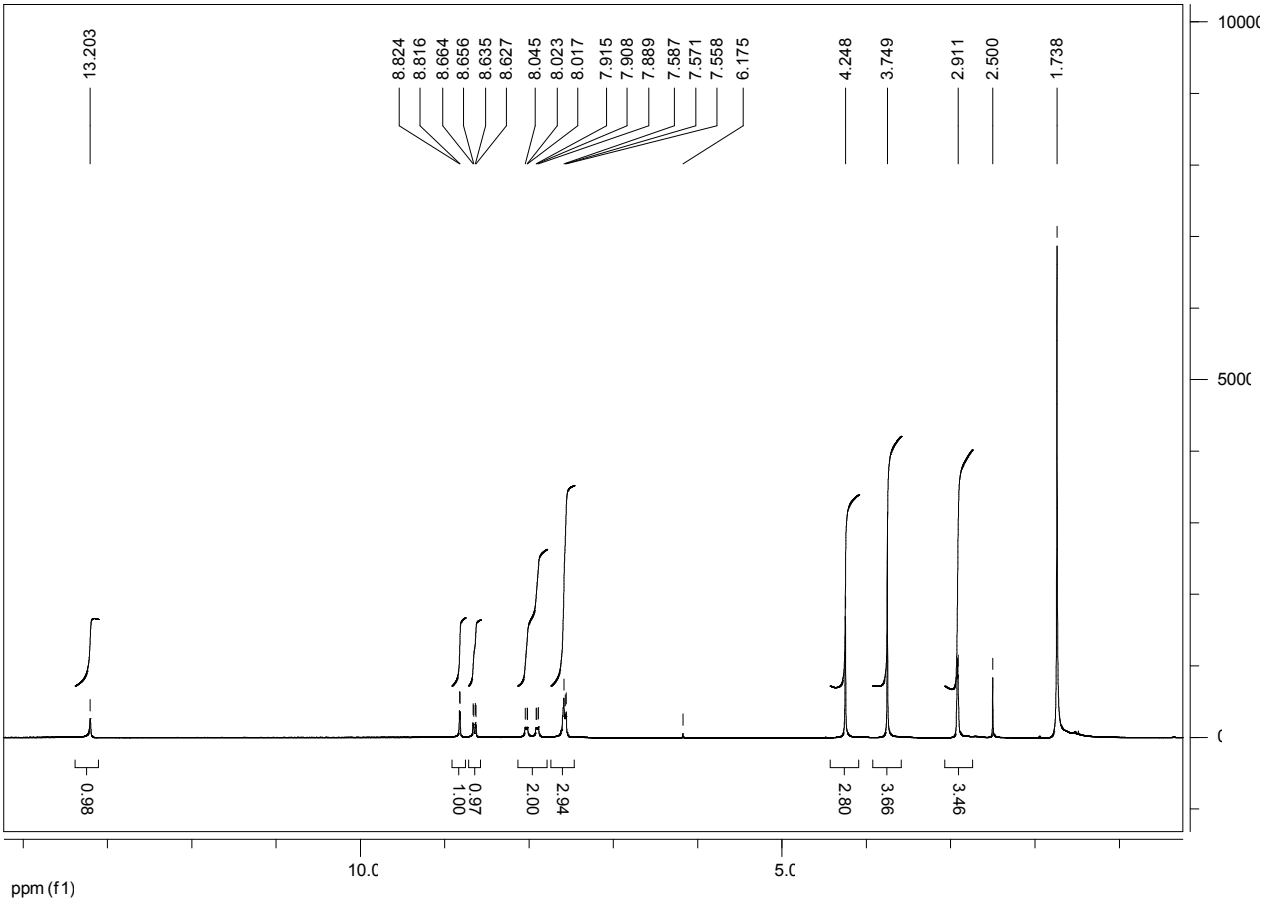

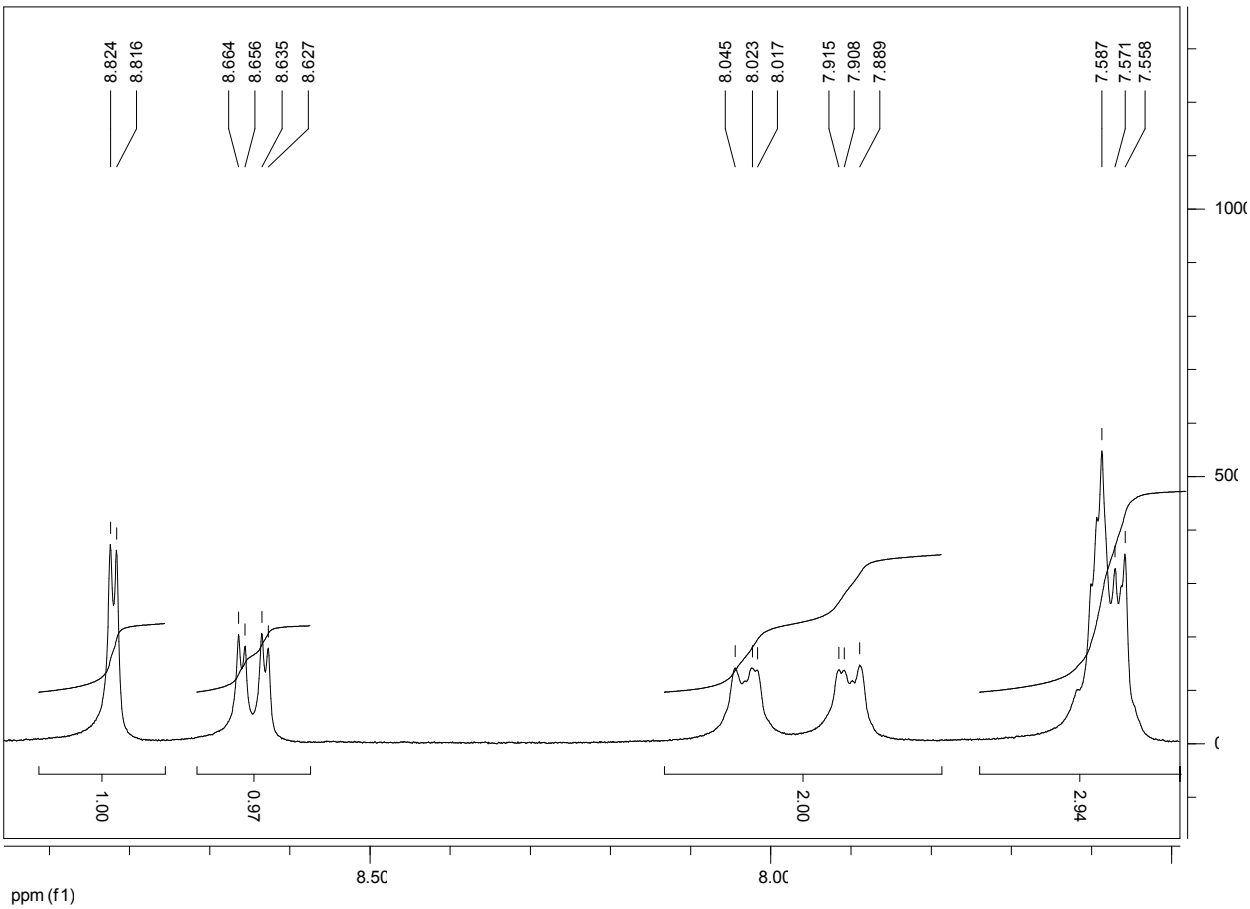
8.824
8.816
8.664
8.656
8.635
8.627
8.045
8.023
8.017
7.915
7.908
7.889
7.587
7.571
7.558
1.00
0.97
2.00
2.94
8.50
8.00
ppm (f1)

1-(2-Methoxyethyl)-2-[4-methoxy-3-(4,4,5,5-tetramethyl-[1,3,2]dioxaborolan-2-yl)-phenyl]-1*H*-benzoimidazole (Compound 21)

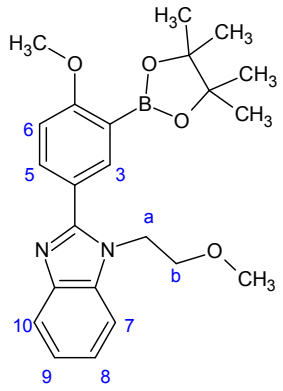

^{1}H NMR (300 MHz, $CDCl_3$)

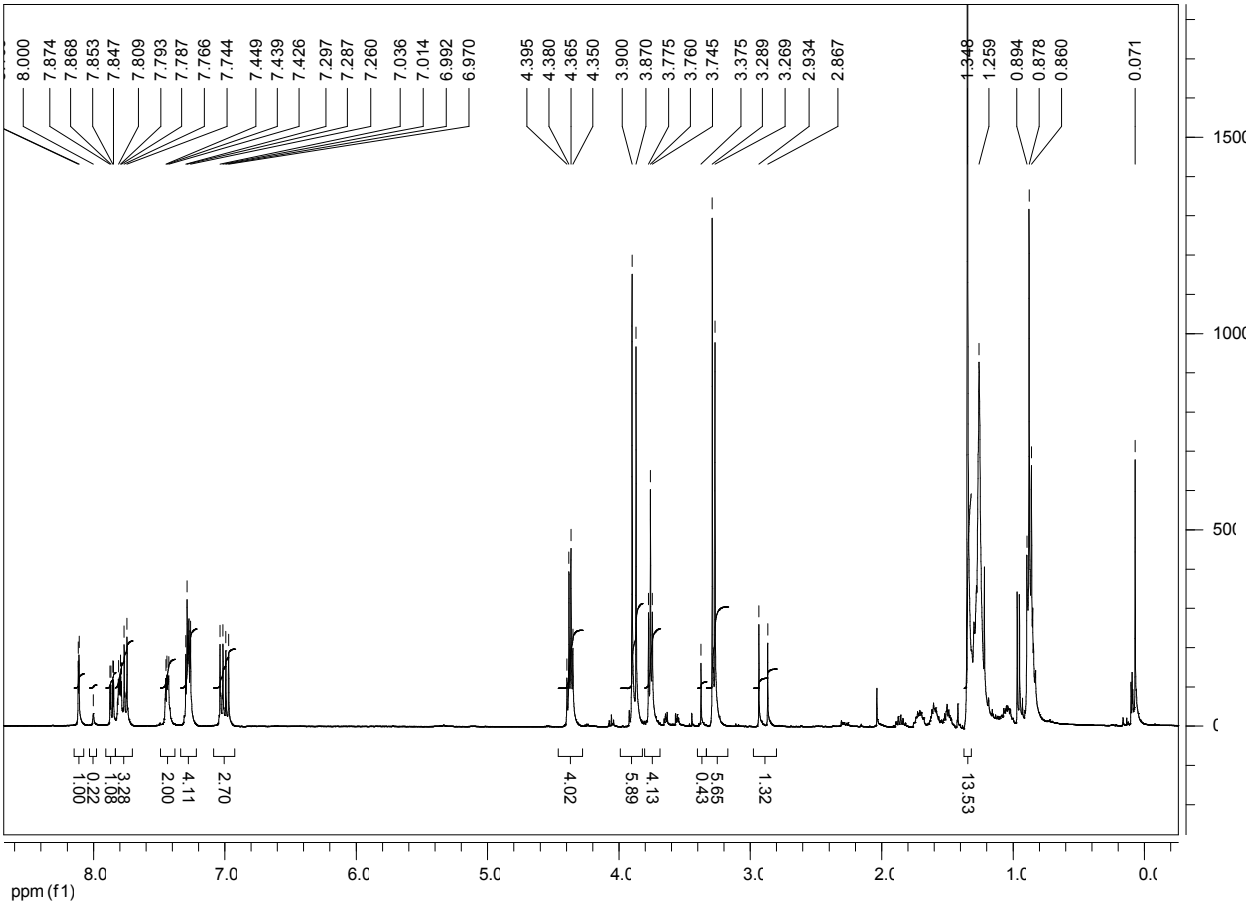

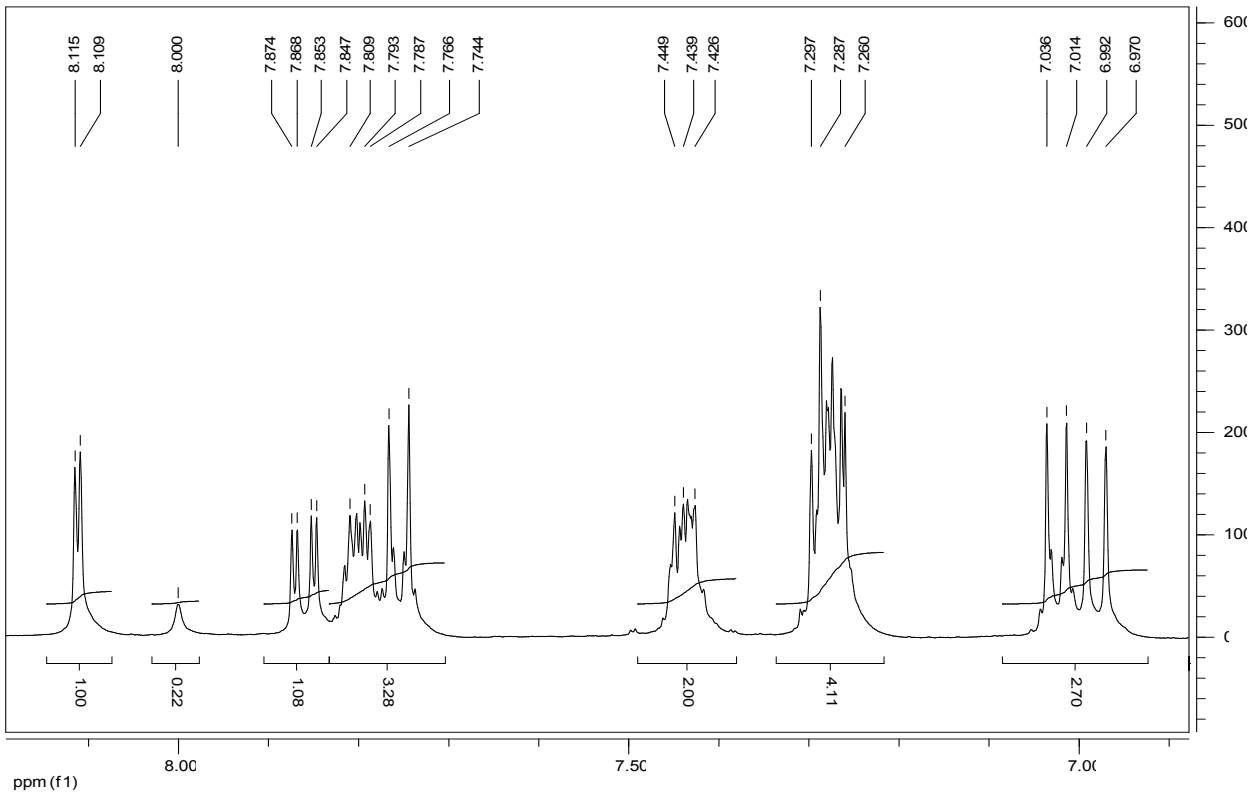
8.115
8.109
8.000
7.874
7.868
7.853
7.847
7.809
7.793
7.787
7.766
7.744
7.449
7.439
7.426
7.297
7.287
7.260
7.036
7.014
6.992
6.970
1.00
0.22
1.08
3.28
2.00
4.11
2.70
8.00
7.50
7.00
ppm (f1)

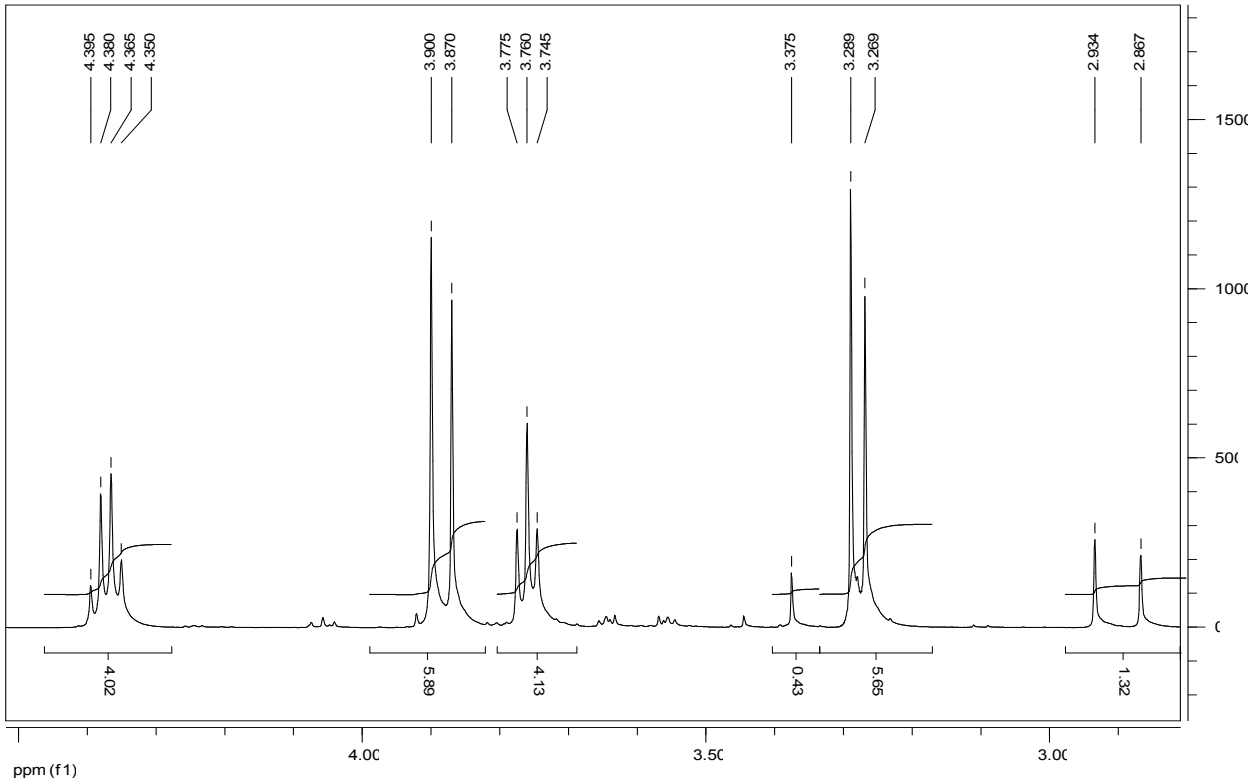
4.395
4.380
4.365
4.350
3.900
3.870
3.775
3.760
3.745
3.375
3.289
3.269
2.934
2.867
4.02
5.89
4.13
0.43
5.65
1.32
4.00
3.50
3.00
ppm (f1)

2-(4'-methoxyphenyl)benzimidazole (Compound 23)

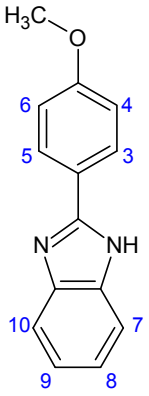

^{1}H NMR (300 MHz, $CDCl_3$)

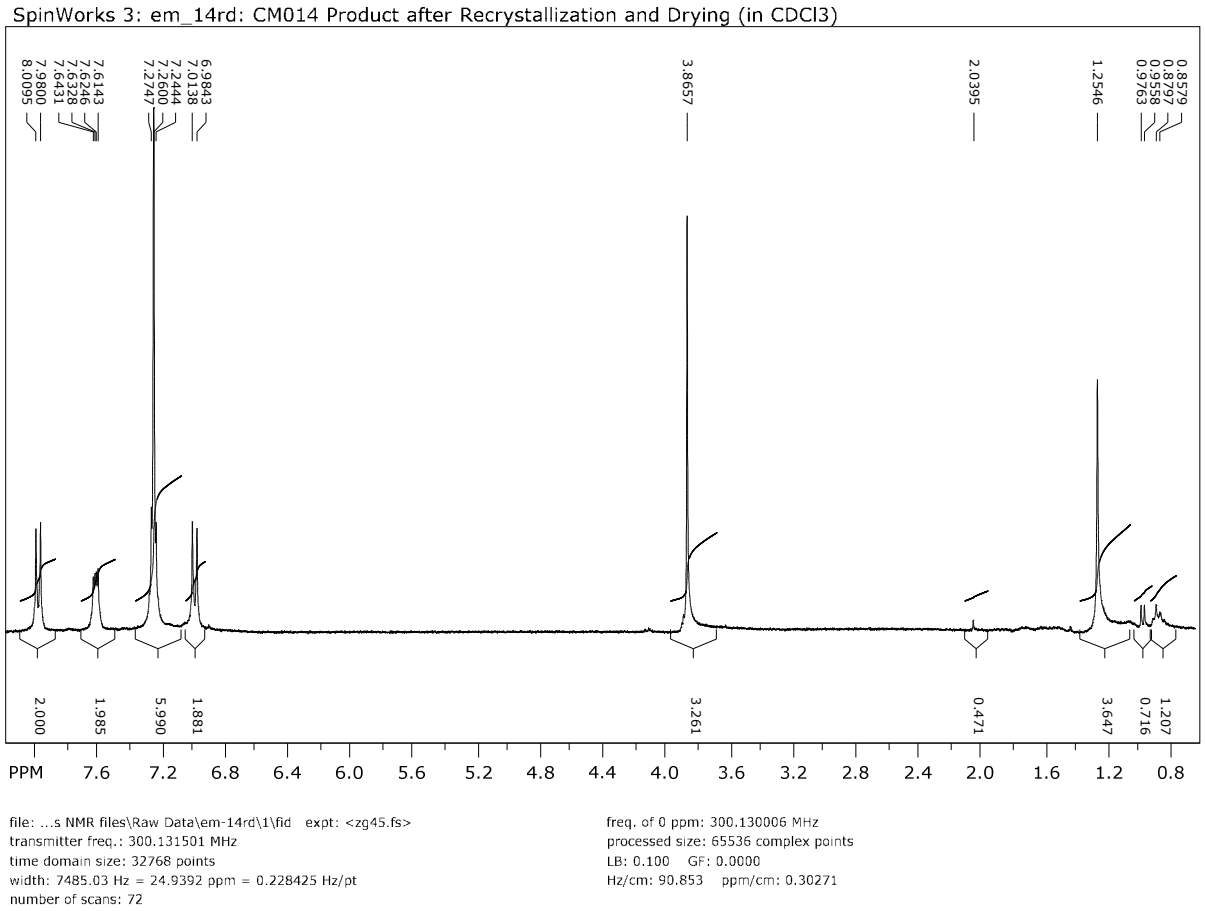

file: ...s NMR files\Raw Data\em-14rd\1\fid expt: <zg45.fs>
transmitter freq.: 300.131501 MHz
time domain size: 32768 points
width: 7485.03 Hz = 24.9392 ppm = 0.228425 Hz/pt
number of scans: 72

freq. of 0 ppm: 300.130006 MHz
processed size: 65536 complex points
LB: 0.100 GF: 0.0000
Hz/cm: 90.853 ppm/cm: 0.30271

1-(2-Methoxyethyl)-2-(4-methoxyphenyl)benzimidazole (Compound 24)

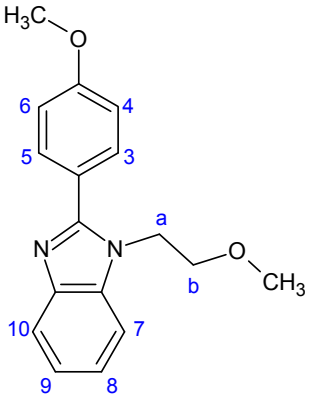

^{1}H NMR (300 MHz, $CDCl_3$)

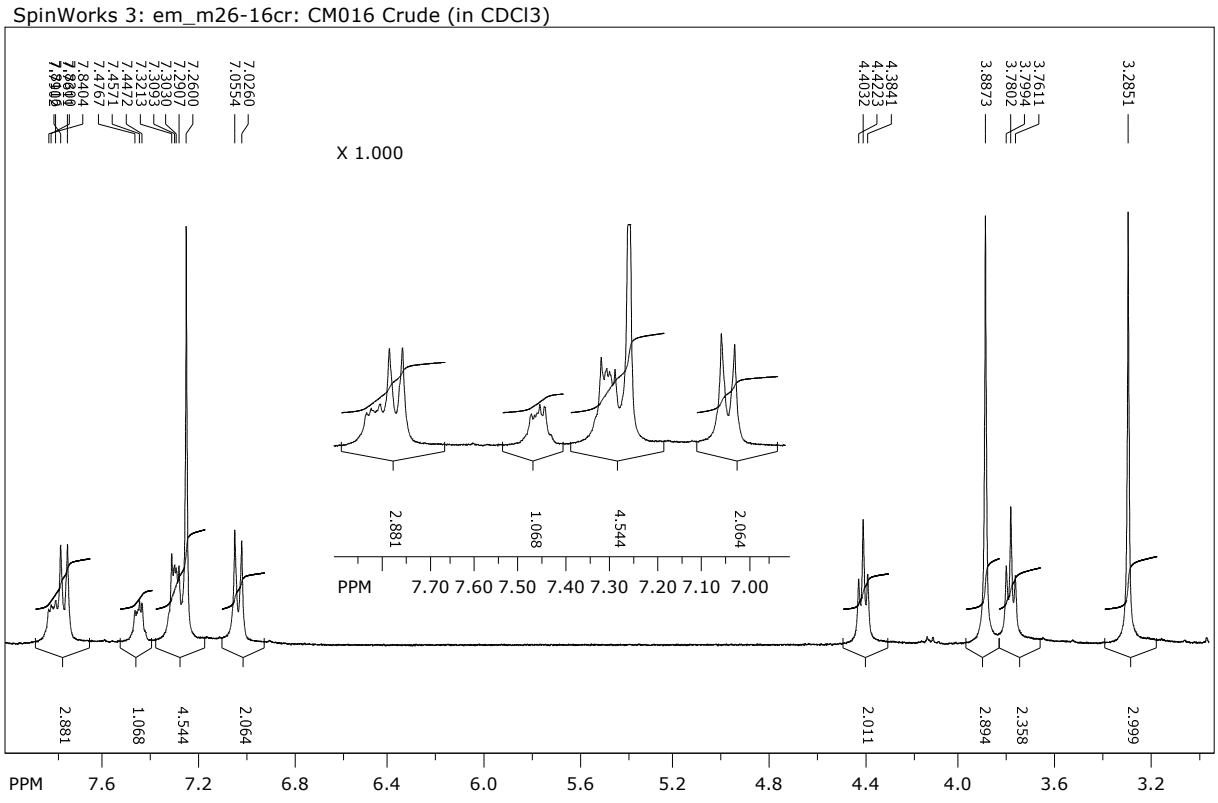

file: ...R files\Raw Data\em_m26-16cr\1\fid expt: <zg45.fs>
transmitter freq.: 300.131501 MHz
time domain size: 32768 points
width: 7485.03 Hz = 24.9392 ppm = 0.228425 Hz/pt
number of scans: 32

freq. of 0 ppm: 300.130006 MHz
processed size: 65536 complex points
LB: 0.100 GF: 0.0000
Hz/cm: 61.012 ppm/cm: 0.20328

Fourth Generation Tweezer (Compound 25)

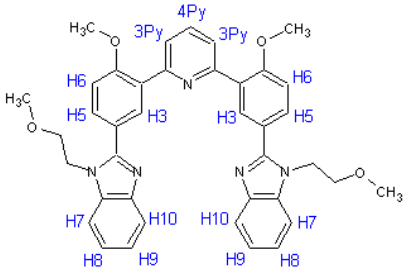

^{1}H NMR (300 MHz, $CDCl_3$)

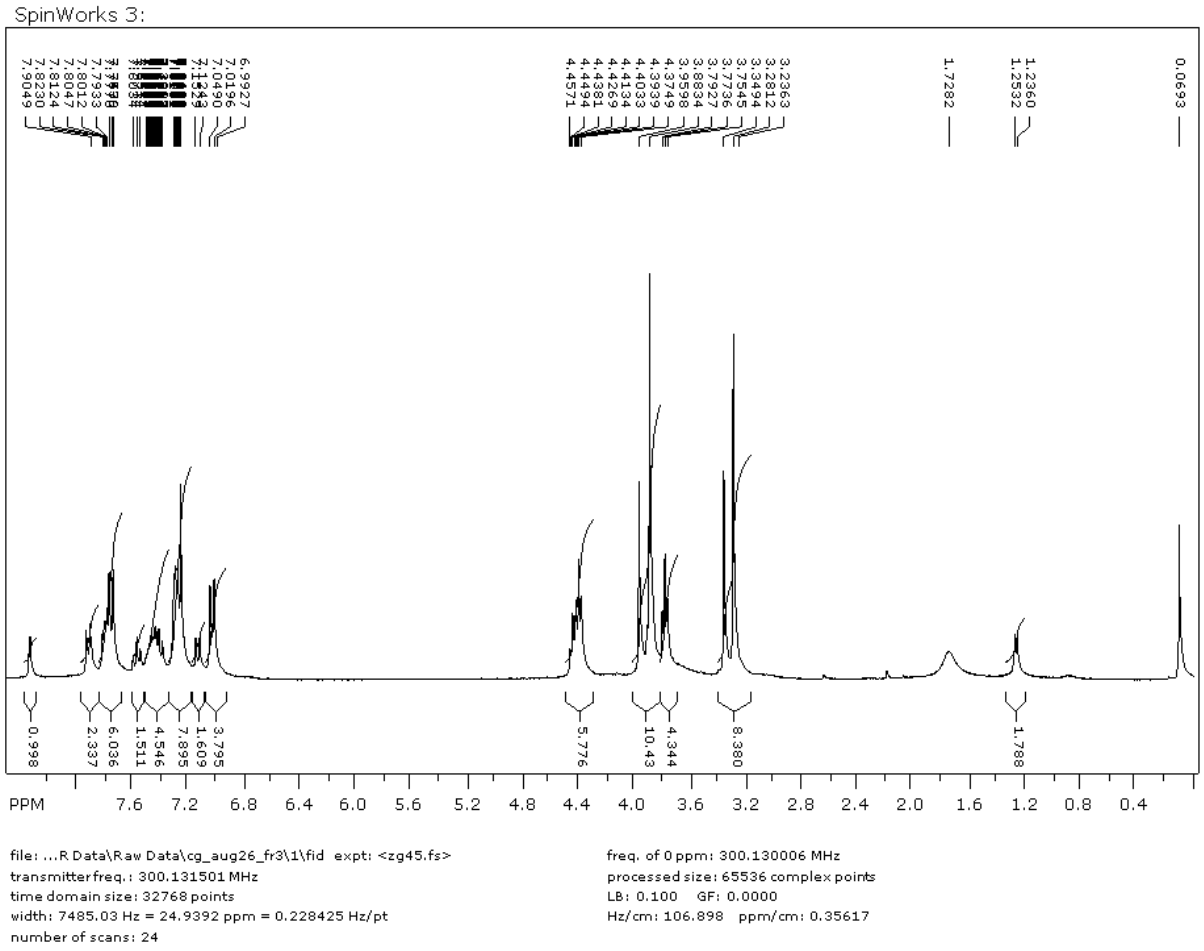

file: ...R Data\Raw Data\cg_aug26_fr3\1\fid expt: <zg45.fs>
transmitter freq.: 300.131501 MHz
time domain size: 32768 points
width: 7485.03 Hz = 24.9392 ppm = 0.228425 Hz/pt
number of scans: 24

freq. of 0 ppm: 300.130006 MHz
processed size: 65536 complex points
LB: 0.100 GF: 0.0000
Hz/cm: 106.898 ppm/cm: 0.35617

SpinWorks 3:

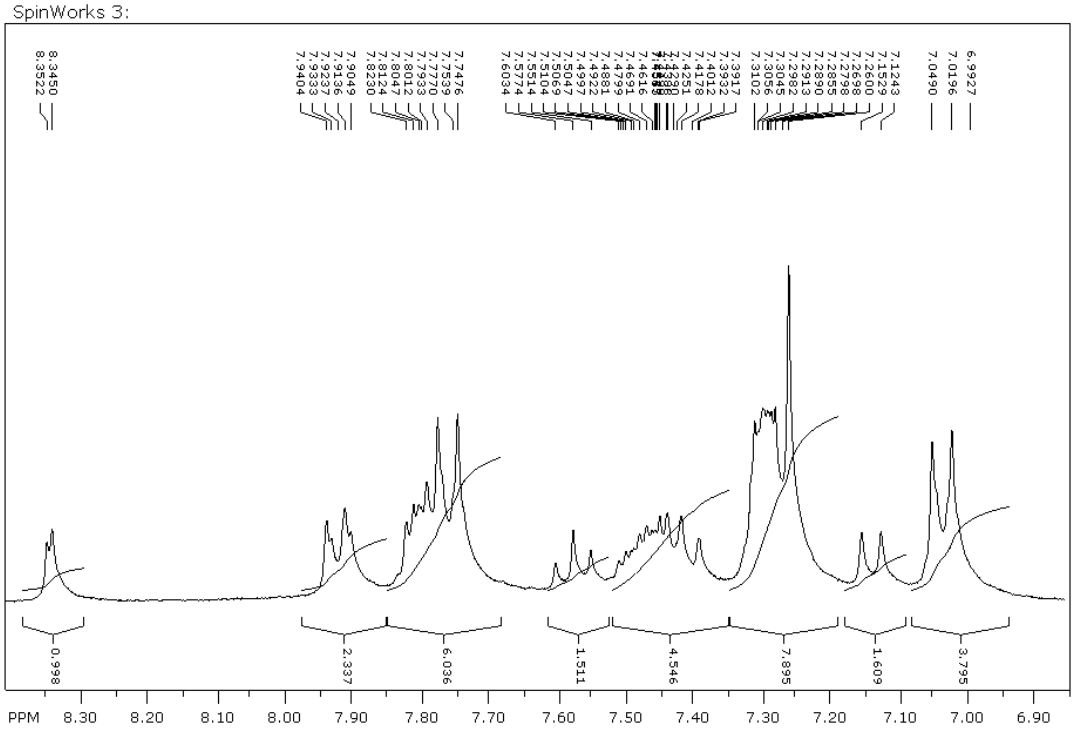

file: ...R Data\Raw Data\cg_aug26_fr3\1\fid expt: <zg45.fs>
transmitter freq.: 300.131501 MHz
time domain size: 32768 points
width: 7485.03 Hz = 24.9392 ppm = 0.228425 Hz/pt
number of scans: 24

freq. of 0 ppm: 300.130006 MHz
processed size: 65536 complex points
LB: 0.100 GF: 0.0000
Hz/cm: 19.511 ppm/cm: 0.06501

SpinWorks 3:

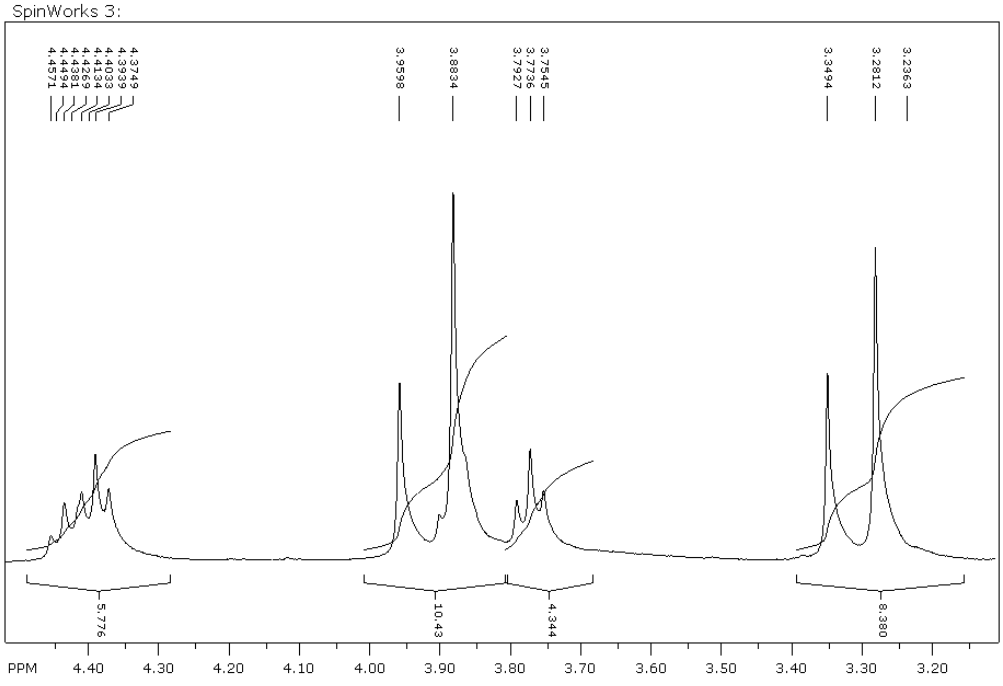

file: ...R Data\Raw Data\cg_aug26_fr3\1\fid expt: <zg45.fs>
transmitter freq.: 300.131501 MHz
time domain size: 32768 points
width: 7485.03 Hz = 24.9392 ppm = 0.228425 Hz/pt
number of scans: 24

freq. of 0 ppm: 300.130006 MHz
processed size: 65536 complex points
LB: 0.100 GF: 0.0000
Hz/cm: 17.642 ppm/cm: 0.05878

Failed Reactions

Caffeine Tweezer (Mono-Substituted)

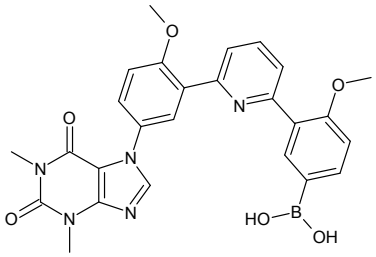

^{1}H NMR (500 MHz, $CDCl_3$)

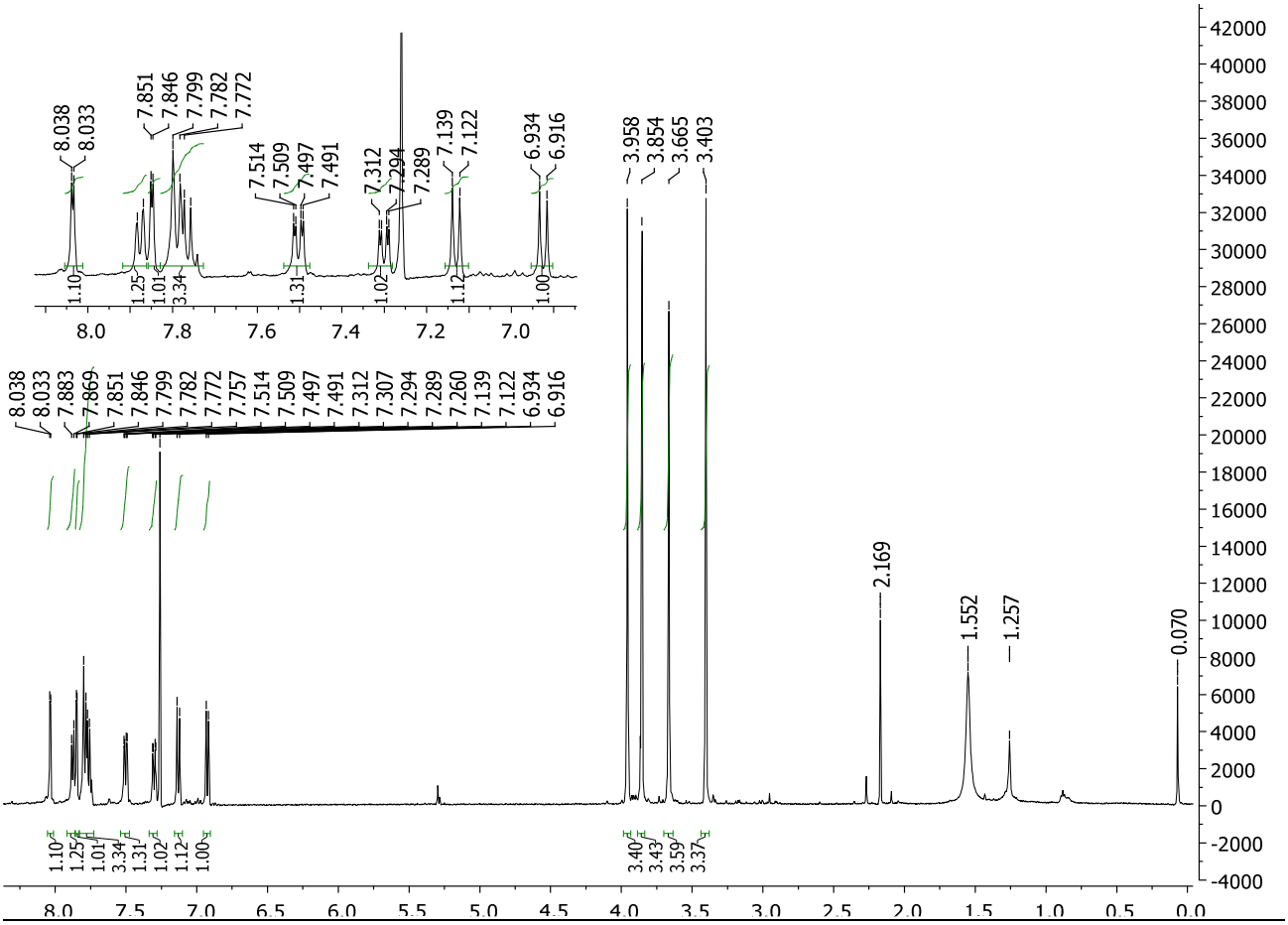

Halogen-Lithium Exchange Reaction (3rd Generation tweezer)

^{1}H NMR (300 MHz, $CDCl_3$)

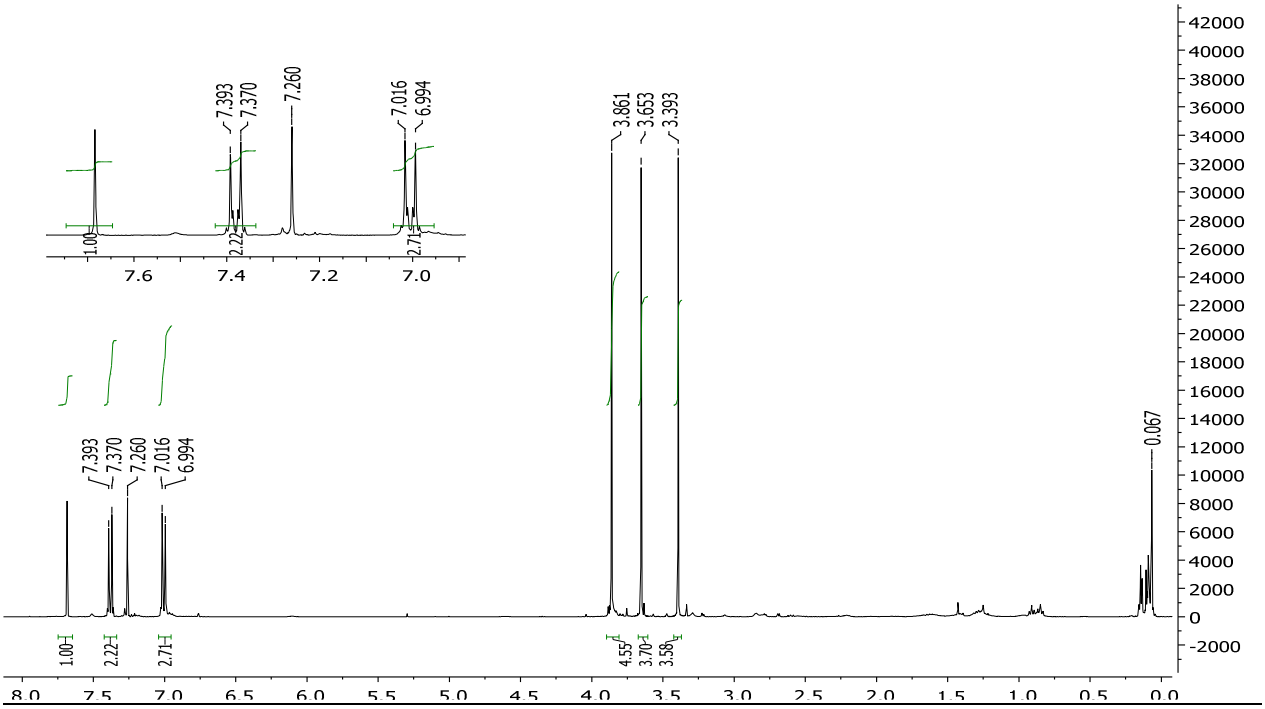

Halogen-Lithium Exchange (UNIT 1 PEG boronic acid)

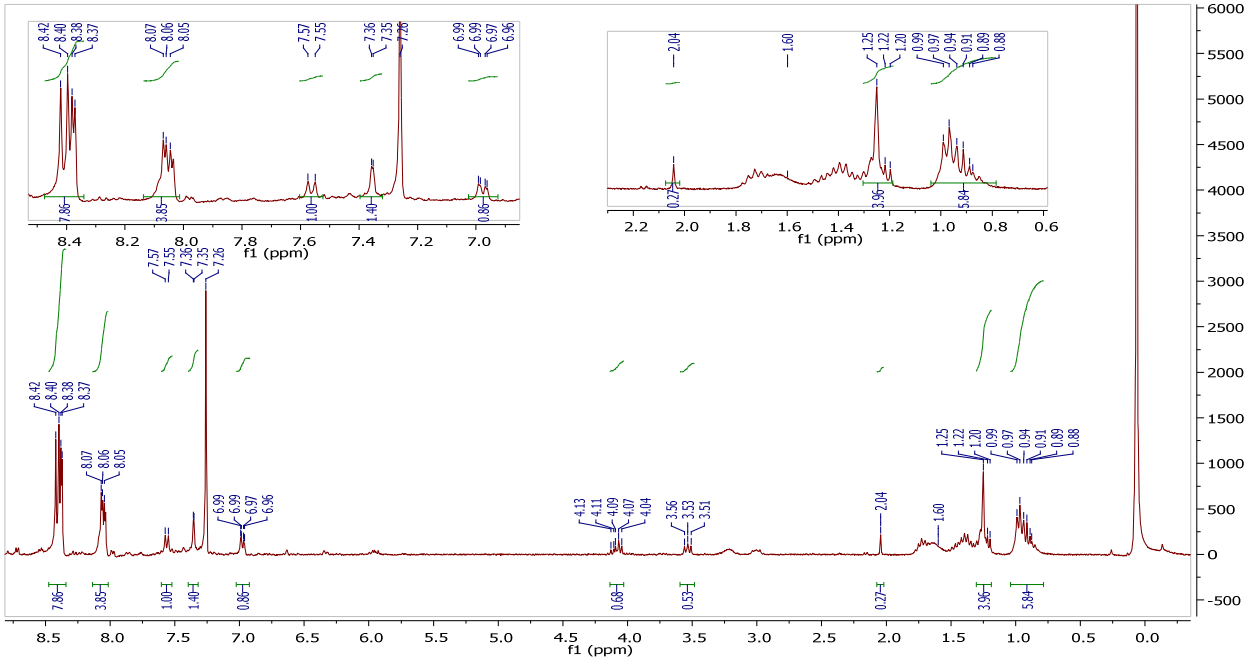

Grignard Reaction (UNIT 1 PEG boronic acid)

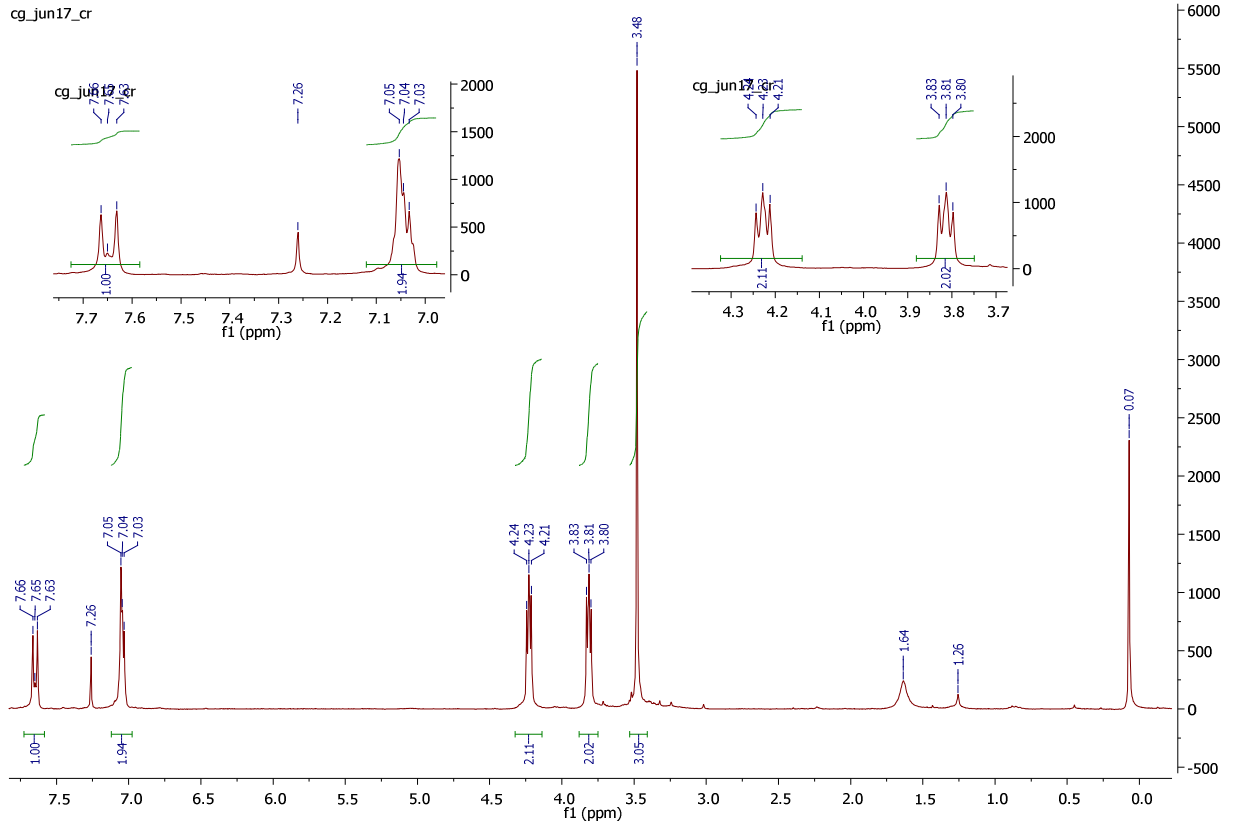

Suzuki Coupling reaction (Synthesis of 2nd Generation tweezer)

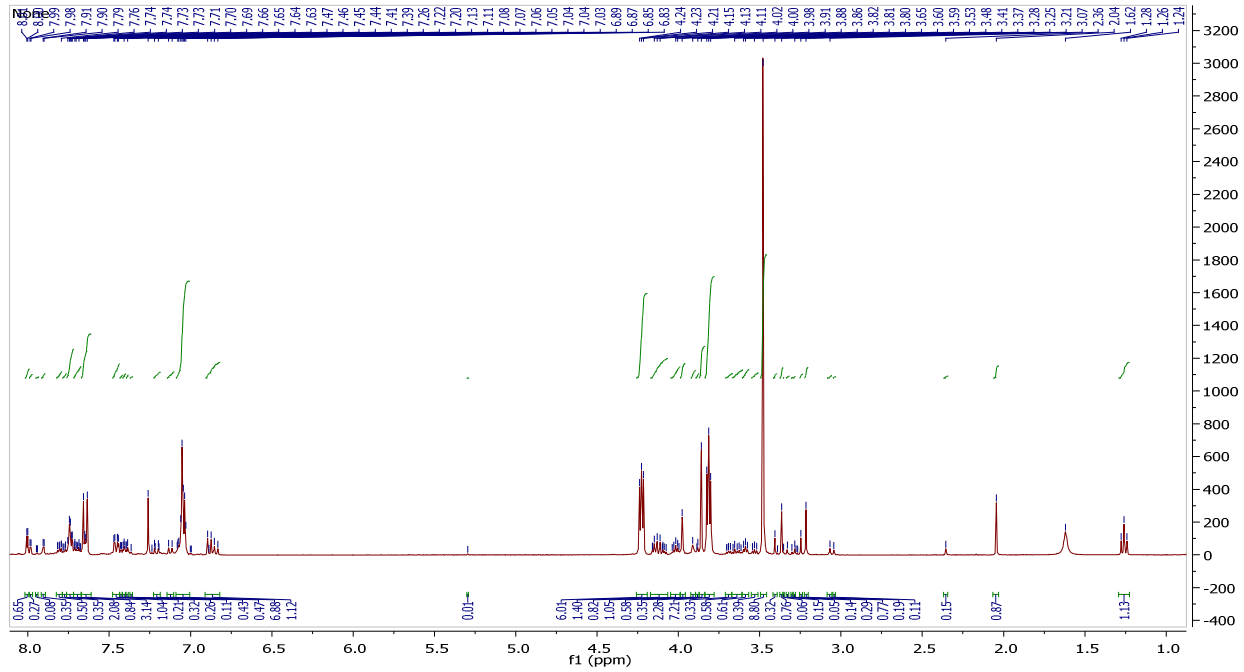

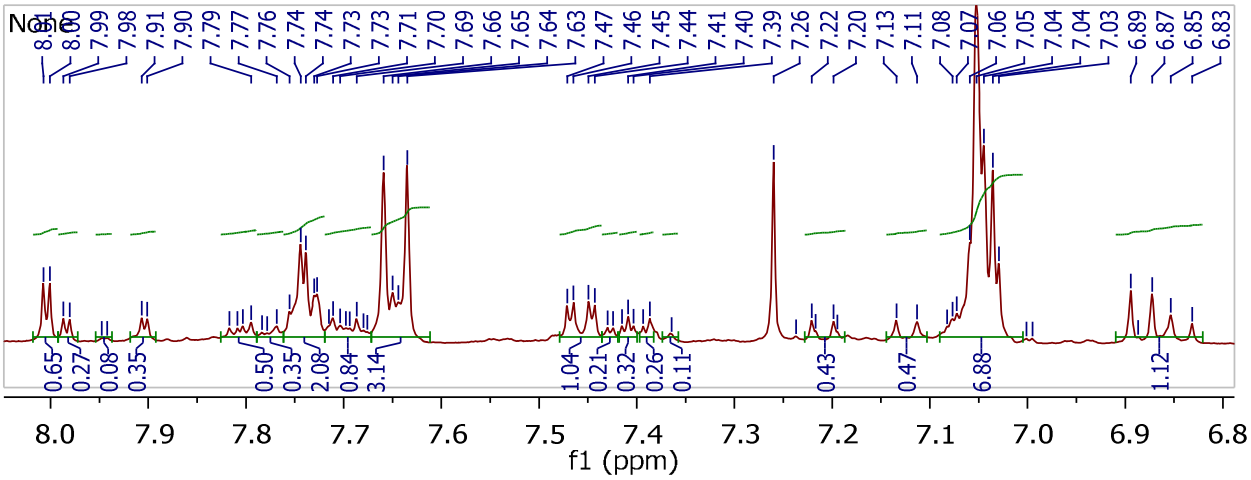
None
8.01 8.00 7.99 7.98 7.91 7.90 7.79 7.77 7.76 7.74 7.74 7.73 7.73 7.71 7.70 7.69 7.66 7.65 7.64 7.63 7.47 7.46 7.45 7.44 7.41 7.40 7.39 7.26 7.22 7.20 7.13 7.11 7.08 7.07 7.06 7.05 7.04 7.04 7.03 6.89 6.87 6.85 6.83
0.65 0.27 0.08 0.35 0.50 0.35 2.08 0.84 3.14 1.04 0.21 0.32 0.26 0.11 0.43 0.47 6.88 1.12
8.0 7.9 7.8 7.7 7.6 7.5 7.4 7.3 7.2 7.1 7.0 6.9 6.8
f1 (ppm)

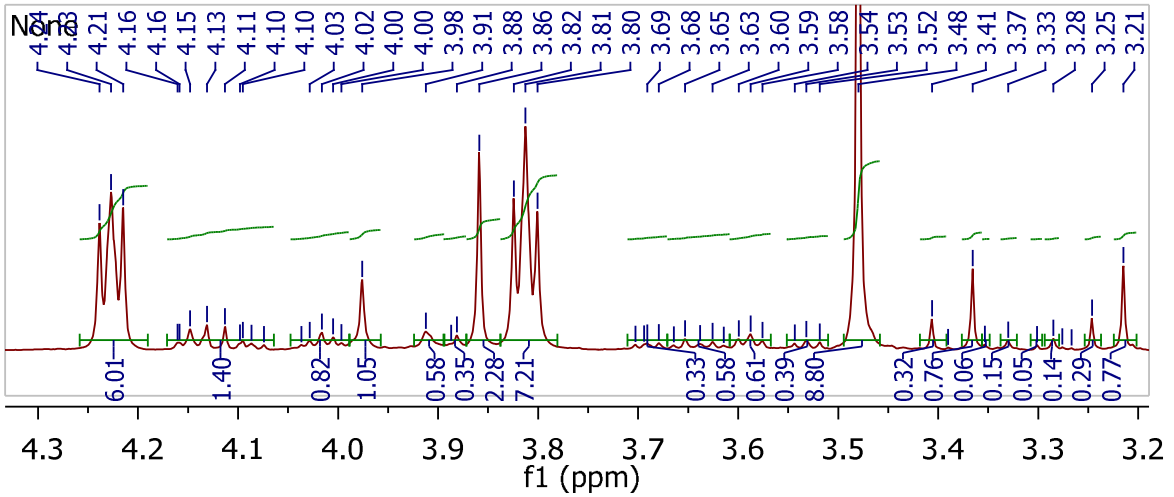
None
4.24 4.23 4.21 4.16 4.16 4.15 4.13 4.11 4.10 4.10 4.03 4.02 4.00 4.00 3.98 3.91 3.88 3.86 3.82 3.81 3.80 3.69 3.68 3.65 3.63 3.60 3.59 3.58 3.54 3.53 3.52 3.48 3.41 3.37 3.33 3.28 3.25 3.21
6.01 1.40 0.82 1.05 0.58 0.35 2.28 7.21 0.33 0.58 0.61 0.39 8.80 0.32 0.76 0.06 0.15 0.05 0.14 0.29 0.77
4.3 4.2 4.1 4.0 3.9 3.8 3.7 3.6 3.5 3.4 3.3 3.2
f1 (ppm)